I.M. Imyanitov and E.V. Chubarina

ELECTRICITY OF THE FREE ATMOSPHERE

TRANSLATED FROM RUSSIAN

Published for the National Aeronautics and Space Administration
and the National Science Foundation, Washington, D.C.
by the Israel Program for Scientific Translations

GLAVNOE UPRAVLENIE GIDROMETEOROLOGICHESKOI SL
MINISTROV SSSR
GLAVNAYA GEOFIZICHESKAYA OBSERVATORIYA im. A. I. VOEIKOVA

Main Administration of the Hydrometeorological Service of the
USSR Council of Ministers
Main Geophysical Observatory im. A. I. Voeikov

I. M. Imyanitov and E. V. Chubarina

ELECTRICITY OF THE FREE ATMOSPHERE

(Elektrichestvo svobodnoi atmosfery)

Results of Measurements Carried Out During the International Geophysical Year and Year of International Geophysical Collaboration

Gidrometeorologicheskoe Izdatel'stvo
Leningrad 1965

Translated from Russian

Israel Program for Scientific Translations
Jerusalem 1967

NASA TT F-425
TT 67-51374

Published Pursuant to an Agreement with
THE NATIONAL AERONAUTICS AND SPACE ADMINISTRATION
and
THE NATIONAL SCIENCE FOUNDATION, WASHINGTON, D.C.

IPST Cat. No. 1841

Translated and Edited by IPST Staff

Printed in Jerusalem by S. Monson
Binding: Wiener Bindery Ltd., Jerusalem

Available from the
U.S. DEPARTMENT OF COMMERCE
Clearinghouse for Federal Scientific and Technical Information
Springfield, Va. 22151

VII/13/5

Table of Contents

ANNOTATION

This monograph is based on data obtained in systematic aircraft soundings of the electric field of the atmosphere during the International Geophysical Year and the Year of International Geophysical Collaboration. In addition to detailed tables of the initial data, this book gives, for the first time, data on the structure of "fair" weather electric field, and on the distribution of electric space charges and potentials in these conditions. Data on the electric structure of stratus clouds are also given.

The book on the whole gives a general picture of the electric structure of the atmosphere on cloudy and cloudless days. It is intended for specialists in the field of the physics of the atmosphere and for specialists in those engineering fields in which manifestations of atmospheric electricity are encountered.

INTRODUCTION

Toward the end of the nineteen fifties, it was finally clarified that the primary electric generators which charge the earth's atmosphere and which lead to the appearance of the electric field of the atmosphere are situated in the troposphere at some altitude above the earth's surface. At the same time, most of the data on the electricity of the atmosphere have been collected in surface measurements. Only at the end of the forties and in the fifties were some investigations undertaken which made it possible to obtain direct data on the electricity of the free atmosphere. However, these data were obtained sporadically and did not make it possible to obtain a typical picture of the electric structure of vertical cross sections of the atmosphere.

Surface measurements in most cases did not make it possible to get an idea of the large-scale distribution of charges in the atmosphere and, of course, gave totally insufficient information on the meso-scale inhomogeneities, and even less on the microphysical characteristics of the free atmosphere. The complexity of the calculation of the distribution of charges in the atmosphere from data on the distribution of the field intensity in one plane makes it possible to obtain a solution only under some simplifying assumptions regarding the position of the charges, and this only for the simplest cases. In measurements made in the atmosphere near ground level, this solution is complicated by the fact that the electrode effect very strongly affects the measurement results.

After it had been found by occasional investigations in the free atmosphere that, even on clear days, the field intensity may not only decrease with altitude, but also increase, it became clear that the usual extrapolation of surface data on the free atmosphere by introducing some stipulated regularity of the field decrease with altitude may lead to inaccurate results.

The fact that the basic data on atmospheric electricity were mainly obtained from surface measurements did not make it possible to get an idea of the distribution of charges with a horizontal extent significantly exceeding the vertical extent. It was found that, despite the long duration of the measurements of atmospheric electricity, which extends over one hundred years, the macro-scale electric characteristics of stratus clouds had not been studied at all, and their role in the general scheme of atmospheric electricity processes had not been clarified. On the other hand, these clouds, although they are considerably less active electrically than thunderstorm clouds, cover about half of the globe, extending over an area approximately 200-300 times as large as that covered by thunderstorm clouds. Accordingly, electric processes in stratus clouds, which are hundreds of times less active than in thunderstorm clouds, may have a considerable effect on electric processes in the atmosphere.

It has not been clarified how often an increase of potential gradient with altitude is observed in the surface layer. Moreover, the regularities in behavior of the space charges of different signs distributed in the atmosphere, which appear in this case, also remain unclear.

It can be affirmed without exaggeration that only the macro-scale electric characteristics of thunderstorm clouds, and to some extent of shower clouds, have been somewhat systematically studied. And although a large part of these data remains disputable and incomplete, the electric characteristics of the free atmosphere in other cases were known only for some cases, the typicalness of which has still to be determined.

At the same time, data on the electric characteristics of the free atmosphere are important not only for the science of atmospheric electricity itself, but also for the physics of clouds and for a number of engineering fields. The role of electric forces in drop coalescence and, consequently, in the development of clouds and precipitation, is well known. By following the movement of space charges and the distribution of currents in the atmosphere, it is possible to obtain complete information on the mixing conditions in the atmosphere. The electric characteristics of clouds are in a number of cases the most characteristic quantity determining the state of the clouds, and are of particular importance in the study of active cloud modification.

The problem of the electrostatic hazard for aircraft, which is closely related to the conditions of electrification of bodies in clouds, is well known. The need to solve this problem increases with the increasing rate of aircraft electrification (we recall that the electrification is proportional to the third power of the aircraft velocity). The problem of indications signaling the approach to thunderstorm clouds, so important for the safety of aircraft, can be solved by studying the structure of electric fields in the atmosphere. A study of the distribution of conductivity or of the field intensity at high altitudes can serve as a means of indicating anomalously ionized regions of artificial origin.

There is therefore nothing surprising in the fact that in the absence of experimental data on the electricity of the free atmosphere, general considerations, hypotheses, and schemes, which explain either the atmospheric electricity as a whole or some of its peculiarities, abound. The necessity to explain phenomena which the investigator encountered inevitably led to the propounding of such schemes. On the other hand, the setting up of hypotheses and schemes which were not confirmed by sufficient experimental data resulted in their being insufficiently reliable and contradictory. The soundest hypothesis from the point of view of the general concepts and the most fantastic hypothesis were often both considered as equally probable owing to the absence of data which would have made it possible to compare the theory with the facts.

Under these conditions, it seemed necessary to begin systematic investigations of the electric characteristics of the free atmosphere, since such investigations, giving a solution to important practical problems, would at the same time make it possible to analyze general problems also. Favorable possibilities for such investigations appeared during the International Geophysical Year and the following Year of International Collaboration.

In the first place, in the USSR, it was planned to investigate the vertical distribution of the electric field intensity. These measurements, permitting

determination of the potential of the atmosphere, and in most cases the distribution of space charges in it, thus make it possible to obtain a general picture of the large-scale distribution of charges in the atmosphere.

It was planned to carry out the measurement at three points in the Soviet Union — Leningrad, Kiev, and Tashkent. Several points were necessary, firstly, in order to find out how much the studied characteristics depend on the latitude, and, secondly, to determine to what extent the potentials and field intensities at various points of the globe vary synchronously.

The investigations were carried out from aircraft, since this made it possible to determine simultaneously additional meteorological characteristics, such as the type of clouds and the altitudes of their boundaries, the presence of precipitation, the level of its appearance, etc. In the same soundings, other investigations connected with the IGY program, for example measurement of the vertical distribution of condensation nuclei, were carried out simultaneously.

The results of data processed from more than 2000 soundings are considered in the present work. The initial sounding data are given in the book "Materialy nablyudenii napryazhennosti elektricheskogo polya atmosfery na razlichnykh vysotakh po dannym samoletnogo zondirovaniya v period MGG i MGS (1958-1959)" [Observation Data concerning the Intensity of the Atmospheric Electric Field at Various Altitudes from Aircraft Sounding during the IGY and Year of International Geophysical Collaboration (1958-1959)], published by Gidrometeorizdat in 1963.

The measurements were carried out using equipment developed by V. G. Bordulina, N. P. Ziganov, and V. V. Mikhailovskaya, and built in the experimental workshops of the Main Geophysical Observatory [GGO].

The measurements in Leningrad, Kiev, and Tashkent were carried out by groups of aerologists under the direction of E. V. Chubarina, I. V. Spasskaya, and K. E. Tserfas.

The data for the present work were processed under the direction of E. V. Chubarina, by the technicians of the department of atmospheric electricity of GGO, T. A. Basukova, V. V. Uksusova, and G. G. Agafonova.

All the works connected with both the development of the equipment and the organization of the measurements and the processing were directed by I. M. Imyanitov.

Chapter I

INVESTIGATIONS OF THE ELECTRIC FIELD IN THE FREE ATMOSPHERE AND THEIR IMPORTANCE FOR THE DETERMINATION OF THE NATURE OF ITS ORIGIN

Experimental investigations of the electric field in the atmosphere were restricted until recently to measurements near ground level. These measurements, conducted at a number of stations, sometimes extending over decades, made it possible to clarify a number of characteristic features of the behavior of the electric field in the surface layer, and to establish its relationship to other elements of atmospheric electricity, such as the conductivity of the atmosphere, the air-earth current, etc.

It has been established that in fair* weather conditions, the electric field is usually directed as though the earth were negatively and the atmosphere positively charged. The mean field intensity at the ground level is about 130 v/m. During precipitation and particularly during thunderstorms, as well as in a number of other cases, the field may change direction and reach approximately 10,000 v/m.

These investigations, in particular, established that the intensity of the atmospheric electric field undergoes variations, which take place simultaneously all over the globe. Synchronous variations both in the diurnal and in the annual course are observed. These so-called unitary variations of the electric field of the atmosphere are most easily determined by measurements over oceans and in polar regions in fair weather conditions. Electric field measurements, performed at continental stations, are subjected to the influence of a number of local factors, which modify the conductivity in the surface layer and therefore do not allow a simple determination of unitary variations.

Field measurements over the oceans, carried out by Mauchly /95/, showed (Figure 1) that a maximum is observed in the diurnal variation at approximately 19 hr GMT and a minimum at 3 hr GMT. This variation is observed both over the Indian, Atlantic and Pacific oceans (curve 4, based on the data of 59 diurnal series), and in polar regions (curve 3, based on Sverdrup's data /108/).

Further investigations /114/ showed that the diurnal unitary field variation is in many ways similar to the diurnal variation of the intensity of thunderstorm activity, calculated for the whole globe (Figure 1, curves 1, 2, 3 — the area occupied by thunderstorms over the globe). The thunderstorm activity is estimated in this case by the area occupied by thunderstorms, which is calculated from data on the number of days with thunderstorms and on the diurnal variation of thunderstorm activity in the given regions.

* "Fair" weather is the term applied to weather in which the electric field is little dependent on local conditions (no clouds, precipitation, fogs, dust, strong wind, etc.).

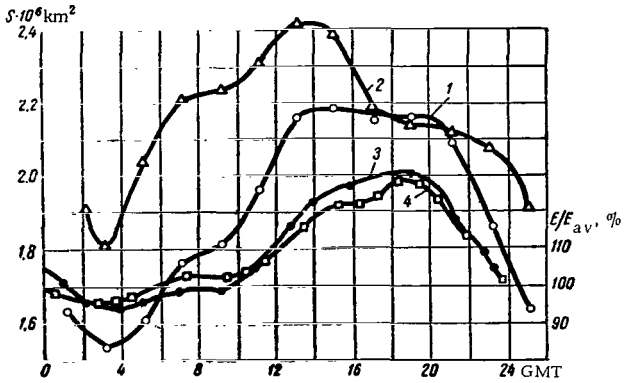

FIGURE 1. Diurnal variations of thunderstorm activity (1 and 2) and relative diurnal variations in the electric field intensity E/E (%) over oceans (3 and 4).

1—according to Brooks /68/, 1921; 2—according to Krumm /89/, 1959; 3—from measurements in polar regions on the ship "Maud"; 4—from measurements over oceans on the ship of the Carnegie Institute.

The close similarity between the two curves suggested that a causal relationship exists between thunderstorm activity around the earth and the electric field in the atmosphere.

The few measurements of the electric-field variation with altitude which were carried out in the nineteen twenties to forties showed that its intensity decreases fairly rapidly with altitude. At the same time, measurements on mountains and airborne measurements also established that the air conductivity increases with altitude, obeying a law close to exponential.

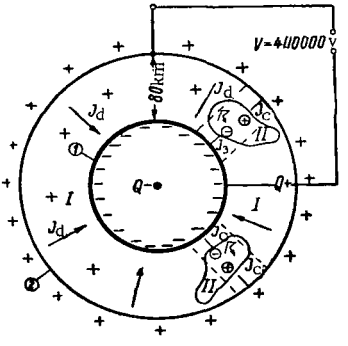

FIGURE 2. Diagram illustrating the theory of the spherical condenser.

I—regions of "fair" weather; II—regions occupied by thunderstorms; 1— the earth; 2—ionosphere; J_c— charging currents; J_d— discharge currents.

The existence of a latitudinal variation in the field intensity near the ground level has been established. The mean field intensity is minimum at the equator and rises toward the moderate latitudes.

These and a number of other facts have been explained by means of a theoretical model (the theory of the spherical condenser). This theory is usually /83, 60/ used for explaining processes of atmospheric electricity.

According to this theory, the electric field of the atmosphere exists owing to the fact that a negative charge Q_- and a positive charge Q_+ are concentrated on the earth (1) (Figure 2) and in the

upper layers of the atmosphere (the ionosphere) (2), respectively, which serve as condenser plates. These charges create some potential difference V between the plates, as a result of which an electric field is observed in the atmosphere. Owing to the atmospheric conductivity, an electric current J_p, which tends to discharge the condenser, flows between the ionosphere and the earth's surface. The density i_p of this current is constant with altitudes and equal to $E_h\lambda_h$, where E_h is the field and λ_h is air conductivity at the altitude h. The atmospheric field should decrease with altitude, following an exponential law, since the conductivity, as indicated above, increases with altitude by an exponential law. Since the conductivity at an altitude of 6 km is approximately 10 times as high as that at the earth's surface, the electric field at this altitude will be only 10 % of its value at ground level.

To maintain the charges on the plates of the above-mentioned condenser, the appearance of charging currents, which compensate for the indicated discharge current, is obviously necessary.

It is assumed that charging currents J_c are created in all the regions of the globe occupied by thunderstorms (regions II, Figure 2), where the field has a direction opposite to that observed in fair weather regions I. Since the charges Q of the earth and the atmosphere are determined by the relationship between the charging and discharging currents, an intensification in thunderstorm activity should be associated with a rise in the charges, and consequently, with an increase in the potential difference V between the earth and the ionosphere. A rise in the potential difference V should lead to an intensification of the field and of the discharge currents as long as the discharge current has not become equal to the total charging current. It should be borne in mind in this connection that, owing to the good conductivity of the earth and of the ionosphere, charges which come into contact with them spread over the whole surface of the corresponding sphere in a very short time (a matter of seconds). Thus, variations in the potential difference V should occur on the whole globe practically simultaneously. A decrease in thunderstorm activity should be associated with corresponding decreases in the potential difference V and the atmospheric field intensity.

If we assume that the whole current J_c to the earth and to the ionosphere, which is created by thunder clouds, is proportional to the area covered by thunderstorms, the close correlation between the variation of the thunderstorm activity and the unitary variation of the potential gradient (see Figure 1) becomes clear.

Electric processes, causing the appearance of a field in the atmosphere, can be simply described by means of the electric scheme shown in Figure 3, which follows from the scheme of Figure 1.

As a result of the charging currents J_c created by thunderstorms, the ionosphere and the earth are continuously being charged by positive and negative charges, respectively; a leakage current J_d appears in regions of fair weather and a potential difference V between the earth and the ionosphere is created. In quasistationary processes, it can be assumed that for the earth as a whole the sum of discharge currents is equal to the sum of charging currents. If R is the resistance of a vertical air column between the earth and the ionosphere having a cross section of 1 cm^2, then

from Ohm's law, the density of the discharge current i_d will be

$$i_d = \frac{V}{R}.$$

On the other hand, since the current density will be the same in any cross section, the following equation can be written

$$i_d = E_h \lambda_h,$$

where E_h and λ_h are respectively the field intensity and air conductivity at any level.

Comparing both equations we obtain

$$\frac{V}{R} = E\lambda. \qquad (1)$$

This equation is useful since it relates the electric characteristics V, common to the whole globe, to the electric characteristic R of an air column above the place of measurement and to the local characteristics of the field intensity E_h and the conductivity λ_h, measured at any altitude, in particular at ground level.

Variations in the field intensity E at the ground level may, in accordance with equation (1), be attributed to one of three factors (or to any combination of them).

1. Variations in E due to variations in V, with R = const and λ = const. Such variations should be detected at all stations of the globe. In this case current density variations follow variations of the potential V.*

2. Variations in E due to variations in R, with V = const and λ = const. Such variations are detected only at stations which are situated in the zone of variation of R. Variations in R are usually connected with the passage of cloud systems, fronts, and with the appearance of large polluted air masses.

The vertical current density undergoes variations only at stations over which R varies.

It should be noted that the main part of the atmospheric electrical resistance is concentrated in its lower layers (R_2 and R_3 in Figure 3). Thus, for example, half of the whole resistance R is concentrated in fair-weather conditions in the 0-2 km layer. About 66 % of the whole resistance R is concentrated within the 0-6 km layer (Figure 3, the variation of the resistance R with the altitude H).

The variation of the air resistance is due to the appearance of aerosols in the atmosphere affecting its state of ionization, which again usually occurs in the troposphere, mainly in its lower and middle layers. The main variations of R will therefore occur in the lower layers of the atmosphere. But a 50 % increase in the air resistance in the 6-80 km layer causes a variation of approximately 9 % in the field intensity at ground level and a 50 % increase in the air resistance in the 0-6 km layer causes a variation of approximately 8 % in the field intensity at ground level.

Consequently, resistance variations in the upper layers of the atmosphere, caused by variations in the ionization rate, can be manifested in a

* Since the potential of the earth is usually taken equal to zero, the potential difference between the earth and the ionosphere is numerically equal to the potential of the ionosphere.

variation in the field intensity at ground level. Thus, the latitudinal variation of the field intensity may be due to the fact /83/ that the density of cosmic radiation, being the main ionizer at high altitudes, increases from the equator to high latitudes due to the deflecting action of the magnetic field of the earth. This should lead accordingly to an increase in the conductivity of the upper layers of the atmosphere as one moves toward high latitudes. Thus, the field in upper layers of the atmosphere at higher latitudes is "short-circuited", which in turn results in an increase in the field intensity at ground level.

3. Variations in E due to local variations in λ when V = const and R = const. If E and λ are measured simultaneously, it is very simple to eliminate variations in E which are due to variations in λ. If the conductivity λ in some thin layer rises, for example, by a factor n, then the field intensity E decreases by a factor n. The vertical current density in this case does not vary. Local conductivity variations, occurring in the layer adjacent to the earth's surface, have practically no effect on the magnitude of the resistance R of the entire air column.

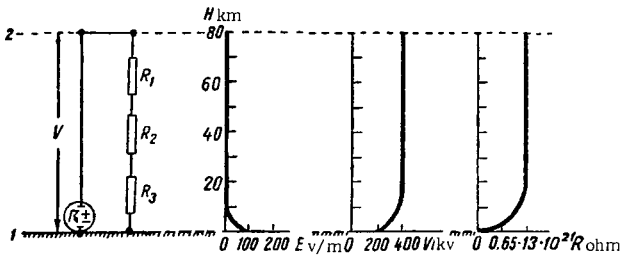

FIGURE 3. Scheme of the electric current circuit according to the spherical condenser theory and the variation of the electric field intensity E, the potential V, and the columnar resistance R of altitude H.

1 — earth; 2 — ionosphere; R_1, R_2, R_3 — resistances of sections of the atmosphere.

If the field variations are caused by several of the considered factors, it is possible, by comparing data of field and conductivity measurements at a number of stations, to isolate field variations due to variations in V, R and λ. An example of such an analysis is given by P. N. Tverskii /59/.

To carry out such a comparison successfully, particularly for individual seasons, months, and even days, it is necessary to be able to isolate unitary variations during the corresponding period. Such measurements can be carried out reliably only at marine, high-mountain, and polar stations. It is necessary in this case that the variations in R and λ have a small effect on the field measured at the station. In other words, the station should be situated in a fair-weather region. In order to be sure that the variations in the field over the station are caused by variations in V, it is necessary to compare the readings of several such stations. To increase the probability of several marine or polar stations being simultaneously situated in fair-weather regions, it is necessary to carry out simultaneous observations at a large number of stations, daily and continuously. It should, however, be borne in mind that such an analysis

is founded on the basic assumption of the spherical condenser theory that there exists some spherical equalization layer, and is valid only when this condition is fulfilled.

It should also be noted that surface measurements, permitting isolation of variations in V and R on the basis of certain assumptions, do not make it possible to find out their absolute values. Reliable data on the potential V of upper layers, and on the resistance R, can be obtained only by direct measurements.

The spherical condenser theory has undergone, in the course of time, some partial variations. Thus, for example, Israel and Kasemir /84/ showed that a comparatively rapid equalization of the potential in high layers of the atmosphere may take place below the ionosphere, at an altitude of the order of 60 km, at which, due to high conductivity, charges are distributed uniformly over the whole surface in less than 300 sec. Their work led to, in particular, the important conclusion that the altitude of the equalizing layer depends on the charging rate. The data on the variation of the conductivity with altitude, etc., were somewhat more accurately determined in a number of investigations.

However, all these additions and corrections did not significantly change the theory described. Despite the fact that the theory of the spherical condenser explains a number of phenomena observed in nature, it remains hypothetical, since no data directly confirming its basic assumptions are available.

In the first place, it should be noted that until now the potential difference between the earth and the ionosphere has not been measured and it has not been confirmed that this difference, the same at a given time for the whole ionosphere, undergoes variations which cause the appearance of a unitary variation in the electric field intensity in the atmosphere.

A second very important factor, which would determine the correctness of the theory and which has not found sufficient experimental confirmation, are numerical data on the balance of currents which charge and discharge the earth and the ionosphere. This balance of currents, as follows from the above, will be different for regions with different physico-geographical conditions. At present, it has been measured at only one or two points of the globe.

It is perfectly obvious that for a given section of the earth's surface the balance of currents must not be equal to zero; it must equal zero only for the earth's surface as a whole. Thus, for the Kew Observatory (Cambridge, England) this balance appears as follows /116/:

TABLE 1

Charge carried in by charging currents	Q_c C/km^2 year
Lightning discharge	−20
Point-discharge currents	−100
Charge carried away by discharge currents	Q_d C/km^2 year
Conduction current	+ 60
Precipitation currents	+ 20
Total	−40 C/km^2 year

As can be seen, the charge Q_d consists of a number of components. The role played in the balance by the point discharge currents is notable.

On the other hand, these are the least amenable to investigation, since it is difficult to compare currents from an artificial point discharge with currents flowing in natural conditions from trees and bushes, hills and mountains, houses and masts, etc., under strong electric fields. The sign of individual current components may vary from point to point on the earth's surface. Investigations of V. V. Zykova /10/, carried out in the South Sakhalin geophysical observatory showed, for example, that in Sakhalin, point-discharge currents can, in contrast to England, transport to the atmosphere a negative electric charge and that other regions can also exist in which the point-discharge current component has the same sign. Thus, this most important component of the currents, which creates the charge exchange between the earth and the atmosphere, cannot at present be correctly calculated either quantitatively or with respect to sign.

To date there are no data on the balance of currents in regions with the highest thunderstorm activity. The relationship between the unitary variation and the diurnal variation of the thunderstorm activity for the whole globe also requires quantitative determination. The earlier practice of estimating thunderstorm activity from the number of days per year with thunderstorms does not constitute a sufficiently correct criterion. It is known that thunderstorms in South Africa, for example, give a considerably larger number of thunderstorm discharges, and these discharges carry larger charges than those in Europe /116/. The mean areas occupied by individual thunderclouds and the lifetime of the latter also differ at different latitudes.

The current carried by lightning considerably depends on the topography of the terrain. Thus, the amplitudes of lightning currents in the Caucasus Mountains are approximately half those on the plain /58/, although the number of discharges per each thunderstorm in the Caucasus is larger.

It should also be taken into account that the interrelation between the thunderstorm activities of individual regions of the earth may also vary; this should lead to a phase shift in the unitary variation. Thus, according to Brooks' data /68/, five world thunderstorm centers were observed: Central Africa — 150 days with thunderstorms per year; central Brazil — 106 days; the region of the Isthmus of Panama — 135 days; southern Mexico — 142 days; and Java — 220 days. According to data of the World Meteorological Organization /70/ obtained later, the most powerful center is situated in Central and West Africa (at five stations more than 200 days with thunderstorms are observed). The thunderstorm activity of this center thus seems to have increased recently, and the thunderstorm center in the Malay Archipelago to have weakened and somewhat shifted. It looks as if the center of the Malayan region moved to the southern part of the Malacca Peninsula. In 1952, 80 days with thunderstorms were observed in Java. The character and distribution of thunderstorm centers of the Western Hemisphere was somewhat different: the center in the southern Mexico and Isthmus of Panama regions weakened and shifted, while the activity of the Brazil thunderstorm center intensified. These data, given by V. I. Arabadzhi /3/, point to the need for careful study of thunderstorm activity in connection with the unitary variation of the electric field.

These conclusions of course require serious improvement and verification. The available data on the variation of the number of days with thunderstorms per year may be due both to variations in the observation

technique, in the number of stations, etc., and to ordinary random variations in thunderstorm activity from year to year.

These improvements, along with an estimate of the relation between thunderstorm activity, determined from the number of days with thunderstorms per year, and the currents transported by lightning, and point discharges for various regions of the globe, together with measurements of the unitary variation, constituted an object of investigations during the IGY.

An analysis of the diurnal variation of the area occupied by thunderstorms, carried out by Krumm /89/, also showed that a shift of the maximum area occupied by thunderstorms toward noon hours by Greenwich time is observed.

In order to estimate the role of thunderstorms as generators charging the earth and the ionosphere, Gish and Wait /79/, and Stergis, Rein, and Kangas /107/ measured the conduction current above thunderclouds. It was assumed that this current is equal to the current charging the earth under the clouds.

From aircraft measurements above 21 thunderclouds in the central part of the U.S.A., Gish and Wait determined that the mean current flowing upward from one thundercloud was 0.5 amp. Since according to Brooks' data /68/, 1800 thunderstorms take place simultaneously on the earth, the total charging current is approximately 900-1000 amp. Assuming that the number of 1800 given by Brooks for the number of thunderstorms which exist simultaneously on the earth is underestimated, and assuming in addition that individual thunderclouds may consist of several thunderstorm centers, Gish and Wait considered that their measurements confirmed the assumption of equality of thunderstorm currents to the total fair-weather air—earth current.

Somewhat later, Stergis et al. measured the currents above thunderstorms in Florida. From data of 25 balloon soundings, the measured current from one thundercloud amounted on the average to 1.3 amp. These data seem exaggerated. Firstly, as indicated by Holzer /82/, part of the flow lines had to terminate again at the earth. This would reduce the current by approximately 15 %. Secondly, as shown by investigations of the fields above showers and thunderclouds /11/, 20-30 % of the clouds have a negative polarization, and therefore the total current above regions occupied by shower and thunderclouds may be half that calculated by Stergis et al. Thus, serious corrections in the balance calculations of currents in thunderstorm and fair-weather regions are necessary.

It should be noted also that not all the observed effects are satisfactorily explained by the spherical condenser theory. Recently, mainly by measurements in the free atmosphere, investigators obtained new data which do not fit into the framework of this theory. Let us consider some results which contradict the spherical condenser theory.

The diurnal variation of the area occupied by thunderstorms varies from season to season and from period to period. Let us compare the data of Brooks (Figure 1, curve 1) with those of Krumm (Figure 1, curve 2), which refer to different periods. At the same time, the diurnal unitary variation of the field remains approximately constant by phase and amplitude both when averaged over several years, and when measured for individual months /31/ and even, as will be shown below /15/, for individual days.

This result suggests that there exists some factor, more stable than the area occupied by thunderstorms, which determines the diurnal unitary variation of the field.

It should also be noted that if thunderstorm activity is the basic source charging the earth as a whole, a close similarity between the annual unitary variation of the field (determined by N. A. Paramonov /45/) and the annual variation of the area occupied by thunderstorms should exist. This similarity should be displayed even more clearly than in the case of the diurnal variation, since when comparing the annual variations, there is no need to make assumptions regarding the character of the diurnal variation of the thunderstorm activity.

A comparison of the curves of the annual unitary variation of the field /45/ and of the mean number of thunderstorms /89/ leads, however, to an unexpected result; these curves are opposite in phase (Figure 4).

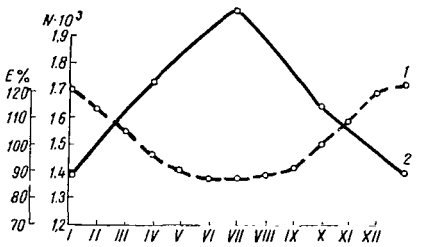

FIGURE 4. Annual unitary variation of the field E (curve 1) /45/ and of the mean number of thunderstorms N (curve 2) /89/.

Thus, either the estimate of the role of thunderstorm activity in the formation of unitary variations cannot be reduced to the magnitude of area occupied by thunderstorms, or apart from thunderstorms, there also exist in the atmosphere other sources charging the earth and the atmosphere, which affect at least relatively slow variations of the field intensity.

Ignoring a number of other facts, which do not fit into the framework of the spherical condenser theory, and which have been established in the study of the electricity of the free atmosphere (we return to these later), we consider another theory which explains the existence of the electric field of the atmosphere.

In 1949, Ya. I. Frenkel' /62/ generalized a number of his works on the theory of atmospheric electricity phenomena. In particular, he proposed a theory of the origin of the electric field of the earth differing from that described above. Frenkel' assumed that most types of clouds are electrically polarized (form electric dipoles). The field intensity inside these dipoles was assumed equal to about 10,000 v/m. Polarized clouds should induce charges on the earth's surface, and the amount of charges induced by all the clouds is what produces the observed field of the earth. The difference in atmospheric conductivities under clouds and in fair-weather zones is due to the appearance of some excess charge on the earth's surface, the field of which is superimposed on the field of the induced charges and ensures the existence of the fair-weather field in large cloudless regions (for example, in the Sahara Desert).

In accordance with this theory, it was assumed that the ionosphere (or high, conducting layers of the atmosphere) does not play an important role in processes connected with atmospheric electricity, and the electric field of the atmosphere was explained as being entirely due to the interaction of electric phenomena in the troposphere and their interaction with the earth.

According to this theory, the unitary variation of the field intensity may be due to variations in the conditions of charging of the earth as a whole. Potential variations of upper layers may in this case proceed asynchronously and, in general, are not directly related to the field intensity variations at the earth's surface. The field in regions of "disturbed" weather is opposite in direction to the field in regions of fair weather. Variations in the charging conditions of the earth as a whole are determined according to the theory developed by Frenkel', using a relationship which follows from the equality of the currents in regions of fair and of disturbed weather:

$$\lambda_1 E_1 S_1 = \lambda_2 E_2 S_2,$$

where λ_1, E_1, and S_1 are respectively the electric conductivity, the field intensity, and the area of the fair-weather region, and λ_2, E_2, and S_2 are the same quantities for the disturbed-weather region. Since, in accordance with the theory, the total positive charge induced by clouds is equal to the negative charge, then $E_1 S_1 = E_2 S_2$.

If λ_1 and λ_2 were equal, the total charge of the earth's surface would thus be equal to zero. However, under clouds whose field can cause point discharges of surface objects, particularly under thunderclouds and shower clouds, it can be expected in accordance with the theory that $\lambda_2 > \lambda_1$, from which it follows $E_1 S_1 > E_2 S_2$, i.e., in this case the earth's surface as a whole should have a negative charge, uniformly distributed in regions of fair and disturbed weather. The positive charge remaining in the atmosphere in zones of "disturbed" weather, is transported, according to Frenkel', by air currents to the fair-weather region.

Frenkel' also considered in close detail a number of elementary processes connected with charging of cloud particles and charge separation. However, the almost complete absence of data on space charges in clouds and on the rate of their separation, along with the absence of data on the charges of individual particles, did not make it possible to check the theory as a whole by comparing it with the actually observed conditions.

The first attempts made in the Main Geophysical Observatory to verify the quantitative assumptions of this theory by measuring electric fields in the free atmosphere, particularly in clouds, showed /27/ that the electric field in most clouds, including cumulus clouds, is lower by one to two orders than the values calculated theoretically.

Thus, Frenkel' could not explain the appearance of the electric field of the earth. However, the same measurements showed that the spherical condenser theory also cannot explain a number of observed phenomena. Seventy soundings of the electric field variation with altitude gave a different picture from that based on the spherical condenser theory.

The measurements showed that the electric field in a number of cases decreases with altitude considerably faster than had been assumed (Figure 5 /27/). The field at an altitude of several kilometers sometimes drops to zero and even changes sign (see Figure 6a /27/). In other words, the electric field due to charges of the earth is compensated by a volume

charge of the atmosphere, concentrated in a few lower kilometers. The variation of the electric field under clouds differs from that in fair-weather days (Figure 5 /27/), but the observed field variation is not directly due to fields created by clouds, but to increased space charges originating and spreading out from clouds.

It has been observed that the whole region of field rise is concentrated in the zone under the cloud base. The field distribution indicated the appearance of a negative space charge near the earth.

The potentials at altitudes of 2-4 km may already be close to those expected in the ionosphere. The variation of these potentials is much larger than that necessary for the appearance of a unitary variation according to the spherical condenser theory (Figure 6b /27/). In some cases, the potential is observed to decrease at certain altitudes (Figure 6a /27/).

Sagalyn and Fausher /100, 101/ studied the conductivity distribution with altitude and confirmed the results of the field measurements. It was found that the conductivity below the inversion layer usually varies little with altitude, and only increases above this layer, approximately following an exponential law. The decrease in conductivity is apparently due to an increase in the pollution content of the atmosphere, which leads to the attachment of light ions to heavy nuclei. As a result the field in the lower part of the troposphere is formed by space charges situated on particles, the displacement of which, due to the electric field, is small. It could be expected that in these conditions, beside conduction currents, a considerable role can be played by convective electric currents, which have in the past been neglected. The existence of such currents, reaching significant values in the free atmosphere, was shown for the first time by Kraakevik /87, 88/. These currents could attain considerable magnitudes only in the lower layers of the troposphere, often under inversions. The existence of convective currents flowing to the earth was observed for the first time by Izergin /22/.

It was found that these phenomena can be explained if, discarding the spherical condenser theory, we assume that the observed electric field of the atmosphere occurs due to an exchange of charges between the earth and the troposphere /27/, the charges being created largely due to the appearance of clouds. In contrast to the theory advanced by Frenkel', in this case clouds which contribute to the appearance of strong electric fields are not necessary.

Charges which reach the earth become common for the whole of it, and form a field observed in cloudless regions as well as field variations common for the whole globe. Charges which remain in the atmosphere are carried by air currents and together with the charges on the earth create local fields and variations of the field of the atmosphere. Thus, according to this scheme, some upper-layer potential common for the whole earth, which determines the behavior of the unitary field variation, cannot be expected.

It is important to note that the monograph /27/ demonstrates the possibility of the participation of the whole cloudiness in the charge exchange between the earth and the atmosphere, and not only of thunderclouds, as assumed in the spherical condenser theory.

Charge exchange between the troposphere and the ionosphere is, of course, also possible /85/. This is due to lightning strokes. In this case, the atmospheric electric field results from charge exchange developing according to the scheme troposphere—earth, troposphere—ionosphere, the two zones

little affecting eath other . In this case, the current directed to the upper layers of the atmosphere is small compared with the currents between the earth and the troposphere.

The disagreement between the observed phenomena and the basic spherical condenser scheme recently led to the creation of a number of new hypotheses and assumptions about the basic factors which maintain the electric field of the atmosphere and cause its variation.

In the work of V. I. Gerasimenko /7/, for example, it is pointed out that the diurnal variation of the sea area illuminated by the sun is very similar to the diurnal unitary variation. Since Müleisen's data /97/ indicate the charging of water upon evaporation, it can be assumed that the diurnal variations of the evaporation area may cause the variation in the charging of the earth as a whole. This scheme, chiefly attractive in that it explains the stability of the diurnal unitary variation, gives rise to a number of objections. The principal one is that according to the data of a number of authors (given, for example, in /86/), water evaporation does not cause charging. The contradiction between Müleisen's experiments and most known experiments may be due partly to the fact that in Müleisen's experiments the evaporation area was much larger than the evaporation area in other experiments, partly to a difference in the chemical composition in the evaporating water, and partly perhaps to experimental error.

The first results of the study of the electric field in the free atmosphere may suggest that charging of the atmosphere could be effected by electrification of its aerosol content. This process does not concern the capture of air ions by heavier particles, but electrification due either to evaporation of aerosol particles or to attachment of these particles with subsequent separation.

In addition to Müleisen, V. D. Reshetov /51, 52/ recently worked in this direction. Reshetov assumed that aerosol particles acquire a charge which depends on the pH of the given aerosol. For $pH < 5$, negative charges should form on aerosol particles; for $pH > 5$, positive charges form on aerosol particles. Since for sea-water $pH \approx 9$, this may lead to positive charging of the atmosphere and negative charging of the earth. The diurnal variation of this charging, according to Gerasimenko's data /7/, may be proportional to the illuminated surface of the oceans.

Laboratory experiments carried out by V. I. Kraav /35/, disproved the basic assumption on which Reshetov's scheme is based. According to Kraav's data, upon spraying aqueous solutions of both low and considerable pH values, the drops are always negatively charged. Of course, the results of /35/ could be affected by the chemical composition of the solutions investigated and by their concentration, but it clearly follows from the work that the value of the pH of the solution does not determine the sign of the charge.

At the same time, it should be noted that the contribution of the evaporation from oceans and the role of aerosols in the electrification of the atmosphere can be clarified only by appropriate experiments in the free atmosphere.

The role played by various sources of electrification and accumulation of charges in the atmosphere can be determined and consequently, the correct scheme describing the electric processes in the atmosphere can be selected, only on the basis of a study of the electricity of the free atmosphere and, first of all, of a study of the distribution of the field and space charges /21/.

The distribution of the field with altitude, the time variations of the atmospheric potential at various altitudes, and their synchronism with the unitary variation make it possible to get an idea of the correctness of given hypotheses. Such data could be obtained by making prolonged systematic measurements in the free atmosphere. The investigation program of the International Geophysical Year therefore included soundings of the electric field of the atmosphere at various altitudes.

In the USSR, aircraft were used for this purpose, which also made it possible to carry out additional investigations of the microstructure of clouds, of the distribution of condensation nuclei in the atmosphere, etc. These investigations give additional data on the electrification conditions of the atmosphere.

Measuring the variation of the electric field E with the altitude h from an aircraft, it is possible to calculate the potential V_h of the layer at the altitude h by the formula

$$V_h = \int_0^h E\,dh.$$

Such measurements are hindered by two difficulties:

a) an aircraft cannot ascend to the boundary of the ionosphere and, consequently, cannot measure its potential;

b) measurements of the field at altitudes higher than 10 km are very difficult. At an altitude of 10 km, for example, the field E can be expected not to exceed 5-10 v/m (see Figure 3).

The rapid decrease of the electric field with altitude, although complicating measurements at considerable altitudes, makes it possible at the same time to determine the potential of the ionosphere from measurements only up to relatively low altitudes, since the potential of the atmosphere at an altitude of 10 km should not, in theory, differ by more than 20-25 % of the potential of the ionosphere (see Figure 3). As indicated, the main variations in the potential of the ionosphere are due to processes in the lower layers.

Aircraft measurements of the field variation with altitude thus make it possible to check the basic assumption of the spherical condenser theory, i.e., the existence of an equalizing layer situated at an altitude of 60-100 km, as well as to measure its potential variations.

This theory is obviously correct if the variations of the layer potential are related to the unitary variation, and the potential itself varies with altitude monotonously and identically at all the measurement points.

If we assume that the horizontal components of the atmospheric electric field can be neglected, then from data on the variation of the electric field with altitude, a very important electric characteristic of the atmosphere — the density ρ of space charges — can be calculated.

The Poisson equation in this case can be written in the form:

$$\frac{\partial E}{\partial z} = 4\pi\rho.$$

In other words, by differentiating the curve $E=f(h)$ is it possible to determine the value of ρ at various altitudes h.

Aircraft soundings of the electric field, carried out in different meteorological conditions, also make it possible to determine the electric charges of clouds and their role in the creation of electric charges in the atmosphere.

The distribution of the field and space charges with altitude, and also its diurnal variation, permit the regularity of variation of charges in the atmosphere to be determined and the correctness of other hypotheses concerning the origin of atmospheric electricity, for example the schemes of Müleisen and Reshetov, to be checked. If the field variations with altitude are determined only by the conductivity height distribution, this means that atmospheric aerosols are charged only as a result of ions from the atmosphere settling on them. Thus, aerosol electrification of the atmosphere plays a minor role. If, however, the field distribution in the atmosphere is not determined by the conductivity distribution in it, this indicates the important role of the electrification of aerosols in the generation of atmospheric electricity. These schemes are considered in more detail in the following sections of the book.

It should be noted that investigations of the electric field in the atmosphere help to solve a wider range of problems than does the general picture of the distribution of the electric field, its potentials and space charges in the atmosphere, and the determination of the origin of the atmospheric electric field.

Investigations of the electricity of stratus clouds, while answering questions specific to atmospheric electricity (how, where, when, in what amounts, and due to what do space charges accumulate, and what are the fields that result), help at the same time in answering a number of general questions concerning the physics of clouds and contribute to the solution of applied problems.

As was shown in /81/, the coalescence efficiency of drops with sizes of 600 and 100 μ considerably depends on the electric field intensity. In the absence of an external field, only about 30 % of the collisions between drops of these sizes lead to coalescence. In the presence of an external field of approximately 15 v/cm, the rate of coalescing drops reaches approximately 90 %. The coalescence of smaller drops can be expected to depend to a larger extent on the external electric field, since the relative velocities of such drops are lower and, consequently, the coalescence of small drops is more difficult than the coalescence of large drops.

Processes of cloud and precipitation development, therefore, considerably depend on the magnitude of the electric field in them. The growth of particles and fall of precipitation is usually associated with an increase in the electric field, and this field in turn contributes to the growth of particles. An investigation of this process helps to clarify important problems concerning the physics of clouds and atmospheric electricity. This kind of investigation should be based, on one hand, on a study of field magnitudes and particle spectra in clouds, and on the other hand, on laboratory measurements of the coalescence efficiency of drops of different sizes in the presence of electric fields. The first part of this problem is solved by field measurements in clouds.

Data on the electricity of clouds can serve as a very good criterion in determining their state. Vertical development of clouds, beginning of precipitation, and its intensification are associated with variations in the electric field of the cloud. In the limiting case, clouds themselves

demonstrate the intensity of processes in them by generating lightning. Measurement of the field in clouds is therefore highly useful for indicating their state; this is true both when studying natural processes in clouds /11/, and in particular, when studying processes in artificially modified clouds /30/. Such an indication of the state, however, has been used till now only for intense convective clouds. The possibility of applying it to stratus clouds is dependent on the study of their electrification. However, until recently, data on their electricity have been extremely scanty.

Data on the electricity of the free atmosphere, and in particular, on the electricity of clouds, are necessary for the development of warning systems to prevent the entry of an aircraft into thunderclouds /6, 28/.

Recently, there have been increasing attempts to work out methods for the introduction of considerable artificially created space charges into the atmosphere /112, 93/. The development of this technique has two principal aims: to investigate air motions in the atmosphere by labeling definite air portions with space charges, and to investigate the variations in the state of clouds under the effect of introduced space charges. Solution of both problems requires knowledge of the "background" — the characteristic values of the fields and space charges in the atmosphere and in clouds.

Without dwelling on a number of other problems requiring a study of cloud electricity, e.g., /117, 42, 20/, to some of which we return in the following, we pass to a discussion of the investigation results.

Chapter II

ORGANIZATION OF MEASUREMENTS AND DATA PROCESSING METHOD

§1. BRIEF DESCRIPTION OF A DEVICE FOR MEASURING THE ELECTRIC FIELD IN THE FREE ATMOSPHERE

Three aircraft of the type LI-2 were instrumented for measurements of electric fields in the free atmosphere. The instruments used were electrostatic fluxmeters.

Figure 5 gives the circuit diagram of an aircraft electrostatic fluxmeter /24/, developed by I. M. Imyanitov and V. V. Mikhailov and used in the above-described investigations.

The device consists of two identical sensing units located in the upper and lower parts of the fuselage at the intersection of neutral lines of the aircraft, so that they were influenced only by the vertical component E_z of the atmospheric field, and by the field E_Q due to the aircraft's charge; the horizontal components E_x and E_y were not measured. The measuring plates of the sensors are situated at the same level as the airplane surface. The output voltage from the sensors is fed to the input of the amplifiers and from there to a synchronous detector using a 6 × 6 tube. The plate circuit of the detector includes a milliammeter, and terminals for connecting an automatic recorder are fitted.

The instrument has four sensitivity ranges: ±5, ±25, ±250, ±2500 v/cm. The largest signal produces a current of 1 ma at the output. The instrument's scale is linear, and tests showed that instrumental error is less than 5 %. The lag of the instrument is less than 1/50 sec, and it is fed from the aircraft's power supply system. The operation of the instrument is described in detail in the monograph /24/.

The instrument has subsequently been somewhat modified. To simplify the processing of the measurement results, the direct voltages from the outputs of the two channels, being proportional to the field intensities E^A and E^B at the locations of the pickups, are applied to an additional stage consisting of two double-triode bridges. The unbalance current of one bridge is proportional to the field intensity in the atmosphere, since the vacuum tube bridge solves the equation

$$E = aE^A - bE^B.$$

The second tube bridge makes it possible to determine the aircraft charge Q_a, by solving the equation

$$Q_a = -(cE^A + dE^B).$$

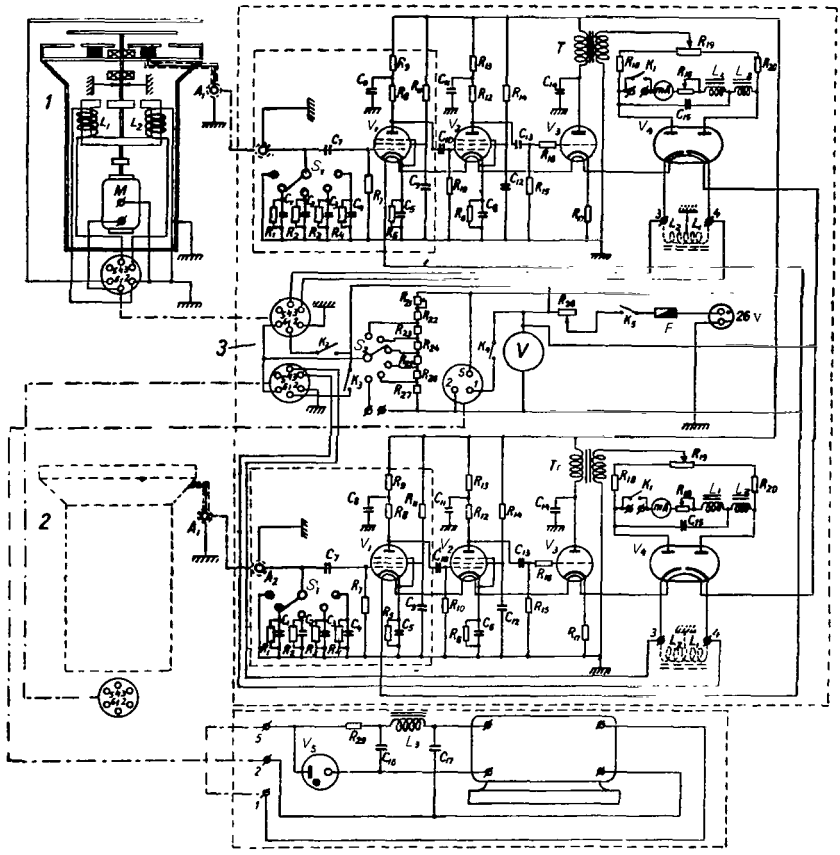

FIGURE 5. Circuit diagram of an aircraft electrostatic fluxmeter.

1 and 2—sensors; 3—block containing amplifiers, synchronous detectors, and power supply unit.

The circuit digram of the auxiliary unit is given in Figure 6.

A chart record of the instrument operating with the auxiliary unit is shown in Figure 7.

The instrument circuit also includes a calibration device and a circuit for checking the sensitivity in the first and second measurement ranges.

The sensitivity checking circuit makes it possible, by simply depressing a toggle switch, to check the stability of the instrument's sensitivity and to determine, in the case of sensitivity loss, the reason for it (deterioration of the input insulation or change of the amplification).

The range selector-switch has a fifth position, in which the input of the instrument is short-circuited. In this position, the voltage on the output, which corresponds to no-signal on the input, was determined.

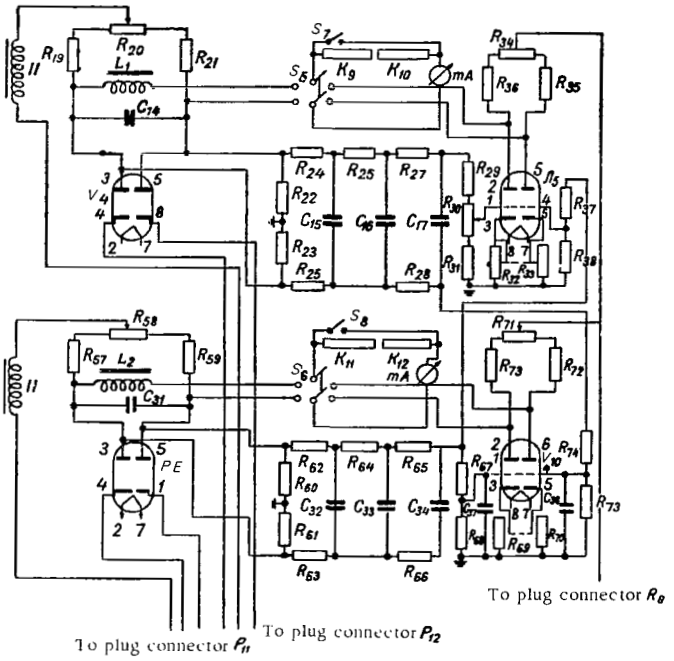

FIGURE 6. Circuit diagram of an auxiliary unit for direct measurement of the field intensity and the aircraft charge.

The calibration device includes special covers which are put on the sensors; by applying a known voltage to electrodes mounted in these covers, it is possible to calibrate the instrument accurately.

During operation of the equipment on each flight, the stability of the instrument's readings in the absence of an external field and the steadiness of its sensitivity were checked, and the necessary correction of the readings made.

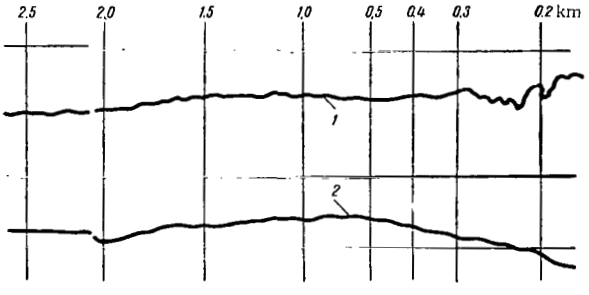

FIGURE 7. An oscillographic recording of the instrument operating with the auxiliary unit.

1— recording of the aircraft charge; 2—recording of the vertical component of the atmospheric field. The vertical lines give the altitude (in km).

Full calibration of the instruments and necessary adjustments were periodically carried out.

§ 2. DETERMINATION OF THE DISTORTION FACTORS

The use of two sensors made it necessary to take into account, in addition to distortions introduced in the electric field of the atmosphere by the aircraft as a conducting body, also the influence on the results of the measurements of the proper charge of the aircraft, acquired by the latter in collisions with cloud and precipitation particles, and also due to the exhaust gases.

Owing to the distortions in the position of the equipotential surfaces of the atmospheric field introduced by the aircraft's fuselage, the instrument will measure, not the true atmospheric field E, but the field E_E proportional to the true one /29/:

$$E_E^A = k_E^A E; \quad -E_E^B = k_E^B E.$$

We denote by the index A quantities referring to the upper sensor, and by B, quantities referring to the lower sensor.

In addition, the instruments may be influenced by the field E_Q of the proper charge of the aircraft:

$$E_Q^A = -k_Q^A Q; \quad E_Q^B = -k_Q^B Q,$$

where k_E^A, k_E^B, k_Q^A, k_Q^B are proportionality factors. Then, the following field intensity arises in the general case at the upper sensor:

$$E^A = k_E^A E - k_Q^A Q,$$

and at the lower sensor:

$$E^B = -k_E^B E - k_Q^B Q.$$

Solving this system of equations, it is possible to determine the true intensity E* of the atmospheric field and the aircraft charge Q:

$$E = \frac{k_Q^B E^A - k_Q^A E^B}{k_Q^B k_E^A + k_Q^A k_E^B}, \quad Q = \frac{-k_E^B E^A - k_E^A E^B}{k_Q^A k_E^B + k_E^A k_Q^B}.$$

Using the notation

$$a = \frac{k_Q^B}{k_Q^B k_E^A + k_Q^A k_E^B}, \quad b = \frac{k_Q^A}{k_Q^B k_E^A + k_Q^A k_E^B},$$

$$c = \frac{k_E^B}{k_Q^B k_E^A + k_Q^A k_E^B}, \quad d = \frac{k_E^A}{k_Q^B k_E^A + k_Q^A k_E^B},$$

* Here and in the following, we deal only with the vertical component E of the atmospheric field.

we obtain

$$E = aE^A - bE^B; \quad Q = -(cE^A + dE^B). \tag{2}$$

Thus, for calculating the true atmospheric field and proper aircraft charge, the coefficients b, c, and d, which in turn can be calculated knowing the factors k_E^A, k_E^B, k_Q^A, k_Q^B, have to be known.

These factors were determined experimentally, using an aircraft model. To determine k_E^A and k_E^B, the model was placed in an artificial electric field between condenser plates with an area of $3 \times 3\,m^2$ and an air gap of 2 m. A voltage of 2 kv from high-voltage rectifiers was applied to the plates. The aircraft model was suspended on a silk thread parallel to the plates in the center of the condenser (Figure 8a). The electric field in the condenser was considered uniform and given, and the field intensity on the surface of the aircraft model at the sites of the sensors was determined from the magnitude of the induced charge.

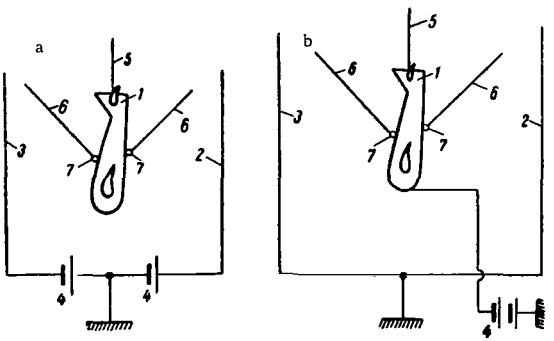

FIGURE 8. Schematic diagram of the model set up for the determination of the distortion coefficients for the external field (a) and the proper charge (b).

1— aircraft model; 2 and 3— condenser plates; 4—voltage source; 5—insulator thread for suspending the model; 6—silk thread for suspending the test ball; 7—test ball P.

The magnitude of the induced charge was determined by means of a small insulated metal test ball, which was brought into contact with the corresponding point of the model surface. The charge carried by the ball was proportional to the density of the surface charge of the model at the point of contact. Measuring the ball's charge by means of an electrometer, it is possible to determine the field intensity at the model surface. The factors k_E^A and k_E^B show by how many times the field intensity at the aircraft model differs from the field intensity in the condenser.

To determine the factors k_Q^A and k_Q^B, a charge was applied to the aircraft model (Figure 8b) and the electric field intensity E_Q created by this charge was determined at the sites of the sensors; k_Q^A and k_Q^E are the factors of proportionality between the charge applied to the aircraft model and the field intensity at its surface at the sites of the sensors.

Results of the measurements carried out on the aircraft model are given in Table 2.

TABLE 2.

Object	a	b	$c\frac{\text{e.s.u.}}{\text{v/cm}}$	$d\frac{\text{e.s.u.}}{\text{v/cm}}$	Number of measurements
Model	0.38 ± 0.02	0.42 ± 0.03	$(0.053 \pm 0.02) \times 10^{-5}$	$(0.053 \pm 0.02) \times 10^{-5}$	140
Aircraft	0.38	0.42	1.32×10^{3}	1.32×10^{3}	

TABLE 3

Date, hour	Altitude, m	E^A v/cm	E^B v/cm	E^A/E^B
29 May 1959, 6 hours . . .	1600	5.60	5.25	1.07
	3000	6.30	5.90	1.07
	3300	15.40	15.70	0.98
29 May 1959, 18 hours . .	1300	2.94	2.73	1.08
	1400	3.50	3.36	1.04
	1500	3.36	3.29	1.02
	2000	3.78	3.64	1.04
17 June 1959, 6 hours	2500	2.31	2.17	1.07
	2900	2.59	2.45	1.06
	3000	2.87	2.66	1.08
	3100	2.87	2.73	1.05
	3200	2.80	2.66	1.05
18 July 1959, 18 hours . . .	2400	1.68	1.54	1.09
11 June 1959, 6 hours . . .	200	4.90	4.58	1.08
	400	4.20	3.85	1.09
	500	4.20	3.85	1.09
	600	4.55	4.20	1.08
	700	4.90	4.55	1.08
	800	4.55	4.20	1.08
	900	4.20	3.85	1.09
	1000	3.85	3.50	1.10
	3800	1.96	1.82	1.08
	4100	1.54	1.47	1.05
	4200	1.47	1.32	1.11
	4300	1.19	1.12	1.07
	4000	1.12	0.98	1.14
29 June 1959, 15 hours . .	5300	665	630	1.06
	5400	595	490	1.21
2 July 1959, 18 hours . . .	3300	13.3	12.6	1.06
17 December 1959, 18 hours	1700	13.6	12.9	1.05
			Mean	1.08

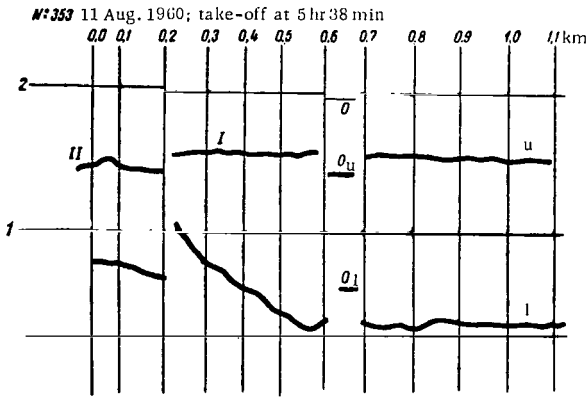

FIGURE 9. An oscillographic recording obtained during operation of the instrument without the auxiliary unit.

1—base line; 2—line for marking the sensitivity and special phenomena; vertical lines — altitude marks (in km); I and II—sensitivity ranges; O—short-circuited input; u, l—recordings from the upper and lower sensors.

Since the factors k_Q^m (for the model) and k_Q^a (for the aircraft) are connected by the relation $k_Q^a = \frac{k_Q^m}{n^2}$, where n is the similarity coefficient between the model and the aircraft (in our case $n = 50$), the coefficients c and d were recalculated for the aircraft /29/.

The factors finally obtained for calculating according to formulas (2), the intensity of the atmospheric electric field and the aircraft charge, are given in Table 2.

Imperfect modeling of the aircraft and measuring errors may lead to errors in the determination of the distortion factors. To check the correctness of the determined factors, it was decided to compare the model measurements with the aircraft measurements. For this purpose, cases were chosen where, during the aircraft's flight, the atmospheric field was equal or close to zero, and the aircraft charge was fairly considerable.

In this case, if $E=0$, then $\frac{E^A}{E^B} = \frac{k_Q^A}{k_Q^B}$. From the model measurements, it was obtained that $\frac{k_Q^A}{k_Q^B} = 1.08$.

Results of measurements of the field intensity by the upper E^A and lower E^B sensors in flights around Leningrad are given in Table 3.

Thus, the distortion factors measured on aircraft models with a high degree of accuracy are close to the true factors.

The data in Table 3 also make it possible to determine the influence of space charges, arising in the atmosphere upon the electrification of aircraft, on the measurement results. Despite the opinion expressed in /113/, it follows that during flights in clouds, where the field intensities

due to charging may be tens and sometimes hundreds of times higher than the field intensities measured in the atmosphere, additional space charges have practically no effect on the measurement results. The opinion of the authors of /113/ is obviously the result of the fact that, despite accepted recommendations /24/, they used collectors which were incorrectly positioned.

§ 3. PROCESSING OF SOUNDING DATA

The readings of the aircraft instrument used for measuring the field intensity were recorded on photographic paper by a K4-51 automatic optical recorder. The chart speed was 0.5 mm/sec. After the flight, the photographic paper chart was developed and the altitudes, sensitivities, and meteorological conditions were marked on it in accordance with the entries in the aircraft's log book (Table 4).

TABLE 4

Log book of aircraft sounding of the electric field of the atmosphere

Point _____

Date _____ Observer _____

Flight time: take-off _____ hours _____ min

landing _____ hours _____ min

Cloudiness (type, coverage): take-off _____

landing

Control calibration parameters: before the flight _____

in flight

Sensitivity at take-off _____

Ascent			Descent			Remarks
marks	altitude	observed phenomenon (clouds, rain, smoke, optical phenomena)	marks	altitude	observed phenomenon	

With the change of sensitivity, corresponding deviations appear in the third recorder loop recorded on the chart. Deviations of different magnitudes serving to mark specific phenomena and synchronize the records

in the log book with the recording on the chart, can be created in the same loop. An example of the instrument record without the auxiliary stage is shown in Figure 9.

The recorder chart ready for processing includes:

1) a straight base line, which separates the chart into two equal parts;

2) two recording lines of the galvanometer readings, which are proportional to the field intensities acting on the upper and lower sensors respectively;

3) a line on which are marked the altitudes, spatial points, and the sensitivity range (in places of a sensitivity change the line is discontinuous, being displaced vertically).

In the processing of the paper charts, the mean ordinates for each 100 m of altitude were measured and referred to the middle of the layer.* Applying the method of equal areas and using a graticule, the ordinates were read with an accuracy of 0.5 mm (which corresponds to a field intensity of 0.04 v/cm), according to which E^A and E^B, representing the fields measured by the upper and lower sensors, were calculated. Next, the intensity of the atmospheric electric field and the aircraft charge were calculated by formulas (2).

To simplify data processing, the instrument's calibration figures were used to prepare tables for the field intensity (Table 5) and for the aircraft charge (Table 6) in advance.

TABLE 5

Ordinate, mm	$0.38\,E^A$	$0.42\,E^B$
0.5		
1.0		
1.5		
. . .		
. . .		

TABLE 6

Ordinate, mm	$1.18\,E^A$	$1.32\,E^B$
0.5		
1.0		
1.5		
. . .		
. . .		

In the preparation of the tables, the ordinates were taken at 0.5 mm intervals, since accuracy in reading the ordinates did not exceed 0.5 mm.

The procedure in the processing of the charts is shown in Table 7.

TABLE 7

Altitude, m	Sensitivity	Ordinate α_1, mm	$\alpha_1-\alpha_0$ mm	α_2 mm	$\alpha_2-\alpha_0$ mm	$0.38E^A$ v/cm	$0.42\,E^B$ v/cm	E v/cm	$1.18E^A$ v/cm	$1.32\,E^B$ v/cm	Q e.s.u.

* The averaging along the vertical also includes some horizontal averaging. During sounding the aircraft usually climbed spirally, with a mean horizontal velocity of approximately 50-60 m/sec and a vertical ascent velocity of 4-5 m/sec. Therefore, in averaging the field over 100 meters vertically, it was simultaneously averaged over a horizontal path of about 1000 m; the scale of horizontal averaging increased with altitude, since the ascent velocity kept decreasing.

In Table 7, α_1 and α_2 are the ordinates taken from the readings of the upper and lower sensors; α_0 is the zero ordinate.

When using the tables, the calibration stability was carefully followed.

A recording when the instrument worked with the auxiliary units is given in Figure 7. Curve 1 represents the recording of the aircraft charge, and curve 2, the direct recording of the intensity of the electric field of the atmosphere. As before, the mean ordinates for 100-meter layers were taken, and from the calibration data, E and Q were determined.

If the instrument's sensitivity is maintained constant, it is possible to prepare Table 8, which is based on the calibration of the instrument.

TABLE 8

Ordinate, mm	E v/cm	$Q \times 10^{-3}$, e.s.u.

The chart-processing procedure when using the auxiliary units is shown in Table 9.

TABLE 9

Altitude, m	Sensitivity	α_0	α_1	$\alpha_1-\alpha_0$	E	α_2	$\alpha_2-\alpha_0$	Q

The final processing stage was the filling in of "Tables of Data on the Measurement of the Field Intensity in the Free Atmosphere", in which field intensity data at various altitudes, obtained after processing, were entered.

The data on the variation of the field intensity with altitude were used to calculate the potential of the atmosphere at an altitude of 6000 m.

$$V_{6000} = \int_0^{H=6000} E(H)\,dH. \qquad (3)$$

The variation of the space-charge density with altitude can be calculated by the formula

$$\rho = \frac{1}{4\pi}\frac{dE}{dH} \simeq \frac{1}{4\pi}\frac{\Delta E}{\Delta H}, \qquad (4)$$

or

$$\rho = 2.66\frac{\Delta E}{\Delta H},$$

where E is expressed in v/cm, H in meters, and ρ in e.s.u./m^3.

The space charge of an air column extending between 0 and 6000 m with a basis of 1 m^2 is calculated by integrating the curve $\rho = f(H)$.

$$Q_{0-6000} = \int_{0}^{H=6000} \rho(H)\, dH,$$

or

$$Q_{0-6000} = 2.66\,(E_{100} - E_{6000}), \qquad (5)$$

where E_{6000} is the mean intensity of the electric field at an altitude of 6000 m and E_{100} is the mean intensity of the electric field in the first 100-meter layer.

The measurement results were entered in a table, which included, in addition to the indicated data, information on the meteorological situation.

During soundings, the measurements started from an altitude of 30 m, since below this level, the distortion factors are considerably affected by the proximity of the earth. In the following the 30 m level will be denoted as zero level.

Chapter III

FAIR-WEATHER ELECTRICITY

The present chapter deals with the structure of the electric field on cloudless days, as well as on days with slight cloudiness, not exceeding 20-30 % (if the field variation with altitude is monotonous). Such days are called fair-weather days.

§ 1. VARIATION OF ELECTRIC-FIELD INTENSITY AND SPACE CHARGES WITH ALTITUDE

Studies of the electric-field variation with altitude* on fair-weather days showed that the observed electric-field profiles can be classified into four basic groups:

Group I — positive field intensity monotonously decreasing with altitude;

Group II — positive field intensity monotonously decreasing with altitude and changing sign at a definite altitude;

Group III — field intensity not varying monotonously with altitude, but having a maximum, usually at an altitude of 300-700 m, and often changing sign at an altitude of 3000-4000 m;

Group IV — "sluggish" electric-field profile varying little with altitude.

Only 3 % of the profiles observed in clear weather did not fall under this classification.

Group I. This group includes profiles having an exponential decrease of the electric-field intensity with altitude. Of the 425 profiles observed in clear weather (of which 415 belong to different groups of the proposed classification), 141 such profiles were observed, constituting approximately 34 % of the total number of profiles investigated on fair-weather days. Up to altitudes of 2000-3500 m, these profiles are well expressed by the equation:

$$E = E_0 e^{-aH}, \qquad (6)$$

where $a = 1\,\text{km}^{-1}$, if the altitude H is expressed in kilometers; E_0 is the electric field at the surface. The value of E_0 is determined by extrapolating the field profile up to the earth's surface, since aircraft measurements begin from 30 m, in order to eliminate the distorting effect the proximity of the earth has on the readings of the lower sensor.

* In the following, the variation of the electric field with altitude is called the electric field profile.

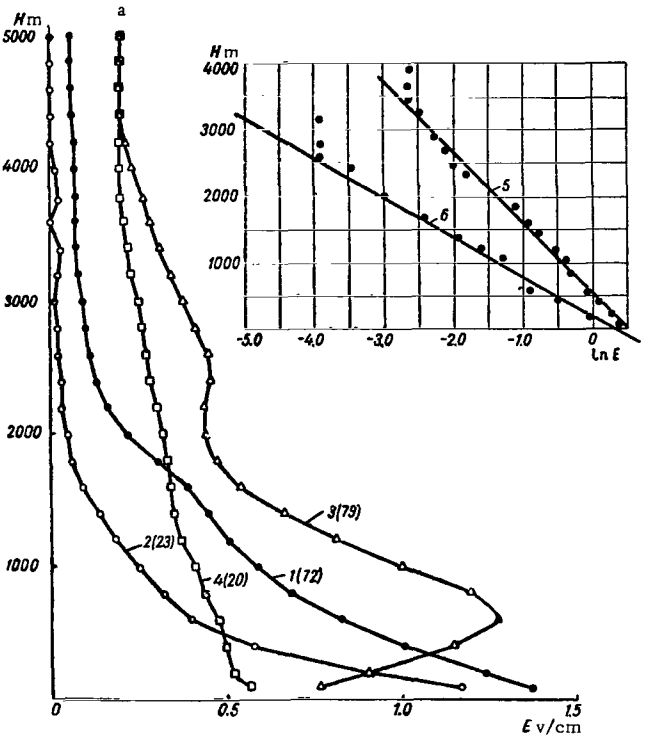

FIGURE 10a. Variation of the electric field E with altitude H on clear days, for Leningrad.

1—profile of Group I; 2—of Group II; 3—of Group III; 4—of Group IV; 5 and 6—curves 1 and 2 drawn in a semilogarithmic scale (see formula (6), a = 1 up to an altitude of 3000 m). Here and in other figures the numbers in parentheses denote the number of soundings.

Figure 10 gives profiles of Group I, observed at all three sounding points. In the upper right corner of each graph is the variation of the field with altitude in semilogarithmic scale. It gives an idea of how accurately formula (6) describes the true variation of the field (curve 5). The table corresponding to the graph is given in Appendices I-III. The exponential term with $a = 1\,km^{-1}$ describes the field variation only in the lower layer of the atmosphere: for Leningrad up to approximately 3000 m, for Kiev and Tashkent up to an altitude of approximately 1500 m. At these altitudes, the graph plotted in a semilogarithmic scale has a break point; the points also lie on a straight line, but with a different slope. Consequently, above the indicated altitudes also, the field variation with altitude is exponential, but with a different exponent. The total field variation with altitude can thus be described by a sum of two exponentials; the power of the second exponential is close to $0.4\text{-}0.5\,km^{-1}$. It is interesting to compare these results with those of Clark /74/.

In his measurements in polar regions and over the oceans (Greenland), as well as 3000 m above Chesapeake Bay, Clark also obtained exponential profiles of the electric field, but the exponent was approximately

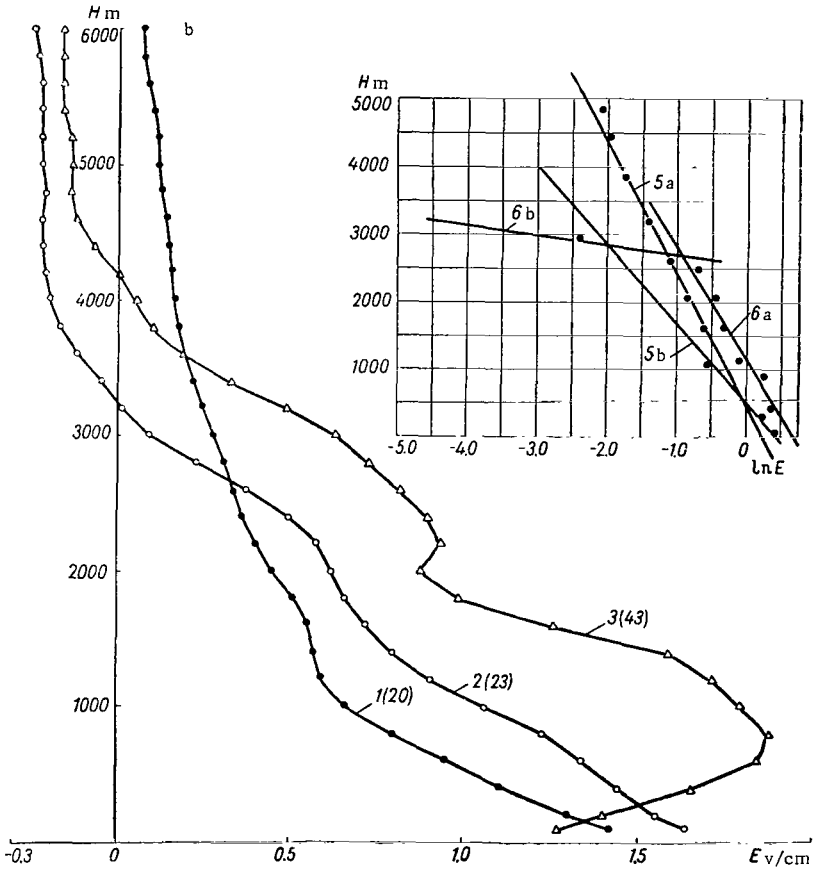

FIGURE 10b. Variation of the electric field E with altitude H on clear days, for Kiev.

1—profile of Group I; 2—of Group II; 3—of Group III; 5 and 6—curves 1 and 2 plotted in a semilogarithmic scale (see formula (6), for curve 5, $a = 1$ up to an altitude of 1500 m. $a = 0.4$ at altitudes from 1500 to 5000 m; for curve 6, $a = 0.6$ up to an altitude of 3000 m).

0.25 km^{-1}. The electric field profiles considered in this work, belonging to Group I, also decrease exponentially, but the exponent is 1 km^{-1}, and above 2-3 km approximately 0.4-0.5 km^{-1}, i.e., the rate of the field decrease with increasing altitude is considerably higher in this case than that given by Clark. This may be due to the fact that the conductivities at the surface over the continents are lower and, consequently, the field intensity over the continents decreases more sharply with increasing altitude than over the oceans. The difference in the exponents determines to what extent the distributions of space charges over land and over the ocean differ.

The variation of space charges with altitude H in the case under consideration is obviously similar to the variation of the field. It can be calculated by Poisson's formula. Substituting equation (6) in equation (4),

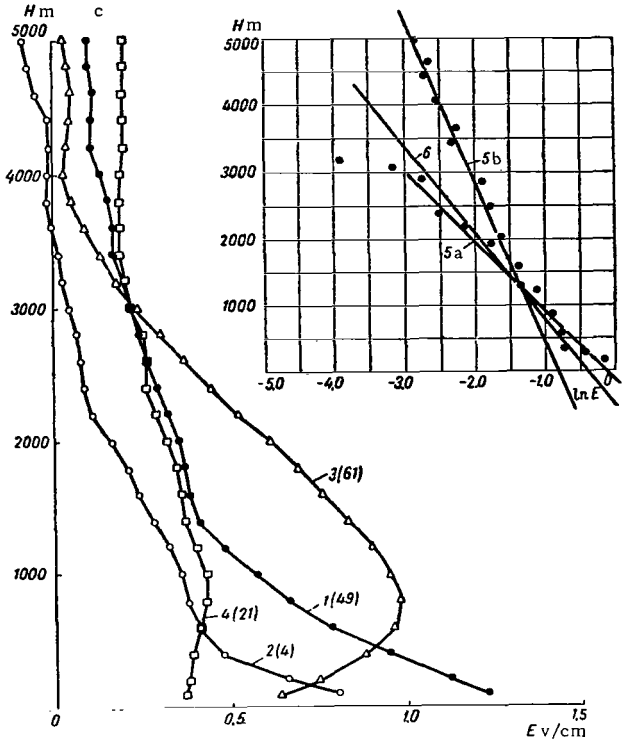

FIGURE 10c. Variation of the electric field E with altitude H on clear days, for Tashkent.

1—profile of Group I; 2—of Group II; 3—of Group III; 4—of Group IV; 5 and 6—curves 1 and 2 plotted in a semilogarithmic scale (see formula (6), for curve 5, $\alpha = 1$ up to an altitude of 1500 m, $\alpha = 0.5$ for altitudes from 1500 to 5000 m; for curve 6, $\alpha = 0.6$ up to an altitude of 3000 m).

we obtain an equation for the variation of ρ with altitude for profiles of Group I

$$\rho = \frac{aE_0 e^{-aH}}{4\pi}. \qquad (7)$$

The variation of the space charge density with altitude for the corresponding electric-field profiles of Group I is given in Figure 11. This variation was obtained by differentiating the experimental curve $E = f(H)$ (Appendices IV and V).

Group II. In 50 cases (~12 %), the electric field decreased with altitude according to an exponential law up to altitudes of 2500-3000 m, above this becoming either zero or negative. These profiles belong to Group II.

The field variation in this group is described by the formulas:

for Leningrad

$$E = E_0 e^{-H}, \qquad (8)$$

for Kiev

$$E = E_0 e^{-0.6H},$$

for Tashkent

$$E = E_0 e^{-0.6H}, \quad (8)$$

where H is expressed in km.

Figure 10 gives field profiles of Group II, observed at all the three sounding points. In the upper right corners of each graph, the field variation with altitude is given in a semilogarithmic scale (curve b).

Usually, the altitude of the curve break is approximately 2.5-3 km. The table corresponding to the graph is given in the Appendices I-III. The space charge density variation with altitude corresponding to the field profiles of Group II is shown in Figure 11.

Group III. This group of electric field profiles encountered in fair weather includes those profiles where the monotonous variation of the field intensity with altitude is upset. The profiles usually have a maximum at an altitude of 500-700 m, and at an altitude of 3500-4000 m the field often changes sign.

Out of 425 profiles, 183 (~43 %) were of this type.

It should be noted that a similar field variation is also observed on cloudy days. On clear days, profiles of Group III are connected with the appearance of smoke and dust and with the presence of a temperature inversion, the inversion boundary usually passing somewhat higher than the maximum field intensity.

Figure 10 gives electric field profiles of Group III for all three points, and Figure 11 gives their corresponding variation of the space charge density. The data corresponding to the graphs of Figure 10 are given in Appendices I-III, and the data corresponding to Figure 11, in Appendices IV-V.

As can be seen from the graph, profiles of Group III are the result of a separation of the positive and negative charges in the atmosphere. In cases where this separation did not lead to the appearance of an excess positive charge in the atmosphere, the field of which would exceed the field intensity created by the negative charge of the earth, the atmospheric field at no point changes sign. If the excess positive charge of an atmospheric layer from the surface to an altitude H is larger than the charge of the earth, the field intensity at this altitude changes sign.

Group IV. This group includes profiles for which the field varies little with altitude (Figure 10). The number of such profiles is relatively small, 41 out of 425 (~10 %). Profiles of this group are usually connected with comparatively low values of the electric field at ground level. These profiles correspond to the case where the space charge of the atmosphere is small. Profiles of this type are apparently connected with a more or less constant conductivity variation with altitude.

Thus, on clear days, we may expect to encounter profiles of Groups I and III more frequently; they are obviously the basic types. Profiles of Groups II and IV were observed in only 22 % of the cases.

Despite the fact that the above classification of field profiles is to some extent arbitrary, it corresponds to definite processes in the atmosphere, i.e., to different charge distributions in the atmosphere.

Profiles of Group I are observed in cases where, in the investigated region, the field intensity from the negative charge of the earth is only

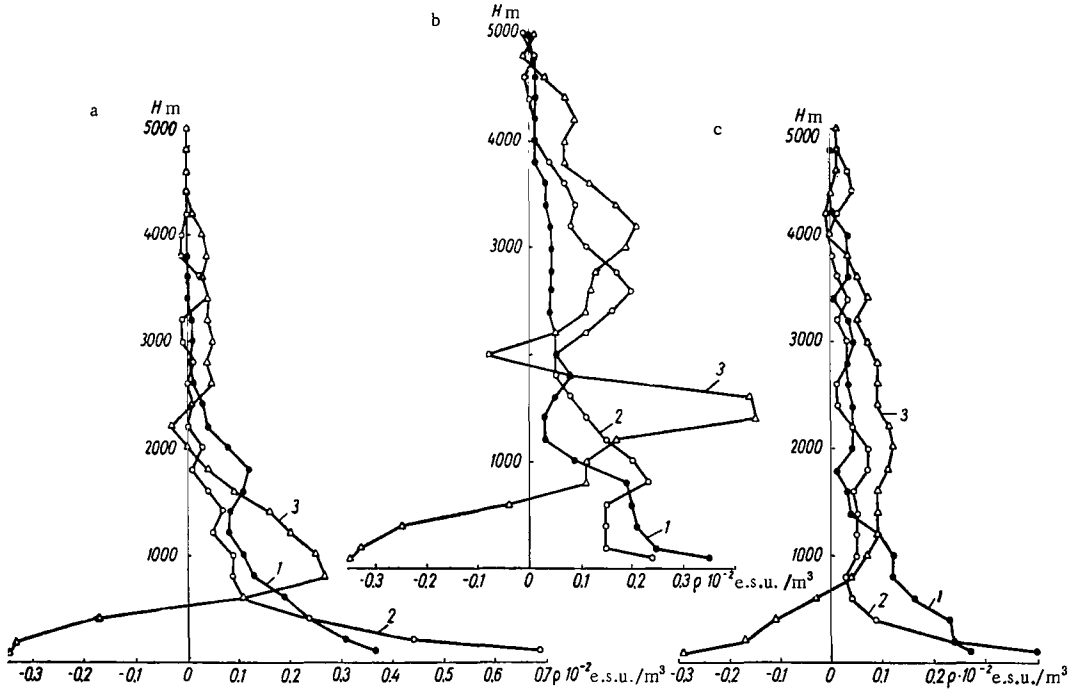

FIGURE 11. Variation of the space-charge density ρ with altitude H on clear days.

a—Leningrad; b—Kiev; c—Tashkent; 1—profile of Group I; 2—of Group II; 3—of Group III.

partially compensated up to the measurement altitude by the field due to the atmospheric charge.

If the field intensity due to the positive charge of the atmosphere is higher than that due to the negative charge of the earth, then field profiles of Group II are observed.

Profiles of Group III are connected with the separation of positive and negative charges in the atmosphere. In cases where this separation did not result in an excess positive charge in the atmosphere, the field of which exceeded that of the negative charge of the earth, the atmospheric field at no point changed sign. Profiles of Group II obviously represent transitions from profiles of Group I to profiles of Group III. For these profiles, the negative charge of the earth is compensated by the atmospheric charge at some relatively low altitude, 2500-4000 m. If the positive charge of an air column with a unit cross section exceeds the negative charge of the earth's surface, then above this level the field intensity changes sign. In the opposite case, it remains equal to zero.

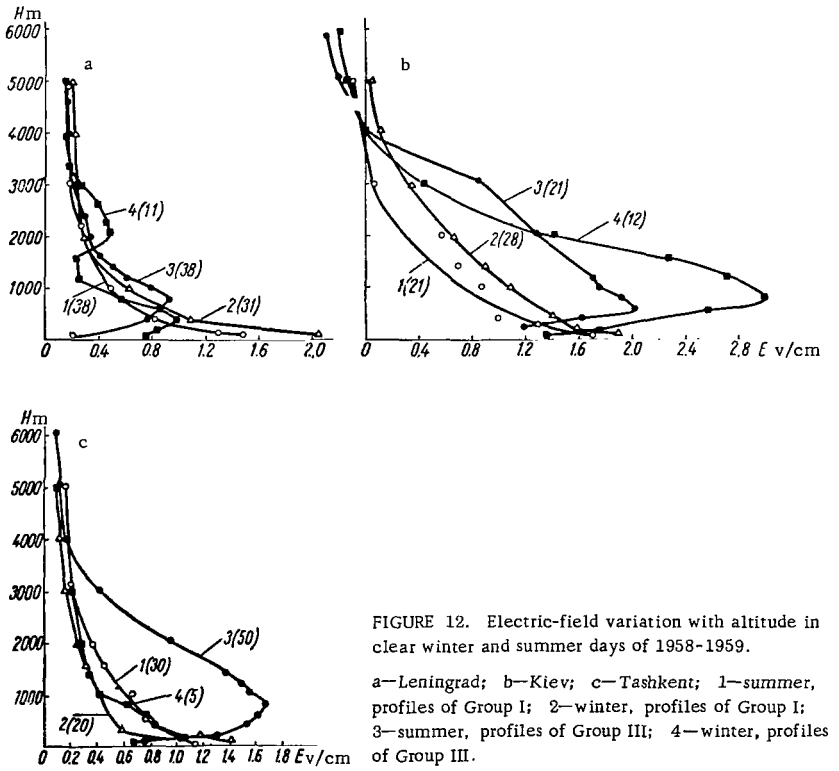

FIGURE 12. Electric-field variation with altitude in clear winter and summer days of 1958-1959.

a—Leningrad; b—Kiev; c—Tashkent; 1—summer, profiles of Group I; 2—winter, profiles of Group I; 3—summer, profiles of Group III; 4—winter, profiles of Group III.

It is interesting to follow the summer-to-winter variation in the electric-field profiles for clear days. Figure 12 shows profiles of Groups I, II, and III for the summer (May-September), and for the winter (November-March). It was found that profiles of Group III are most often characteristic

of summer; in winter months they are rarely observed, and mainly on days after disappearance of cloudiness. A particularly large difference between winter and summer profiles is observed in Tashkent. There, profiles of both Groups I and II, and profiles of Group III show lower field intensities in winter than in summer. The summer maximum is higher than the winter maximum. The same can be said of Group-III profiles for Leningard, although there is not such a sharp difference between winter and summer profiles. For Kiev, the converse was observed, and the difference between winter and summer profiles is considerable.

The differences in the positions of the summer and winter maxima are obviously due to differences in the turbulence regimes of the atmosphere in the summer and in the winter. Since the atmosphere is more turbulent in summer than in winter, the field maximum is situated higher in summer than in winter. The converse relationship between the summer and winter maxima obtained for Kiev is difficult to explain; it may be due to the small number of ascents used for the averaging. For the profiles of Groups I and II, the electric field intensities at ground level are higher in winter than in summer. The center of gravity of the space charges lies closer to the earth in winter than it does in summer.

§ 2. DIURNAL TRANSFORMATION OF THE ELECTRIC-FIELD AND SPACE-CHARGE PROFILES

It is interesting to follow the diurnal variation in the electric-field profiles, from which it is also possible to get an idea of the variation in the atmospheric charge distribution.

Figure 13 shows the diurnal variations of the profiles of Group I. The shaded areas indicate the variations in the space charge-density from the surface to 1000 m, from 1000 m to 2000 m, from 2000 m to 3000 m, and higher up.

Figure 13 gives the mean profiles of all Group-I profiles encountered at given hours of the day. The number of cases for each observation period was small, and it is therefore impossible to eliminate the influence of individual fluctuations, although the standard deviations (given in Appendices VI-XI) for these profiles are small, which indicates a small difference between the field profiles taken for the averaging. Local time is given in all cases.

It would seem that the field variation with altitude should be smoothest during daytime hours, i.e., when the developing convective motions in the atmosphere spread the atmospheric charge over large layers; the charge near ground level should then be smaller than in the calm night hours and increase with height. The measurement data, however, showed a different picture. At 14 hr local time, the maximum charge is observed in the first thousand meters from the surface, decreasing toward morning and evening. It is obvious that the total charge of the atmosphere over the observation place varies diurnally (as can be seen from the figure, the area of all the shaded squares varies diurnally), and the largest charge of the whole atmospheric column is observed at 14-15 hr local time.* Probably, at

* It is impossible to determine the time of occurrence of the maximum or minimum accurately, since we only have data for the actual times of the soundings, and do not know what takes place in between.

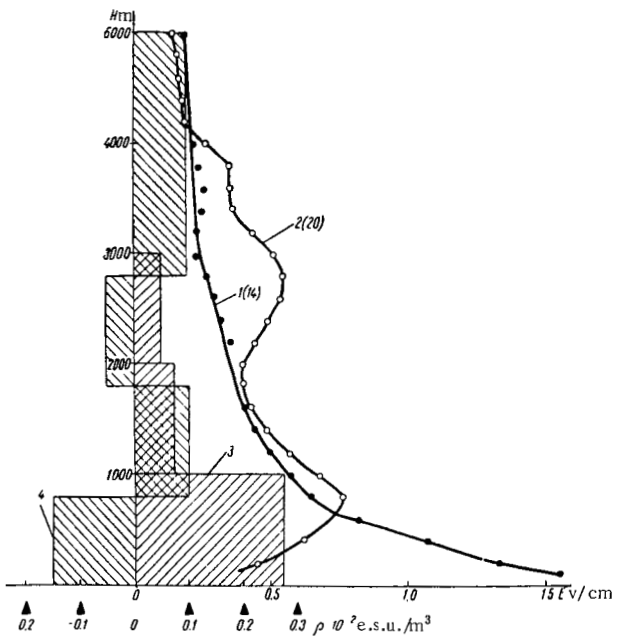
H m
6000
4000
3000
2000
1000
2(20)
1(14)
3
4
0
0.5
1.0
1.5 E v/cm
0.2
-0.1
0
0.1
0.2
0.3 ρ 10 ² e.s.u./m³

a

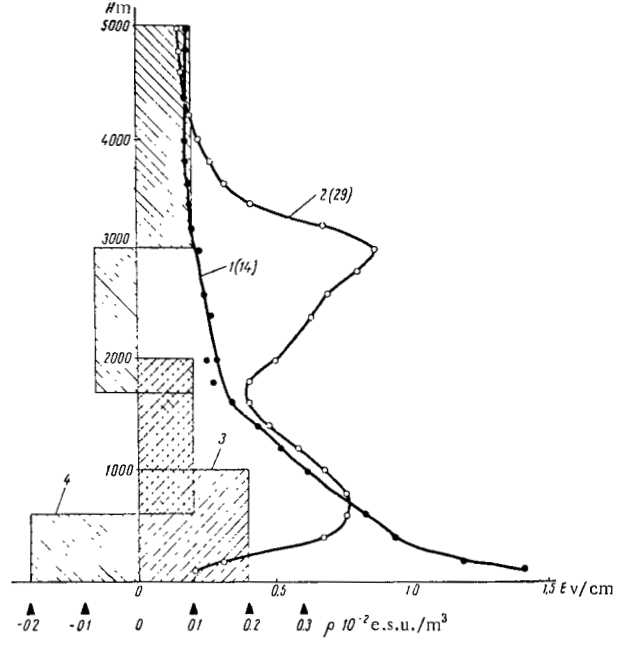
H m
5000
4000
3000
2000
1000
2(29)
1(14)
3
4
0
0.5
1.0
1.5 E v/cm
-0.2
-0.1
0
0.1
0.2
0.3 ρ 10 ⁻² e.s.u./m³

b

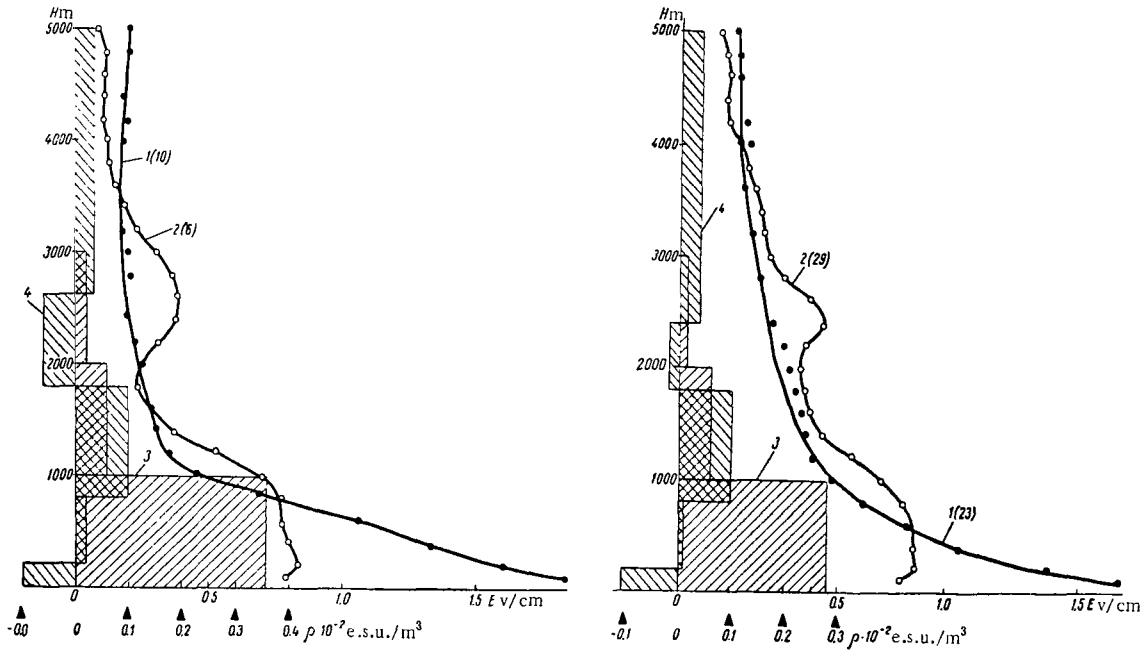

FIGURE 13a-d. Transformation of field profiles of Groups I(1) and III (2) and of space-charge profiles of Groups I (3) and III (4) in the course of the day (24 hr) during 1958-1959.

Leningrad: a—2 hr; b—5 hr; c—14 hr; d—17 hr.

this time, the amount of pollution in the atmosphere increases, and consequently, the conductivity decreases and the electric field increases. It is also possible that aerosol particles in the atmosphere may be electrified for some reason, e.g., by contact electrification or by electrification caused by separation of particles from the earth.

All the above refers to the electric-field profiles observed in Leningrad. In Kiev and Tashkent, a similar diurnal variation of the field profiles is observed, but the number of measurements made at these points is smaller. If the two measurements made at 12 hr in Tashkent are eliminated, then there too, the maximum field intensities, and consequently the maximum atmospheric charge, occur during afternoon hours.

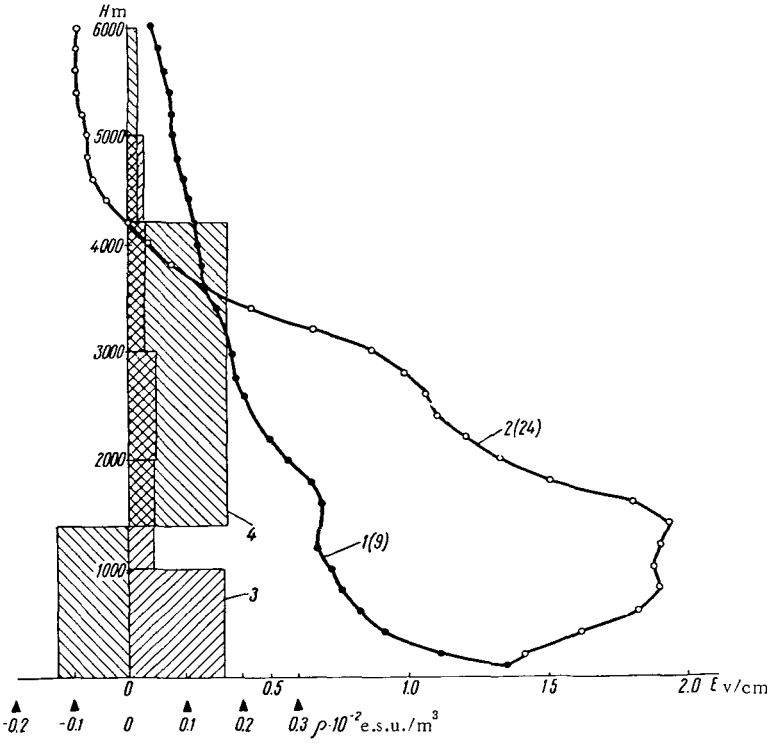

e

FIGURE 13e. Transformation of field profiles of Groups I(1) and III(2) and of space-charge profiles of Groups I(3) and III(4) from 3 hr to 15 hr, during 1958-1959.

Kiev: 3 hr.

Figure 13 also gives the mean electric field profiles of Group III for each flight period during 1958-1959. Figure 14 gives the diurnal transformation of profiles of Group III in June 1959 at Tashkent. It follows from this figure that the negative charge near the surface varies diurnally, the minimum negative charge occurring at 18 hr local time (Figure 15), which is obviously connected with a partial settling of the negative charge on the

earth, as well as with its transport upward by convective currents. Toward this time the total charge decreases. One can clearly see from Figure 14 the diurnal variation of the altitude at which the field of the atmospheric charge compensates the field of the earth (the altitude where the field profile passes through zero), and also the diurnal variation of the altitude of the maximum electric-field intensity. In the region of the maximum electric-field intensity, separation of the negative (below the maximum) and positive (above the maximum) space charges takes place. It follows from Figure 14 that the field intensity aloft may considerably exceed the field at ground level even on clear days.

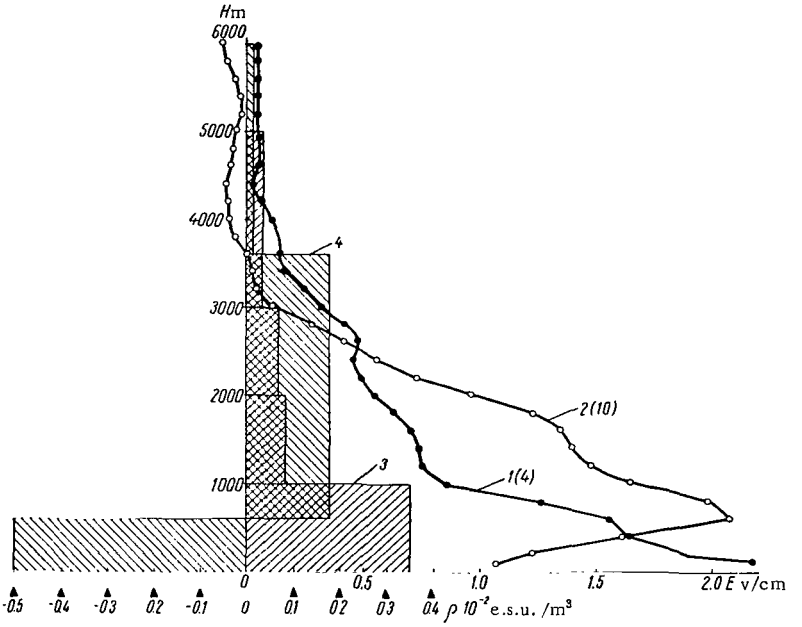

f

FIGURE 13f. Transformation of field profiles of Groups I(1) and III(2) and of space charge profiles of Groups I(3) and III(4) from 3 hr to 15 hr during 1958-1959.

Kiev: 15 hr.

The same can also be said of Figure 13, where the transformation of the profiles of Group III for all the cases observed in 1958-1959 is given. There, for both Leningrad and Tashkent, the maximum charge density is observed during daytime hours.

The curves for Leningrad are characterized by two maxima: a lower one at an altitude of 500-700 m, and an upper one at an altitude of 2500-3000 m.

Firstly, it was assumed that the second maximum is due to space charges left from dissipated clouds. Curves with two maxima were observed in 15 out of 79 cases, when profiles of Group III were observed.

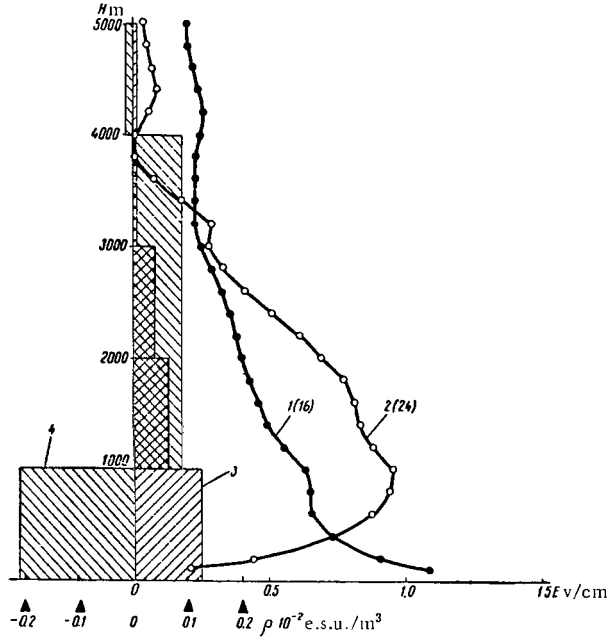
H m
5000
4000
3000
2000
1000
1(16)
2(24)
3
4
0
0.5
1.0
1.5 E v/cm
-0.2
-0.1
0
0.1
0.2
ρ 10⁻² e.s.u./m³

g

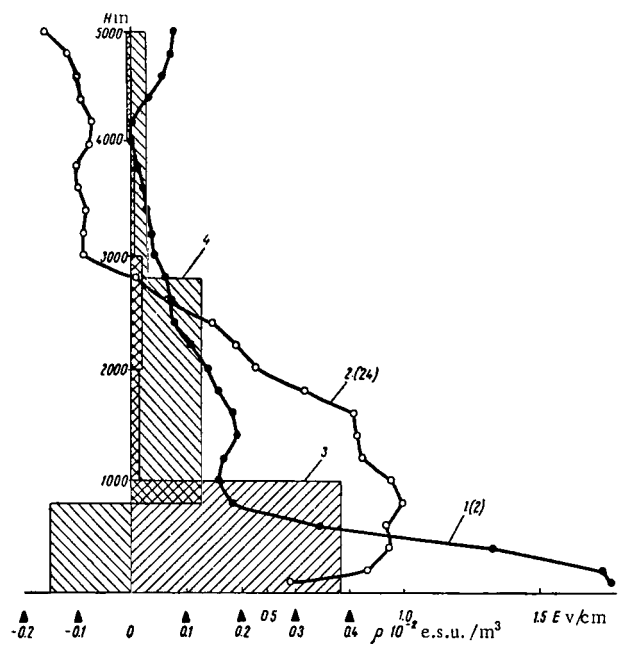
H m
5000
4000
3000
2000
1000
2(24)
4
3
1(2)
-0.2
-0.1
0
0.1
0.2
0.5
0.3
0.4
1.0
ρ 10⁻² e.s.u./m³
1.5 E v/cm

h

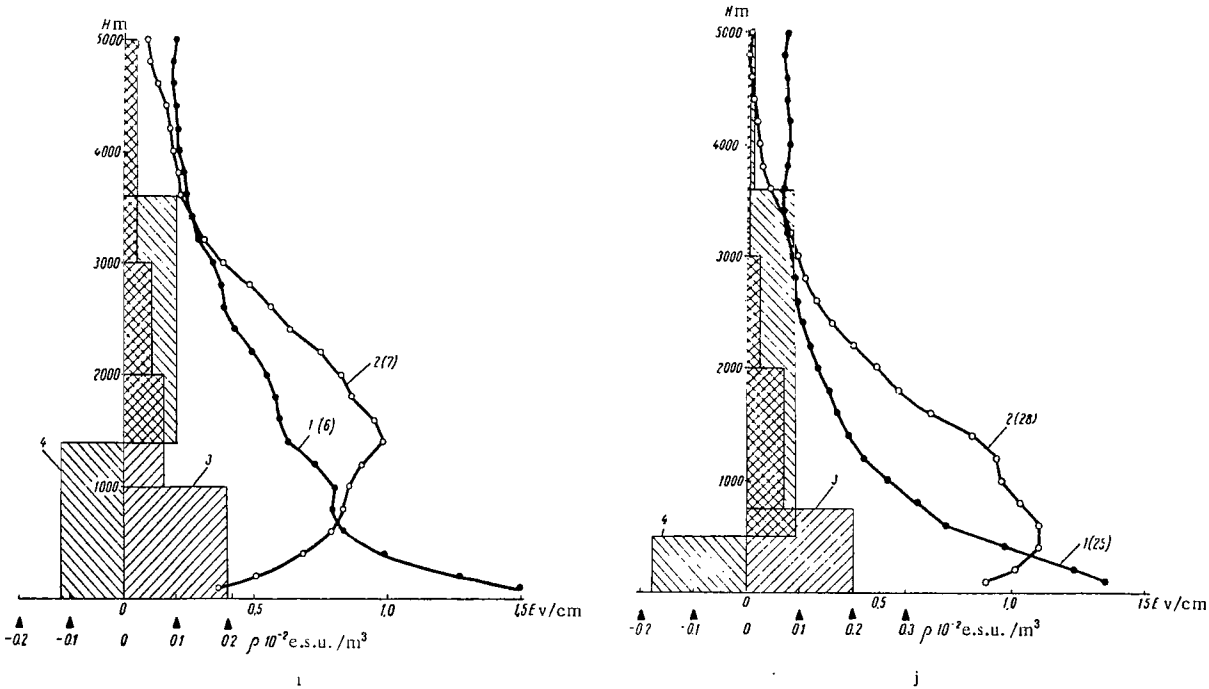

FIGURE 13g-j. Transformation of field profiles of Groups I(1) and III(2) and of space-charge density profiles of Groups I(3) and III(4) during the course of the day, during 1958-1959.

Tashkent: g—6 hr; h—12 hr; i—18 hr; j—24 hr.

Although all these profiles were observed on clear days, clouds were observed during the preceding flights. For example: the flight on 24 November 1959, at 6 hr — in the previous flight As were observed in a layer from 1800 to 5500 m; the flight on 26 November 1959, at 6 hr — in the previous flight As were observed from 1800 to 5500 m; the flight on 4 December 1959, at 6 hr — in the previous flight St were observed from 900 to 1200 m; the flight on 5 December 1959, at 3 hr — in the previous flight Sc with light snow were observed from 800 to 1000 m.

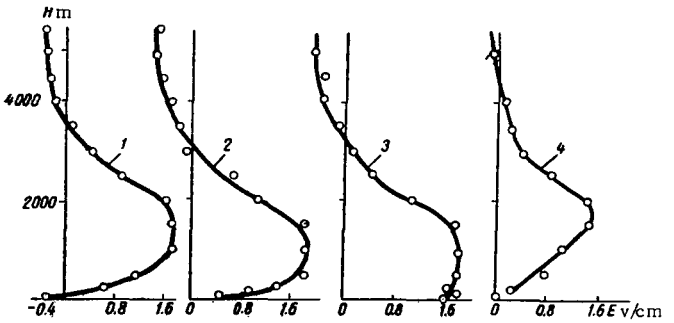

FIGURE 14. Transformation of the field profiles of Group IV during one day (24 hr) in June 1959, in Tashkent (GMT).

1—0 hr; 2—6 hr; 3—12 hr; 4—18 hr.

The field rise at altitudes from 2000 to 3000 m is very clearly outlined in these flights. But at the same time, the relationship between the field peaks and the cloudiness preceding the flight seems insufficiently conclusive, since the form and altitude of the peaks are very stable, and do not coincide with the form and altitude of the field peaks corresponding to the clouds in the previous flights.

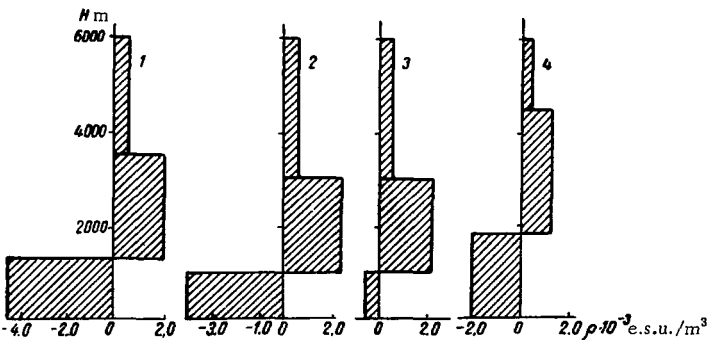

FIGURE 15. Transformation of the space charge profiles during one day (24 hr) in June 1958, in Tashkent (GMT).

1—0 hr; 2—6 hr; 3—12 hr; 4—18 hr.

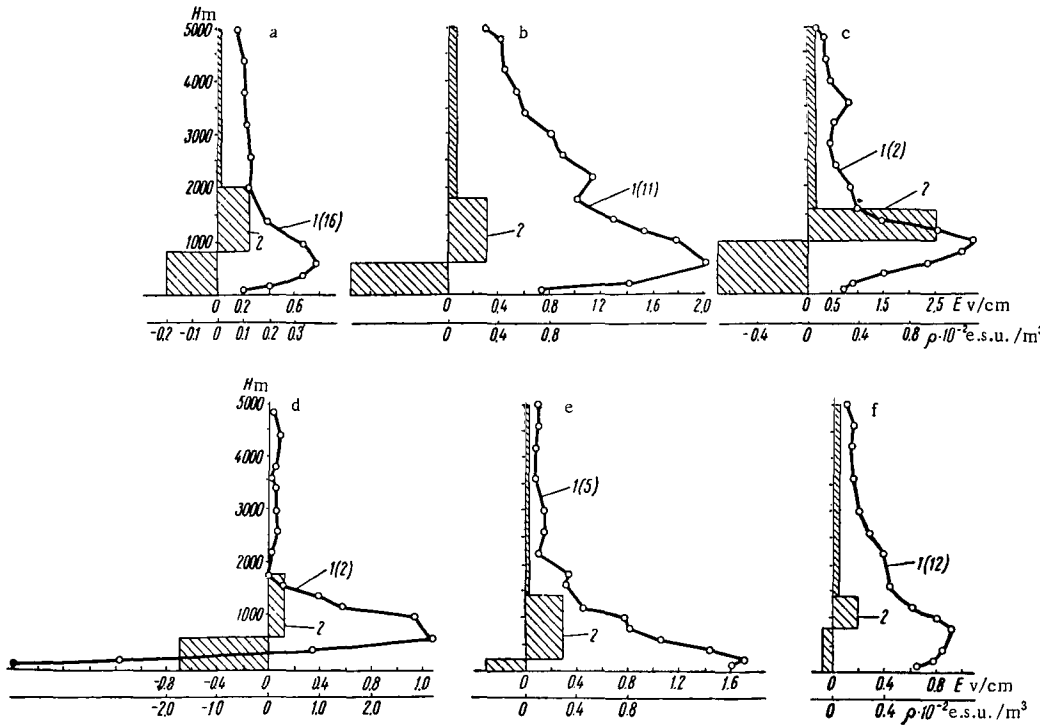

FIGURE 16. Transformation of field profiles of Group III(1) and of the space charge profile(2) in Leningrad.

a—3 hr; b—6 hr; c—7 hr; d—12 hr; e—15 hr; f—18 hr.

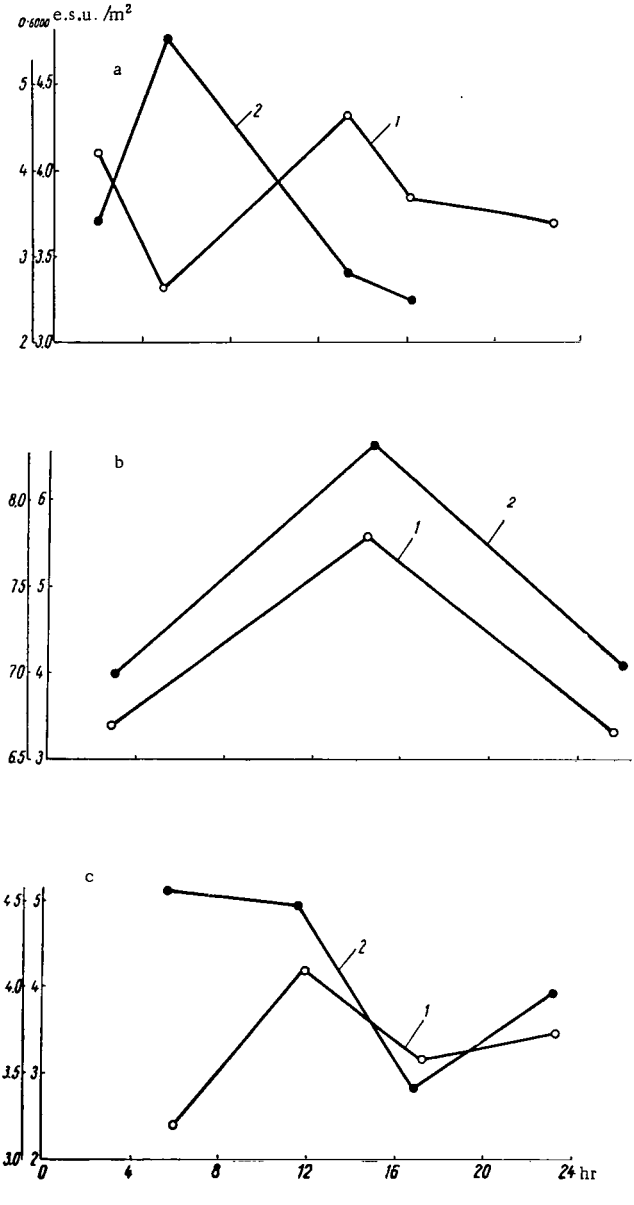

FIGURE 17. Diurnal variation of the charge of an air column with a cross section of 1 m^2 and height of 6000 m.

a—Leningrad; b—Kiev; c—Tashkent; 1—profile of Group I; 2—profile of Group II.

An analysis of the baric topography maps showed that the formation of such field peaks in perfectly clear weather is due to northern winds, which at altitudes from 2000 to 3000 m carry industrial mist and dust from Leningrad (the flight took place in southerly and southwesterly directions from Leningrad). In the case of a wind change, the peak disappears. For example, on 27 November 1959 at 6 hr, with cloudiness 0/0, the wind from ground level to an altitude of approximately 1500 m was westerly, and at an altitude of 1500-2000 m, its direction changed to northeasterly; from approximately 2000 to 3000 m the above-mentioned field peak was observed. On 27 November 1959 at 18 hr, with cloudiness 6/6 Sc, the altitude of its lower limit varying from 600 to 700 , the wind was westerly, and at an altitude of 5000 m it turned to the north, becoming northwesterly; a small field peak connected with the cloud was observed, but the peak at 2000-3000 m was not. The next flight took place on 28 November 1959 at 6 hr, with cloudiness 10/10 Sc, the altitudes of the lower and upper boundaries being 300 and 1000 m respectively; from ground level to an altitude of 1800 m the wind was westerly, and only a peak connected with the passage of the aircraft through the cloud was observed in the field profile.

Thus, during northerly and northeasterly winds a peak is observed, and with a change in the wind direction it disappears.

Profiles of Group III, with the exception of 15 cases connected with the influence of the town, are given in Figure 16. Only a single surface maximum, connected with surface mist, dust and surface inversions, is observed in this case (Appendix XI).

Using formula (5), it is possible, on the basis of data on the variation of the field with altitude, to calculate the charge of a vertical column with a base of 1 m^2 in the layer 0-6000 m. Figure 17 gives the diurnal variation of the charge of an air column of unit cross section. As might be expected, the maximum charge is observed during afternoon hours, which makes it possible to relate the appearance of the maximum to the development of convection. An exception are the diurnal variations in the charge of a unit column in Leningrad and Tashkent, which were observed on days with profiles of Group III. A maximum during morning hours (6 hr), and a minimum during afternoon hours are clearly seen on the graph. The diurnal variation of the charge in these cases is strongly affected by the appearance at the surface of a negative charge, which has a considerable diurnal variation.

If advection is neglected, it is possible to calculate from the variation of the charge Q of the column in the time t, the current density produced by the variation of this charge

$$i = \frac{dQ}{dt} \approx \frac{\Delta Q}{\Delta t} = \frac{Q_1 - Q_2}{t_1 - t_2},$$

where Q_1 and Q_2 are the charges of the air column at the times t_1 and t_2. The current magnitude i is of the order of 10^{-13} to 10^{-14} amp/m^2, i.e., ~1-10 % of the conduction current.

§ 3. DIURNAL VARIATION OF THE ELECTRIC FIELD AT VARIOUS ALTITUDES

By comparing the data of soundings carried out at different times in the course of the day, it is possible to find out the diurnal variations of the field intensity at various altitudes.

The graphs of Figure 18 give the diurnal variation of the electric field with respect to Greenwich Mean Time at altitudes ranging from ground level up to 5000 m, the potential at an altitude of 6000 m, and the charge of an air column between 0 and 6000 m for Leningrad, Kiev, and Tashkent (Appendices XII-XIV).

The field variation at ground level (Figure 18a) is based on the results of observations in Voeikovo, and has two principal maxima: one sharply pronounced, is observed at 5 hr GMT (7 hr true solar time), the second, less strongly pronounced, is observed at 13-17 hr GMT. During ascent, the first maximum disappears at 100 m, while the second is maintained, becoming sharper and somewhat shifted, now occurring at 18 hr GMT. The transformation of the curve of the diurnal electric field variation at various altitudes can be seen from the figure.

As can be seen, at altitudes from 100 to 500 m, the curves obtained very much resemble the diurnal unitary variation of the field intensity common to the whole globe, particularly marked over oceans (the observations of Mauchly /95/, Sverdrup /108/, Lobodin /31/).

The diurnal variation curves are similar to the unitary variation from 100 to 700 m (Figure 18); higher up, they begin to transform, and at an altitude of 3000 m, they are already totally different from the unitary variation curve. The correlation coefficient between the respective diurnal variation and the unitary variation is given to the right of the curves. As can be seen, this coefficient is fairly high, approximately 80-84 % up to an altitude of 2000 m, above which, it decreases, being only 12 % at an altitude of 3000 m (Appendix XV).

The diurnal variation of the charge of an air column has a minimum at 2-5 hr and a maximum at 14-20 hr true solar time. This variation may be considered not to be connected with the influence of surface space charges. Surface space charges give a double diurnal wave; the variation of the charge of a six-kilometer column has, however, only one maximum, its peak occurring at 20 hr true solar time, when convection decreases. The position of this maximum is determined by local time.

It follows from Figure 18b, that among the diurnal variation curves of the electric field at various altitudes, as observed in Kiev, there are also those which are similar to the unitary field variation, but here, the altitude interval of their manifestation considerably closes, and the altitude of their manifestation is higher. At altitudes of 600 and 800 m, the curves are similar to the unitary variation curve, and the correlation coefficients between the diurnal variation at the corresponding altitude and the unitary variation are 71 and 68 %, respectively. Higher, the curves obey laws different from those of the unitary variation.

The diurnal variation of the charge of the air column for Kiev is similar to that obtained in Leningrad, i.e., the minimum occurs at 5-9 hr, and the maximum at 21 hr true solar time.

Over Tashkent (Figure 18c), there is also a layer where the unitary variation appears, but it lies considerably higher than over Leningrad

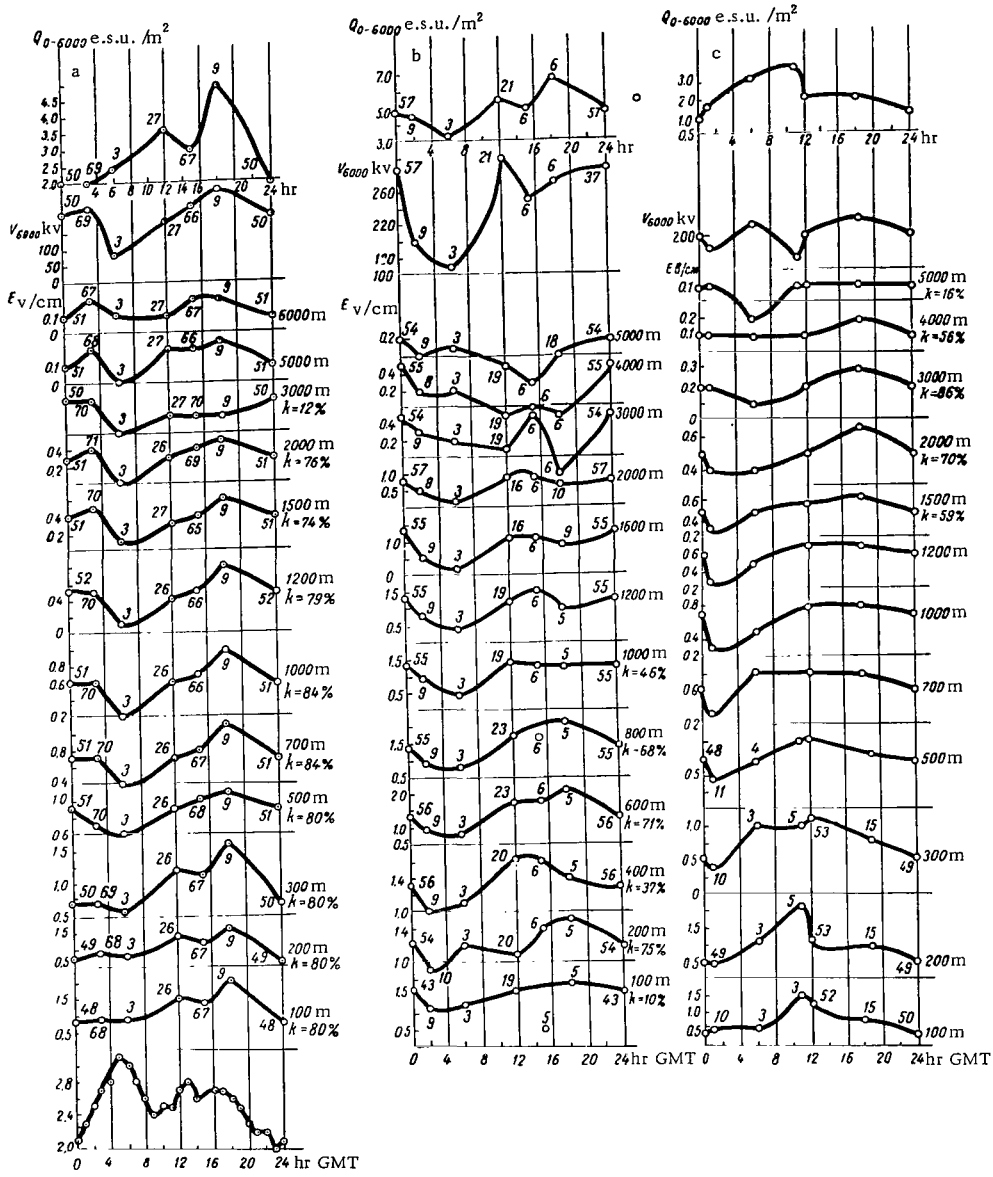

FIGURE 18. Diurnal variation of the electric field E (with respect to GMT) at various altitudes, the potential V at an altitude of 6000 m, and the charge Q of an air column of unit cross section and a height of 6000 m in Leningrad (a), Kiev (b) and Tashkent (c).

The figures near the dots designate the number of soundings; k designates the coefficient of correlation between the respective curve and the unitary variation curve. The altitude at which the measurement was made is indicated in each curve.

and Kiev. Only at altitudes of 2000-3000 m are the curves similar to the unitary wave; the correlation coefficients between the diurnal field variations and the unitary variation are 70 and 86 %. Above and below these altitudes, the correlation coefficients decrease. For Tashkent, the diurnal variation of the charge of an air column from 0 to 6000 m in clear days has a maximum at 17 hr and a minimum at 6 hr true solar time.

The variation of the charge of an air column from 0 to 6000 m obviously determines the variation of the electric field in the lower air layer up to an altitude of approximately 1000 m; as can be seen from Figure 18, these curves are very similar.

The mean charge of an air column from 0 to 6000 with a cross section of 1 m^2, is smaller for Tashkent than for Kiev and Leningrad; for Leningrad it is approximately equal to 3 e.s.u./m^2, for Kiev about 5 e.s.u./m^2, and for Tashkent about 2 e.s.u./m^2. This is obviously due to the fact that a negative charge, reducing the total charge of the atmosphere, often appears in the lower atmospheric layers at Tashkent. Highly characteristic of Tashkent are profiles of Group III, which appear in the case of charge separation in the atmosphere. Owing to the presence of a lower negative charge, the total charge of the column decreases. The diurnal variations of this lower charge obviously determine, in the first place, the diurnal variations of the field at Leningrad, as well as at Kiev and Tashkent.

If we assume that the unitary variation is due to variations in the earth's charge, it obviously appears only in the layer coinciding approximately with the "center of gravity" of the volume charge, i.e., if the measurements are made at a level where the charge of the air column is approximately equal above and below the flight level, then the fields of these charges compensate each other, and the field of the proper charge of the earth can be measured. This is particularly clearly seen for Tashkent, where the phase of the variation of the charge of a unit air column differs from that of the unitary variation, and the latter appears in a fairly narrow layer.

As one moves southward, the space charges spread over a thicker layer of the atmosphere, and their so-called center of gravity rises higher and higher.

It is important to note that the unitary variation at certain altitudes is not only reflected in the mean picture of the diurnal variation of the electric field at various altitudes plotted from a large number of cases, but often in individual days as well. Examining the transformation of the diurnal variation of the electric field with altitude, we notice that at definite altitudes, the diurnal variation of the electric field agrees in phase with the unitary variation (from data of measurements during 24 hours).

§ 4. THE POTENTIAL OF THE ELECTRIC FIELD OF THE ATMOSPHERE AT AN ALTITUDE OF 6000 m AND ITS TIME VARIATION

Measurements of the potential of the high layers of the atmosphere should help in determining the correctness of the hypothesis which likens these layers and the earth to the plates of a gigantic spherical condenser with charges of opposite signs.

By integrating the curve $E=f(H)$ is it possible to calculate the potential V of the atmosphere at an altitude H. From the data of this work, the potential at an altitude of 6000 m on days with profiles of Group I should be equal to approximately 90 % of the potential of the ionosphere; therefore, the potential of the ionosphere on these days exceeds the potential measured at 6000 m by approximately 10 %. According to Clark /74/, the potential of the ionosphere is approximately 20 % higher than the potential at 6000 m. Gish /80/ estimates the potential at an altitude of 6000 m to be about 70 % of the potential of the ionosphere, assumed by him equal to 400 kv; consequently, the potential at an altitude of 6000 m should be approximately 280 kv.

The potential variations at an altitude of 6000 m should thus be largely similar to the potential variations of the ionosphere. Deviations from this similarity may result mainly from deviations of the atmospheric conductivity from the "normal" values. Since these variations occur mainly in the layer between 0 and 3-4 km, and usually lead to a decrease in the conductivity, the calculated values of the ionospheric potential may turn out to be somewhat overestimated.

The spherical condenser theory assumes that: 1) the potential should rise with altitude; 2) the diurnal variations of the potential at an altitude of 6000 m should agree in phase and amplitude with the unitary variation; 3) these variations and the potential values at the same level should be the same at all observation points if local effects (clouds, high-spreading dust, and others) are eliminated.

Figure 19 gives the variations of the electric potential with altitude, observed in 1958 at Leningrad, Kiev, and Tashkent.

Curve 1, based on Gish's formula /80/, represents the theoretically calculated potential variation with altitude; the points give the measured values of the potential, and the circles give the potential values at altitudes where the curve has a maximum, so that higher up, the potential decreases. It follows from the behavior of the curves that the monotonous rise of the potential with altitude is often upset, even on clear days.

Appendix XVI gives tables of the potential distribution at an altitude of 6000 m. The most probable potential value, on all days (both clear and cloudy), lies between 80 and 300 kv with a maximum of about 200-240 kv. In this case, the most probable value of the ionospheric potential is 220-260 kv. The histogram of the atmospheric potential, referred to all the days, is highly elongated, i.e., many very high potential values are observed. On individual fair-weather days, the potential over the observation place may reach 500 kv, and on cloudy days, potentials of $+3 \cdot 10^7$ and $3 \cdot 10^6$ v are observed.

The diurnal potential variations at 6000 m are mostly dissimilar to the unitary variation and differ for all three observation points at the same time. Figure 20 gives the mean diurnal potential variations of the atmosphere over Leningrad, Kiev, and Tashkent during June, September, and December 1958. We see that they all differ by phase and are dissimilar to the unitary variation. Figure 21 gives the results of simultaneous potential measurements at the three points. The days of the month on which soundings were made are plotted along the abscissa, and the potential values, along the ordinate.

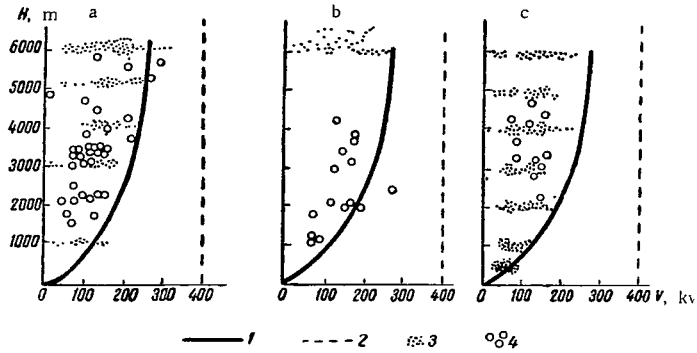

FIGURE 19. Variation of the potential V with altitude H.

1— calculated from Gish's data /80/; 2— value of the potential of the ionosphere /80/; 3— measured values of the potential at the given altitude; 4— value of the potential at points where it began decreasing with altitude. a— Leningrad (75 soundings); b— Kiev (30 soundings); 3— Tashkent (50 soundings).

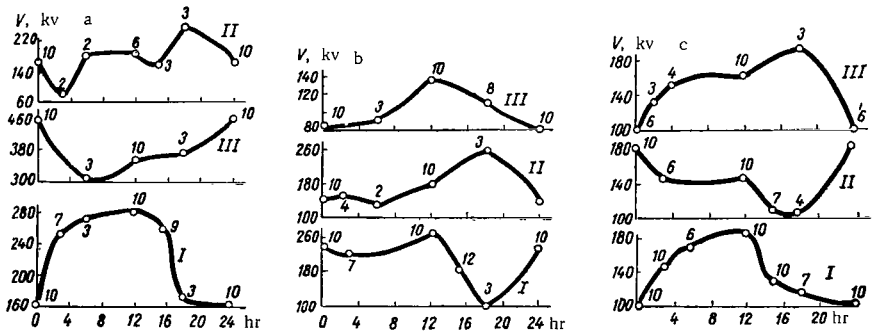

FIGURE 20. Diurnal variation of the atmospheric potential V at an altitude of 6000 m.

a— June 1958; b— September 1958; c— December 1958 (hours, GMT). I— Leningrad; II— Kiev; III— Tashkent. The figures at the plotted points give the number of soundings.

§ 5. ANNUAL VARIATION OF THE ELECTRIC POTENTIAL OF THE ATMOSPHERE AT AN ALTITUDE OF 6000 m, AND OF THE CHARGE OF AN AIR COLUMN IN THE 0-6000 m LAYER

Long-period variations in the electric potential and charge of the atmosphere (annual variations in particular) should be the most stable characteristics of the electric state of the atmosphere, since they are less affected by irregular processes than short-period variations.

As was mentioned above, the annual variation of the characteristics of the atmospheric electricity has a global character, i.e., it is

identical for the northern and southern hemispheres owing to the general variation of the earth's charge.

Thus, the annual variation of the atmospheric electric field near the earth, with minimum and maximum monthly-mean values occurring in the summer and winter months in the northern hemisphere (i.e., respectively, the winter and summer months in the southern hemisphere), is given in /45/.

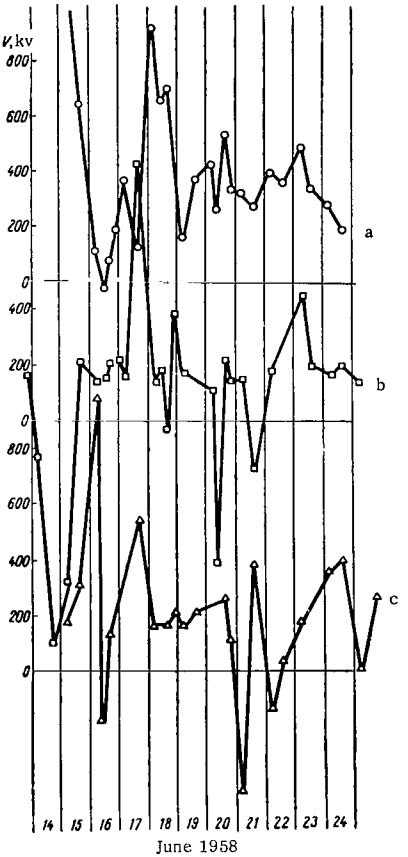

FIGURE 21. Time variation of the atmospheric potential V at an altitude of 6000 m.

a — Leningrad; b — Kiev; c — Tashkent.

The annual variations of the space charge density at ground level, obtained for different points of the globe, are given in /41/. It is pointed out that the annual variations of ρ in different places, in different years, and obtained using different instruments, are always characterized by reduced values for the summer months (May-October) and increased values for winter months (November-April).

The air conductivity λ at ground level also has an annual variation which is the inverse of the space charge variation /43/.

The idea that annual variation effects appear only in the surface layer, and a simple explanation of this variation by increased and reduced release of radioactive emanations from the soil as dependent on the degree of its coverage by snow (or ice), does not explain the existence of the same variation in equatorial regions and, as will be shown further, the fact that the annual variation of the field and space charge extends to considerable altitudes.

The large difference in the amplitudes of the annual variation of the field in the northern and southern hemispheres /45/ suggests that the general annual variation for the whole globe is determined by the seasonal variation in the northern hemisphere. The seasonal variation is more clearly manifested over continents, and the land area in the northern hemisphere is slightly more than five times that in the southern hemisphere.

It is therefore possible that the seasonal variations in the northern hemisphere prevail over the seasonal variations in the southern hemisphere, producing common variations for the entire globe.

According to Wilson's theory, it is natural to assume that the annual variation of the electric field (the annual unitary variation) is due to the

annual variation of the thunderstorm activity over the whole globe, if we assume that recharging of the earth takes place mainly in thunderstorm regions. Krumm /89/ computed the annual variation of the total number of thunderstorms (see Figure 4) over the whole globe. It was found that the annual variations of the field intensity and mean number of thunderstorms are not similar, but even opposite in phase, i.e., maximum thunderstorm activity occurs in the northern summer, when the minimum field strength is observed.

Gerasimenko /7/ found that the diurnal unitary variation of the electric field agrees in phase and amplitude with the diurnal variation of the illuminated area of the ocean, and attempted on this basis to conjecture the reasons for the variation of the earth's charge, which causes the unitary variation.

Calculations of the annual variation of the illuminated ocean surface, made by Saluvere /53/, showed that it is not similar to the annual unitary variation of the potential gradient, but has two maxima (in March and September), and two minima (in summer and winter).

Consequently, the annual variation of the potential gradient is not correlated with the variation of the illuminated ocean surface, and none of the related charging mechanisms explain the annual variations of atmospheric-electric quantities.

Thus, it can be considered established at present that such atmospheric-electric characteristics as the field, space charge, and conductivity near ground level have an annual variation which is common for the whole earth. However, there is no satisfactory explanation of these variations. It is impossible to find out to what extent the indicated variations are localized in the surface layer of the atmosphere, and in what way the charge exchange between the earth and the atmosphere affects them.

The data obtained from aircraft sounding made it possible to determine the annual variations of such electric characteristics of the atmosphere as space charge, potential at definite altitudes, electric field at definite level, etc.

The results of soundings during four years (1958-1961) are considered in the present section. Sufficient ascents took place every month to enable determination of the monthly-mean values of the measured quantities. The results obtained were used to plot graphs of the annual variation of the space charge of a unit air column with a base of 1 m^2 in the layer 0-6000 m. The annual variation of the electric potential at an altitude of 6000 m and of the space charge is shown in Figure 22. The mean smoothed curves are given in the graphs. The smoothing was effected using the formula

$$b = \frac{n_1 a + 2n_2 b + n_3 c}{n_1 + 2n_2 + n_3} ,$$

where a, b, c are the monthly-mean values of the charge or potential, and n_1, n_2, and n_3 are the corresponding number of cases from which these means were obtained (Appendix XVII).

In Leningrad, the annual variation of the atmosphere's charge, calculated only for clear days, shows a maximum in February-April and a minimum in June-December. In Kiev and Tashkent, the maximum

charge is observed in winter months, and the minimum charge in summer and autumn months.

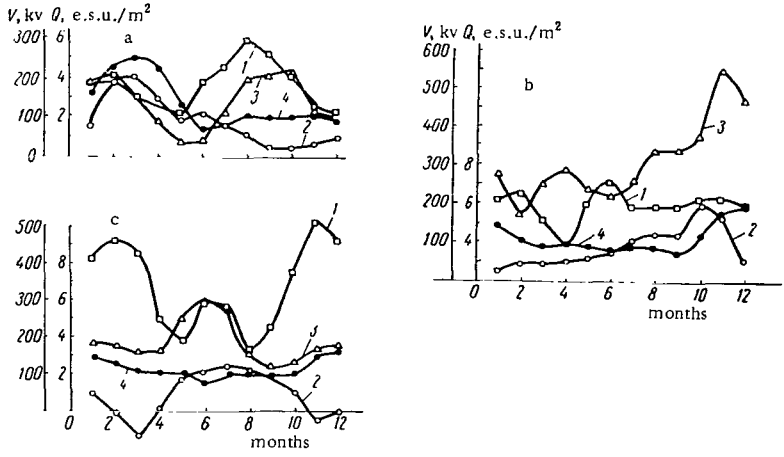

FIGURE 22. Annual variation of the potential V of the atmosphere at an altitude of 6000 m and of the charge Q of a unit air column 6000 m high on days with any weather (1 and 2) and on clear days (3 and 4), from data of measurements made during 1958-1961.

a — Leningrad; b — Kiev; c — Tashkent.

The picture from the annual variation plotted from all the days is less clear. In Leningrad, the annual variation of the atmosphere's charge on all days is very similar to the charge variation only on clear days, the two variations agreeing in phase, but differing somewhat in amplitude. In Kiev and particularly in Tashkent, the differences are larger. In Kiev, on all days, the minimum charge is observed in winter-spring months, and the maximum charge in autumn months. In Tashkent two minima (March and November) and two maxima (summer and winter) are observed.

Thus, on clear days, the annual charge variation in the 0-6000 m atmospheric layer resembles in general lines the annual unitary variation of the field. In Tashkent only is the relative amplitude considerably smaller than in Kiev and Leningrad, and smaller than the relative amplitude of the mean unitary variation of the potential gradient. The annual variations of the charge of an atmospheric column in Kiev and Tashkent considerably differed from one another in all the days, both by the positions of the extrema, and by the magnitudes. It should be borne in mind that only the excess charge of an atmospheric column is given, i.e., the variations given in the figures are not of the whole atmospheric charge, but only of the uncompensated charge. The charge equal to it in magnitude and opposite in sign obviously either settled on the earth, or spread upward, or was carried to neighboring regions by advective currents. If we assume that most of these charges settled on the earth, then in order to explain the reasons for the annual unitary variation, the annual charge variation during all days should be considered, although it is considerably less similar to the annual variations of the electric characteristics of the

atmosphere (given in the literature /41, 45/) than to the annual variation of the charge of an atmospheric column on clear days only.

The annual charge variation on clear days is similar in general lines to the annual unitary variation of the potential gradient given by N. A. Paramonov /45/, and it might be thought that the charge of opposite sign, which settles on the earth mainly caused this variation, if these variations were quantitatively equal. According to Paramonov's calculations, the maximum amplitude of the annual variation of the potential gradient amounts to ~ 40 % of the mean, and the largest deviation from the mean in the annual variation of the space charge of an atmospheric column amounts to ~80-90 %. The mean charge of an atmospheric column on clear days from the three observation points is ≈ 3 e.s.u./m^2; it can create an electric field at ground level of ~ 110 v/m. The mean deviation of the charge of an air column for all the observation points is ~2 e.s.u./m^2 and it can create a variation of the electric field of ~60-75 v/m. If we extrapolate these data on the atmospheric charge to the whole globe, i.e., assume that the mean variation of the earth's charge is ~ 2 e.s.u./m^2, then the mean annual charge variation over the whole earth will be $\Delta Q = 2$ e.s.u./$m^2 \times 5 \times 10^{14}$ m^2 = 10×10^{14} e.s.u. = $3 \times 3 \times 10^5$ coulombs (the area of the earth is 5×10^{14} m^2).

If we assume that the charge under consideration is created only over land and the land area amounts to approximately 1/3 of the total surface of the earth, then the value obtained for the variation of the earth's charge owing to settling of atmospheric space charge on the earth should be divided by 3,

$$\Delta Q \approx 1 \cdot 10^5 \text{ coulombs.}$$

As is known (see, for example /34/), 50 % of the whole surface of the earth is covered with clouds, and therefore 50 % are found in clear-weather regions. This means, that the total variation of the earth's charge due to charge settling from the atmosphere in fair weather regions will be

$$\Delta Q \cong 0.5 \cdot 10^5 \text{ coulombs.}$$

Variation of the charge only on clear days takes place because it is precisely on these days that the annual variation of the atmospheric charge agrees in phase with the annual unitary variation of the potential gradient. If the mean charge of the earth is approximately -3×10^5 coulombs, then the calculated variations of the earth's charge amount to about 15 % of the whole charge of the earth. According to data of /45/, the amplitude of the annual unitary variation for the whole earth is ~ 16 %. If the considered process of charge exchange between the atmosphere and the earth is a measure of the variation of the earth's charge, then the settling of charges from the atmosphere on clear days can roughly explain the observed variations.

The annual variation of the charge of an atmospheric column on all days, i.e., including cloudy days, does not agree in phase with the annual unitary variation of the potential gradient. The contribution of the charge arriving on the earth on these days should be larger than on clear days.

The annual variation of the charge of a unit air column, characterizing the charge exchange between the earth and the atmosphere as a whole,

shows that this exchange is very intensive, and that the magnitude of the variation of this charge is sufficient to explain the observed annual variations of the potential gradient. However, owing to the absence of similar data for the whole earth, it is impossible to carry out the necessary averaging over the surface of the globe, and it is therefore impossible to find phase relationships which would make it possible to determine the source of the annual field variations.

The annual variation of the electric charge of an air column while reflecting the general conditions of charge exchange between the earth and the atmosphere, does not show how the atmospheric charge is stratified, or to what extent the variation of the electric field at ground level is connected with space charges in the surface layer.

It was therefore desirable to examine the annual variation of space charges at various levels. Since the separation level of space charges of different signs in the atmosphere is usually at an altitude of 300-700 m, and the field intensity changes sign at an altitude of 3500-4000 m, the annual charge variations in the layers 0-500, 500-3500, and 3500-6000 m were investigated (Appendix XVIII).

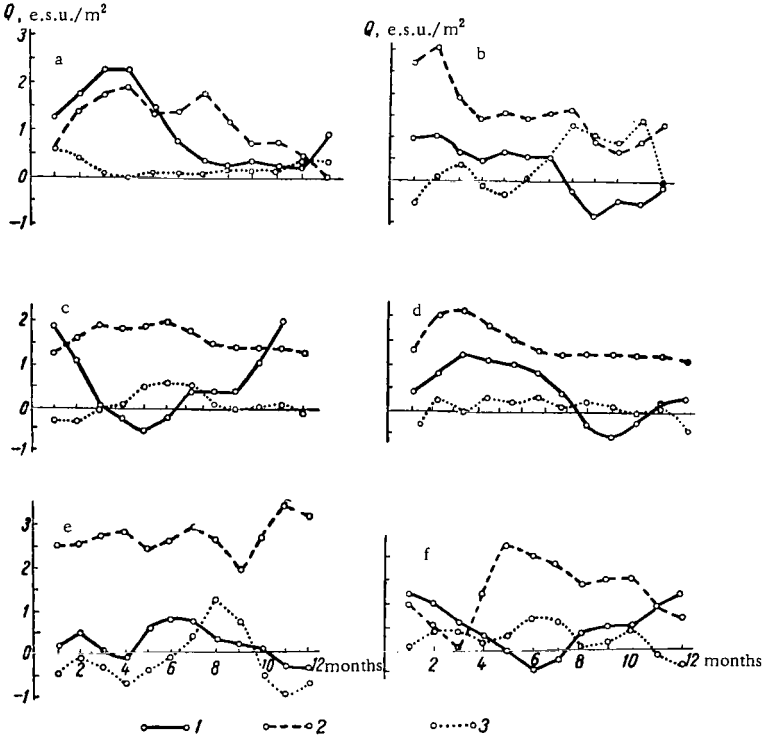

FIGURE 23. Annual charge variation of an air column in the layer 0-500 m (1), in the layer 500-3500 m (2), and in the layer 3500-6000 m (3).

In "fair" weather days; a— Leningrad; b— Kiev; c— Tashkent; in all the days; d— Leningrad; e— Kiev; f— Tashkent.

Figure 23 gives the annual variations of the atmospheric charge in the indicated altitude intervals. It is interesting that the charge variations in the lower 500-m layer in Leningrad and Kiev are very similar and have the same phase as the annual space charge variations measured at ground level /41/. In Tashkent, the annual variation of the atmospheric charge in the lower 500-m layer agrees in phase with the annual unitary variation of the potential gradient /45/, exceeding it in amplitude. The mean amplitude of the given variation for all the towns is approximately 2 e.s.u./m^2, so that the above-mentioned considerations apply in this case.

Considering the annual charge variation in the next 500-3500 m layer, and comparing it with the total charge variation in the 0-6000 m layer, we can see that, of all the three curves which give the space charge variation in different layers, this curve most resembles, particularly for all days, the variation of the charge of the entire 6000 m air column. The magnitude of the charge in this layer is largest, so that in some cases it may exceed the total charge of the atmosphere. It may therefore be concluded that the main charge of the atmosphere lies in the 500-3500 m layer.

The layer of this maximum charge is that where low- and medium-level clouds form and disintegrate, and therefore it is not surprising that it is precisely in this layer that the maximum space charge of the atmosphere is observed. More surprising is the fact that this is the maximum charge layer on clear days also. From elementary concepts a different result might have been expected, i.e., at least on clear days the main charge is situated in the lowest layers of the atmosphere and that it has a decisive role in the magnitude and variation of the charge of the entire 6000 m atmospheric column.

The high values of charges in the 500-3500 m layer are due also to the fact that this is the thickest layer. But, on the other hand, had the electric field always decreased according to an exponential law with a power close to 1, then charges larger than those in the lower atmospheric layer should not have arisen in this case, and the variation of the charge of the entire column would always be determined by the charge variation in the lower atmospheric layer. Days with profiles of Group III obviously played a large part in the formation of the opposite distribution. In addition, charges from disintegrated clouds remaining in the atmosphere could also create some charge accumulation in the 500-3500 m layer.

The fact that even on clear days the charges in the upper 3500-6000 m layer were larger than assumed was unexpected. They are comparable in magnitude with the surface charges in the lower 500 m layer. On cloudy days, the charge in this high layer sometimes even exceeds that in the lower layer. Its variation is very often similar to that of the charge in the 500-3500 m layer.

Thus, on clear days, the mean charge Q in the 0-500 m layer is ~ 0.7 e.s.u./m^2; in the next 500-3500 m layer, ~ 2.0 e.s.u./m^2; and in the upper 3500-6000 m layer, ~ 0.5 e.s.u./m^2.

On all the days, $Q_{0-500} \approx 0.5$ e.s.u./m^2, $Q_{500-3500} \approx 2.0$ e.s.u./m^2, and $Q_{3500-6000} \approx 0.5$ e.s.u./m^2.

Thus, the main part of the electric charge of the atmosphere is concentrated in the 500-3500 m layer, the largest annual charge variations being connected with this layer. The annual variation of the space charge in the 0-500 m layer may even be the opposite of that in higher layers. This

obviously explains the lack of similarity between the annual variation of the field and of the space charge near the earth's surface.

The annual potential variation differs from the annual variation of the charge of a unit column even on clear days (see Figure 22).

On clear days with a monotonous decrease in the electric field with increasing altitude, the variations of the potential and of the space charge of the atmosphere should be similar in the case of field profiles of Group I. In fact, if the electric field decreases by an exponential law

$$E = E_0 e^{-ah},$$

the potential at an altitude H will be

$$V_H = \int_0^H E e^{-ah}\, dh = \left[-\frac{E_0}{a} e^{-ah} \right]_0^H = \frac{E_0}{a}\left(1 - e^{-aH}\right). \qquad (9)$$

The charge of an air column with an altitude H and base of 1 m^2 will be

$$Q_H = \frac{E_0}{4\pi}\left(1 - e^{-aH}\right). \qquad (10)$$

The ratio $\frac{Q_H}{V_H} = \frac{a}{4\pi}$, i.e., constant for the given state of the atmosphere, and therefore the variation of the potential should be similar to the variation of the charge of a unit air column. The nonparallelism observed in the given graphs should obviously be attributed to days with a nonmonotonous variation of the electric field with altitude in clear weather and to the variation of a.

The annual variation of the atmospheric potential on clear days at Leningrad and Kiev has a minimum in May-June and a maximum in autumn and winter months. In Leningrad, a secondary minimum is observed in November-December, but these two points are based on a smaller number of cases than the rest.

Thus, the phase of the annual potential variation on clear days at Kiev and Leningrad agrees with that of the annual unitary variation. In turn, the variation at Tashkent has a reverse course — a maximum is observed in summer months, obviously due to the fact that, because of the rise in the content of dust and other impurities in the atmosphere there during the summer months, the electric field in the lower layers of the atmosphere and the electric potential of the atmosphere increase. The annual potential variation, based on the data of all days for Tashkent, closely resembles the annual unitary variation of the potential gradient and, in addition, a secondary weak maximum in summer months is observed against the background of a fairly deep minimum. The annual potential variation at Leningrad and Kiev, based on the data of all days, has a minimum in April and a maximum in August (Leningrad) and in June (Kiev); during the remaining months at Kiev, the variation is weakly pronounced.

§ 6. RELATIONSHIP BETWEEN THE ELECTRIC FIELD OF THE ATMOSPHERE AND CONDENSATION NUCLEI* /64/

The influence of air pollution on the electric characteristics of the atmosphere has been apparent for many years. A variation in the content of aerosols (in particular, of condensation nuclei) brings about, in the first place, a variation in the air conductivity λ, which is related to the concentration n of light ions by

$$\lambda = ekn, \tag{11}$$

where e is the elementary charge (4.8×10^{-10} e.s.u.), and k is the mean mobility of light ions ($1\ cm^2 v^{-1} sec^{-1}$).

Recombination of light ions can usually be neglected in the lower layers of the atmosphere, and then

$$n = \frac{q}{4\pi D (r'z + rN)'}, \tag{12}$$

where, on the average, the rate of ion production is $q \approx 10$; $D \approx 3 \times 10^{-2}$ is the diffusion coefficient; r' and z are respectively the mean effective radius and concentration of all nuclei; r and N are the mean radius and concentration of drops.

In the absence of clouds, $N = 0$, and then

$$n = \frac{q}{(4\pi Dr) z} = \frac{q}{\beta z}. \tag{13}$$

where the coefficient $\beta = 4\pi Dr$, according to data of special measurements carried out from time to time at a small number of points, is of the order of 4×10^{-6}.

It is known that the vertical conduction current $i = E\lambda$ in undisturbed conditions usually differs little from the average value, taken equal to 10^{-6} e.s.u. $cm^{-2} sec^{-1}$. A variation of the conductivity λ under a constant value of i should cause a variation of the electric field E, which depends in this case (according to (11) and (13)) on the nuclei concentration z:

$$E = \left(\frac{i\beta}{ekq}\right) z. \tag{14}$$

For the above-indicated mean values of the individual parameters, the coefficient A which relates E to z is calculated by the formula

$$A = \left(\frac{i\beta}{ekq}\right) \tag{15}$$

and is approximately equal to 3×10^{-6}. Independently of this estimate, the value of A can be calculated from data of simultaneous measurements of E and z.

In aircraft soundings of the atmosphere, the concentration z' of condensation nuclei was measured simultaneously with the recording of the field intensity. Results of observations of condensation nuclei by means

* The results of observation of condensation nuclei are kindly submitted by E. S. Selezneva.

of a Scholz counter /1/, carried out under the direction of A. L. Dergach and E. S. Selezneva, are published in /9, 54, 56/.

The observation and data processing techniques differed in certain respects: the mean field intensity was determined for each 100 m layer, whereas condensation nuclei at altitudes up to 1 km were measured at 250 m intervals, and above 1 km, at 500 m intervals. These differences should mainly affect the shape of the curves characterizing the vertical distribution of E and z'.

To calculate the coefficient $A'=\left(\frac{E}{z'}\right)$, use was made of data of measurements of E and z' in 25 ascents. The values of A' were calculated only up to an altitude of 2.5 km. At higher altitudes, owing to the considerable decrease in aerosol concentration, the recombination of light ions (which was not taken into consideration in the derivation of formula (15)) plays a significant role. This limitation can be easily overcome by partly modifying the processing technique. In fact, for sufficiently large z, according to (15), $E\approx Az$; whereas for very small z, taking into account recombination

$$cE\approx\frac{A}{2}z,$$

where c is some coefficient.

The inexpediency of determining the values of A for considerable altitudes (above 2.5 km) is due to measurement errors, which must considerably affect the result for small values of E and z.

Table 10 gives the distribution of different values of the coefficient A'. (for altitudes less than 2.5 km). In the calculation of recurrency as percentages, rarely encountered anomalous (negative) values of A' were excluded. On the average, $A'\approx3\times10^{-6}$, i.e., within the limits of possible error, it agrees with the above-indicated value of the coefficient A. From the experimentally obtained relationship $A'=A$ (using the definition $A'=\frac{E}{z'}$) follows the approximate equality $z'\approx z$. Consequently, it is highly probable that most aerosol particles are condensation nuclei.

TABLE 10.

$A\cdot10^6$	0-1	1.1-2	2.1-3	3.1-4	4.1-5	5.1-6	6.1–7	7.1-8
Number of cases	19	27	25	14	12	5	10	3
Recurrency, %	15	21.5	20	11	9.5	4	8	2.5
$A\cdot10^6$	8.1-9	9.1-10	10.1-11	11.1-12	12.1-13	13.1-14	14.1-15	15
Number of cases	1	1	1	2			1	1
Recurrency, %	1	1	1	1.5			1	1

When analyzing the type of distribution of some essentially positive quantity, it is convenient to use a logarithmically normal grid first /40/. The data given in Table 10 were used to plot a graph of $P(L)$ as a function of L (Figure 24), where $P(L)$ is the probability that $l\leqslant L$, using here the notation $l=\lg A'$. As follows from this figure, in the scales chosen, the

experimental points lie along a straight line with a comparatively small spread. This shows that the distribution of the values of the coefficient A is satisfactorily described by a logarithmically normal law, which is particularly often used to characterize the size distribution of particles, for example of cloud drops, emulsion grains, and a number of artificial aerosols (a calculation made by N. Kolmogorov for a special case — the size distribution of particles obtained as a result of fractionation — is inaccurately called Kolmogorov's law in one of the recent works /40/).

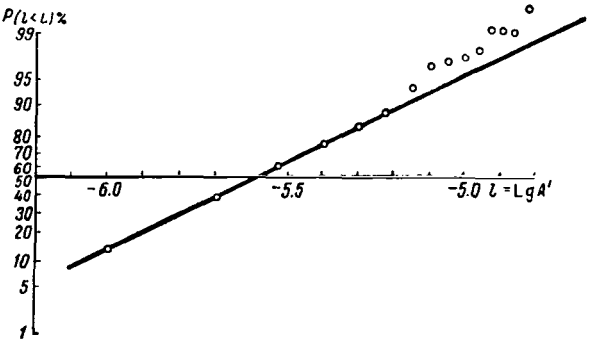

FIGURE 24. Recurrence of mean values of coefficient A', not exceeding a given value.

The case under consideration is closely related to the size distribution of particles, since, by substituting in formula (15) the value $\beta = 4\pi Dr'$ and using Einstein's relationship $\left(\frac{k}{D} = \frac{e}{kT}\right)$ and the numerical values of the physical constants, we obtain (for T = 300°)

$$A = \left(\frac{4\pi ikT}{qe^2}\right) r' = \left(2.3 \cdot 10^6 \frac{i}{q}\right) r', \qquad (16)$$

where k is the Boltzmann constant, and T, the absolute temperature.

For the above-indicated mean values of i and q, it is possible to write approximately

$$r' = 4A. \qquad (17)$$

In contrast to the usually considered distribution of individual values of r' in a given sample, the results obtained here (Table 10) characterize the recurrency of the mean values of r' for different samples (measurements). An estimate of the recurrency (as percentages of the total number of measurements) of different mean values of r' (in microns) on the basis of Figure 24 and relationship (17) is given in Table 11. Despite their tentative nature, these data are of interest since in most cases there is no information on the mean sizes of aerosol particles in natural conditions.

TABLE 11.

r'_{mean}, μ	<0.05	0.05-0.1	0.1-0.2	0.2-0.3	0.3-0.4	0.4-0.5	>0.5
Recurrency, %	20	30	30	10	5	2	3

A shortcoming in the aircraft sounding data used here (according to the elements E and z) is the fact that, given the possibility to estimate the mean sizes of aerosol particles in the absence of clouds, they are insufficient for determination of the mean particle charges. However, even limited information on individual details concerning the distribution of particle charges are of interest.

From the vertical profiles of the field $E(h)$, obtained in aircraft sounding, the mean space charge densities $\rho(h)$ at various altitudes h were regularly calculated. These data can be used for estimating the mean excess charge per one nucleus $\theta=\left[\frac{\rho(h)}{z'(h)}\right]$. The values of θ are determined more or less accurately in cases where the numerator and denominator of the fraction are sufficiently large (in practice, for altitudes up to 2.5 km). Above this level, measurement errors begin to have a considerable effect, and therefore it is not advisable to calculate θ.

By comparing data on ρ and z', it was found that θ is $10^{-11}-10^{-12}$ e.s.u. /nucleus. Consequently, the observed space charges to which the electric field of the atmosphere is due are created by a small part (1/100-1/1000) of the total number of aerosol particles (nuclei). The question naturally arises of whether or not there exist any indications enabling identification from among the multitude of particles of those responsible for the creation of space charges. Often (mostly without sufficient grounds) charges of different signs were related to different particle size-fractions. If the particles of interest differed in size, the value of θ could be expected to vary appreciably with altitude. However, calculations showed that θ essentially does not vary up to altitudes of 2-2.5 km. It has already long been established that natural radioactive particles have a predominantly positive charge. They should, consequently, participate in the creation of the atmospheric space charge, but to what extent they do so is difficult to estimate at present. The estimates obtained here do not contradict the assumption that radioactive particles may play an important role in this connection.

In conclusion, we consider the vertical profiles of the electric field $E(h)$ and of the condensation nuclei concentration $z'(h)$. Profiles of the Group I /16/ frequently are encountered (approximately 35 % of all cases), when the electric field $E(h)$ is an exponentially decreasing function of the altitude

$$E=E_0e^{-ah}. \tag{18}$$

For h = 2-2.5 km, $a\approx 1\ \text{km}^{-1}$, for altitudes larger than 2.5 km, $a\approx 0.4$-0.5. On the average, the concentration of nuclei $z'(h)$ often decreases with increasing altitude, also by an exponential law /9, 54, 56/

$$z'=z_0e^{-\frac{b}{h}}. \tag{19}$$

The value of the coefficient b varies with the observation point from 0.4 to 1.06, differing as a rule for altitudes up to 3 km and higher; the entire profile can be satisfactorily described by a sum of two exponentials. It is interesting to note that, according to the results of many investigations carried out in clear weather, particles are distributed in the atmosphere in layers /37/. This is obviously due to the tier pattern of convective movements.

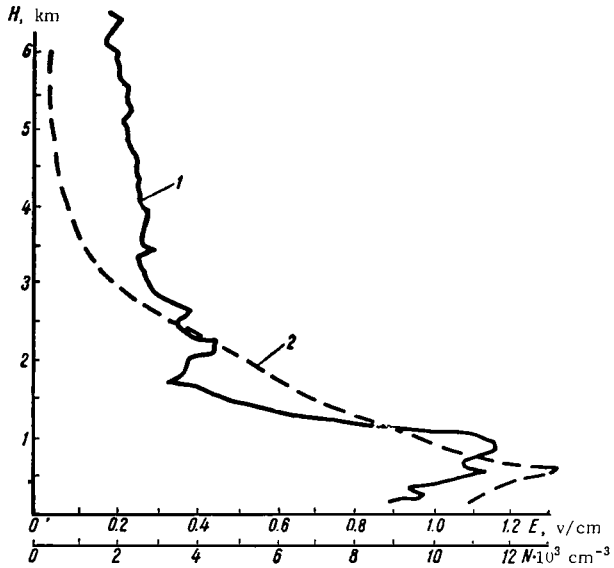

FIGURE 25. Variation of the electric field E (1) and of the concentration N of condensation nuclei (2) with altitude in July 1959 near Leningrad (from 27 soundings).

Along with the monotonous profiles $E(h)$ considered, as often encountered (approximately in 40 % of all the cases) are profiles of Group III, of which a maximum of E at some altitude is characteristic. Figure 25 gives height distribution curves of the electric field and of the concentration of condensation nuclei, based on data obtained during 27 ascents in July 1959. The similarity of the vertical distribution curves of $E(h)$ and $z'(h)$ is displayed not only in the case of the averaged data, but also in the case of data for individual ascents (Figure 26). Figure 26 gives the distribution with altitude of the electric field, the concentration of condensation nuclei, the temperature, and the relative humidity at different hours on 16 July 1959. Despite the above differences in the observation techniques, the curves $E(h)$ and $z'(h)$ are similar to one another in most cases.

We note that a maximum at an altitude of 500-700 m is characteristic of almost all the electric field profiles. A similar maximum at approximately the same altitudes is also observed in the profiles of the condensation nuclei. As a rule, a fairly strong temperature inversion, near the boundary of which $E(h)$ and $z'(h)$ had maximum values, was observed in the morning hours. Toward 8 hr the inversion weakened, transformed into an isotherm or even completely disappeared, but the general pattern of the curves of $E(h)$ and $z'(h)$ with a maximum at some altitude was maintained as a rule. It is probable that the maximum in the distribution of condensation nuclei is maintained after the disappearance of the layer of interception connected with the inversion, owing to the fact that the developing turbulence not only dissolves the layer of aerosol accumulation, but also "feeds" it by new dust portions which are carried from the earth's surface and other sources of pollution.

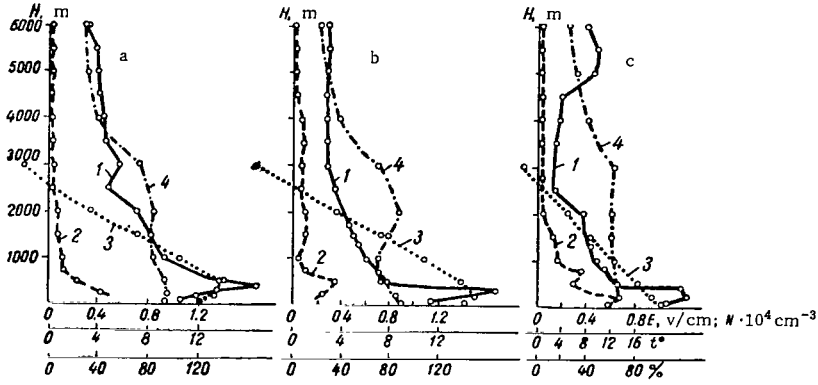

FIGURE 26. Time variation of the altitude distribution of the electric field E (1), of the concentration of condensation nuclei (2), of the temperature (3), and of the relative humidity (4) from data of individual measurements near Leningrad.

a— clear, 3 hr, 16 August 1959; b— clear, 7 hr, 16 July 1959; c— cloudiness 3/3 Cu, Ac, 12 hr, 16 July 1959.

The maximum is as a rule smallest during daytime hours, although the total number of condensation nuclei in the atmosphere may increase. Toward evening, the turbulent motions in the atmosphere decay; the dust, which spreads in a thick layer, begins to settle and the concentration of condensation nuclei in the surface layer increases. At this time, an intercepting layer sometimes begin to form, and at the altitude corresponding to the break point in the temperature curve, a sharp variation of the concentration of nuclei is observed. It should be noted that the condensation nuclei profile has a sharper diurnal variation than the profile of the electric field. The diurnal variation curves of E and z' at different altitudes apparently do not agree as well as the corresponding vertical profiles, but the number of such comparisons made is too small to be conclusive.

Thus, the analysis of the measurements performed produced the following results:

1. The existence of a close relationship between the vertical distribution of condensation nuclei and the atmospheric electric field was established. In cases when an exponential decrease in the field and concentration of nuclei is observed, the coefficients in the powers of the corresponding exponentials are close in magnitude.

2. The agreement between the mean values of the coefficients A and A', obtained by totally different methods, confirms that the relationship between the field and the concentration of condensation nuclei is due to the variation in the air conductivity. This made it possible to estimate the mean sizes of nuclei.

3. The altitude distribution of the condensation nuclei and electric field is significantly affected by the state of the atmosphere, in particular, by the presence of inversions and related intercepting layers.

Chapter IV

ELECTRIC STRUCTURE OF STRATIFORM CLOUDS AND THEIR INFLUENCE ON THE ELECTRIC FIELD OF THE ATMOSPHERE

Stratiform clouds extend over territories hundreds of times larger than those covered by thunder clouds. They may remain for long periods over the same points. Almost half the surface of the earth is covered with stratiform clouds. Therefore, although the electric charges and currents in them are considerably smaller than in thunder clouds, they may play an important role in the general charge exchange between the earth and the atmosphere.

However, the electric properties of these clouds have not been studied much. In works devoted to the investigation of these clouds, data which were obtained during measurements in 1-2 clouds are usually given.

At the same time, data on the electric structure of stratiform clouds are of importance to the theory of cloud electrification, since it is in such clouds that electrification processes connected with the deposition of air ions on water droplets and processes of charge separation under the effect of gravity occur in their purest form. In stratiform clouds not giving precipitation the electrification mechanisms which play a role are only several of the many possible. The fact that charge separation in stratiform clouds is established mainly under the influence of gravity and of the electric field is also important; convective motions in them have a comparatively weak effect on the height distribution of charged particles.

The study of the electric structures of stratiform clouds is also important in order to establish how charge accumulation proceeds in the first stage of thundercloud development.

A study of the transformation of the electric structure of clouds is also important for assessing the effectiveness of cloud seeding. Finally, investigations of the electric properties of clouds are necessary for improving the methods of combating the electrostatic hazard to aircraft.

It is important in the first place to find out the electric macrocharacteristics of these clouds, the distribution of space charges and the electric field in them, and the magnitudes of the charges.

§ 1. INVESTIGATION AND DATA PROCESSING TECHNIQUE

Investigations of nonprecipitating clouds of the stratified St, Sc, and of other types show that the field in them in horizontal flights is relatively

constant, which makes it possible to liken these clouds electrically to infinitely charged layers and to consider all the fields and charge variations in them as dependent only on the vertical coordinate. In these circumstances aircraft sounding has a special advantage over other types of vertical sounding. This is due to the fact that simultaneously with the vertical sounding, the measurements are horizontally averaged, which considerably reduces the influence of local inhomogeneities on the measurement results.

In order to determine typical features of the electric structure of clouds, a method for comparing clouds of a given type has to be found. Analysis of measurement results showed that it is convenient to compare different clouds by reducing them to a single thickness. For this purpose, the sections of the oscillograms on which the variation of the electric field in the clouds was represented were divided into 10 equal sections regardless of the thickness of the clouds to which these oscillograms referred.

The field values, which were averaged over intervals equal to 1/10 of the cloud thickness and referring to the same interval numbers in each cloud, were compared with one another; in this way, electric structures typical of the kinds of clouds investigated were obtained.

It should be said that the use of this method is based on the idea that all clouds of a given type have a similar electric structure or some typical structures; such factors as temperature, humidity, and their distribution in the atmosphere, etc., either do not have a significant effect on the form of these structures, or their effects are identical in the clouds investigated. Nevertheless, by analyzing the clouds under investigation, it was found out that there are indeed only a certain number of basic types of charge distribution in them, and that the expected similarity in the charge distribution does in fact exist. The determination of the variation of the electric field with altitude in clouds made it possible to use Poisson's equation and to obtain the charge and potential distribution in the investigated clouds for a one-dimensional problem.

§ 2. ELECTRIC STRUCTURE OF STRATIFIED CLOUDS

In this section the data on 116 stratified St clouds investigated in 1958-1959 are analyzed.

The thickness of the investigated clouds varied from 100 to 1000 m, their mean thickness being 600 m; the mean altitude of their bases was approximately 350 m (there were cases, however, when the clouds began almost at ground level, from 30-50 m). The mean field intensity E in St-type clouds was 1.0 v/cm. The external values of the electric field were in the range from +5.5 to −15 v/cm. The mean maximum and minimum intensities for all the clouds did not exceed +2.1 v/cm and 0.3 v/cm, respectively. More detailed characteristics of the investigated clouds are given in Appendix XIX.

Appendix XIX gives, in addition the extremal values of the electric field E_{max} and E_{min}; the mean maximum ρ_{max} and minimum ρ_{min} space charge densities in the clouds; the potentials at an altitude of 6000 m; the charge

Q_{0-6000} of an air column in the layer 0-6000 m; and the potential difference between the top and base of cloud.

The distribution of the field in these clouds (averaged over thickness intervals of 100 m) is given in Appendix XXVI.

It can be seen that the prevailing field intensities were in the range from −1 to +3 v/cm. They amount to more than 80 % of all the measured values of the field.

The dependence of the mean and maximum field intensity on the cloud thickness as well as the excess space charge densities in these clouds are given in Appendices XXVII and XXVIII.

It follows from the data given in this appendix that the mean field intensity in clouds more than 200 m thick depends only slightly on their thickness. The maximum field intensity increases with the cloud thickness, but the rate of this increase is slow.

Appendix XXVIII gives the influence of the cloud thickness on the field at all the three investigation points. It can be noticed that as one moves to the south, the maximum field intensities increase with the cloud thickness faster than the mean intensities.

The investigated clouds differed in their electric structure, but almost all the structures could be reduced to four basic types.

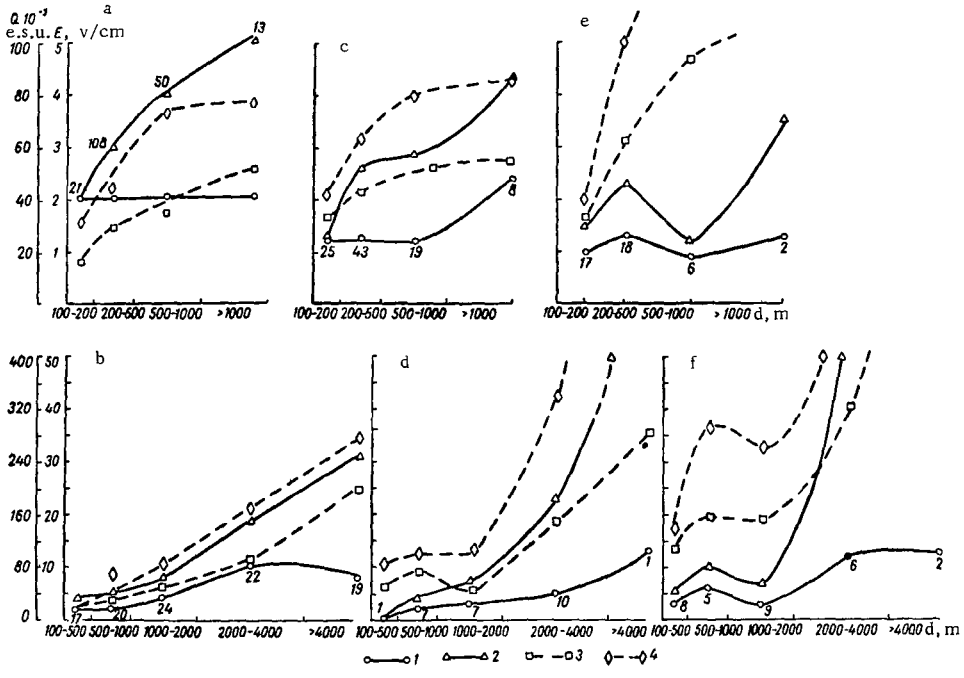

FIGURE 27. Mean field intensity E (1), maximum field intensity E_{max} (2), mean Q (3) and maximum $\overline{Q}_{max}$ (4) rate of aircraft charging as a function of the cloud thickness d.

The figures on the curves give the number of soundings. Leningrad: a—Sc; b—Ns; Kiev: c— Sc, d — Ns; Tashkent: e— Sc, f— Ns.

From the data of 70 soundings in Leningrad, positively polarized clouds were observed in 28 cases (41 %); positive space charges were situated in their upper part, and negative charges in their lower part. In this case, an excess positive charge was observed in the clouds. The field variation with altitude in the cloud in this case is shown in Figure 28a (the ordinate gives the reduced cloud altitude). The field variation in individual clouds is close to the averaged variation.

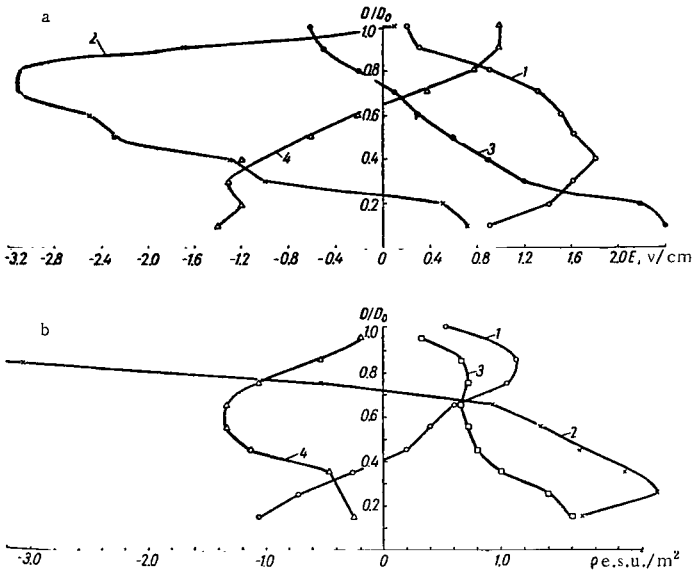

FIGURE 28. Reduced variation of the electric field E (a) and of the space charge (b) in St-type clouds.

1 — positively polarized clouds (27 cases); 2 — negatively polarized clouds (7 cases); 3 — positively charged clouds (16 cases); 4 — negatively charged clouds (6 cases).

Figure 28b gives the charge distribution in the cloud. The mean positive charge situated in the upper part of the cloud is approximately $+2.5$ e.s.u./m^2 with a mean space charge density of about 2.2×10^{-2} e.s.u./m^3, and the mean negative charge is -2.5 e.s.u./m^2 with a mean density of -1.6×10^{-2} e.s.u./m^3. The mean excess positive charge of the cloud is 2.7 e.s.u./m^2 with a density of 0.7×10^{-2} e.s.u./m^3. Appendix XLa gives the field variation with altitude in clouds of a given electric structure on individual days. The value of σ, the root-mean-square deviation from the value in individual clouds, is also given there.

In seven cases ($\sim$10 %), a negative cloud polarization was observed. Negative space charges were situated in its upper part, and positive charges in its lower part. The vertical field profile in these clouds is given in Figure 28a. Although the number of investigated clouds is small, the basic features of this variation are fairly clear. The mean magnitude of the upper, negative charge in these clouds is -9 e.s.u./m^2 with a mean

charge density of about -0.5×10^{-2} e.s.u./m^3; the mean magnitude of the lower, positive charge is approximately 9 e.s.u./m^2 with a mean space charge density of 2.4×10^{-2} e.s.u./m^3. The excess charge in this case is small, amounting to 2.5 e.s.u./m^2 with a mean density of 0.7×10^{-2} e.s.u./m^3. It is important to note that the field intensity in clouds of this structure was found to be the highest. Appendix XLb gives the field variation with altitude in clouds of this structure.

A number of the clouds investigated displayed unipolar charge, both positively and negatively charged clouds being observed.

Eighteen clouds (27 % of all the cases) were found to be positively charged. The field variation with altitude in these clouds is shown in Figure 28a and in Appendix XLc. The mean charge of a unit column extending from the cloud base to its top was 7.5 e.s.u./m^2, and the mean space charge density was 2.4×10^{-2} e.s.u./m^3. As a rule, these clouds were 500-1000 m thick.

Six clouds were negatively charged. The field profile in them is shown in Figure 28a and in Appendix XLd. The mean negative charge amounted to -6.4 e.s.u./m^2, the mean charge density being about 1.2×10^{-2} e.s.u./m^3; at the upper and lower cloud boundaries, the charge density decreased sharply. The total charge of the cloud was always positive (with the exception, of course, of unipolar, negatively charged clouds). The negative charge density was lower as a rule than the positive charge density. Data on the space charge densities in clouds of different structures are given in Appendix XXI. Several multiply-charged clouds were observed among those of the St-type. The field intensity and space charge density are highest in multiply-charged clouds. As a rule, multiply-charged clouds are thicker than doubly and singly-charged clouds.

The field vectors above and below charge clouds having unipolar charge were most often opposite in direction.

Stratus clouds can considerably affect the variation of the field in the atmosphere. Figure 29a gives the field variation with altitude on days when stratus clouds prevail. Only those cases where clouds of other types did not exist are considered. The field variation on days when St clouds prevail, plotted for 37 ascents, shows that stratus clouds not only modify the field, but also affect its variation beneath the clouds. Under their influence, a negative space charge appeared near the earth's surface. A negative space charge was also observed somewhat higher than the clouds, at altitudes of 1800-3000 m and higher than 5000 m.

The field profiles on days when stratified clouds prevail resemble the field variation in the case of profiles of Group III on clear days, i.e., in the zone occupied by stratified clouds, the atmosphere transfers charges to the earth.

It follows from the data of Figure 29a that the mean field intensity under stratified clouds in the layer 0-200 m is lower than on days with fair weather, and this is due to the appearance of a negative space charge at the earth's surface. Under the influence of stratified clouds, the potential at an altitude of 6000 m decreases (Appendix XIX, V_{6000}); whereas on clear days it amounts to 220 kv, on days when stratified cloudiness prevails, it is equal to 170 kv. The total charge of a unit air column in the layer 0-6000 m (Appendix XIX, Q_{0-6000}) is hardly influenced by stratified clouds.

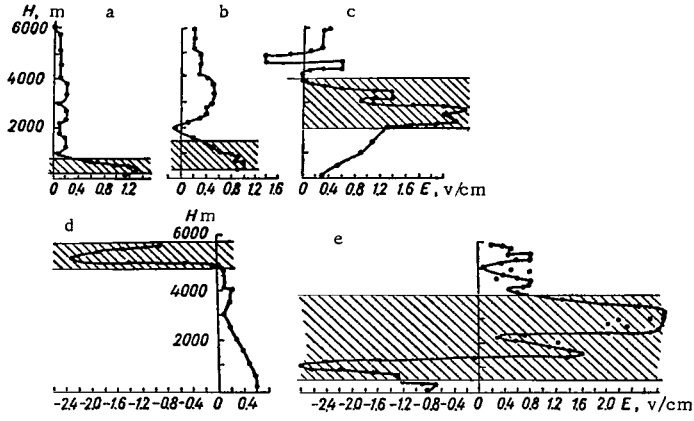

FIGURE 29. Field variation with altitude near Leningrad when clouds of some single type prevail in the absence of all other types.

a — St (37 cases); b — Sc (117 cases); c — As (30 cases); d — Cs (11 cases); e — Ns (75 cases). The shaded area denotes the region occupied by the clouds.

It should be noted that the potential difference between the upper and lower boundaries of stratified clouds depends largely on their thickness and may be considerable, sometimes on clear days, even exceeding the potential of the atmosphere at an altitude of 6000 m. The dependence of the potential difference ΔV on the cloud thickness is shown in Table 12, which is based on data of observations made in 1959.

TABLE 12.

Cloud thickness, m	100-200	200-500	500-1000
ΔV, kv	16	47	-177

It follows from the data of Table 12 that the potential difference ΔV in clouds thicker than 500 m has the opposite sign and is comparable in magnitude to the potential V_{6000} in clear weather.

Appendix XXXV gives summary data on the electric characteristics of clouds with different electric structures.

The relationships between the electric structure and the mean thickness of clouds and between the electric structure and the mean altitude of their lower boundary are given respectively in Appendices XXXIa and XXXIb. We see that doubly-charged clouds are thicker than singly-charged ones. There are still insufficient data on clouds with a more complex electric structure than those considered.

The mean altitude of the lower boundary of clouds apparently plays an insignificant role in the formation of some type of electric structure.

The electric characteristics of stratified clouds vary somewhat from summer to winter. This is illustrated by the data of Appendices XXXII and XXXIII, from which it follows that in winter, the absolute mean values $\overline{E}$ and mean maximum values E_{max} of the field intensity are lower. The potential differences (V_u—V_l) between the upper and lower cloud boundaries and

both the mean $\overline{Q}$ and the absolute mean maximum $|\overline{Q}_{max}|$ values of an aircraft's charging rate are considerably smaller in winter.

§ 3. ELECTRIC STRUCTURE OF STRATOCUMULUS CLOUDS

In this section, data of investigations in 1958-1959 on approximately three hundred and fifty stratocumulus clouds are analyzed.

The thickness of the investigated clouds varied between 100 and 1800 m. Their mean thickness was 500 m, and the mean altitude of the lower boundary was about 800 m.

The mean field intensity in them was +0.3 v/cm, the maximum E_{max} = 14.0 v/cm, the minimum E_{min} = −16.0 v/cm. More detailed electric characteristics of these clouds are given in Appendix XIX.

In individual clouds, the mean values of the field intensity may differ considerably from those given in Appendix XIX.

Appendix XXVI gives the probability of mean field intensity values (averaged over thickness intervals of 100 m) in stratocumulus clouds. Over 80 % of the measured values of the field were in the range from −2 to 4 v/cm, with almost 50 % in a narrow interval from 0 to 2 v/cm.

The dependence of the mean E and maximum E_{max} (calculated as the mean of the absolute maximum values for all the clouds) field intensity, and also of the excess space charge ρ, on the cloud thickness is given in Appendices XXVII, XXVIII, and XXIX. Figure 27 gives the dependence for different observation points. The mean field intensity in stratocumulus clouds depends only slightly on their thickness, and the mean maximum field intensity increases almost linearly with the cloud thickness. The dependence of the field intensity of clouds on their thickness does not vary appreciably with geographical latitude.

Winter and summer stratocumulus clouds have somewhat different characteristics, as can be seen from the data of Appendices XXXII, XXXIII and XXXIV. It follows from these data that clouds with a negative polarity prevail in summer and clouds with a positive polarity prevail in winter. The field intensity in summer clouds is higher than in winter clouds; the mean excess charge of clouds is also larger in summer.

The electric structures of stratocumulus clouds also differed, but like the structures of stratus clouds, they could be reduced to four basic types. Only a certain number of clouds (about ten) had a more complex structure, not corresponding to those given below.

Of the approximately 170 clouds investigated in Leningrad, 85 were positively polarized. In this case, an excess positive charge was observed in the clouds. The variation of the field E with altitude in clouds of this structure is shown by curve 1 in Figure 30a (the ordinate gives the reduced cloud height). The variation of the field in individual clouds is close to the averaged variation shown in Figure 30a. Appendix XLIa gives the field variation with altitude in individual clouds (reduced variation). The small value of the root-mean-square deviation σ from the mean value is not worth considering.

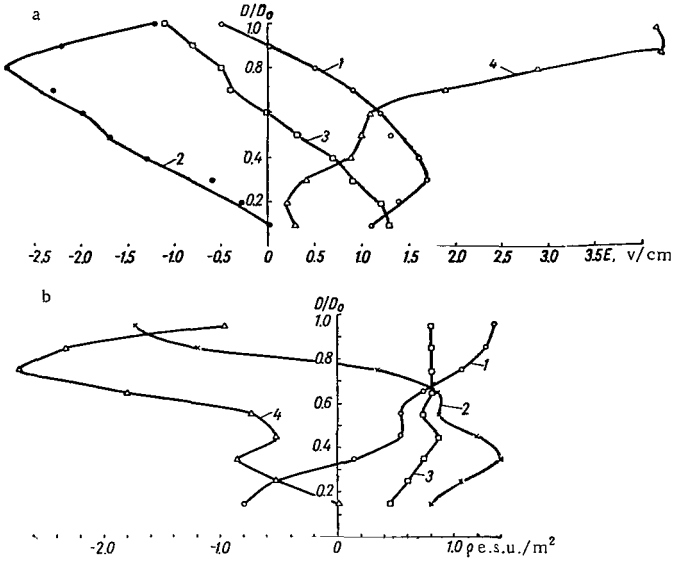

FIGURE 30. Reduced variation of the field E (a) and of the space charge (b) in Sc clouds.

1 — positively polarized clouds (77 cases); 2 — negatively polarized clouds (23 cases); 3 — positively charged clouds (41 cases); 4 — negatively charged clouds (13 cases).

The lower third of the cloud had a negative space charge of -1.6 e.s.u./m^2 with a mean density of -2.1×10^{-2} e.s.u./m^3. The mean excess positive charge of the cloud was 4.2 e.s.u./m^2 with a mean density of 1.1×10^{-2} e.s.u./m^3. The upper two thirds of the cloud had a positive charge of 5.8 e.s.u./m^2 with a mean density of 1.6×10^{-2} e.s.u./m^3. By representing the electric structure of the cloud as two oppositely charged layers with an excess positive charge, it is possible to obtain the data given in Appendix XXX.

Twenty-six clouds have a negative polarization and an excess positive charge. The field variation in these clouds is shown in Figure 30a (2). The variation of the field in individual clouds is given in Appendix XLIb. It is significant that the field in these clouds was negative. The upper third of the clouds has a negative charge of -5 e.s.u./m^2 with a mean density of 4.1×10^{-2} e.s.u./m^3; the lower two thirds had a positive charge of 7.5 e.s.u./m^2 with a mean density of 2.6×10^{-2} e.s.u./m^3. The mean excess positive charge was 2.5 e.s.u./m^2, and its mean density is 0.3×10^{-2} e.s.u./m^3. The field rose and fell almost linearly, i.e., the space charge density in the corresponding sections was constant over the height of the clouds. The electric structure of this cloud can also be represented as two oppositely charged layers with an excess charge. Data on this structure are given in Appendix XXX.

Many stratocumulus clouds were unipolar. Forty one clouds had a positive charge. The field profile in these clouds is shown in Figure 30a (3)

(Appendix XLIIIc). It is important to note that such a variation of the field is often observed also when the electric field above and below the cloud is positive. The charge of these clouds was on the average 6.9 e.s.u./m^2 with a mean space charge density of 2×10^{-2} e.s.u./m^3.

Fourteen clouds were found to be negatively charged. The field variation with altitude in this case is shown in Figure 30a /4/ and in Appendix XLIIId. As follows from these data, the negative charge is concentrated mainly in the upper half of the cloud. The magnitude of this charge was about -11 e.s.u./m^2 with a mean density of -1.9×10^{-2} e.s.u./m^3. The space charge density in the upper part of the cloud exceeded this value by a factor of three. Clouds of this structure had the highest field intensities.

In addition to the types of structures considered, several cases were observed when the charges in the clouds were small, and the fields created by them were hardly noticeable. These cases are referred to uncharged clouds. Multiply-charged clouds were observed in 9 cases. The influence of the cloud thickness and of the altitude of its base on the type of electric structure is shown in Appendices XXXIa and XXXIb. It is seen that with increasing mean cloud thickness there is a tendency for the electric structure to become complex. The altitude of the lower cloud boundary does not affect the type of structure to any significant degree.

Stratocumulus clouds considerably affect the field profile. Figure 29b gives the field variation with altitude in days with stratocumulus clouds. The curve is based on the data of 117 soundings on days when there were no clouds of other types. Stratocumulus clouds reduce the field at the earth's surface and increase it at high altitudes; like stratus clouds, they change the field direction above the upper boundary and give rise to a negative space charge above the clouds. The field profile greatly resembles the profiles of group III on clear days. In Figure 29b, the range of altitudes at which the stratocumulus clouds were situated on the days of the investigations is shaded.

Figures 31 gives the field variations with altitude in the presence of stratocumulus clouds with a given type of electric structure and in the absence of clouds of other types. The ordinate gives the reduced heights, i.e., the heights obtained by dividing the region from the earth to the cloud into five parts, the clouds itself into ten parts and, finally, the region above the cloud into five parts. For each part, the mean electric field intensity was found.

As can be seen, the indicated profiles show both general features and sharp differences. Thus, in all cases, the electric field below the cloud varies very little, and the space charge below the cloud is therefore very small. Below positively polarized and positively charged clouds, the electric field values are higher on the average than below negative and negatively polarized clouds. Below positively polarized and positively charged clouds the mean space charge is negative, and below negatively polarized and negatively charged clouds, positive.

The field profiles in clouds were discussed above.

A layer of negative charge is situated above all clouds except in the case of negatively charged clouds, above which a layer of positive charge is situated. Above this layer, the field intensities and the charges are small.

The potential of the atmosphere at an altitude of 6000 m on days when stratocumulus clouds prevail is approximately 170 kv, i.e., somewhat lower than the potential V_{6000} in clear-weather days. In turn, the mean charge in the layer from 0 to 6000 m ($\overline{Q}_{0-6000}$) is one third that as on days with clear weather (Appendix XIX).

The potential difference between the upper and lower boundaries of stratocumulus clouds depends to a large extent on their thickness, often amounting to an appreciable fraction of the atmosphere's potential on clear days at 6000 m, and sometimes even exceeding it. In many cases, the potential difference between cloud boundaries has a sign opposite to the potential of the atmosphere in the 0-6000 m layer. Table 13 gives the potential difference ΔV between the upper and lower boundaries of 90 stratocumulus clouds investigated in Leningrad in 1959.

TABLE 13.

Cloud thickness, m	100-200	200-500	500-1000	1000-1800
ΔV, kv	2	27	-40	-235

It should not be considered that clouds of large thicknesses necessarily have a negative potential drop. In many cases, a positive potential difference is also observed; thus, from investigations in 1958, the potential difference between the boundaries of stratocumulus clouds more than 1000 m thick was about 100 kv.

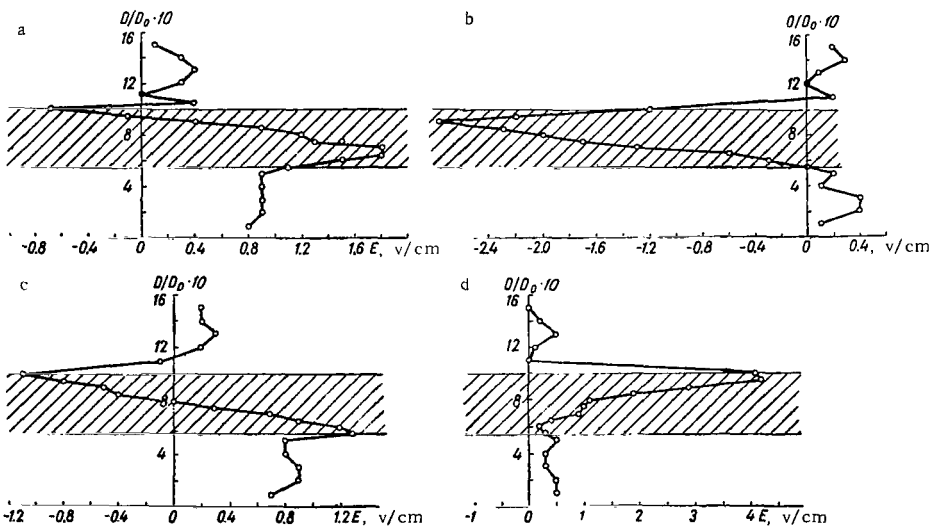

FIGURE 31. Variation of the electric field E with the reduced height D/D_0 in the presence of stratocumulus clouds with a definite type of electric structure and in the absence of clouds of other type.

a — in the case of positively polarized clouds (72 cases); b — in the case of negatively polarized clouds (20 cases); c — in the case of positively charged clouds (38 cases); d — in the case of negatively charged clouds (10 cases).

§ 4. ELECTRIC STRUCTURE OF ALTOSTRATUS CLOUDS

In this section, data of investigations on 218 clouds are analyzed.

The mean field intensity in them was about −2 v/cm, the maximum being 6.5 v/cm and the minimum 14.5 v/cm. The mean thickness of the investigated clouds was 950 m, and the mean altitude of their lower boundary 3400 m. More detailed data on these clouds are given in Appendix XIX. In individual clouds, the field may appreciably deviate from the mean values given. Appendix XXVI gives data on the distribution of the measured field values in altostratus clouds. The field values are averaged over a layer 100 m thick. More than 80 % of all the cases are found within the field range from −1 v/cm to 6 v/cm, with more than 50 % of all the values within the range from −1 v/cm to 3 v/cm.

The mean field intensity in these clouds, according to data of measurements in Leningrad and Kiev, increases with the thickness, and the maximum field intensity in them increases very strongly with the thickness. The mean field intensity in thick clouds is on the average (Appendices XXVII-XXIX) 8 times as high as in thin clouds, and the maximum field intensity is 26 times as high. The potential difference between the cloud boundaries increases very rapidly with its thickness. When the cloud thickness increases by less than a factor of 10, the potential difference $(V_u - V_l)$ increases by more than a factor of 40.

Since both the mean $|\overline{Q}|$ and the maximum mean $|\overline{Q}_{max}|$ aircraft charge also strongly increases with the cloud thickness, it can be assumed that with increasing thickness of clouds, their liquid water content and the particle sizes in them increase considerably. Although special measurements have not been made, it can be said with certainty that the high field intensities in thicker clouds are no doubt connected with the enlargement of the particles in them up to the size of rain particles, and, in a number of cases, with the appearance of precipitating zones in them.

The electric state of altostratus clouds varies greatly with the changing of the seasons (Appendices XXXII-XXXIV). In summer, both the mean $|\overline{E}|$, and the maximum mean values $\overline{E}_{max}$ of the field are considerably higher than in winter at all the observation points. Accordingly, the potential difference $(V_u - V_l)$ between the upper and lower cloud boundaries is larger; the excess space charge in clouds is also larger as a rule, and so on.

This intensification of the electric phenomena occurring in clouds is particularly noticeable in the passage from winter to summer in Tashkent. It should be noted that these clouds often consist of solid particles in winter.

The four basic electric structures indicated above are also observed in altostratus clouds.

According to data of measurements in Leningrad, of 89 clouds investigated, 26 had a positive polarization (Figure 32, curve 1 and Appendix XLIIa). The upper positive charge was approximately 3 e.s.u./m^2, the lower positive charge was 4.8 e.s.u./m^2, and the excess charge was negative, being equal to −1.9 e.s.u./m^2.* If we represent the cloud as a polarized layer with an excess negative charge, then the upper polarized charge will be 2.9 e.s.u./m^2 and the lower polarized charge, −2.9 e.s.u./m^2.

* [We suggest this sentence should read: The upper positive charge was approximately 3 e.s.u./m^2, the lower negative charge was −4.8 e.s.u./m^2, and the excess charge was negative, being equal to −1.8 e.s.u./m^2.]

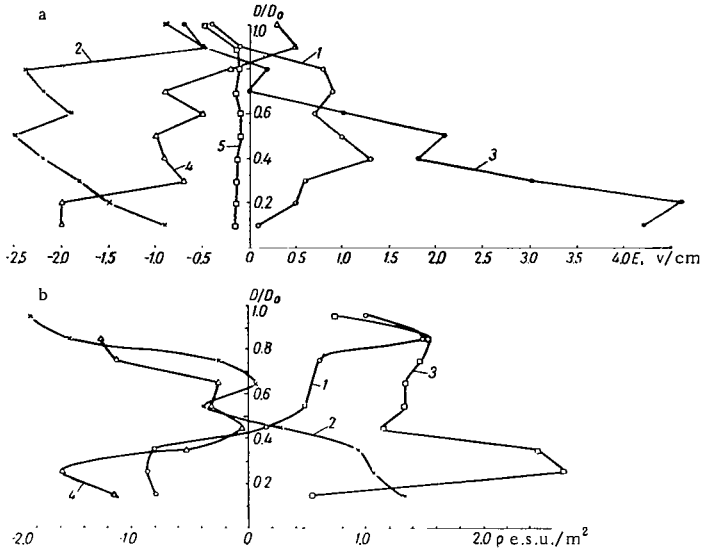

FIGURE 32. Reduced variation of the electric field E (a) and of the space charge (b) in clouds of the type As.

1 — positively polarized clouds (26 cases); 2 — negatively polarized clouds (23 cases); 3 — positively charged clouds (18 cases); 4 — negatively charged clouds (10 cases); 5 — weakly charged clouds.

The spread of the individual values from the mean value is comparatively small (Appendix XLIIa). In 23 cases, a negative cloud polarization was observed. The upper, negative charge was -3.2 e.s.u./m^2 and the lower, positive charge, 3.2 e.s.u./m^2. The excess charge was zero (Figure 32b, curve 2 and Appendix XLIIb).

It should be noted that in the case of this structure, the field maintains negative values throughout the whole cloud thickness.

In both types of polarized clouds, the charges were concentrated at their boundaries; in the middle part of the clouds, the space charges were negligibly small. Positively charged clouds were observed in 18 cases (Appendix XLIIc and Figure 32), the mean charge in them being 15.7 e.s.u./m^2; since the number of clouds investigated is small, the mean deviation σ. (Appendix XLIIc) is comparatively large.

In 10 of the clouds investigated, only negative space charges with a mean value of -6.1 e.s.u./m^2 were observed (Figure 32a, curve 4 and Appendix XLIId). In this case too, all the measured fields were negative.

Finally, in 10 cases very weakly charged clouds in which the field hardly varied with altitude were observed (Appendix XLIIe).

The dependence of the electric structure of clouds on their thickness and on the altitude of their lower boundary may be seen from the data of

of Appendices XXXIa and XXXIb. It follows from Appendix XXXIa that, in general, thick clouds have a tendency toward a more complex electric structure. The altitude of the lower cloud boundary does not appreciably affect the type of electric structure (Appendix XXXIc).

Altostratus clouds greatly affect the field variation with altitude. Figure 29c gives the field variation with altitude in days when only clouds of this type were observed. The range of altitudes at which the investigated clouds were observed is shaded.

As follows from the figure, altostratus clouds appreciably modify the field at the earth's surface. A considerable negative space charge is created under the cloud, which rises up to the lower boundary of the cloud. The potential at an altitude of 6000 m rises up to 265 kv (Appendix XIX). The potential difference between the cloud boundaries is about 87 kv on the average. The field variation with altitude again resembles the profiles of group III during clear weather, but the mean field intensities are considerably higher than during clear weather.

§ 5. ELECTRIC STRUCTURE OF CIRROSTRATUS CLOUDS

The comparatively small number of cirrostratus clouds investigated /48/ makes it possible to make only a general estimate of their characteristics, without claim to a high reliability of the mean data given (Appendix XIX). The mean field intensity in cirrostratus clouds is 0 v/cm, the maximum absolute value is 20.0 v/cm, and the minimum, 9.0 v/cm. The mean thickness of the investigated clouds is about 1100 m, and the mean altitude of their lower boundary 5500 m.

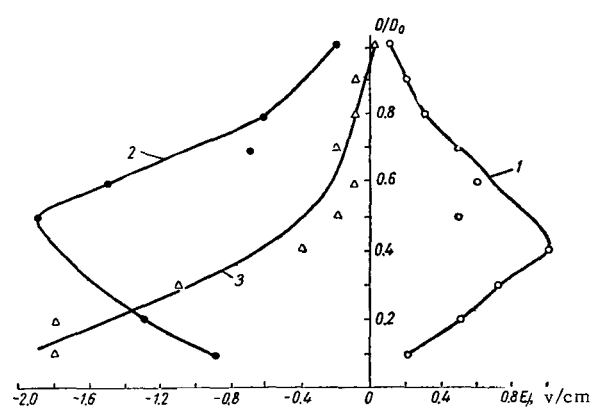

FIGURE 33. Reduced variation of the electric field E in Cs clouds.

1 — positively polarized clouds (8 cases); 2 — negatively polarized clouds (6 cases); 3 — negatively charged clouds (2 cases).

More detailed data on these clouds are given in Appendix XIX. In specific parts of the cloud, the field may appreciably differ from the mean values given. Appendix XXVI gives data on the distribution of the mean field intensities in cirrostratus clouds. The intensities are averaged over layers 100 m thick. Over 80 % of all the field values fall into the interval from −2 to 4 v/cm, and over 50 % into the interval from −2 to 1 v/cm.

The electric structures of cirrostratus clouds may be more complex than those considered earlier.

Of the 48 clouds investigated over Leningrad, 8 were positively polarized (Figure 33, curve 1, and Appendix XLIIIa). The charge in the upper part was 2.7 e.s.u. /m^2, and in the lower part −2.6 e.s.u./m^2; the excess charge was 0.1 e.s.u./m^2.

Six clouds were negatively polarized. The charge in their upper part was −3.5 e.s.u./m^2, and in their lower part, 1.6 e.s.u. /m^2; the excess charge was −1.9 e.s.u./m^2 (Figure 33, curve 2, and Appendix XLIIIb). Two clouds were found to be of single-negative charge (Appendix XLIIIc).

Six clouds had in the lower part a positive charge of a mean density of 3.5 e.s.u./m^2, in the central part, a negative charge with a mean density of −3.7 e.s.u./m^2 and in the upper part again a positive charge with a density of 3.5 e.s.u./m^2. The excess charge of the cloud was positive and equal to 3.3 e.s.u./m^2 (Appendix XLIIId).

Six cases were observed where there was a positive charge in the middle of the cloud and negative charges in its upper and lower parts (Appendix XLIIIe).

In 9 clouds negative, positive, again negative and positive charges alternated, the whole cloud having a small positive charge (Appendix XLIIIf). In 9 cases, the clouds were found to be very weakly charged (Figure 33, curve 3, and Appendix XLIIIg).

Cirrostratus clouds considerably affect the variation of the field with altitude. We return to Figure 29d, which gives the field variation with altitude on days when clouds only of the type under consideration were observed. The range of altitudes at which the clouds under consideration were observed is shaded; under these high-lying clouds, the field at the earth's surface is reduced. A positive charge, but of smaller magnitude than in the case of clear weather profiles of group I, remains under the cloud. The 6000 m potential is somewhat higher than on days with clear weather. The potential difference between the cloud boundaries is −323 kv on the average (Appendix XIX). Thus, Cs clouds considerably affect the electric field throughout the whole thickness of the troposphere.

§ 6. ELECTRICITY OF NIMBOSTRATUS CLOUDS

The appearance of nimbostratus clouds in the atmosphere has a very large effect on its electric characteristics.

Precipitation, which is capable of generating a significant electric current, considerably modifies the electrification conditions of clouds and of the atmosphere and makes possible their charging to significant potentials, creating considerable space charges.

However, it still remains unclear how precipitation particles from stratus clouds are charged (this being the process in the clouds which leads to their charging), how the conditions of development of a cloud affect its electric characteristics, and how its electric characteristics affect the development of the cloud.

Investigations in recent years have shown that the existence of nimbostratus clouds is closely related to their electric properties.

On one hand, the electric characteristics of clouds are the result of their development and can (particularly the macrocharacteristics) serve as an indicator characterizing the state of the cloud. As was shown earlier, a number of the electric characteristics of many forms of clouds vary considerably with a variation of the air moments in them /26/, with the enlargement of particles /19, 96/, and with a variation of cloud properties such as thickness.

On the other hand, a number of processes which determine the state of clouds depend on their electric characteristics. In particular, as the electric charges of small drops grow, the probability of their collisions increases if the charges are of different signs /38, 5/ and the electric forces can have a decisive role in this case. With the rise of the electric field, the coalescence efficiency of colliding drops with a diameter of hundreds of microns increases, amounting to less than 1/3 in the absence of an electric field, and reaching almost 9/10 in fields of 15 v/cm /81/. It can be expected (although this effect has not yet been studied experimentally) that an even greater role than this might be played by the electric field in the coalescence of cloud drops.

Investigations on nimbostratus clouds may be helpful to some extent in studying the development conditions of thunder clouds, although a complete identification of the conditions of their development, reducing the differences only to the scales of the phenomena as assumed by Chalmers /71/, cannot be expected. The point is that here is a current connected with precipitation charging nimbostratus clouds, and this aspect of the process is common for nimbostratus and for stratocumulus clouds, although the conditions of particle electrification in the two types of clouds are no doubt different. The electric processes taking place in stratocumulus clouds may be considered as occurring and as being quasi-stationary, this considerably facilitating study of the conditions of their charging by precipitation. In nimbostratus clouds, as well as in cumulonimbus clouds, conduction and diffusion currents occur, which reduce the polarization and charge of the clouds. At the same time, the large electric fields existing in thunder clouds, which give rise to point discharges on the earth and from drops in clouds, affecting processes of particle freezing and vapor transport, generation of lightning, etc., cause the processes in cumulonimbus clouds to differ from those in nimbostratus clouds. The investigation of the electric characteristics of nimbostratus clouds is also important for the study of atmospheric electricity in general, supplementing the information on the electric state of the atmosphere and the conditions of its charging.

Many investigators pointed out the importance and complexity of investigating the electric structure of nimbostratus clouds. Sivaramakrishnan /106/ wrote in 1962: "In any discussion on the origin of electricity carried by rain and of charges causing variation of the field,

it is necessary to consider the electric structure of the cloud." He goes on to say: "Very little, however, is known about the electric structure of clouds giving a continuous rain, i.e., nimbostratus clouds... ." He also mentions the experimental difficulties of such an investigation. Chalmers /71/ wrote in 1958: "Electric effects undoubtedly occur in connection with nimbostratus clouds, but these are much less intense than those associated with cumulonimbus clouds, and are therefore less easily investigated." He goes on to say: "The electric structure of nimbostratus clouds is not only of interest in itself, but the results obtained may also have some bearing on the problems of charge separation in cumulonimbus clouds."

The first attempt at establishing the electric structure of nimbostratus clouds was made by Chalmers /71/. In his calculations, he used data on the air-earth current and on the field at the surface upon the passage of these clouds. He also made a number of assumptions regarding the conditions under which electrification of precipitation particles takes place and the levels where this occurs. Using the above method, Chalmers obtained several possible electric structures of these clouds.

The first experimental investigations /17, 20/ generalized the macrocharacteristics of nimbostratus clouds. For the first time, experimental data on the magnitudes and vertical distribution of the electric field in these clouds were examined and an attempt was made at determining their electric structure.

In /17/, in particular, it was pointed out that the electric structure of nimbostratus clouds in a number of cases is more complex than the structure of other clouds of stratified forms. We assumed that these results could to some extent be due to differences in the data-processing methods used.

This section gives results of a further study of data obtained during systematic soundings of the electric field variation with altitude using the technique described earlier.

To obtain typical profiles of the electric field in the case of nimbostratus clouds, the method of reduced altitudes, mentioned at the beginning of the chapter, was used.

In data-processing, considerable use was made of data given in /39/. Separate comparisons were made of the field intensities at the reduced altitudes below the clouds, in the clouds, and above them. The data of investigations carried out in Leningrad were mainly used.

It is known /71/ that nimbostratus clouds from which rain falls have different electric characteristics to those from which snow falls. An attempt was therefore made to find out the respective features of clouds giving liquid and solid precipitation.

Electric structure of rain-producing nimbostratus clouds

The field distribution in these clouds is shown in Figure 34. The cases in Figure 34a correspond to positive cloud polarization, and the cases in Figure 34b to negative polarization. Judging from the number of cases, both polarizations are equally probable in nimbostratus clouds.

Let us consider the case in Figure 34a. The graph is based on the averaging of data on 31 clouds with a mean thickness of ~2500 m and a mean altitude of the lower boundary of ~800 m. The field under the cloud is positive, small in magnitude, and weakly decreasing with altitude. A negative charge is situated in the lower part of the cloud, and a positive charge in the upper part. The charge density at the top and the base of the cloud is higher than in its center.

The charge of the air under the cloud is 0.8 e.s.u./m^2. The charge situated in the lower third of the cloud is −15 e.s.u./m^2. The charge in the center of the cloud is very small, amounting to −1.5 e.s.u./m^2. A charge of 10 e.s.u./m^2 is situated at the upper boundary of the cloud. A positive charge of 2.7 e.s.u./m^2 is situated in a layer of 1000 m above the cloud. The cloud on the whole is not only polarized, but also charged negatively with a charge of −5 e.s.u./m^2. The whole atmospheric layer up to an altitude of 6000 m is also charged with a negative charge of −2.7 e.s.u./m^2 on the average. The potential at an altitude of 6000 m on days with clouds of this type is ~1500 kv, on the average reaching ~32×10^3 kv on individual days.

Let us consider Figure 34b, where the case of a negative cloud polarization is shown. The graph is based on the averaged data on 27 clouds having a mean thickness of 2000 m and a mean lower boundary altitude of 900 m.

The field under a typical cloud is negative and weakly decreases, which corresponds to a small positive charge under the cloud (about 3.0 e.s.u./m^2). The charge in the lower part of the cloud is positive, amounting to approximately 11.4 e.s.u./m^2. The charge of the upper two-thirds of the cloud is negative, amounting to approximately −10.5 e.s.u./m^2. Above the cloud, there is a negative charge of about −3 e.s.u./m^2.

The cloud as a whole has a small positive charge (about 1 e.s.u./m^2). The whole layer of the atmosphere from the surface to an altitude of 6000 m has a negative charge of approximately −2 e.s.u./m^2. The potential at an altitude of 6000 m in the case of clouds of this type is on the average 700 kv, reaching 4000 kv on individual days.

Electric structure of snow-producing nimbostratus clouds

The distribution of the electric field in these clouds is shown in Figure 35.

The case in Figure 35a corresponds to a positive cloud polarization, and the case in Figure 35b to a negative cloud polarization; the case in Figure 35c is somewhat specific, being intermediate between the first two. From the number of different polarization cases, the first two are equally probable, the third occurring considerably more rarely.

We now consider the case of Figure 35a, which presents the distribution of the electric field in a positively polarized cloud, based on data on 37 clouds with a mean thickness of 2000 m and a mean lower boundary altitude of approximately 1000 m.

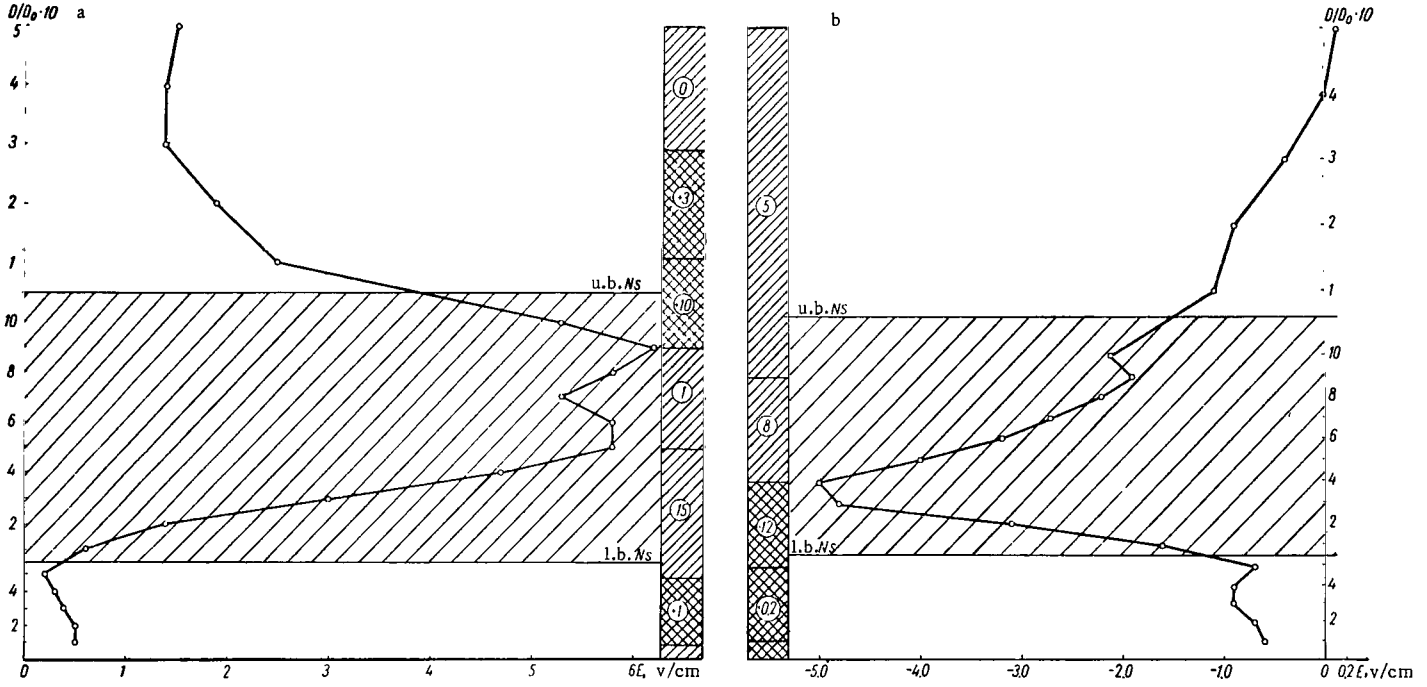

FIGURE 34. Reduced variation of the electric field E and of the charge distribution q in Ns clouds from which precipitation is in the form of rain, from data of measurements made in Leningrad during 1958-1963.

a — positively polarized clouds (31 cases); b — negatively polarized clouds (27 cases); l.b.and u.b. — lower and upper cloud boundaries. The encircled figures give the magnitude of the charge in e.s.u. /m^2.

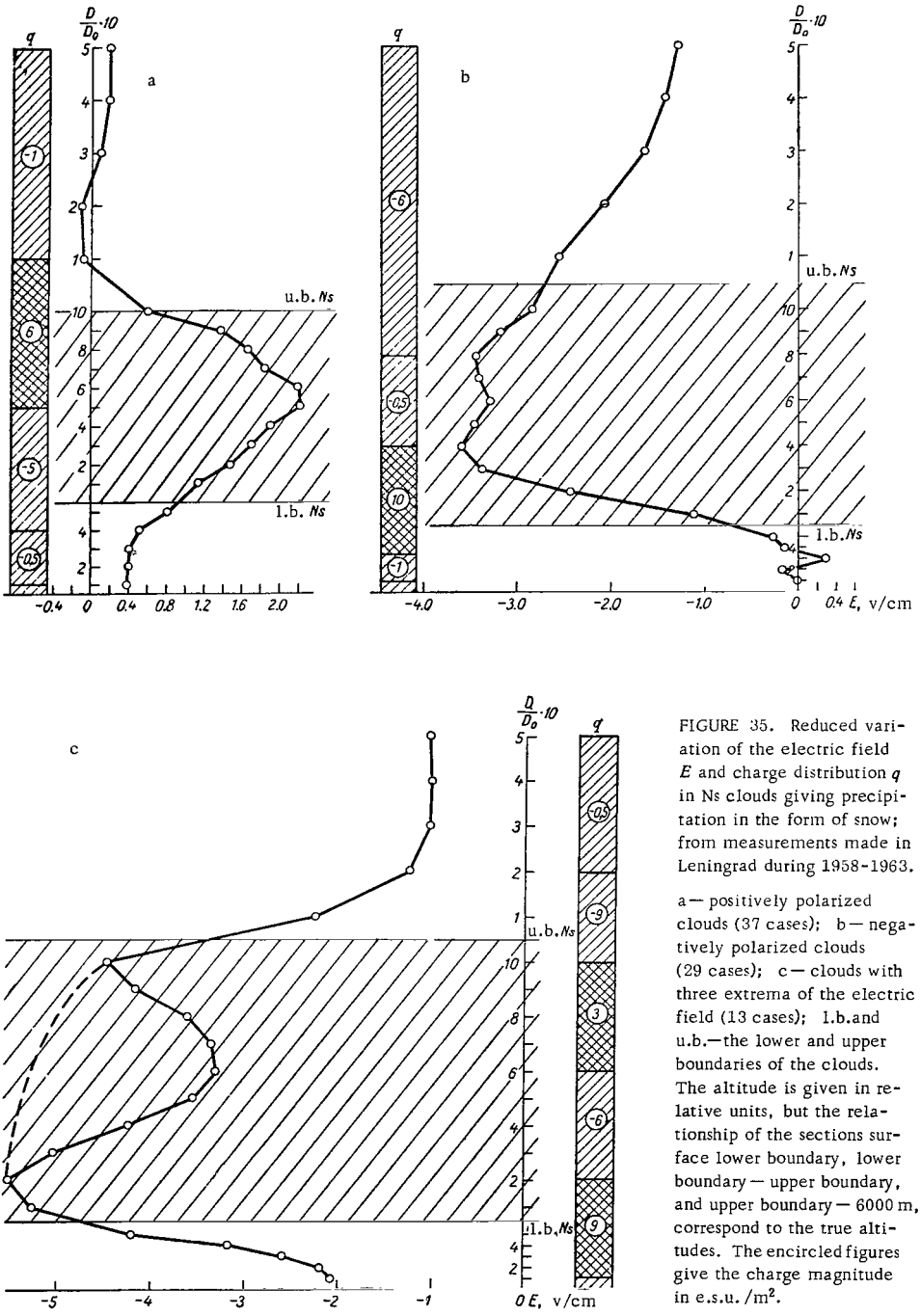

FIGURE 35. Reduced variation of the electric field E and charge distribution q in Ns clouds giving precipitation in the form of snow; from measurements made in Leningrad during 1958-1963.

a — positively polarized clouds (37 cases); b — negatively polarized clouds (29 cases); c — clouds with three extrema of the electric field (13 cases); l.b.and u.b.—the lower and upper boundaries of the clouds. The altitude is given in relative units, but the relationship of the sections surface lower boundary, lower boundary — upper boundary, and upper boundary — 6000 m, correspond to the true altitudes. The encircled figures give the charge magnitude in e.s.u./m^2.

The electric field under a typical cloud is positive and rises slightly with altitude. In the lower half of the cloud, and immediately beneath it, the electric field rises almost linearly. In the upper half of the cloud, the field decreases, this decrease being steeper in the upper part of the cloud. Above the cloud, the field continues first to decrease to small negative values, and then slowly returns to small positive values; at the maximum sounding altitude, it becomes equal to 0.2 v/cm. The negative charge beneath the cloud is about -1 e.s.u./m^2; the negative charge in the lower part of cloud is about -4 e.s.u./m^2; the positive charge in the upper part of the cloud is approximately 5 e.s.u./m^2; the negative charge above the cloud is approximately -0.8 e.s.u./m^2. The cloud as a whole is positively charged (2 e.s.u./m^2). The whole atmospheric layer up to an altitude of 6000 m is also positively charged (0.5 e.s.u./m^2).

The potential at an altitude of 6000 m is 250 kv on the average.

Let us consider the distribution of fields in negatively polarized nimbostratus clouds giving precipitation in the form of snow. The graph of the field variation with altitude in this case is based on averaged data on 29 clouds with a mean lower boundary altitude of $\sim$600 m, and a mean thickness of $\sim$3000 m (Figure 35b). The electric field under a typical cloud is mainly negative and slightly decreases with altitude, which corresponds to a positive charge under the clouds of $\sim$06.e.s.u./m^2. The absolute value of the electric field in the lower third of the cloud rises steeply up to the maximum value ($\sim$3.6 v/cm). In the center of the cloud the field varies only slightly with altitude, and in the upper third it decreases; this decrease is approximately linear and continues by the same law also above the cloud. The charge in the lower part of the cloud is approximately 9 e.s.u./m^2, in the center of the cloud approximately -0.3 e.s.u./m^2, in the upper third of the cloud approximately -2.7 e.s.u./m^2, and above the cloud approximately -3.5 e.s.u./m^2.

The cloud as a whole is positively charged ($\sim$6 e.s.u./m^2). The whole atmospheric layer up to 6000 m is also positively charged ($\sim$3 e.s.u./m^2).

The potential at an altitude of 6000 m is about 600 kv. In a few cases clouds were observed which had a negative electric field and extrema in both their upper and lower parts.

The electric field distribution in these clouds is given in Figure 35c, which is based on averaged data on 13 clouds with a mean thickness of $\sim$3300 m and a mean lower boundary altitude of $\sim$600 m.

The electric field under such a cloud is negative, increasing with altitude, slightly at first, and then more and more steeply as it approaches the cloud. The field in the lower quarter of the cloud continues to increase in absolute value; it then decreases, increasing again in the upper part of the cloud. The steepest increase is observed at the upper boundary of the cloud. The electric field above the cloud decreases sharply in absolute value.

The positive charge under the cloud is equal to $\sim$5.6 e.s.u./m^2. The positive charge in the lower part of the cloud is equal to $\sim$4 e.s.u./m^2; the negative charge in the center of the cloud is equal to approximately -6 e.s.u./m^2; the positive charge in the upper part of the cloud is equal to $\sim$3 e.s.u./m^2; the negative charge above the cloud is equal to approximately 9 e.s.u./m^2. The cloud as a whole has a small negative charge of -0.5 e.s.u./m^2.

The entire atmosphereric layer from the surface to 6000 m is also negatively charged (-3 e.s.u./m^2). The potential at an altitude of 6000 m is -1700 kv.

In real clouds, the actual values of the field may differ from the mean values given above; for example, field intensities reaching approximately -23 v/cm have been observed in individual clouds. The mean field intensities exceed 15 v/cm (Appendix LII).

Electric structure of mixed nimbostratus clouds

In this section, clouds which precipitate rain or snow, but in which the 0° isotherm passes through the cloud, are considered. In this case, direct use of the technique used earlier for finding the characteristic structure leads to the conclusion that such clouds consist of four charges lying one above the other. It has been assumed that the electric structure of the cloud in this case is affected by the altitude of the 0° isotherm.

We recall that the method of reduced altitudes can give positive results if in the averaging sections the observed structure is a function of the altitude alone. The averaging was therefore made for the reduced thicknesses corresponding to the altitude intervals between the lower cloud edge and the level of the 0° isotherm, and between the level of the 0° isotherm and the altitude of the upper cloud edge. The field distribution in these clouds is shown in Figure 36, which is based on averaged data obtained during flights in mixed nimbostratus clouds over Leningrad, Kiev, and Tashkent.

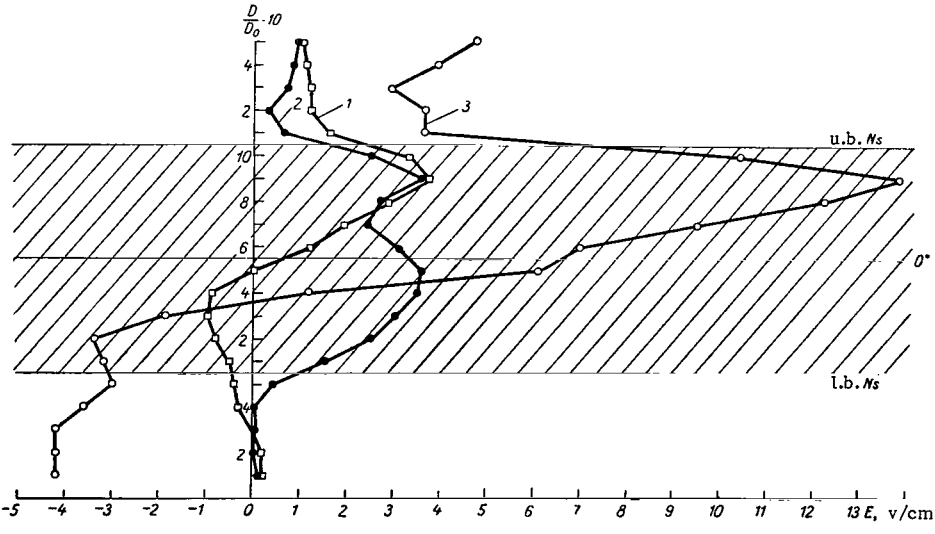

FIGURE 36. Reduced variation of the electric field E in Ns clouds of a mixed structure.

1 — Leningrad, 1958-1962 (52 cases); 2 — Kiev, 1960-1963 (11 cases); 3 — Tashkent, 1960-1961 (16 cases); l.b. and u.b. — the lower and upper boundaries of the clouds.

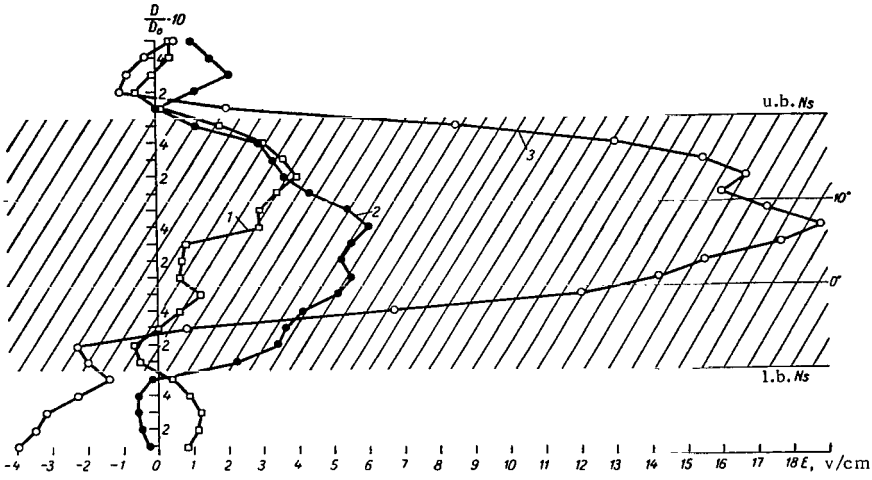

FIGURE 37. Reduced variation of the electric field E in Ns clouds of a mixed structure.

1 — Leningrad, 1960-1962 (18 cases); 2 — Kiev, 1960-1962 (7 cases); 3 — Tashkent, 1960-1961 (10 cases); l.b. and u.b. — lower and upper boundaries of the clouds.

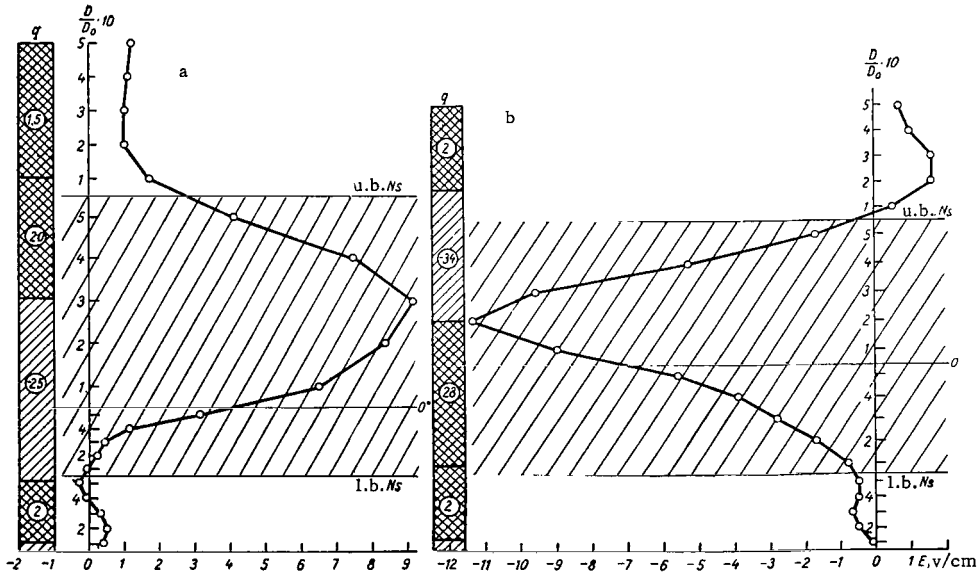

FIGURE 38. Reduced variation of the electric field E and charge distribution q in Ns clouds of a mixed structure, based on measurements made in Leningrad during 1958-1963.

a — positively polarized clouds (36 cases); b — negatively polarized clouds (15 cases); l.b. and u.b. — lower and upper cloud boundaries. The encircled figures give the charge magnitude in e.s.u./m^2.

It should be noted that allowance for the passage of the 0° isotherm showed clouds of this type to have a comparatively simple typical structure, surprisingly resembling in external form that obtained by Simpson and Scraze for cumulonimbus clouds. Figure 36 plainly shows that the maximum fields and charges in mixed nimbostratus clouds occur in the region above the 0° isotherm. As a rule, a small positive charge is situated beneath the cloud and in its lower part, a large negative charge higher up, and a large positive charge in the upper part of the cloud. Above the cloud, there is generally a small positive charge.

We conclude from the graph that the passage of the 0° isotherm through a cloud apparently has a significant effect on the electrification processes in it.

The influence of the temperature in clouds on their electrification processes is considered in more detail in Figure 37, where field profiles pertaining to the following altitude intervals are presented: ground level — the lower cloud boundary; the lower cloud boundary — the 0° isotherm; the 0° isotherm — the −10° isotherm; the −10° isotherm — the upper cloud boundary; and above the upper cloud boundary. Based on a small number of cases, these graphs show, despite insufficient averaging, that the region of the field maximum, or the region of charge separation in clouds of mixed structure, lies in the temperature interval from 0° to −10° and −12°, i.e., in the temperature range where liquid and solid particles most probably coexist and where intensive electrification processes, connected with their coexistence, occur.

The data of Figures 36 and 37 also show the rate of increase in electrification in mixed nimbostratus clouds as one moves to the south. The maximum field in a "typical" cloud over Leningrad is approximately 4 v/cm, over Kiev 6 v/cm, and over Tashkent more than 19 v/cm. With decreasing latitude, the mean values of the field in clouds also increase (about 1 v/cm over Leningrad, about 3.5 v/cm over Kiev, and more than 11 v/cm over Tashkent). The charges in the clouds also increase accordingly. A more detailed examination of the electric structure of mixed nimbostratus clouds showed that several types of cloud polarization are also encountered among them, the most typical being positive polarization (36 out of 60 cases) and negative polarization (15 out of 60 cases).

The graphs corresponding to these types of polarization are given in Figure 38.

Let us consider in Figure 38a the case of positive cloud polarization. The graph is based on averaged data for 36 clouds having a mean thickness of about 3500 m and a mean lower boundary altitude of approximately 800 m. The electric field under the cloud and in its lower third is very low and decreases slightly with altitude, which corresponds to a small positive charge under the cloud (about 2 e.s.u./m^2). The lower part of the cloud has a small negative charge (−2 e.s.u./m^2). There is a large negative charge (about −24 e.s.u./m^2) in the immediate vicinity of the 0° isotherm. The upper part of the cloud has a large positive charge (approximately 16 e.s.u./m^2), and the layer near the clouds has a positive charge (approximately 3 e.s.u./m^2). Higher up, the charge is practically zero. The total charge of the cloud is negative (about −8 e.s.u./m^2). The total charge of the atmosphere is also negative (approximately −2 e.s.u./m^2).

The potential at an altitude of 6000 m is approximately 2000 kv.

Let us consider the case (Figure 38b) when the polarization of the cloud is negative. The graph is based on averaged data for 15 clouds with a mean thickness of approximately 3000 m and a mean lower boundary altitude of 900 m.

The electric field under the cloud and in the cloud is negative and becomes positive only above the cloud.

Beneath the cloud and in its lower part, the electric field intensity is low, slightly decreasing with altitude, which corresponds to a small positive charge under the cloud (about 0.8 e.s.u./m^2).

The maximum field intensities occur somewhat higher than the 0° isotherm.

The positive charge in the cloud is approximately 29 e.s.u./m^2, and the negative charge at the upper cloud boundary is approximately -30 e.s.u./m^2. Directly above the cloud, there is a layer of negative charge (-3 e.s.u./m^2), and higher up, a layer of positive charge (3 e.s.u./m^2). As a whole, the cloud is almost uncharged, and the total charge of the atmosphere is small and negative, about -2.5 e.s.u./m^2. The potential at 6000 m is approximately -2000 kv.

Typical structures of nimbostratus clouds

The typical structures obtained for nimbostratus clouds are given in Figures 34, 35, and 38. As can be seen, the electric structures of pure-water clouds, snow clouds, and mixed-structure clouds are very similar.

Mixed-structure clouds are positively polarized in about 70 % of the cases, water clouds in about 54 % of the cases, and snow clouds in about 47 % of the cases. A positive charge in the case of negative cloud polarization, and a negative charge in the case of positive cloud polarization generally exists in the lower part of the cloud and beneath it. It should be noted that individual clouds may have electric fields and structures differing from the mean typical ones described above. Figure 39 gives the field variation in a cloud the lower part of which contained a positive charge, and the upper part, a negative charge (actual altitude given in Figure 39). It follows from the figure that, beginning from an altitude of 500 m, precipitation falling from it is negatively charged.

Figure 39 also shows the field distribution in a cloud of a mixed structure, in which, with a "normal" structure, field intensities reaching 150 v/cm and space charge densities exceeding 1 e.s.u./m^3 (i.e., close to the values encountered in thunder clouds) were observed.

As indicated earlier, Chalmers /71/ studied in England the electric current and field at ground level upon the passage of nimbostratus clouds. He pointed out that after averaging the data of all observations, the current density from snow-producing clouds is equal to -3.5×10^{-12} amp/m^2, and the field intensity is equal on the average to -57 v/cm, whereas in the case of rain-forming clouds, the mean total vertical current is equal to $+3.8\times10^{-12}$ amp/m^2 with a mean field intensity of -176 v/m. Although Chalmers specially points out that under conditions prevailing in England, the fall of liquid precipitation from pure water clouds is improbable, the

analysis technique applied by him did not make it possible to check this assumption, and we shall consider Chalmers' data as pertaining both to mixed, and to pure-water clouds.

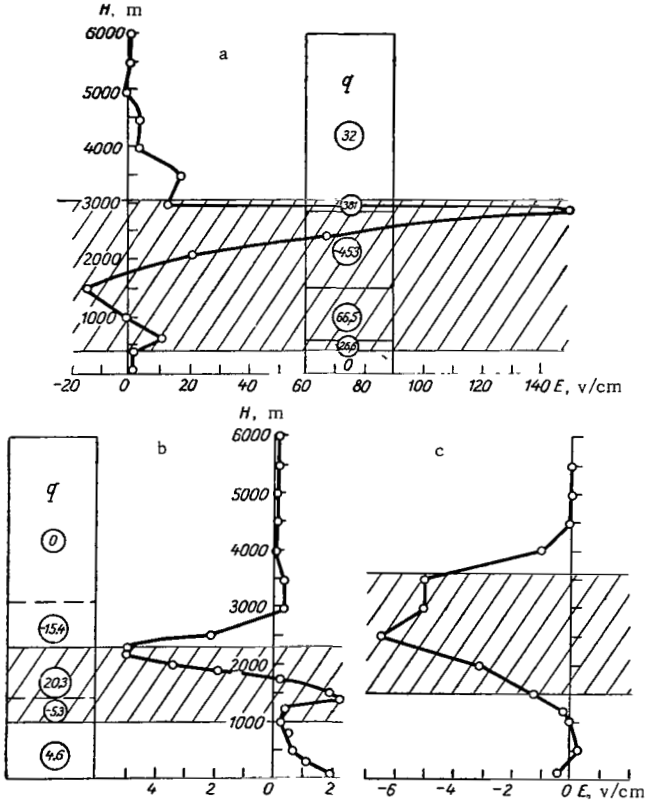

FIGURE 39. Reduced variation of the electric field E and electric structure in individual Ns clouds having a mixed structure.

a — Leningrad, 26 August 1959, 6 hr, mixed-structure clouds; b — Leningrad, 17 December 1959, 18 hr, cloud entirely in the region of below 0°C; c — Leningrad, 16 June 1959, 17 hr 30 min, "warm" cloud. The encircled numbers give the charge magnitude in e.s.u./m^2.

Chalmers' data show that negatively charged particles fall out from snow clouds in the case of a negative field, whereas in the case of other types of nimbostratus clouds, the so-called mirror effect appears, i.e., the electric field at ground level beneath the clouds has a sign opposite to the precipitation current from them. Sivaramakrishnan /106/, who studied in India the electric characteristics associated with nimbostratus clouds (also at ground level), also points out the existence of the mirror effect on the basis of over 200 observations. The conditions under which Sivaramakrishnan carried out his measurements made it possible for him to study the electricity only of those clouds which gave liquid

precipitation. In contrast to the data of Chalmers /71/, Simpson /105/ noticed that in England the sign of the charge of snow flakes at ground level is opposite to the sign of the field, and that with clouds giving snow, positive fields are observed when the snow flakes are negatively charged.

Chalmers /71/ attempted on the basis of his observations and some general considerations to determine the electric structures of snow- and rain-forming clouds. The absence of actual data on the processes of the electrification of precipitation particles, or at least on the levels at which this electrification occurs, made it necessary for him to consider several possible schemes assuming the electrification of particles to occur either in the clouds, or at ground level, or between the cloud and the earth.

Data on the height distribution of the potential in the case of rain-precipitating nimbostratus clouds, which were obtained by Chalmers /71/, are given in Figure 40 (Appendix XLIV). Curve 1 corresponds to Chalmers' assumption that electrification is observed in that region of the cloud where snow melting takes place. Figure 40 also gives the experimental curve 2 obtained by us for positively polarized rain-precipitating clouds. As can be inferred from a comparison of the curves, Chalmers succeeded in satisfactorily conveying the general character of the curve. Our data unambiguously show that in the case of rain-precipitating clouds, the main process of precipitation particle electrification takes place in the clouds. In clouds of a mixed structure, the main electrification zone is situated in the region of the 0° isotherm.

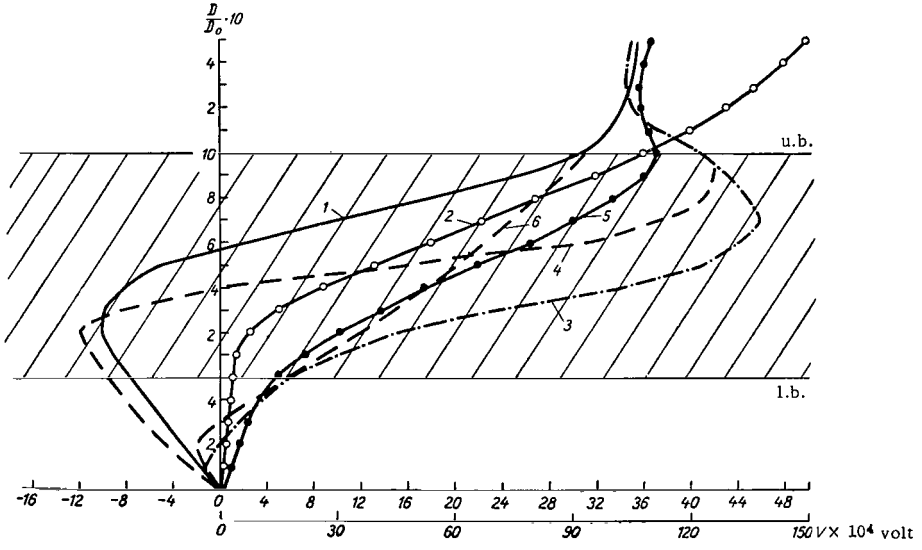

FIGURE 40. Potential distribution in rain and snow nimbostratus clouds.

1 — "warm" clouds (calculated by Chalmers /71/ on the assumption that the electrification of drops takes place in the clouds); 2 — Ns rain clouds (obtained from measurements made at GGO); 3 — snow clouds (potential distribution calculated by Chalmers /71/ on the assumption that the particles are electrified in the cloud); 4 — potential distribution (calculated by Chalmers /71/ on the assumption that particle electrification takes place at the surface); 5 — height distribution of potential (obtained from measurements made at GGO); 6 — calculated by Chalmers /71/ for rain clouds on the assumption that particle electrification takes place at the surface; l.b. and u.b. — lower and upper cloud boundaries.

This result largely explains the data obtained by Reiter /99/ on the conduction current and field at a number of mountain stations when these happen to be situated in nimbostratus clouds. In those parts of mixed-structure clouds where only snow was observed, a positive field occurs during 90 % of the whole observation period; in regions where both rain and snow were observed simultaneously, this ratio fell to approximately 30 %. In regions with rain alone, the ratio became equal to only 10 %. Despite all the difficulties connected with observation in mountains, when the position of the station with respect to the cloud is not accurately known, the closeness of the earth affects the processes in the clouds, and it is not known whether other clouds affect the measurement results. Reiter's data are well explained by Figures 34, 35, and 38.

The probability of a negative field appearing in the region of the 0° isotherm increases as one moves downward, and approaches 90 %.

The results of Chalmers' calculations /71/, referring to snow-precipitating clouds, are also given in Figure 40. Curve 3 is plotted on the assumption that the main charging of snowflakes takes place within the cloud, and curve 4 on the assumption that the charging takes place at ground level, or at a low altitude. For comparison, our data (curve 5), obtained by integration of the experimental curve of Figure 35a, are plotted on the graph. Curve 5 is in closer agreement with curve 3, obtained by Chalmers, and thus the conclusion that the main electrification processes in these clouds are connected with collisions and fractionation of snowflakes inside the cloud is confirmed. In fact, the space charge distribution obtained for snow-precipitating clouds unambiguously indicates that the electrification of snowflakes takes place in the middle of the cloud.

The discrepancy between curve 3, obtained by Chalmers, and the experimental data (Figure 35b and c) is explained naturally if we remember that Chalmers, in contrast to other authors, did not observe the mirror effect in the case of snow-precipitating clouds, i.e., he mainly studied positively polarized clouds. If the mirror effect mentioned by Simpson /105/ appears in the case of mixed clouds, and the current in the case of a negative field is positive, the use of Chalmers' scheme /71/ is conducive to the dependence represented by curve 1 in Figure 40. This dependence, corresponding to the case of charging inside the cloud, is similar to the one obtained experimentally.

Thus, the electricity of nimbostratus clouds is connected in all cases with processes which take place in the clouds themselves. The appearance of a negative cloud polarization is apparently connected with electrification mechanisms other than those acting in positively polarized clouds. From the field variation in these clouds the conclusion may be reached that also in this case the electrification of particles takes place inside the cloud.

Only in individual cases can it be assumed that the electrification of precipitation particles takes place at ground level. It is possible that the mechanisms which lead both to a positive and to a negative cloud polarization take place in almost all the clouds investigated, and that differences in polarization are due to the fact that one of the electrification mechanisms predominates. Thus, for example, in mixed clouds, electrification upon snow melting, electrification upon disintegration of snow particles, charging due to decrease of the conductivity in clouds, charging due to contact potential difference, and so on, may lead to different electrification signs.

An illustration of the field variation in the case of simultaneous action of two mechanisms (one more powerful than the other, but comparable in magnitude) may possibly be the field variation in snow-precipitating clouds, shown in Figure 35c. It can be assumed that this field variation is caused by the presence in the cloud of a mechanism which leads to intensive negative polarization (the curve completed by the broken line) and of a less powerful mechanism which leads to positive polarization.

Chapter V

SCHEME OF ELECTRIC PROCESSES IN THE ATMOSPHERE

§1. STRUCTURE OF THE ELECTRIC FIELD OF THE FREE ATMOSPHERE

It was already mentioned in Chapter I that many assumptions made on the basis of the spherical condenser theory can be checked by means of systematic soundings of the atmospheric electric-field variation with altitude. As shown by data given in this work, the variation of the electric field with altitude even on fair-weather days is often not monotonous; the field on days when stratified clouds prevail generally has a maximum at definite altitudes. The variation of the electric potential with altitude is accordingly also not monotonous.

The time variations of the potential at an altitude of 6000 m at various observation points were found not to be synchronous and were equal neither by amplitude nor by phase, for both diurnal and annual variations. These variations were also found to disagree with the corresponding unitary variations of the field (see Figures 1 and 18). The relative diurnal variations of the potential at a height of 6000 m amounted to 28, 22, and 50 % in Leningrad, Kiev, and Tashkent respectively during the International Meteorological Interval in June 1958.

The mean values of the potential during the variation periods also differ considerably from those calculated on the basis of the spherical condenser scheme. During the International Meteorological Interval in June 1958, the mean potential at an altitude of 6000 m was approximately 230 kv in Leningrad, 160 kv in Kiev, and 370 kv in Tashkent. During the International Meteorological Interval in September 1958, the values of the potential at these points were 220, 170, and 110 kv, and during the International Meteorological Interval in December 1958, they were 140, 140, and 150 kv.

The mean potential values on fair-weather days at an altitude of 6000 m during 1958-1961 were 140 kv in Leningrad, over 300 kv in Kiev, and about 205 kv in Tashkent (Appendices XVI and XVII).

Stratified clouds cause large deviations both of the mean values of the potential at an altitude of 6000 m, and of their variations at individual observation points (Appendix XVIII).

The diurnal unitary variation of the potential gradient was observed at the stations only in comparatively narrow altitude intervals. Above and below these altitudes, the electric field variation was determined mainly by the variation of the local space charges in the atmosphere.

On the other hand, Clark /74/ observed in measurements made over oceans unitary variation of the potential at an altitude of 6000 m. The number of measurements at Clark's disposal was small (only 5 full soundings and another one the results of which were extrapolated to the required altitude), and the time of the soundings was not very successfully chosen (it did not coincide with the time of the diurnal maximum). The 6 points obtained by Clark lay near the variation curve of the potential at an altitude calculated from data on the diurnal unitary variation, which was measured during the voyage of Carnegie in 1928-1929 on the basis of the spherical condenser theory. The correlation coefficient between the measured and calculated potentials was 0.89. The calculated potential of the ionosphere was 290 kv ± 10 %.

According to our measurements, this quantity should on the average amount to 220-260 kv on clear days, but for Kiev, for example, it increases to approximately 340 kv, and for Leningrad decreases to 170 kv.

At the same time, on fair-weather days, potentials exceeding the values of 220-260 kv and 290 kv are often observed at an altitude of 6000 m; much smaller, including negative, potentials can also be observed. These cases cannot be due to redistribution of the voltages as a result of conductivity variations in individual sections of the atmosphere.

In fact, processes taking place in the troposphere generally lead to an increase in resistance in the lower layers of the atmosphere. The measurements made by Clark /74/ over oceans pertain to the purest conditions. Measurements over the continents are made under considerably more polluted conditions, and consequently, lower conductivities exist in the lower layers of the atmosphere. According to Uchikava's data /111/, for example, the appearance of an inversion causing accumulation of pollutants in the exchange layer of the atmosphere almost doubles the atmospheric resistance in this layer. Similar variations follow from the works of Sagalyn and Fausher /100, 101/. Thus, a decrease in the potential at an altitude of 6000 m cannot be attributed either to a resistance decrease in the lower layers, or to a corresponding resistance increase in the atmospheric layers above 6000 m.

There are two possible ways of explaining the appearance of potentials at an altitude of 6000 m which exceed that of the ionosphere. It should be assumed either that space charges created by a mechanism different from that responsible for the vertical redistribution of the conductivity exist above the place of measurement, or that there is no potential difference between the earth and the ionosphere which would determine the electric field profile and its variation together with the vertical conductivity distribution. Small and even negative potentials at the height of 6000 m may be explained only by the influence of space charges of the atmosphere.

Thus, the number of relationships obtained cannot be explained by the spherical condenser theory in its present form. We will now consider a possible way of explaining the observed effects.

§2. CHARGE EXCHANGE BETWEEN THE EARTH AND THE ATMOSPHERE, AND THE MECHANISM DETERMINING ELECTRIC FIELD VARIATIONS COMMON TO THE ENTIRE GLOBE

The solution of the system of equations common to the whole earth and describing electric processes in the atmosphere and charge exchange between the earth and the atmosphere involves the description of generation and separation of charges in the atmosphere, of conduction currents in it, and the effect of the electric field on these processes.

As long as there are no data on these processes, one should consider individual components of the overall balance of currents which produce charge exchange.

Essentially, two approaches to the solution of the problem of charge exchange between the earth and the atmosphere are possible. A conducting atmosphere can be considered and, by determining the external emf's acting in it, the currents may be calculated and the dynamics of the process thus studied from the electrodynamic point of view. Obtaining the instantaneous values of the charge distribution in the atmosphere in successive time intervals, it is possible to solve the electrostatic problem for each interval and, by comparing successive distributions, to solve by means of certain assumptions the problem of how one quasistatic distribution transforms into another. It is more convenient to interpret the measurements described in the preceding chapters in the second way.

Let us consider the solution of the problem of the field and charge distribution in a neutral system consisting of a poorly conducting medium (Figure 41) bounded by two concentric "ungrounded" highly conductive spheres (1) and (2) (i.e., the scheme on which the spherical condenser theory is based).

Suppose a point charge $-q$ is somehow removed from a neutral, poorly conducting atmospheric medium and transferred to sphere (1). Suppose the region from which this charge is removed lies at a distance h_1 from the internal sphere (the earth). Then at the moment immediately after the charge transfer, the field in the whole space between spheres (1) and (2) can be represented as being due to a charge $+q$; a charge $-q$, which is uniformly distributed over the whole surface of sphere (1) (or concentrated in its center); and charges induced in the sphere as follows: $-q_1$, situated at a point lying on the straight line joining the center of the sphere and the center of the charge $+q$ at a distance $h_1' = \frac{h_1}{i + \frac{h_1}{R}}$ from the surface of the sphere; a charge $+q_1$, situated in the center of the sphere (or uniformly distributed over its surface); a charge $-q_2$, induced by the charge $+q$ in the hollow sphere (2); a charge equal to it $+q_2$, which provides the quasineutrality of sphere (2) and which is uniformly distributed over sphere (2); and two infinite series of charges, consisting of successive reflections of the considered charges in the opposite sphere and of the reflections of these reflected charges. The rapid decrease in the importance of these reflected charges with increasing number of the term in the series makes it possible to retain only the first terms of the expansion in the solution of this problem (in our case), and to consider only the effect of these. Since the real altitudes of charge formation in the atmosphere, not exceeding 10 km, are

very small compared with the radius of the earth, it can also be assumed that $h_1' = h_1$ and $h_2' = h_2$. The distribution of the charges will then resemble that shown in Figure 42.

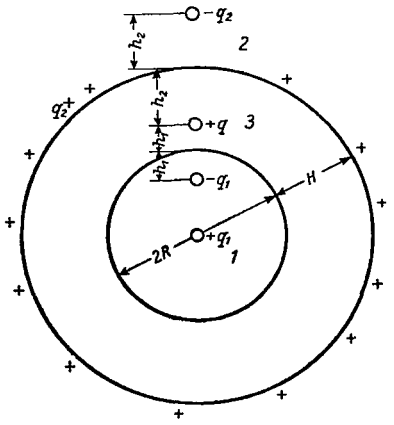

FIGURE 41. Distribution of induced charges in the system of the earth (1), ionosphere (2), and atmosphere (3).

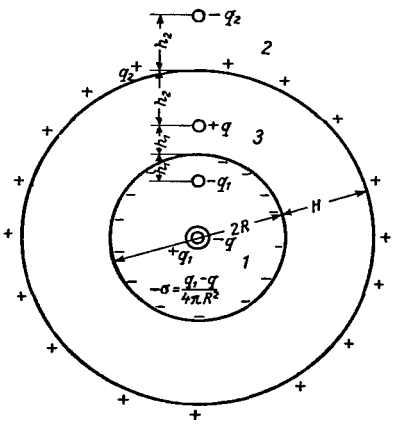

FIGURE 42. Distribution of proper and induced charges in system of the earth (1), ionosphere (2), and atmosphere (3).

An important result of these considerations is the conclusion that the settling of a charge on the conducting sphere (1) leads to the appearance of a local field, created by the charges $+q$, $-q_1$, $-q_2$, in addition to a weaker field common to the whole surface between the concentric spheres, which is created by the charges $-q$ and $+q_1$ (situated on the surface of the internal sphere), and by the charge q_2 (situated on the internal surfaces of the external sphere).

It follows from Gauss' theorem that $q_1 + q_2 = q$, and therefore, the field in the entire space between the spheres will be created by the charge $-q + q_1 = -q_2$ on sphere (1), and by the charge $+q_2$ on sphere (2), and will thus be confined in space (3).

Neglecting the curvature of the spherical surfaces, the magnitudes of the charges q_1 and q_2 can be given by the expressions:

$$q_1 = q\frac{h_2}{h_1 + h_2}, \quad q_2 = q\frac{h_1}{h_1 + h_2}. \tag{20}$$

The error due to the neglect of the surface curvature amounts to a fraction of q_1 and q_2 which does not exceed $\frac{h_1}{R}$, i.e., negligibly small.

This dependence of the magnitude of the induced charges, which create the field outside the disturbance zone, on the altitude of the charge in a poorly conducting zone leads to the following conclusions:

a) in cases where the altitude of charge location in a poorly-conducting zone is very small compared with the zone thickness, the transfer of a charge of opposite sign to the internal sphere does not cause the appearance of a field on the whole sphere, and the field disturbance is of a local nature;

b) the field intensities on the surface of the internal conducting sphere and the potential difference between the spheres largely depend on the ratio of the altitude of the center of the charge (which remains in the poorly conducting zone) to the whole thickness of the latter.

If we apply the model under consideration to the earth, atmosphere, and ionosphere, it is found that for altitudes of charge appearance from 0 to approximately 10 km and an altitude of the ionosphere of about 100 km (or 60-70 km according to the data of Israel and Kasemir /84/), only less than a tenth of the total charge reaching the earth participates in the creation of the general field of the earth and its variations. In this case, thunderstorm activity cannot cause more than a tenth or a twentieth of the observed diurnal variations in the electric field.

The balance of currents between the earth and the atmosphere in thunderstorm and nonthunderstorm regions is estimated with errors apparently not exceeding 50 %. As is shown in the works of Gish and Wait, Stergis, Rein and Kangas /79, 107/, currents from thunderclouds do not in any case exceed 2000 amp over the entire surface of the earth. It is indicated in /31/ that this figure is overestimated, since a number of thunderclouds are negatively polarized. On the other hand, the magnitude of the earth's charge and its variations, considered in /60/, is estimated with an error not exceeding 50 % /15/.

The balance of the currents in the earth-atmosphere system and the appearance of a unitary variation in accordance with the spherical condenser scheme are guaranteed by assuming that the whole charge from thunderclouds reaching the earth provides for unitary variations. From the point of view of the above-given considerations, in order to obtain the observed unitary field variations, the amount of charge arriving from thunderclouds and consequently, the currents from them, must be ten times larger, which is actually observed. To eliminate this contradiction, it is assumed that the altitude of the region in which charges are induced is low, and comparable with the altitude at which excess charges appear. Applied to the atmosphere, this affirmation means that region (2) is situated in a poorly-conducting part of the atmosphere. But in this case, charges of region (2) cannot participate in the creation of relatively fast field variations such as the diurnal unitary field variations. Then, to obtain relatively short-period field variations common to the whole globe, they should be assumed to be created only by a variation of the total charge of the globe. As an alternative, it could be assumed that the total effect of all thunderclouds creates some superposition

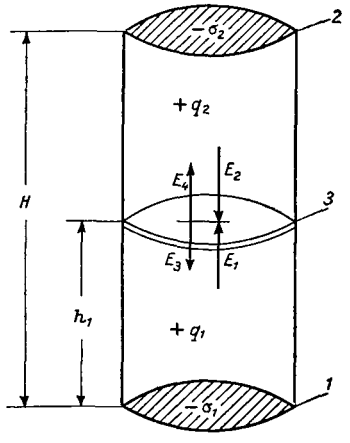

FIGURE 43. Scheme illustrating the calculation of the altitude at which the unitary variation appears.

1—earth; 2—ionosphere; 3—the layer where the unitary variation appears; q_1 and q_2—charges of a unit atmospheric column, lying above and below the layer (3); σ_1 and σ_2—the densities of charges induced in (1) and (2); E_1, E_2, E_3 and E_4—the fields created respectively by the four charges mentioned.

of the fields of all the local induced charges which appears as the general field of the earth but, as was shown by Pierce /98/, an estimate of the role of thunderclouds in this case shows that only 1/20 of the diurnal unitary variation can be attributed to this mechanism, if we assume that $h_1+h_2 \gg h_1$ (Figure 42) and thus neglect the effect of charges reflected in the atmosphere. Consequently, this mechanism of field creation does not play an important role.

The altitude at which those charges induced by the charges appearing in the atmosphere occur strongly depends on the rate at which the charges in the atmosphere appear. Using the above-indicated fact that the diurnal unitary variation over continents appears in a definite altitude range, the effective altitude h_1+h_2, where region (2) in the atmosphere for processes lasting 24 hours begins, can be calculated.

The relaxation time in the atmosphere, which is determined by its conductivity, does not exceed 400 sec in fair-weather conditions, and rarely exceeds 4000 sec even when the atmosphere is relatively strongly polluted, so it is negligibly small compared with the time of passage of the diurnal field wave. It may therefore be assumed that the effective altitude of region (2), from data on the diurnal variation, is close to the effective altitude also for faster field variations which last more than several hundreds or even thousands of seconds.

We now estimate the altitude of region (2). The appearance of the unitary variation only in a comparatively thin layer at some altitude h_1 may be due to the fact that at this altitude, the fields due to atmospheric space charges lying above and below this layer and to charges induced by the latter in the earth and in the upper conducting layers of the atmosphere compensate each other, as is shown in Figure 43. In this case, the condition of the appearance of unitary variation in a layer high up can be written in the form

$$E_1+E_2+E_3+E_4=0, \tag{21}$$

where E_1 is the electric field due to atmospheric space charges q_1 lying below the level where the unitary variation appears; E_2 is the electric field due to atmospheric space charges q_2 lying above this level; E_3 and E_4. are the fields due to charges induced in the earth and in upper layers of the atmosphere respectively.

If the atmospheric charge at some altitude h is $\rho=\rho(h)$, then, neglecting the curvature of the earth in the one-dimensional problem, which is applicable on clear days, the following expressions can be written for the fields E_1, E_2, E_3, and E_4:

$$E_1=-4\pi q_1=-4\pi\int_0^{h_y}\rho(h)\,dh, \tag{22}$$

$$E_2=4\pi q_2=4\pi\int_{h_y}^{H}\rho(h)\,dh, \tag{23}$$

$$E_3=4\pi\int_0^{H}\frac{H-h}{H}\rho(h)\,dh, \tag{24}$$

$$E_4=-4\pi\int_0^{H}\frac{h}{H}\rho(h)\,dh, \tag{25}$$

where h_y is the altitude at which the unitary variation appears; h is the current coordinate; H is the effective altitude of the boundary of region (2), in which charges are induced by the atmospheric space charges. It should be borne in mind in this connection that in reality the charges σ_2, which create the field E_4, are situated within a given thickness; the time in which their distribution is established may be considerable, but in quai-stationary conditions, a charge which does not have well-defined altitude can be considered as concentrated at some altitude H. Equations (24) and (25) are similar to equation (20); the charges induced by a plane layer of charge ρ, situated between two conducting planes $h_1+h_2=H$ apart, can be calculated from the relationships:

$$\rho_1=\frac{H-h}{H}\rho \quad \text{and} \quad \rho_2=\frac{h}{H}\rho. \tag{26}$$

For many cases on clear days, the space charge variation with altitude can be represented by the formula (Chapter III)

$$\rho=\rho_0 e^{-ah}.$$

Then, substituting in equation (21) the expressions of its terms from (22)-(25),* we obtain

$$-4\pi\rho_0\int_0^{h_y}e^{-ah}dh+4\pi\rho_0\int_{h_y}^{H}e^{-ah}dh+4\pi\rho_0\int_0^{H}\frac{H-h}{H}e^{-ah}dh-$$
$$-\frac{4\pi\rho_0}{H}\int_0^{H}he^{-ah}dh=0.$$

After integrating and carrying out the algebraic transformations, we obtain the equation

$$aHe^{-ah_y}+e^{-aH}-1=0, \tag{27}$$

which relates the altitudes h_y and H.

Equation (27) makes it possible to find H if h_y is known (Table 14). The calculations are made for two values of the coefficient a, which characterize the regularity in decrease of the electric field with altitude: over the continents $a=10^{-3}\,m^{-1}$, and over the oceans $a=2.5\times10^{-4}\,m^{-1}$ (Clark /74/).

TABLE 14. Values of altitude H of equalizing layer (m)

a m^{-1}	h_y			
	200	500	1000	2000
10^{-3}	500	1200	2500	5000
2.5×10^{-4}	400	1000	2000	4000

* Equation (7) gives the dependence of both the proper charges and induced charges on altitude, but formulas (22)-(25) should contain only the magnitudes of the proper charges. However, for a rough estimate of H (7) can be used.

The second solution of equation (27), $H = 0$, corresponds to a change of the reference system, in which the origin of the coordinates is assumed to be situated at the altitude of the effective layer.

Thus, the calculation results strengthen the conclusion obtained earlier: the effective altitude, at which charges induced in the atmosphere are situated, varies within the troposphere and may often drop to its lower layers.

It is not advisable, therefore, to look for the altitude of the equalizing layer from the rate of establishment of an equal potential in the upper layers of the atmosphere (the method of Israel and Kasemir /84/), since the charges which compensate the earth's field are situated at altitudes at which the conductivity is low, and they cannot provide equalization in the required time.

We now consider in more detail the concept of the effective altitude H. If at a distance H from the earth, we produce in a solid metallic body a cavity concentric with the earth, then with the given positions of space charges, the field distribution at the earth's surface will be the same as in the real case. Thus, the field due to charges situated in the atmosphere and on the earth does not penetrate beyond the altitude H. It should then be borne in mind that in reality, the charges which create the field E are situated in some very large layer exceeding H.

The time taken to establish their distribution may be considerable since it is determined by the relaxation time of the field at these altitudes, but in quasistationary conditions the vertically distributed charge can be considered as concentrated at some altitude H.

Thus, the second "condenser plate" is situated at low altitudes in a poorly-conducting zone of the atmosphere. Its effective altitude depends on the height distribution of space charges. The field variations close to ground level, having both a global and a local character, will be affected, not only by the magnitudes of the charges in the atmosphere, also by their height distribution. An upward displacement of the space charges will result in a decrease in the field at ground level, and a downward displacement will result in an increase in the field. An increase in atmospheric turbulence in cases where the charges are created high up contributes to a rise in the field at ground level, and when the charges are created at the earth's surface, it contributes to a decrease in the field at ground level. It should be noted that this process does not often take place in pure form, since atmospheric turbulence, in addition to displacing charges, often contributes to their appearance, which may mask its influence on the field variation at the surface due to the variation of the altitudes of already existing charges.

We now consider somewhat closer the influence of the height distribution of charges on the creation of field variations at ground level. The field E_g at ground level can be represented as a sum of the field due to the proper charge of the earth E_e and of the field due to local space charges of the atmosphere E_a:

$$E_g = E_e + E_a. \tag{28}$$

As indicated above, only a certain fraction m of the charge Q reaching the earth will create a field common to the whole globe

$$E_e = m \frac{Q}{R^2}, \tag{29}$$

where R is the radius of the earth.

The field due to the space charges in the atmosphere is

$$E_a = 4\pi n \int_0^H \rho \, dh, \tag{30}$$

where n gives the fraction of the lines of force from a charge situated in the atmosphere which enclose the earth.

The values of m and n depend on the height distribution of space charge sources in the atmosphere, on its conductivity, and on the atmospheric turbulence

$$E_g = m \frac{Q}{R^2} + 4\pi n \int_0^H \rho \, dh. \tag{31}$$

Processes resulting in an upward displacement of charges cause a decrease in m and n; processes resulting in a downward displacement of charges cause an increase in m and n. For the indicated values of the effective altitudes, n may vary from 0 to 1. The value obtained for m is averaged over the whole globe, and can therefore vary within narrower limits. For a given region (equation (20)) $m_i = \frac{h_{1i}}{H_i}$, where h_{1i} and H_i are respectively the altitude of the excess charge q_i and the effective altitude in the region i.

For the earth as a whole

$$E_e = \frac{\sum_{i=1}^{i=t} m_i q_i}{R^2} = \frac{\sum_{i=1}^{i=t} \frac{h_i}{H_i} q_i}{R^2}. \tag{32}$$

If we introduce the concept of some mean excess charge density $\overline{q_i}$ in the atmosphere, then

$$m = \frac{\sum_{i=1}^{i=t} m_i}{t} = \frac{\sum_{i=1}^{i=t} \frac{h_i}{H_i}}{t}. \tag{33}$$

It follows from formula (33) that, although m_i in the i-th region can, like n, vary from 0 to 1, on the average, m should naturally vary over the earth's surface within considerably narrower limits. However, the global effects on the value of m over the whole surface of the earth (the change of seasons with allowance for the difference in the distribution of continents and seas of both hemispheres, the diurnal variation of the continental area illuminated by the sun, etc.) may be expected to lead to variations in m and to corresponding variations in E_a.

Local time variations in n may be considerably larger than variations in m, thus causing considerable variations in the local field E_a

$$E_a = 4\pi \sum_{j=1}^{j=s} \frac{H - h_j}{H} q_j, \tag{34}$$

where h_j and H are the altitudes of the charges q_j and the effective altitude in the given region respectively. Introducing the concept of some altitude average charge $\overline{q}$, an expression characterizing n can be obtained

$$n = \frac{\sum_{j=1}^{j=s} \frac{H - h_{1j}}{H}}{s}. \qquad (35)$$

The altitude of the charges h_{1j} can vary from 0 to H, causing the indicated variation in n from 0 to 1, and accordingly, a considerable variation in the local field.

The following conclusions may be drawn from the present section.

1. The electric field in the atmosphere is due to the action of charges situated throughout the troposphere and on the earth's surface.

2. Global variations in the electric field are determined by the time variations, averaged over the whole surface of the earth, of both the magnitudes of the charges reaching the earth, and of the height distribution of the charges left in the atmosphere; they therefore depend on such factors as the height distribution of charge generation zones, the rate of charge separation, the conductivity profile of the atmosphere, and turbulent mixing in the atmosphere.

3. Local variations of the atmospheric electric field are determined both by the magnitude of the charges situated in the atmosphere, and by their height distribution. Local variations therefore depend on such factors as the rate of appearance and separation of local charges, and the conductivity and turbulence profiles of the atmosphere.

§ 3. SCHEME OF ELECTRIC PROCESSES IN FAIR-WEATHER REGIONS

A simple scheme of the electric processes in fair-weather regions follows from the analysis given in the previous sections. We assume that the conductivity λ in an atmosphere free from space charges increases with the altitude h according to some law $\lambda = \lambda(h)$, and that an electric field of the earth with an intensity E at the surface is "applied" in this region. During the equalization time $T = \frac{4.6\varepsilon}{4\pi\lambda}$, a steady current i is established in the atmosphere, and the field distribution with altitude will have the form

$$E(h) = \frac{i}{\lambda(h)} = \frac{E_g \lambda_g}{\lambda(h)}, \qquad (36)$$

where E_g and λ_g are the field at the surface and conductivity respectively. If the conductivity increases with altitude by an exponential law, as is the case over oceans and polar regions and more rarely over continents, the field will decrease with altitude by the same law.

This case is shown in Figure 44. As indicated in Chapter III (see Figure 10), such profiles are indeed observed over continents during fair weather in approximately 40 % of the cases. We called them profiles

of Group I. With these profiles, the field variations common to the whole earth may clearly appear at all altitudes, their amplitude decreasing with altitude in accordance with the increase in conductivity. This case is similar to that investigated by Clark /74/. In cases where, for some reason, additional space charges arise at some altitude in the atmosphere, the field profile may differ from that considered above. Let us assume, for example, that the conductivity within some altitude interval does not rise, but remains constant. Then in stationary conditions, the field in this section will not vary with altitude, i. e., there will be no space charges in this zone. If in the same altitude interval the conductivity decreases with altitude, a region of negative space charge arises in this altitude interval, and the field there will rise with altitude.

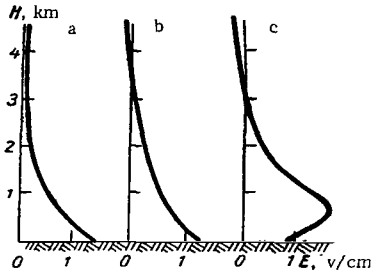

FIGURE 44. Field profiles.

a—in an atmosphere without additional space charges; b—in an atmosphere into which positive space charges are carried; c—in an atmosphere in which charge separation and generation takes place.

If some charge is transferred by air currents to the atmospheric region under investigation, or it arises as a result of the fall of charged particles by gravity, extrema may appear on the field profiles. The field profiles in these cases will be similar to that of Group III shown in Figure 44c. Profiles of this type very often appear in fair-weather zones due to dust in the lower layers of the atmosphere and the resulting decrease in conductivity, as was shown in the section dealing with the effect of pollution in the atmosphere on the field variation with altitude.

In the case of profiles of Group III, the electric field high up will be largely determined by the distribution of local space charges, and the unitary variations of the field will affect only some very narrow altitude interval, where the field of the local space charges is comparatively weak. The potential over these regions will accordingly depend not only on the field common for the whole earth, but also on the magnitude and height distribution of the local space charges.

The stratification of space charges (which is characteristic of profiles of Group III) may result, as zones where these profiles appear become sources of charging of the earth and affect the magnitudes of the unitary variations.

If additional positive space charges arrive in a zone with a conductivity decreasing exponentially with altitude from some other regions of the earth, as a result of advective transfer, the electric field due to the earth's charge may already be "shielded" at relatively low altitudes. In this case, the field naturally does not penetrate above the "shielding" layer. This is the way in which the profiles of Group II (Figure 44b) arise. It should be noted that the altitude at which the field drops to zero is in the case of Group-II profiles close to the altitude at which the "center of gravity" of the positive space charge is situated in the case of Group-III profiles. This confirms the assumption regarding the role of advective transfer of positive charges in the formation of Group-II profiles. In the case of Group-II

profiles, the potential of high layers of the atmosphere depends largely on the magnitude and position of local space charges.

It should be noted that the field variations over continents and oceans differ considerably in their rates of field decrease with altitude even in the case of group-I profiles. Over continents the coefficient in the exponent (formula (6), Chapter III) is $a = 1\,\text{km}^{-1}$, whereas, according to Clark's data /74/, over oceans $a = 0.25\,\text{km}^{-1}$. This difference, being the result of the increased degree of pollution over the continents as compared with over the oceans, indicates that the potential of high layers of the atmosphere also should differ considerably over oceans and over continents. In fact, the potential V at an altitude H in the case of Group-I profiles is

$$V = \int_0^H E\,dh = \int_0^H E_0 e^{-ah}\,dh = -\frac{E_0}{a}\left[1 - e^{-aH}\right]. \qquad (37)$$

If we assume that the exponential rise in conductivity can be extrapolated to considerable altitudes (50-100 km) then, neglecting the second term in the brackets, we find that the potential at these altitudes will be four times as large over oceans as over continents. This once more emphasized the difficulty to which the concepts of the spherical condenser theory lead.

It should also be recalled that seasonal variations of the field profiles, which are connected with a variation of the coefficient a for profiles of Groups I and II, and with a variation of the altitude and amplitude of the maximum in the case of Group-III profiles, are observed.

Under different measurement conditions, these seasonal variations appear differently. In Leningrad and Tashkent, for example, the value of the coefficient a increases in passing from summer to winter. The field maxima in the case of Group-III profiles lie lower in winter than in summer. Generally, in these regions, the main space charges in the atmosphere are observed to approach the earth when passing from summer to winter. This is in agreement with the fact that convective air motions are weaker in winter than in summer, and the transport of space charges due to eddy diffusion decreases.

These peculiarities of the field variation in Leningrad are also due to the fact that the surface air ionization decreases in winter owing to the snow cover, which prevents the release of radioactive emanations. A decrease in the rate of ionization contributes to a decrease in the surface air conductivity, which results in an increase in the field intensity in the surface layer during winter.

In Kiev, the opposite variation of the field profiles upon the transition from winter to summer is observed, and although these variations are smaller in absolute magnitude than those in Leningrad and Tashkent, they are appreciably large. The Kiev anomaly is connected with peculiarities in the height distribution of atmospheric pollution. According to E. S. Selezneva /54/, the vertical distribution of nuclei in the Kiev region decreases with altitude more sharply in summer than in winter.

It was mentioned in Chapter III that diurnal variations in the rate of decrease of the field with altitude and of the altitudes and magnitudes of the field maxima are also observed. Along with the seasonal and diurnal variations in the charge of an air column extending from 0 to 6000 m, the mentioned variations in the altitude of the "center of gravity" of the space

charges in the atmosphere, leading to a modification of the effective altitude, affect diurnal and seasonal variations of both the local and possibly the unitary surface field.

The fact that the effective altitude at which charges induced in the atmosphere are situated is only a few kilometers or even hundreds of meters above the earth's surface leads to another conclusion. The field lines from the atmospheric charges diverge almost equally toward the earth's surface and into the atmosphere (50-60% of the total number of lines ending at the earth). A direct result of this is that the actual field from the proper charges of the earth, with which the corresponding fields from the atmospheric charges inevitably combine, is approximately only 0.66 of the observed field even in fair-weather regions. Accordingly, the total charge of the earth should amount to about 3.5×10^5 coulombs, if we take, as is accepted, a value of 130 v/m for the mean electric field intensity at ground level.

The data of the last three sections lead to the conclusion that, even in fair-weather conditions, the field variation with altitude and the diurnal variation over continents are mainly due to variations in the magnitude and position of the space charges in the atmosphere. The field variation with altitude is closely related to the distribution of impurities in the atmosphere, and is therefore dependent on convection in the atmosphere. In conditions other than fair weather, the pollution in the atmosphere should have an even larger influence.

§ 4. ELECTRICITY OF STRATUS CLOUDS WHICH DO NOT PRODUCE PRECIPITATION

It follows from the data given above that stratus clouds considerably modify the electric state of the atmosphere. Separated charges exist in the clouds, and these may be spread out and carried by air currents into neighboring regions of the atmosphere, and also may reach the earth in convective currents. It is highly probable that this charge circulation in the earth-atmosphere system plays a role in the creation and maintenance of the electric field of the atmosphere, and the regularities of this circulation affect the laws of variation of the electric field. In the presence of stratus clouds, a negative space charge is almost always observed at the surface, decreasing the electric field strength at the surface.

The potential of the atmosphere at an altitude of 6000 m varies considerably on cloudy days. On clear days, this potential is V_{6000} = 200-220 kv, and the charge of an air column 6000 m high with a base of 1 m^2 is Q_{0-6000} = 2.5-3.0 e.s.u./m^2. St clouds as a rule reduce the total potential of the atmosphere, evidently owing to the negative charge beneath them and to the fact that the electric fields above the clouds very rapidly fall off to zero, i.e., the field from the charges of the cloud compensates the electric field of the earth.

Sc clouds also somewhat modify the total potential of the atmosphere, evidently owing to the negative charge beneath the clouds. The potential drop in the cloud itself is negligible, and on the average positive. Above the cloud, a region of negative field contributing to a decrease in the total

potential is often observed, and higher up, the field is positive and remains considerable up to altitudes of 5000-6000 m.

Owing to the negative charges below and above the cloud, the total charge of an air column is smaller than on clear days.

Clouds of the As form raise the potential of the atmosphere and reduce the total charge of an air column mainly due to a redistribution of the charges in the atmosphere, since the potential drop in the cloud itself is negligible on the average (approximately 90 kv), and the excess charge of the cloud is about 1 e.s.u./m^2.

Cs clouds do not, on the average, modify the potential and charge of the atmosphere. In individual cases, Cs clouds reduce the total potential of the atmosphere, mainly owing to a potential drop at the cloud boundaries (Appendix XIX).

The distribution and magnitude of charges in the atmosphere in the case of Ns clouds vary within wide limits; the potential of the atmosphere and the charge of an air column are considerably larger than in clear weather.

The highest electric field intensities were observed in Ns clouds, being approximately 200 v/cm in mixed Ns clouds.

Appendix XXVI gives the percentage distribution of electric fields in stratified clouds. The electric fields most often encountered have intensities of from −1 to +3 v/cm, the fields in high-altitude crystalline clouds of the type Cs very often being negative.

Studies of the electric field variations inside stratified clouds showed that mainly four types of field variations in the clouds are encountered; these correspond to four types of cloud electrification: 1) positively polarized clouds with an excess positive charge; 2) negatively polarized clouds with an excess positive charge; 3) positively charged unipolar clouds; 4) negatively charged unipolar clouds.

In addition, uncharged clouds are encountered, in which the electric field is small and hardly varies. Uncharged clouds amount to approximately 4 % of all St and Sc clouds, approximately 11 % of all As clouds, and approximately 13 % of all Cs clouds; uncharged Ns clouds were not observed. Clouds with three, four, and more charges are also encountered. Among St and Sc, the percentage of multiply-charged clouds is low ($\sim$ 5 %), and among As amounts to approximately 10 %. Multiply-charged Ns and Cs clouds are more often encountered.

The equation of the variation of the electric field with altitude z in the middle part of stratified clouds can in general be written in the form

$$E = a + b(z - h) + c(z - h)^2, \qquad (38)$$

where a, b and c are coefficients, z is the vertical coordinate (measured upward from the cloud base), and h is the altitude in the cloud at which the maximum field intensity occurs. This equation may be suitable for describing the four basic types of electric structures.

Table 15 gives the mean thicknesses of singly-charged, doubly-charged and multiply-charged clouds. It follows from the table that with increasing cloud thickness, the number of charges in it increases.

As the thickness of the clouds increases, their electric characteristics change: the mean and maximum field intensities in the cloud, the potential difference between the boundaries of the cloud, and the rate of aircraft charging all increase (see Figure 27). It is interesting to note that with

increasing cloud thickness, the ratio of the maximum to the mean field intensity increases (it is clearly seen in the graphs of Figure 27 that the mean and maximum field curves diverge); this is due to the increase in nonuniformities in thick clouds.

The charges of a cloud also depend on its vertical thickness: thicker clouds contain larger charges. The space charge density is also higher in thicker clouds (Appendix XXVII).

The thickness of clouds increases as a result of an increase in their liquid-water content and the concentration of drops. Since these elements were not measured in our investigations, it is only possible to get an idea of this from indirect data, e.g., from the aircraft charge, which was measured in all the investigations. For a given aircraft sounding at a constant velocity, the charge increases with increasing concentration of particles and liquid-water content of the cloud, and, although there is no simple formula relating all these elements, it can nevertheless be affirmed that in places where the number of particles is large and their size larger, the charging of an aircraft is more intensive, as shown in /14/.

TABLE 15

Type of cloud	Position of charges in the cloud				
	+	−	±	∓	Multiple-charged clouds
St	200	200	450	450	700
Sc	260	210	400	430	700
As	640	700	800	900	1500
Ns	630	700	940	600	2000

The last two columns of Appendices XXVII-XXIX give the aircraft charges (the mean, $|\overline{Q}|$, and the maximum, $|Q_{max}|$, in clouds of different thicknesses). We can see that with increasing cloud thickness, aircraft charging in them increases very strongly, and consequently, the concentration and sizes of the drops rapidly increase with the cloud thickness. It can be assumed that the increase in the extremal values of the field in clouds is connected with the increase in these elements.

A number of observed peculiarities in the structures of stratus clouds can be explained by means of a very simple scheme.

Suppose that under the influence of the electric charge of the earth and of the space charge of the atmosphere, a field intensity E_{a_1} has set up at the lower cloud boundary, and an intensity E_{a_2} at the upper cloud boundary (Figure 45). Let the atmospheric conductivity at these levels have the values λ_1 and λ_2. Then, if a cloud with conductivity λ_0 appears in the atmosphere ($\lambda_0<\lambda_1$ and $\lambda_0<\lambda_2$), we can write for the stationary conditions, which set in approximately after a time $\tau=\frac{1}{4\pi\lambda}$, an equation based on the assumption of a constant vertical current

$$\lambda_1 E_{a_1}=\lambda_2 E_{a_2}=\lambda_0' E_0'=\lambda_0'' E_0'', \qquad (39)$$

where λ_0' and λ_0'' are respectively the conductivities in the lower and upper parts of the cloud, and E_0' and E_0'', the field intensities at the respective

points of the cloud. Field discontinuities arise on the cloud boundary:

$$\Delta E_1 = E_{a_1} - E_0' \text{ and } \Delta E_2 = E_0'' - E_{a_2}$$

or, using equation (39),

$$\Delta E_1 = E_{a_1} - E_{a_1}\frac{\lambda_1}{\lambda_0'} = E_{a_1}\left(1 - \frac{\lambda_1}{\lambda_0'}\right)$$

and

$$\Delta E_2 = E_{a_2}\frac{\lambda_2}{\lambda_0''} - E_{a_2} = E_{a_2}\left(\frac{\lambda_2}{\lambda_0''} - 1\right).$$

The following charges then appear on the cloud boundaries:

$$\Delta q_1 = \frac{\Delta E_1}{4\pi} \text{ and } \Delta q_2 = \frac{\Delta E_2}{4\pi},$$

or

$$\Delta q_1 = \frac{E_{a_1}}{4\pi}\left(1 - \frac{\lambda_1}{\lambda_0'}\right) \text{ and } \Delta q_2 = \frac{E_{a_2}}{4\pi}\left(\frac{\lambda_2}{\lambda_0''} - 1\right). \quad (40)$$

Since the conductivity in the cloud may be up to 20 times as low as that in a clear atmosphere /36, 100, 101/ the field in the cloud rises accordingly. The calculation demonstrated can be improved by introducing the relationship between the conductivity and particle spectrum in the atmosphere, if we know the size and height distribution of particles in the cloud, the distribution of the ionization intensity over the cloud thickness, and other parameters necessary for a complete solution of the ionization-recombination equation for an aerosol layer, in which the distribution of particles and consequently, also of the conductivities are given (this solution was obtained to the first approximation by I. B. Pudovkina and Yu. S. Sedunov /48/). However, such a calculation in the case of real clouds hardly gives more than the calculation we have presented, owing to insufficient data on the microstructure of the clouds investigated.

It is obvious that under normal conditions, when the field is positive, the upper part of the cloud will be positively charged, and the lower part, negatively charged. Since the conductivity below an inversion is low and increases sharply in the inversion itself /100, 101/, the charge q_2 forming at the upper boundary of a stratified cloud, which usually appears under an inversion, is naturally larger than the charge q_1 arising at its lower boundary. An increase in the conductivity with altitude should lead to the same effect. The positive charge acquired by a cloud is therefore larger than the negative charge.

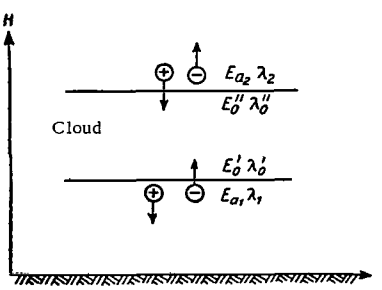

FIGURE 45. A scheme illustrating the charging of a poorly conducting layer by conduction currents.

The conductivity of clouds is lower, the larger the number of particles in them. An increase should therefore be observed in zones where the number of cloud particles increases. These zones can be found from the increase in the aircraft charge. In fact, comparing the fields in stratified clouds in summer and winter (Appendices XXXII, XXXIV), we find that in summer the mean values of the field intensity and its mean

absolute and maximum values, as well as the excess space charges are larger than in winter; the aircraft charge is also larger in summer. Comparison of the field and charges in stratus and stratocumulus clouds also shows that these are larger in stratocumulus clouds than in stratus clouds, which can again be attributed to the fact that the conductivity in stratocumulus clouds is lower, since an aircraft is more intensively charged in them than in stratus clouds.

The scheme presented can explain the observed phenomena quantitatively in a number of cases since the field intensity in stratus clouds is as a rule only 3-5 times as high as the field in a clear atmosphere, and this, as already indicated, approximately corresponds to the conductivity values in clouds.

It should be noted that the appearance of clouds having a charge of a single sign can be relatively simply explained by the existence under or above the cloud of a poorly conducting layer, which is connected with the appearance of a large number of particles, for example, of dust admixtures, or with the transfer of a charge of one sign by convection or diffusion. In fact, a layer with a high dust content is very often situated under clouds, particularly under subinversion clouds. In this case, the influence of a reduced conductivity may lead (in a field of normal direction, according to the scheme considered above) to the formation of a negative charge under this cloud, and of a positive charge in the cloud.

The appearance in a cloud and its surrounding zone of an updraft or downdraft may lead to the same effect, i.e., unipolar cloud charging. If u is the mobility of light ions which create the conduction current and E is the field at the cloud boundary, then the displacement velocity of the ions in the field is $v=uE$. The field at the boundary of the clouds investigated varied from one to several v/cm with a mobility of 2-4 $cm^2/sec \cdot v$. This means that the velocity of the ions will be $\sim$1-10 cm/sec. If the mean velocity of the updraft is $w>v$, then in the case of cloud charging by a conduction current i_{con} a cloud will acquire in a field of normal direction a negative charge spread throughout the whole cloud thickness, and in a negative field, a positive charge. Cloud drops passing through the upper cloud boundary will evaporate, and a positive space charge due to ions left after the evaporation of drops will appear in the air above the cloud. If $w \lesssim v$, the negative charge will also occupy the main part of the cloud volume. If the cloud is engulfed by a descending current with a mean velocity w, and $w>v$, then the cloud in a normal direction field will have a unipolar positive charge. Drops falling under the cloud also evaporate, and the ions left in them form a negative space charge beneath the cloud. If $w \lesssim v$, the main part of the cloud will be positively charged. Thus, vertically oriented air motions with velocities of $\sim$1-10 cm/sec should lead to unipolar cloud charging.

The appearance at one of the boundaries of stratus clouds of considerable diffusion currents (i.e., a large gradient of the space charge density and considerable turbulence) may obviously lead to unipolarly charged clouds. Thus, for example, this scheme explains the appearance of a negative charge beneath a cloud as being due to turbulent motions under the cloud which spread the negative charge, which, in turn, is accumulated by the current i_{con} in the lower part of the cloud, and the whole region between the cloud and the earth gradually fills with a negative charge.

In fact, as shown by M. A. German /8/, the turbulent mixing coefficient k in St-Sc clouds is approximately 40-50 m^{-2}. Under observed space charge density gradients $\frac{\Delta\rho}{\Delta z}$, of the order of magnitude of 10^{-11}-10^{-12} e.s.u./cm^4, beneath clouds, the diffusion current is $i_d = k\frac{\Delta\rho}{\Delta z} \sim 10^{-16}$-$10^{-17}$ amp/cm^2. Thus, the diffusion current may in a number of cases amount to an appreciable fraction of the total current. Since the conduction current beneath clouds is usually smaller than the normal values (owing to the decrease in field intensity and in conductivity as a result of the pollution of the atmosphere, which usually occurs under inversions), the diffusion current can sometimes be assumed as being equal to the conduction current and to considerably affect the transport of space charges. At the upper boundary of stratus and stratocumulus clouds, turbulent motions, which usually appear under inversion layers, are weak, and spreading of the positive charge is hindered. As a result, the excess positive charge in the clouds should grow even more.

This scheme, however, cannot explain certain peculiarities of the electric structure of stratus clouds. In 75 % of the cases, a positive polarization of stratocumulus clouds did in fact occur in a positive field, but in 10 % of the cases, it occurs in a negative field. In addition, in 10 % of the cases, the field above the cloud was positive and below the cloud negative. Negative polarization of stratocumulus clouds occurred in 1/3 of the cases in a negative field (as is required by the scheme under consideration), in 1/3 of the cases in a positive field, and in approximately 1/3 of the cases, the field above the cloud was positive and below the cloud negative. Unipolar negative cloud charges arose in five out of thirteen cases in a positive field, in three cases in a negative field, and in five cases, the field above the cloud was positive and below the cloud negative.

We now consider in more detail the height distribution of the field in clouds of a given electric structure. For this purpose, we examine the field profiles occurring in the case of stratocumulus clouds. Figure 31 gives the height distribution of the field in the case of stratocumulus cloudiness polarized positively (Figure 31a) and negatively (Figure 31b), charged positively (Figure 31c) and charged negatively (Figure 31d). In all the plottings, relative heights D/D_0 are used where for D_0, equal to unity, the altitude of the lower boundary of the clouds, the thickness of the clouds, and the distance between the upper boundary of the clouds and the upper sounding level (6000 m) were successively taken. The data given refer to days when only stratocumulus clouds prevailed. As follows from the graphs of Figure 31, all the basic electric structures arise in a positive atmospheric field.

By comparing the graphs of Figure 31, an attempt can be made to explain them on the basis of an assumption regarding the role of vertical air motions in the creation of unipolar clouds from initially polarized ones. In fact, a comparison of the above-mentioned pairs shows that the charge distribution in a cloud shown in Figure 31a transforms into the distribution shown in Figure 31b, if the distribution curve of the field is "lowered" with respect to the lower cloud boundary. This may occur either upon the appearance of a downdraft, or due to the existence of a layer of reduced conductivity above the cloud.

The field distribution shown in Figure 31a transforms into the distribution shown in Figure 31d, if the distribution curve of the field is "lifted" with respect to the cloud. This may occur either in the case of an updraft, or upon the appearance of a reduced conductivity zone above the cloud. Since usually the air above a cloud is pure, it is highly probable that an initially normally polarized cloud begins to transform into a negatively charged one due to the presence of an updraft in it. It should be noted that the vertical dimensions in the relative scale used are strongly distorted. The mean altitude of the lower cloud boundary is approximately 500 m, the mean cloud thickness varies approximately from 200 m for unipolarly charged clouds to 400 m for polarized clouds, and the thickness of the zone between the upper cloud boundary and the sounding ceiling is approximately 5000 m. The negative charge zones above polarized clouds and above positively charged clouds, and the positive charge zones above negatively charged clouds, extend over a layer thicker than the cloud itself. The appearance of even comparatively thin clouds thus significantly affects the field distribution throughout the whole thickness of the atmosphere.

The absolute value of the field in negatively polarized and negatively charged clouds is higher than in other types of clouds.

The negative cloud polarization cannot be explained by some removal of charges occurring in the cloud due to conduction currents in a normal field. It should be noted that the charges in a negatively polarized cloud arose in a field having a direction not conducive to their appearance. In fact, the conductivity in these clouds is certainly lower than in a clear atmosphere. Consequently, the normal field of the earth should be several times stronger in them. The potential drop in a cloud of 400 m mean thickness should have been from about +50 to −200 kv, whereas it is approximately −50 kv. Thus, due to charge generation and separation in the cloud, a potential difference of at least −100 kv, and sometimes even −250 kv, is created.

It can be similarly assumed that positively polarized clouds are largely connected with active generation of charges in them. This confirms the assumption that the negative charge is small, and that the field above them, as well as above negatively polarized clouds, almost does not decrease up to altitudes of 6000 m.

Also notable is the fact that the potential differences between the upper and lower cloud boundaries ΔV in a number of clouds of all the forms considered are comparable with the potential at 6000 m (V_{6000}) in clear weather, sometimes exceeding it, and often even being comparable to V_{6000} by absolute value, although opposite in sign.

It should be assumed that stratified clouds begin to behave in a number of cases not as a passive resistance but as voltage generators.

In analyzing the initial data, it can be assumed that charges accumulate in thin clouds (up to 500 m) according to the considered scheme of charge accumulation in a section of high resistance. In thicker clouds, additional charge generation arises, and this may play the basic role in clouds thicker than 1000 m.

The generation mechanism of these charges is at present not at all clear; even less clear is the way in which strongly charged clouds arise in cases where the external field does not contribute to it, and charges are not carried away from the cloud with precipitation. It is obvious that to be

able to answer these questions, a more detailed study into the elementary mechanisms of charging of particles in these clouds and into the conditions of charge transport from them is necessary. The observed charge generation in clouds requires that large particles in them should be positively charged, and small particles, negatively charged. It is, however, not so simple to decide which electrification mechanism in these finely-dispersed and often purely warm clouds can develop to a sufficient extent. The mechanism of diffusion and random electrification cannot provide the necessary unipolarity in the charging of small and large particles in these clouds; an analysis of Wilson's mechanism leads to the same conclusion. For certain reasons particle charging in a field cannot provide the required electrification, and the mechanism of Elster and Geitel in Sartor's modification /102/ gives a weakening rather than an intensification of the field in the cloud for our conditions.

To explain the observed effect, it would be possible at first sight to use the electrification mechanism considered by Ya. I. Frenkel' /62/. Owing to the electrokinetic potential of water, drops capture negative ions from the air, becoming negatively charged. Since the charge of drops is proportional to their radius, a negative charge should accumulate in the lower part of the cloud.* In reality, as pointed out in a number of cases (where charge generation took place in clouds), they were positively charged in the lower part. There are no grounds for assuming that drops with an electrokinetic potential of an opposite sign, which would lead to positive charging of drops, may appear in a cloud.

In attempting to find a possible electrification mechanism, one should consider the mechanism of electrification due to the contact potential difference between large and small particles. D. Turner /110/ noticed that raindrops of different radii have different salinities, the NaCl content varying by a factor of three for drops with radii from 0.15 to 0.25 mm. S. M. Shmeter /65/ showed that the concentration of chlorides in rainwater is closely related to the sizes of the cloud drops. The chlorine concentration in drops of radii 1-15 μ rapidly decreases with increasing drop radius, decreasing by a factor of almost 10^4 for drops with a radius of 15 μ as compared with its value for drops with a radius of 1 μ. The chlorine concentration in drops with radii between 20 and 100 μ depends only slightly on the radius. On the basis of the data of E. S. Selezneva /55/ and D. Turner /110/, it may be concluded that as the particles grow further, the chlorine concentration in drops with a radius larger than 200 μ again rises.

The difference in the chemical composition of different sized particles should result in their electrification on coming into contact and then dispersing. As was shown in /25/, the maximum potential to which a large particle of radius R (from which small particles split off on contact) is charged is $V_{max} = V_c \frac{R}{d}$, where V_c is the contact potential difference between the materials of the two particles, and d is the distance 10^{-6}-10^{-7}cm at which charge exchange between the particles stops. A particle of radius 30 μ can be charged by this mechanism in the case of $V_c = 10^{-2}$ v up to tens of volts, and in the case of $V_c = 0.1$ v, up to hundreds of volts.

Depending on the chemical composition of the large and small particles, the contact potential difference may charge the large particles when

* In subinversion clouds, where large drops accumulate in the upper part, the mechanism considered by Frenkel' can explain the negative polarization.

particles of different sizes split off either positively or negatively. We now consider this very powerful electrification mechanism in the clouds being studied.

We calculate the charge which is acquired by a target particle of radius R, falling through a uniform monodisperse cloud of small drops of radius r with a concentration n. Let the fall velocity of the large and small drops be v_1 and v_2 respectively. Suppose the fraction captured from the total number of particles colliding with the large drop is $1-k$. Then the number of collisions where coalescence with the large drop does not occur will be

$$N = kn(R+r)^2(v_1 - v_2)t, \tag{41}$$

where t is the duration of the process.

The charge acquired upon each such collision will be $q=pV_c r$, where p is a factor close to unity, and V_c is the contact potential difference between the large and small particles. As long as the potential of the large particle (which is much lower than that corresponding to the maximum charge Q acquired by it) depends only slightly on its potential /14/, the particle acquires a charge $Q=Nq$ in the course of one second.

Suppose a drop of radius $R = 30\,\mu$ (fall velocity ~ 11 cm/sec) falls through a cloud containing drops of radius $r = 5\,\mu$ (fall velocity ~ 0.6 cm/sec) with a mean concentration of $100\,\text{cm}^{-3}$. In this case, the drop undergoes during a period of 1000 sec about 50 collisions over a path of 100 m in the cloud, and these collisions can be assumed to occur without coalescence, i.e., $k = 1$. During each collision and subsequent separation, a small drop will acquire a charge of one sign, and the large drop are of another sign. Let us assume that large drops are being charged positively. The charge q_1 acquired by the small drops is roughly equal to $q=V_c r$ (assuming $p = 1$); in reality, owing to the increase in the capacity of the small drop when situated near the large drop, the value of q will be somewhat larger. If $V_c = 0.1$ v, then $q = -1.5\times10^{-7}$ e.s.u., and the large drop will acquire a charge $Q = +1.5\times10^{-7}\times50 \sim 10^{-5}$ e.s.u. over the indicated 100 m path. In a 500 m thick real cloud, this charge may grow to 5×10^{-5} e.s.u. The potential thus acquired by the large drop along a 500 m path is only 5 v, and along a 100 m path, about 1 v. These potentials are much lower than the maximum potential V_{max} which a large drop may acquire in such conditions, and therefore, the effect of charge removal by the small drops can be disregarded /14-25/. The relaxation time of the charge of the large drop, due to the air conductivity, should be not less than 1000-2000 sec in a cloud, and therefore the above magnitude of the charge Q will vary by no more than a factor of two as a result of flowing down into the air.

Actual observations of particle charges in stratus and stratocumulus clouds showed that the charges on particles with a radius of 2-10 μ are very close to those calculated in this work and rise proportionally with the radius, the proportionality factor varying from 13 to 20; drops of 5 μ radius carry a charge of from 0.35×10^{-7} to 0.5×10^{-7} e.s.u. on the average /57, 46, 47, 32/.

As mentioned above, the field in negatively polarized clouds reaches -3 v/cm, and the mean thickness of these clouds is 430 m. For the creation of the corresponding charge, a concentration of large drops (radius 30 μ) amounting to about $10^{-2}\,\text{cm}^{-3}$ is necessary in a 400 m thick cloud. These

electric characteristics can also be obtained by assuming $V_c = 0.01$ v,* but on the assumption that the concentration of drops of these sizes is 10^{-1} cm^{-3}. Data of measurements in clouds /4, 90/ show that such concentrations of large particles are indeed observed both in St and in Sc clouds. The density of the current, charging the cloud, which is produced by these particles is approximately 3×10^{-16} amp/cm^2. It is obvious that if the magnitude of this current decreases several times, the cloud will be charged by conduction current, in accordance with the scheme considered earlier. If the concentration of large particles increases, and the variation of their chemical composition with respect to that of small particles creates a contact potential difference between the respective particles, the cloud charging current due to this contact potential difference may become predominant.

It is premature to calculate in detail the charging of particles which fall in a polydisperse cloud. Such calculations can easily be made on the basis of existing works dealing with the fall of drops in clouds, but they cannot make a real improvement to the presented scheme until the dependence of the contact potential difference on the chemical composition of the particles is found and its dependence on the radius of the particles in the investigated clouds determined more accurately.

The purpose in presenting the above estimates was to show just how powerful a charging mechanism may exist in stratus clouds which do not produce precipitation, and to what comparatively strong cloud-charging effects this may lead.

A natural problem arises — the extent to which the electric characteristics of clouds (the electric field in them and the charges on individual particles) affect processes of cloud development by influencing coalescence and condensation processes.

Disregarding Levin's well-known works /38/ on the effect of electric charges on particles and of the electric field on their relative trajectories, i.e., on the "geometrical" collection coefficient, we note only that the influence of electric forces on the coalescence of colliding drops is not yet clearly understood.

It was shown in a number of works that for charged drops the electric charges of the particles themselves as well as the electric field can modify the collection efficiency. It is pointed out by Telford et al. /109/ that charges of opposite sign $\sim 10^{-4}$ e.s.u. increase the collection efficiency of 130 μ drops by a factor of 2-3 as compared with uncharged drops. The work of Goyer et al. /81/ shows that the collision efficiency of 600 μ and 100 μ drops in a field of 15 v/cm increases by a factor of three compared with that in the absence of a field, reaching approximately 90 % (i.e., 90 out of 100 drops coalesce on colliding in the presence of a field, and less than 30 in the absence of a field.) They noticed that the efficiency of drop coalescence was considerably lower in the case of drops having charges of the same sign. Unfortunately, similar investigations have hardly been carried out for smaller cloud particles, and although it can be expected that the coalescence efficiency of small drops on colliding should depend on the electric field in the cloud and on the charges on the particles to an even larger extent than that of large drops, experimental

* We recall that the diffusion potential of a solution varies by approximately 50 mv if the salt concentration changes by a single order of magnitude.

works in this field have not been carried out. At the same time, Schotland and Kaplin /104/ showed that the coalescence coefficient for uncharged 11-21 μ drops colliding with smaller droplets is very small.

An increase in the collision efficiency may considerably affect cloud development processes, and the role of electric forces may turn out to be crucial in this connection. Sartor and Davis point out /102/ that the convergence of falling drops with radii of 19 and 15 μ increases in a vertical field of 40 v/cm, the collision efficiency rising to 0.1 in this field from zero in the absence of a field where the centers of the drops are initially 6 μ apart (horizontally).

A. Lieberman /91/ and Poteny observed that the introduction of charged drops into a chamber filled with fog accelerated the fog dissipation.

It is therefore important to investigate how the actual field intensities measured in a cloud affect the collision of the small particles, which are the main constituents of stratified clouds.

The significant variation in the magnitude and distribution of space charges in the atmosphere under the influence of all types of stratus clouds including high level clouds should be noted. Stratified clouds cause electric polarization in the atmosphere. The absolute value of the electric charge of the atmosphere in the case of Group I profiles may exceed the charges existing in the atmosphere on clear days by several times.

The appearance of considerable negative charges at ground level creates conditions for their transfer to the earth. The magnitude of these charges is, of course, small compared with those in thunderclouds. The charge in thunderclouds may be 10^2-10^3 times as large as the charges in stratified clouds which do not produce precipitation. However, the area covered by stratified clouds is more than 200 times as large as that covered by thunderclouds.

In these conditions, it is very important to estimate correctly the contribution made by stratified clouds to the electrification of the earth and of the atmosphere. We do not as yet have at our disposal sufficient data for such an estimate, since the data on the electricity of stratus clouds were obtained only at three observation points. However, it is already clear that they do contribute considerably to the creation of the electric field of the atmosphere.

The effect of the mechanism of charge generation is clearly observed in Cs, As, and Ns clouds. It is observed to an even larger extent in these clouds than in low-level clouds that the potential differences between the upper and lower cloud boundaries with regard both to their magnitude and to their sign are not caused by the potential difference between the earth and the atmosphere.

Concluding the present section, we wish to point out that for the first time a general picture of the electric structures of clouds of different stratification forms was obtained; this turned out to be more complex than was previously assumed. It was established that all stratified clouds may in fact be charge generators and play a significant role in the creation of the electric field of the atmosphere.

It is necessary to carry out microphysical investigations of clouds in order to find out the reasons for the occurrence of different electric structures and determine the mechanism of charge generation operating in these clouds. Of considerable interest is laboratory investigation of

the possible occurrence in clouds of a potentially powerful mechanism of particle electrification due to contact potential difference between them. The geographical region covered by these investigations should also be enlarged in order to correctly estimate the contribution made by stratified clouds to charge exchange between the earth and the atmosphere.

§ 5. ELECTRICITY OF NIMBOSTRATUS CLOUDS

In order to understand how charges are created in nimbostratus clouds and to obtain some quantitative estimates of the processes leading to the electrification of clouds, we now consider their charging conditions in more detail.

The complete solution to the problem of the electricity in nimbostratus clouds involves solving a system of equations which includes the ionization-recombination equations for light and heavy ions of both signs and for cloud drops, an equation representing the electrification of large particles, and Poisson's equation.

Such a system of equations could be solved to the first approximation (assuming a constant current at different altitudes) with adequate knowledge of the conditions of particle electrification in clouds, the drop spectrum in them, and other necessary parameters characterizing the microphysics of clouds, in particular the influence of the electric field on the coalescence of drops.

Since the necessary data on clouds are not available, we will deal only with the solution to the problem of the electrification of nimbostratus clouds to the first approximation using data on the electric structures of clouds for this purpose.

The total electric current flowing in the atmosphere at some level can be represented as a sum of four currents

$$I = i_1 + i_2 + i_3 + i_4, \tag{42}$$

where

$$i_1 = E\lambda, \quad i_2 = \sum_m q_m n_m v_m,$$
$$i_3 = k\frac{\partial \varphi}{\partial z}, \quad i_4 = \rho v, \tag{43}$$

and where I is the vertical current density; i_1, i_2, i_3, i_4 are respectively the conduction current density, the precipitation current density, the diffusion current density, and the convection current density; E is the field intensity at the given level; λ is the air conductivity; q_m, n_m, and v_m are respectively the charge, concentration, and fall velocity of precipitation particles; k is the coefficient of turbulent mixing; ρ is the space charge; and v is the velocity of the vertical currents. Equations (42) and (43) are based on the assumption that all the currents move along a vertical axis.

We denote the current density through the upper cloud boundary by I_1 and the current density through the lower cloud boundary by I_2. Then, the time variation of the charge Q of a vertical air column of unit cross section extending from the lower to the upper cloud boundary can be

represented in the form:

$$\frac{dQ}{dt} = I_1 - I_2. \tag{44}$$

We now consider the solution of this equation in the case of the model obtained for a positively polarized nimbostratus cloud, neglecting diffusion and convection currents and assuming that the precipitation current is independent of the electric field. The applicability of this assumption is demonstrated below.

In this case

$$\begin{aligned} I_1 &= i_1 = -\lambda_u(E_u + 2\pi Q), \\ I_2 &= i_2 - i_1 = i_2 - \lambda_l(E_l - 2\pi Q), \end{aligned} \tag{45}$$

where λ_u and λ_l are the conductivities near the upper and lower cloud boundaries in a clear atmosphere, E_u and E_l are the respective electric field intensities before the beginning of the cloud development, or

$$\frac{dQ}{dt} = i_{pr} - (\lambda_u E_u - \lambda_l E_l) - 4\pi(\lambda_u + \lambda_l) Q. \tag{46}$$

If we assume that the precipitation and conduction currents above and below the cloud do not vary with time, then the solution of (46) has the form

$$Q = \frac{i_{pr} - (\lambda_u E_u - \lambda_l E_l)}{4\pi(\lambda_u + \lambda_l)} \left(1 - ce^{-4\pi(\lambda_u + \lambda_l)t}\right), \tag{47}$$

where c is determined from the condition that at the moment $t = 0$, $Q = Q_0$

$$c = \frac{(\lambda_u + \lambda_l)(E_l - E_u)}{\lambda_u E_u - \lambda_l E_l - i_{pr}}.$$

We consider the values of the electric currents for the positively polarized mixed cloud model, making use of the data in Figure 38a. The electric field at the sounding ceiling is ~ 1.2 v/cm. As was shown by Rein, Kangas, and Stergis /107/, even the presence of thunderclouds does not modify the conductivity above them. The conductivity above nimbostratus clouds at an altitude of 6000 m may therefore be taken as equal on the average to the conductivity in a clear atmosphere, i.e., 11.5×10^{-4} e.s.u. (see /83/). The conduction current density at this altitude is then equal to 2×10^{-11} amp/m^2. Since in these conditions, the diffusion coefficient (as shown in /8/) does not exceed tens of m^2/sec and $\frac{\partial \rho}{\partial z}$ does not exceed 10^{-6} e.s.u./m^4, the diffusion current density at this altitude is less than 10^{-14} amp/m^2, i.e., negligibly small compared with that of the conduction current. The convection current i_4 at this altitude, even in the case of a vertical velocity of 3 m/sec, does not exceed 1 % of the conduction current; although the vertical wind velocities above clouds were not measured, a velocity of 3 m/sec is clearly overestimated for the average picture under consideration. Thus, at an altitude of 6000 m the whole current practically reduces to the conduction current.

For our one-dimensional scheme in a quasistationary state, it can be assumed that the sum of all the currents at any altitude is equal to the current at 6000 m, i.e., equal to 1.2×10^{-11} amp/m^2.

Performing similar calculations for the region under the cloud, the conduction current density at the surface can be assumed not to exceed 10^{-12} amp/m^2, the diffusion current density not to exceed 2×10^{-14} amp/m^2, and the convection current density i_4 to equal 10^{-12} amp/m^2 only in the case of vertical wind velocities of 1.5 m/sec, which clearly exceed the possible mean vertical velocity. The precipitation current density i_1 under the cloud should therefore be equal to $\sim1.2\times10^{-11}$ amp/m^2. It is interesting to compare these data with the value of 5×10^{-12}-5×10^{-11} amp/m^2 obtained for the current density in Ireland /75, 76/.

Considering the process of cloud charging as a whole, one should take into consideration that, besides the current in the "external" circuit, a part of the current of the "generator," which charges the cloud, should flow inside the generator.

Conduction, diffusion, and convection currents hinder charge separation in a cloud. If we assume in accordance with German's data /8/, that the coefficient of turbulent diffusion in these clouds is k = 50 m^2/sec, and the gradient of the space charge density in the region of the separation of the upper positive and negative charges is 3×10^{-4} e.s.u./m^4, then the diffusion current density at this level is $\sim5\times10^{-12}$ amp/m^2. The convection current may be equal to this current only when the mean vertical wind velocity is 1 m/sec. Estimation of conduction currents in the cloud is very difficult. But if we assume that in these clouds too, the conductivity is three to four times as low as the normal one /36, 66/, the conduction current density in the clouds should not exceed 1×10^{-11} amp/m^2. The "leakage current" density of the "generator" charging the cloud thus barely exceeds 2×10^{-11} amp/m^2.

Hence, it follows that in regions of charge separation, the precipitation current density should reach 3×10^{-11} amp/m^2. A part of this current, which compensates for the "leakage current," is apparently connected with charge transfer by relatively small drops which do not fall from the cloud.

Formula (47) makes it possible to estimate the equilibrium magnitude of the charge in the cloud, and the time it takes to reach this. If we assume that the conductivity above the upper cloud boundary is 5×10^{-4} e.s.u., then the equilibrium charge Q_{eq} of a unit column for the obtained current density, which is reached after a very long time t, is equal to approximately -5 e.s.u./m^2.

The difference between the measured and calculated values is apparently due to the approximate character of the initial estimates of the conductivity near cloud boundaries. This is confirmed by the fact that a similar calculation, using formula (47), of the charge of an atmospheric column extending from ground level to the upper sounding boundary (where the conductivity varies only slightly) gives a magnitude of the equilibrium charge of the atmosphere close to that found by measurement.

The time to charge equilibrium from formula (47) is $t=\frac{1}{4\pi(\lambda_u+\lambda_l)}\approx100$ sec, i.e., in practice, the time to equilibrium is about 500 sec. Formula (47) was derived on the assumption that the precipitation current is time-

independent. In reality, the precipitation particles from stratus clouds fall at a velocity from approximately 1 to 4 m/sec (the radius of the corresponding drops varies from 100 to 500 μ), i.e., 500-2000 sec are required for precipitation particles to reach the surface. Thus, the electric characteristics of the cloud should have sufficient time to reach equilibrium values until the precipitation particles reach the surface. We should note in this connection that, according to Mason's data /42/, the time taken for precipitation particles to form in a warm cloud should amount to several hours, and rather less in a mixed cloud /4/. Consequently, the mentioned structure will appear only several hours after the formation of the cloud, and almost immediately after the beginning of precipitation.

The positive space charge, forming beneath a mixed cloud, is mostly due to positively charged precipitation particles falling from the cloud. According to radar observations, the increase in drop size in the lower part of nimbostratus clouds is imperceptible. Consequently, their fall velocity is more or less constant. The space charge beneath the cloud and in its lower part varies only slightly with altitude, amounting to about 10^{-3} e.s.u./m^2.

To estimate the relationship between this charge and the precipitation current, the fall velocity of the particles has to be known. In order to estimate the fall velocity of particles, use can be made of Best's formula /67/ with the corrections of Browne, Palmer, and Wormell /69/ for the relationship between the rain intensity R' (mm/hr) and the mean radius $\bar{r}$ of the drops (mm)

$$\bar{r} = 0.35R^{0.25}. \tag{48}$$

Using formula (48) and space charge data, Table 16 can be drawn up.

TABLE 16

Precipitation intensity, mm/hr ...	0.1	1	5	10
Mean radius of precipitation particles, mm	0.2	0.35	0.5	0.6
Mean fall velocity of the particles, m/sec	1.6	3	4	4.6
Mean charge per particle, e.s.u. ..	4×10^{-5}	2×10^{-5}	10^{-5}	0.9×10^{-5}

The most intense precipitation is from mixed and warm clouds. Taking approximately 1 mm/hr as the mean precipitation intensity from such clouds, we obtain that for the indicated current density, the space charge density ρ created by the particles $\left(\rho = \frac{i_1}{v_m}\right.$, where v_m is the fall velocity of the particles) is equal to 0.9×10^{-2} e.s.u./m^3; for a precipitation intensity of 5 mm/hr, $\rho = 0.7\times10^{-2}$ e.s.u./m^3; for a precipitation intensity of 10 mm/hr, $\rho = 0.5\times10^{-2}$ e.s.u./m^3, i.e., the space charge values calculated for precipitation intensities of 0.1-10 mm/hr are close to the total space calculated from data on the field variation with altitude.

Thus, in continuous rains, in contrast to showers /12/, the effect of displacement of the space charge of the air together with drops is either small or nonexistent; this difference is possibly due to the fact that strong

downdrafts, which are absent in the case of nimbostratus clouds, form beneath shower clouds.

On the basis of data from measurements made in India, Sivaramakrishnan /106/ gives the following empirical relationship between the precipitation charge and the field E at ground level

$$q = 0.07(E - 1), \tag{49}$$

where E is the field in v/cm, and q is the charge of 1 cm^3 of precipitation in e.s.u.; in addition, he points out that the charge of a unit rain volume is independent of the intensity of the rainfall. In other words, the mean charge of individual particles is independent of the precipitation intensity.

The electric field in a cloud increases with its charge, and the charge of the cloud increases with the precipitation current. The fact that a relationship between the specific charge of clouds and the rainfall intensity does not exist therefore shows that the assumption made in the derivation of formula (47) that the electrification of precipitation is independent of the field in the cloud is correct.

In order to find the extent to which formula (49), obtained for India, is applicable at mid-latitudes, it is possible to compare the precipitation currents according to Sivaramakrishnan's data with those obtained in the present work. The following formula was derived in /106/ on the basis of (48) and (49)

$$i = -2 \cdot 10^{-2}(E - 1)R', \tag{50}$$

where i is the precipitation current density in e.s.u./m^2·sec, R' is the precipitation intensity in mm/hr, and E is the surface electric field in v/cm.

From formula (50) and the data of Figure 38a, it follows that a measured current density of 1.2×10^{-11} amp/m^2 should occur (if the charging conditions in India and in our latitudes are similar) under a precipitation intensity of about 1.5 mm/hr. The charge of 1 g of precipitation particles will be in this case approximately 0.1 e.s.u. according to formula (49).

As indicated above, however, the mean precipitation intensity for these clouds is 1 mm/hr or less; this made it necessary to assume that the charging rate in clouds at mid-latitudes is often higher than at low altitudes. Thus, when the rainfall intensity is 10 mm/hr, the calculated charge of 1 g of precipitation particles should be approximately 3×10^{-2} e.s.u., when the intensity is 5 mm/hr, it should be approximately 6×10^{-2} e.s.u., and when the intensity is 1 mm/hr, approximately 0.3 e.s.u.

It should be noted that data on the charges of individual particles falling from nimbostratus clouds obtained by different authors are highly contradictory. Thus, it is known that the mean charge of both positively and negatively charged drops varies within 10^{-4} and 10^{-3} e.s.u. /2, 61, 73/, the negative charge being somewhat larger than the positive charge. The number of positively charged drops is approximately equal to the number of negative ones. On the whole, however, the charge carried by precipitation from these clouds is positive. In Ireland, for example, according to /75, 76/, 1 g of positively charged drops carries away a charge of 0.1 e.s.u., and 1 g of negatively charged drops, 0.08 e.s.u. (curiously, the difference between these amounts is approximately equal to the previously mentioned value of 0.1 e.s.u. per 1 g).

The data of Table 16 make it possible to understand why the measured charges of individual particles are small and to determine the charge carried by precipitation from clouds to the earth. In fact, the mean excess positive charge per 1 drop is only about 10^{-5} e.s.u. with actual charges of 10^{-3}-10^{-4} e.s.u.

Such a small difference can be observed only in measurements of a very large number of drops or in direct measurements of integral charges — the charge of a large amount of precipitation or of the precipitation current.

Repeating these calculations for positively polarized water clouds, we obtain that the density of the precipitation current from them is $1.6\times$ $\times 10^{-11}$ amp/m^2. In the cloud itself, the "generator" loses through "leakage currents" are approximately 2×10^{-11} amp/m^2. Thus, the cloud as a whole is charged by a current with a density of about 3.5×10^{-11} amp/m^2.

The mean fall velocity of particles from a rain-producing cloud is somewhat higher than that from a snow-producing cloud. The space charge created beneath a rain-producing cloud is due mainly to the charge of the rain particles. It should be noted that the field in nimbostratus clouds may exceed 10-20 v/cm, i.e., they have such a value under which the coalescence efficiency of colliding rain drops rises very strongly /81/.

We now consider the electrification conditions of negatively polarized nimbostratus clouds (their electric characteristics are represented in Figures 34b, 35b, c, and 28b). The existence of clouds of this polarization was completely unexpected.

It is notable that the space charge in precipitation from "warm" and mixed clouds is positive, i.e., of the same sign as the charge in the lower part of the cloud. The scheme of nimbostratus cloud charging considered above cannot be effective in this case if one does not assume that, apart from the precipitation charge, a considerable charge (of opposite sign to the precipitation charge) situated in small particles and in the air, accumulates under the cloud. This assumption, though it requires an experimental check, seems improbable. The space charge on drops is larger than that usually existing in the air. If, however, drops entrain air charged with an opposite sign to that of the charge of the drops, then, for obvious reasons, the total charge of the air above the cloud should have been smaller than the total charge of the drops, which would have led to a field profile which increases and does not, as is actually observed, decrease with altitude.

Another explanation of negative polarization may be the assumption that in these clouds, positively charged precipitation particles fall from the upper part of the clouds. In this case, it is difficult to explain the formation of the lower, negative charge in the cloud. The conductivity in and below the cloud is very small compared with that above it, and it would seem that a negative compensating charge should have formed in the upper part of the cloud and above it, and not in the lower part of the cloud and below it. One may assume, however, that from the upper part of the cloud, negatively charged precipitation particles, and, from its lower part, positively charged precipitation particles fall simultaneously.

The difference in charging may be due to recharging of drops during their fall, but it might possibly be due to two charging processes in the cloud, as was assumed by Chalmers /71/. It should be noted, however, that if one assumes, as Chalmers does, that in mixed clouds, the electrification in the upper part of the cloud is due to the Workman-Reynolds

mechanism /115/, and in the lower part of the cloud, to melting of particles in accordance with the Dinger-Gunn mechanism /77/, then in pure warm, negatively polarized clouds, some other electrification mechanisms no doubt operate. In particular, the mechanism of electrification due to contact potential difference considered above may lead to considerable electrification. If the space charge created beneath the cloud by positively charged precipitation particles is larger than that created by negatively charged precipitation particles, a positive charge arises in the precipitation zone. In this case, it may turn out that, because drops having a charge of one sign are on the average smaller than those of the opposite sign, both a positive and a negative precipitation current may flow then from the cloud, charging the cloud negatively, or positively, respectively.

In fact, the current i_2 can in this case be represented in the form (see (42) and (43)):

$$i_2 = \sum_{m_+} q_m n_m v_m - \sum_{m_-} q_m n_m v_m,$$

where m_+ denotes summing over positively charged particles and m_- over negatively charged particles, and the space charge of the precipitation can be represented in the form

$$\rho = \sum_{m_+} q_m n_m - \sum_{m_-} q_m n_m,$$

i.e., the total current and space charge of the precipitation may be either of the same or of opposite signs, depending on the fall velocities of the particles and the charge distribution over particles of different sizes.

The two electrification processes may, of course, also take place in positively polarized clouds. In the above calculations, the electrification estimates were based on the total current. Some disagreement between the measured space charge and that calculated from vertical-current data is possibly due (in the case of positively polarized clouds) to preferential electrification of large particles with a charge of one sign, and of small particles with a charge of the opposite sign.

The precipitation particles of negatively polarized snow-producing clouds (see Figure 35b) have a negative charge, and their polarization may therefore be due to the dropping of negatively charged particles from the lower part of the cloud and to positive charging of the upper part of the cloud and the air above it. This is confirmed by the charge distribution: a positive charge is concentrated only in the upper part of the cloud and above it, the central part of the cloud being weakly charged. The space charge of the precipitation under snow-producing positively polarized clouds is almost zero. Whether this is due to the presence of particles of both signs in the precipitation from the cloud, or to the fact that there are charges of opposite signs on the particles and in the air, can only be answered by carrying out an experiment in which both the macrostructure and the charges of individual particles will be measured. That positively polarized "snow" clouds are electrified owing to a variation in their resistance in the electric field of the atmosphere, or in any case, that this field plays a significant role in their electrification is not rejected; the low field intensity inside the cloud in particular, supports this.

It can be expected that electrification processes conducive both to positive and to negative polarization may operate in a number of snow clouds; since their efficiency differs considerably, one may attempt to find clouds in which both types of electrification are superimposed. Figure 35c gives the field variation with two extrema in snow clouds, From the broken curve in the figure we can see how the effects of the two mechanisms are superimposed.

In concluding this section, it is interesting to compare the density of the precipitation current flowing beneath nimbostratus clouds with that of the precipitation current flowing beneath thunderclouds. The density of the latter is on the average 10^{-7} amp/m^2 /79,82/, i.e., 10^4 times as large as the current beneath nimbostratus clouds. The precipitation intensity from thunderclouds is only 100 times as high as that from nimbostratus clouds. Formula (50) does not apply in these conditions, which makes it necessary to assume that mechanism of charge generation different to that in stratus clouds operates in thunderclouds.

Thus, the results of the investigation of nimbostratus clouds show the following:

1. Nimbostratus clouds in the moderate latitudes may be both positively and negatively polarized. As one moves to the south, the electric field and charges in clouds increase.

2. In the case of positive polarization of "warm" and mixed clouds, a positive charge is situated in the upper part of the cloud and above it, a considerable negative charge in the middle and lower parts, and again, a small positive charge beneath the cloud. In positively polarized snow clouds the structure is similar, but there is no positive charge beneath the cloud.

In the case of negative polarization of "warm" and mixed clouds, a negative charge is situated in the upper part of the cloud, a large positive charge in the lower part, and a small positive charge beneath the cloud. In negatively polarized mixed clouds the structure is similar, but the charge beneath the cloud is negative (Table 17).

3. Charge formation in positively polarized mixed and warm clouds proceeds as follows: positively charged precipitation particles fall from the cloud, which results in negative charging of the cloud. The field of this negative charge causes the appearance of a corresponding current in the upper part of the cloud and above it, and the formation of a positive charge in this region. Equilibrium charging conditions in the cloud are reached when the total conduction current above and beneath the cloud compensates the precipitation current.

4. The formation of three charges in a cloud may thus be the result of a single mechanism of charging individual particles. It is interesting to check whether the electrification of thunderclouds can also be similarly explained by a single charging mechanism.

5. The "mirror" effect beneath nimbostratus clouds is connected with the fact that positively charged precipitation particles falling from the cloud charge the latter negatively, which results in the fall mainly of positively charged particles in a negative field and of negatively charged precipitation particles in a positive field.

6. Charge formation in negatively polarized mixed and "warm" clouds may result from the fall of positively charged precipitation particles

from the upper part of the cloud and of negatively charged particles from it lower part.

TABLE 17

Cloud characteristics	Charge, e.s.u./m²			Density of the current charging the cloud, amp/m²	
	upper	middle	lower	beneath the cloud	in the cloud
Positively polarized clouds					
Mixed clouds	+20	−25	+2	1.2×10^{-11}	3×10^{-11}
"Warm" clouds	+10	−16	+1	1.6×10^{-11}	3.5×10^{-11}
Snow-producing clouds ..	+ 6	− 5	−0.5		
Negatively polarized clouds					
Mixed clouds	−34	+28	+2		
"Warm" clouds	−10	+12	−0.2		
Snow-producing clouds ..	− 6	+10	−1		

7. The "mirror" effect may not exist beneath negatively polarized mixed and "warm" clouds as well as beneath positively polarized snow clouds.

8. Charge separation in mixed clouds takes place between the 0° isotherm and the −10 and −12° isotherms, which is an indication of the role of melting and freezing of drops in the electrification of these clouds. At the same time, the field and charges in warm clouds are comparable to those in mixed clouds, which is an indication of the considerable role of drop charging (not connected with phase transformations) in the electrification of nimbostratus clouds.

9. Electrification processes in positively polarized snow clouds are weaker than in mixed and "warm" clouds.

10. The field in mixed and "warm" clouds may exert a considerable influence on the coagulation of precipitation particles in them, since the electric field in them exeeds the values which contribute to intensified coagulation.

§ 6. THE INFLUENCE OF STRATIFIED CLOUDS ON THE AMPLITUDE OF THE ELECTRIC CHARGE OF THE EARTH

The charge Q transmitted to the earth in regions occupied by stratified clouds can be expressed by a formula similar to (32),

$$Q=\sum_{i=1}^{i=n}\left[R^2\int_{\varphi}\int_{\theta} mq\,d\varphi\,d\theta\right], \qquad (51)$$

where q is the charge of a unit atmospheric column in a region where i-th type cloudiness prevails; φ is the latitude; θ is the longitude; m is a coefficient depending on the height distribution of the charge over the point chosen; and R is the radius of the earth.

To solve equation (51), one has either to know q and m over the entire surface of the globe, or to attempt to relate q and m to cloudiness data. The second way is obviously simpler.

Thus, in order to assess the role played in the formation of the electric field of the atmosphere by charge exchange between the earth and the atmosphere on days when stratified clouds prevail, not only the charges arising in the atmosphere under conditions of stratified cloudiness in different seasons and in different physicogeographical regions, and the height distribution of these charges, but also the distribution of these clouds over the earth and the variation of this distribution with time have to be known. Unfortunately, there are no comprehensive data at present either on the charge distribution in stratified clouds, or on the distribution of these clouds. We can therefore make only average, general estimates of the magnitude of the charge transferred to the earth, using the data given above.

As indicated earlier, stratified clouds can be both positively and negatively polarized, and have positive and negative charges; the probability of a given type of electrification may depend on the physicogeographical conditions and on the season. In our estimates, however, we have to assume that the mean charge magnitudes obtained from clouds of different types in the investigation regions can, under proper extrapolation, be used for estimating the charges in clouds over the entire globe.

The mean charges contained in a unit atmospheric column at various latitudes are given in Table 18.

TABLE 18

Cloud form	Charge of a unit atmospheric column 6000 m high, e.s.u./m^2		
	Leningrad, 60°	Kiev, 50°	Tashkent, 40°
St	+ 3.0	+2.3	+ 2.6
Sc	+ 2.0	+2.8	+ 2.0
Ns	+ 2.0	+4.2	+14
As	+10.3	+3.4	+ 4.0

This table presents data on the total charge contained in an air column only 6000 m high, but it should be borne in mind, firstly, that this layer contains the main charges of the atmosphere, and secondly, that non-allowance for charges situated above 6000 m may on the average only underestimate the role of clouds in the formation of the global electric field of the atmosphere. Data on upper-level clouds, under the influence of which the negative charge of the earth may rise in absolute value, are omitted in the table. The effect of these clouds will be somewhat smaller than that of stratus or stratocumulus clouds.

The data of Table 18 show that the electrification of frontal precipitation-producing clouds of stratified form (nimbostratus and altostratus) varies considerably with the latitude of the observation points, whereas local stratified clouds, which do not produce precipitation, generally have approximately the same charges at different observation points.

If we assume that the influence of longitude on the charge distribution in clouds can be neglected, and the influence of latitude is taken into account by extrapolation of the data in Table 18 to higher and lower latitudes, the charges in the atmosphere in the case of stratified clouds can be calculated for the whole earth. Table 19 presents the magnitudes of charges calculated for different latitudes in the case of nimbostratus clouds.

TABLE 19

Latitude interval, degrees	0-10	10-20	20-30	30-40	40-50	50-60	60-70	70-80	80-90°
Charge of a unit atmospheric column, e.s.u./m^2	45	36	27	8	8	3	1.5	1	0.5

The values given in the table were obtained either by interpolation, or by linear extrapolation of the measurement results.

A notable fact is the rapid growth of the charges as one moves to the south. The comparison made above between the data of Sivaramakrishnan /106/ and our calculations shows that nimbostratus clouds in India do in fact become much more intensely electrified than in Tashkent.

It should be noted that the density of the mean electric precipitation current for the clouds investigated by Sivaramakrishnan was about 10^{-9} amp/m^2, i.e., more than 80 times as high as the calculated current densities near Leningrad and 30 times as high as the current densities measured in England. Thus, the charging of the earth by precipitation current is more intense than shown in Table 19 as one moves to the south. Nevertheless, the data of this table have naturally to be improved by subsequent measurements.

To calculate the charging of the earth, it is also necessary to use data on the degree to which earth's surface at various latitudes is covered by clouds of different types. The present work makes use of J. London's data /92/ on cloud cover of different types in the northern hemisphere. The information compiled by London probably constitutes the only summary of data available on the seasonal variation of cloud cover of definite types with latitude. Calculations made with formula /51/, using extrapolated data of Table 18 (see, for example, Table 19) and neglecting the variations in the coefficient m with latitude, show that for the northern hemisphere, the influence of stratified clouds on the charging of the earth as a whole is in accordance with the data in Table 20.

As may be seen from Table 20, the largest contribution to charge exchange between the earth and the atmosphere is made by nimbostratus clouds, this being approximately four times as large as that made by stratus and stratocumulus clouds.

The data obtained can be extended to the southern hemisphere but as the large water areas of the southern hemisphere may considerably modify the latitudinal and seasonal variations of the cloud cover as compared with

the nothern hemisphere and affect the magnitudes of cloud charges, this can only be done in a very approximate manner.

The data given by Shaw /103/ could be the only source, apart from that used, in estimating the areas occupied by clouds, but these data are of a very approximate nature, and more important, they do not make it possible to distinguish the specific types of cloudiness.

TABLE 20. Charge transferred by clouds to the earth in the northern hemisphere (coulombs)

Cloud form	Winter	Spring (April)	Summer	Autumn (October)	Annual average
St, Sc	0.25×10^5	0.25×10^5	0.3×10^5	0.25×10^5	0.27×10^5
Ns	1.2×10^5	1.05×10^5	1.2×10^5	1.15×10^5	1.15×10^5
As	0.5×10^5	0.5×10^5	0.55×10^5	0.65×10^5	0.55×10^5
Total	$\sim 2.5\times10^5$	1.7×10^5	2.05×10^5	2.05×10^5	1.95×10^5

Nevertheless, if we assume that the cloudiness in the southern hemisphere has the same electric charges and the same distribution as in the northern hemisphere, then it can be assumed that -4×10^5 coulombs of the earth's charge will be created by stratified clouds, i.e., the charge of the earth depends not only on thundercloud activity, but also on the activity of stratified clouds (we recall that, as indicated above, the absolute value of the proper charge of the earth does not exceed 3.5×10^5 coulombs).

It is much more complicated to estimate the phase of the field variations (even only the annual variations) caused by these clouds. The approximate nature of the estimated values of the mean charge makes for complete arbitrariness when estimating phase and amplitude relations. In order to estimate the phase, it is necessary to know the longitudinal and latitudinal cloudiness variation, and the influence of different forms of the underlying surface on cloud electrification in greater detail, and also to take into account the variation in the altitude and thickness of the clouds in the indicated conditions. At present, initial data for such estimates are not available. But, as a result of the electric activity of stratified clouds, the charges transferred to the earth are of a magnitude comparable with the entire charge of the earth, and this makes it necessary to look for more precise relationships between the electrification of stratified clouds and unitary variations (first and foremost, the annual unitary variation).

In order to determine these relationships, it is necessary to carry out investigations, similar to those made by us, in various parts of the globe, especially at low latitudes and over the oceans.

Bibliography

1. Aleksandrov, N.N. and O.G. Petrenchuk. Metodika izmereniya yader kondensatsii v svobodnoi atmosfere pri samoletnykh zondirovaniyakh (Technique of Measuring Condensation Nuclei in the Free Atmosphere in Aircraft Soundings).— Trudy GGO, No. 93. 1959.
2. Anikeev, I.S. Elektricheskie zaryady dozhdevykh kapel' i snezhinok (Electric Charges of Raindrops and Snowflakes).— Meterologiya i gidrologiya, No.4. 1951.
3. Arabadzhi, V.I. Nekotorye kharakteristiki elektricheskogo sostoyaniya grozovykh oblakov i grozovoi deyatel'nosti (Some Characteristics of the Electric State of Thunderclouds and Thunderstorm Activity).— Uchennye zapiski Minskogo gosudarstvennogo pedagogicheskogo instituta, No.7. 1957.
4. Borovikov, A.M., I.I. Gaivoronskii, E.G. Zak, V.V. Kostarev, I.P. Mazin, V.E. Minervin, A.Kh. Khrgian, and S.M. Shmeter. Fizika oblakov (Physics of Clouds).— Leningrad, Gidrometeoizdat. 1961.
5. Byutner, E.K. and F.A. Gisina. Effektivnyi koeffitsient zakhvata chastits aerozolya dozhdevymi i oblachnymi kaplyami (Effective Collection Coefficient of Aerosol Particles by Rain and Cloud Drops).— Trudy LGMI, No.15. 1963.
6. Voskanov, A.I., I.M. Imyanitov, M.M. Kulik, and A.P. Chuvaev. O vozmozhnosti bezopasnogo prokhoda samoleta cherez grozovye zony (On the Possibility of Safe Aircraft Passage Through Thunderstorm Zones).— Trudy GGO, No. 67. 1957.
7. Gerasimenko, V.I. K voprosu o prichinakh unitarnoi variatsii elektricheskogo polya atmosfery (On the Causes of the Unitary Variation of the Electric Field of the Atmosphere).— Uchenye zapiski Leningradskogo vysshego inzheniernogo morskogo uchilishcha im. Makarova, No.10. 1958.
8. German, M.A. Nekotorye kolichestvennye kharakteristiki turbulentnogo obmena v oblakakh (Some Quantitative Characteristics of Turbulence Exchange in Clouds).— Trudy LGMI, No.12. 1963.
9. Dergach, A.L. Predvaritel'nye rezul'taty nablyudenii za atmosfernymi yadrami kondensatsii za period MGG (Preliminary Results of Observations of Atmospheric Condensation Nuclei During the IGY).— Trudy GGO, No.105. 1963.

10. Zykova, V.V. O roli tokov s ostrii v podderzhanii otritsatel'nogo zaryada Zemli (On the Role of Point Discharge Currents in the Maintenance of the Negative Charge of the Earth).— Trudy GGO, No.110. 1960.
11. Imyanitov, I.M. and T.V. Lobodin. Issledovanie elektricheskoi struktury livnevykh i grozovykh oblakov (Investigation of the Electric Structure of Shower and Thunderclouds).— Trudy GGO, No.136. 1962.
12. Imyanitov, I.M. and V.V. Mikhailovskaya. Opyt issledovaniya zaryadov chastits osadkov v svobodnoi atmosfere (Experience in the Investigation of Charges of Precipitation Particles in the Free Atmosphere). — Trudy GGO, No.97. 1960.
13. Imyanitov, I.M., V.V. Mikhailovskaya, N.P. Ziganov, and M.B. Strel'tsova. Pribor dlya izmereniya napryazhennosti polya atmosfery v slozhnykh meteorologicheskikh usloviyakh (An Instrument for Measuring the Atmospheric Field in Complex Meteorological Conditions).—Izvestiya AN SSSR, seriya geofizicheskaya, No.9. 1956.
14. Imyanitov, I.M. and A.T. Starovoitov. Nekotorye voprosy teorii elektricheskogo zaryazheniya tel v potokakh (Some Problems Concerning the Theory of Electric Charging of Bodies in Streams).— ZhTF, No.6. 1962.
15. Imyanitov, I.M. and E.V. Chubarina. Nekotorye rezul'taty issledovaniya elektricheskogo polya atmosfery s pomoshch'yu samoletov i sovremennye vozzreniya na ego proiskhozhdenie (Some Results of an Investigation of the Electric Field of the Atmosphere by Means of Aircraft and Recent Views on Its Origin).— Materialy konferentsii po itogam MGG (1960) i meteorologicheskogo izucheniya Antarktidy (1959). Moskva, Gidrometeoizdat. 1961.
16. Imyanitov, I.M. and E.V. Chubarina. Khod napryazhennosti elektricheskogo polya v atmosfere s vysotoi v yasnye dni (Variation of the Atmospheric Electric Field with Altitude on Clear Days).— Trudy GGO, No.110. 1960.
17. Imyanitov, I.M. and E.V. Chubarina. Struktura elektricheskogo polya atmosfery i sovremennye vozzreniya na ego proiskhozhdenie (Structure of the Electric Field of the Atmosphere and Recent Views on Its Origin).— Trudy VNMS, Vol.5, Leningrad, Gidrometeoizdat 1963
18. Imyanitov, I.M. and E.V. Chubarina. Elektricheskaya struktura nedozhdyashchikh oblakov nizhnego yarusa (Electric Structure of Low-Level Clouds not Producing Rain).— Trudy GGO, No.146. 1963.
19. Imyanitov, I.M. and A.P. Chuvaev. K voprosu ob osnovnykh protsessakh, vedushchikh k elektrizatsii v grozovykh oblakakh (On the Principal Processes Leading to Electrification in Thunderclouds).— Trudy GGO, No.67. 1957.
20. Imyanitov, I.M. and K.S. Shifrin. Sovremennoe sostoyanie issledovanii atmosfernogo elektrichestva (Present State of the Investigations of Atmospheric Electricity).— UFN, No.76. 1962.

21. Imyanitov, I. M. Issledovaniya elektricheskogo polya v atmosfere (Investigations of the Electric Field in the Atmosphere).— Informatsionnyi sbornik, No. 5 komiteta MGG GUGMS, Leningrad, Gidrometeoizdat. 1958.
22. Izergin, A. M. Issledovanie sostavlyayushchikh vertikal'nogo elektricheskogo toka na zemlyu (Investigation of the Components of the Air-Earth Current). — Trudy GGO, No. 97. 1960.
23. Imyanitov, I. M. K voprosu ob elektrizatsii i provodimosti grozovykh oblakov (On the Electrification and Conductivity of Thunderclouds).— DAN SSSR, Vol. 109. 1956.
24. Imyanitov, I. M. Pribory i metody dlya izucheniya elektrichestva atmosfery (Instruments and Methods for the Study of Atmospheric Electricity).— Moskva, Gostekhizdat. 1957.
25. Imyanitov, I. M. K voprosu o mekhanizme elektrostaticheskogo zaryazheniya (On the Mechanism of Electrostatic Charging).— DAN SSSR, Vol. 121. 1958.
26. Imyanitov, I. M. Elektricheskaya struktura moshchnykh konvektivnykh oblakov i ee svyaz' s dvizheniyami vozdukha v oblakakh (The Electric Structure of Thick Convective Clouds and Its Relationship with Air Motions in Clouds).— In sbornik: "Issledovaniya oblakov, osadkov i grozovogo elektrichestva," Moskva, Izdatel'stvo AN SSSR. 1961.
27. Imyanitov, I. M. Elektricheskie polya v svobodnoi atmosfere (Electric Fields in the Free Atmosphere).— Trudy GGO, No. 35 (97). 1952.
28. Imyanitov, I. M. Elektricheskie polya v moshchnykh kuchevykh i grozovykh oblakakh i ispol'zovanie dannykh o nikh dlya obkhoda samoletami groz (Electric Fields in Thick Cumulus and Thunderclouds and the Use of Data on Them for Aircraft to Avoid Thunderstorms).—Trudy GGO, No. 97. 1960.
29. Imyanitov, I. M. and V. P. Kolokolov. Issledovaniya raspredeleniya indutsirovannogo i sobstvennogo elektricheskogo zaryada na poverkhnosti samoleta (Investigations on the Distribution of the Induced and Proper Electric Charge on the Surface of an Aircraft).— Trudy GGO, No. 58 (120). 1956.
30. Imyanitov, I. M., M. M. Kulik, and A. P. Chuvaev. Predvaritel'nye dannye ob opytakh po regulirovaniyu razvitiya i izmeneniya sostoyaniya oblakov moshchnoi konvektsii v yuzhnykh raionakh ETS i v Zakavkaz'e (Preliminary Data on Experiments for Controlling the Development and Variation of Powerful Convection Clouds in Southern Regions of the European Territory of the USSR and in Trans-Caucasus).— Trudy GGO, No. 67. 1957.
31. Imyanitov, I. M. and T. V. Lobodin. K opredeleniyu absolyutnoi velichiny unitarnoi variatsii gradienta potentsiala elektricheskogo polya atmosfery (On the Determination of the Absolute Value of the Unitary Variation of the Potential Gradient of the Atmospheric Electric Field). — Materialy konferentsii po itogam MGG (1960) i meteorologicheskogo izucheniya Antarktidy (1959). Moskva, Gidrometeoizdat. 1961.

32. Katsyka, A.P., L.G. Makhotkin, G.D. Petrov, and Chzhao Bo-Lin. Elektricheskie zaryady kapel' oblakov i tumanov (Electric Charges of Drops in Clouds and Fogs).— Izvestiya AN SSSR, seriya geofizicheskaya, No.1. 1961.
33. Kolokolov, V.P. Nablyudeniya po atmosfernomu elektrichestvu (Observations of Atmospheric Electricity).— Informatsionnyi sbornik GUGMS, No.2. 1957.
34. Kondrat'ev, K.Ya. Radiatsionnyi balans Zemli kak planety (Radiation Balance of the Earth as a Planet).— Meteorologiya i gidrologiya, No.1. 1957.
35. Kraav, V.I. Ob aerozol'noi teorii atmosfernogo elektrichestva (On the Aerosol Theory of Atmospheric Electricity).— Trudy GGO, No.120. 1962.
36. Krasnogorskaya, N.V. Izmeneniya elektricheskoi provodimosti vozdukha pri razlichnykh meteorologicheskikh usloviyakh (Variations of the Electric Conductivity of the Air under Different Meteorological Conditions).— Izvestiya AN SSSR, seriya geofizicheskaya, No.4. 1958.
37. Laktionov, A.G. Raspredelenie chastits aerozolei v svobodnoi atmosfere (Distribution of Aerosol Particles in the Free Atmosphere).— Izvestiya AN SSSR, seriya geofizicheskaya, No.3. 1958.
38. Levin, L.M. Issledovaniya po fizike grubodispersnykh aerozolei (Investigations in the Physics of Coarse-Dispersed Aerosols).— Moskva, Izvestiya AN SSSR. 1961.
39. Materialy nablyudenii napryazhennosti elektricheskogo polya atmosfery na razlichnykh vysotakh. 1958-1959 gg. (Data on Observations of the Atmospheric Electric Field at Various Altitudes. 1958-1959).— Leningrad, Gidrometeoizdat. 1963.
40. Makhon'ko, K.P. O kharaktere spektra razmerov chastits radioaktivnoi pyli estestvennogo proiskhozhdeniya (On the Size-Spectrum of Natural Radioactive Dust Particles).— Izvestiya AN SSSR, seriya geofizicheskaya, No.1. 1963.
41. Makhotkin, L.G. and B.L. Sushchinskii. Plotnost' ob'emnogo zaryada v Sestroretske (Space Charge Density in Sestroretsk).— Trudy GGO, No.110. 1960.
42. Mason, B.J. Physics of Clouds. [Russian translation. 1961].
43. Obodenskii, V.N. Kurs meteorologii (A Course in Meteorology).— Sverdlovsk, Gidrometeoizdat. 1944.
44. Paramonov, N.A. Unitarnaya variatsiya gradienta potentsiala elektricheskogo polya atmosfery (Unitary Variation of the Potential Gradient of the Atmospheric Electric Field).— DAN SSSR, Vol.70, No.1. 1950.
45. Paramonov, N.A. O godovom khode gradienta atmosferno-elektricheskogo potentsiala (On the Annual Variation of the Atmospheric Potential Gradient).— DAN SSSR, Vol.71, No.1. 1950.
46. Petrov, G.D. Metodika izmereniya zaryadov i razmerov aerozol'nykh chastits s samoleta (Technique of Aircraft Measurement of the Charges and Sizes of Aerosol Particles).— Izvestiya AN SSSR, seriya geofizicheskaya, No.11. 1959.

47. Petrov, G.D. O raspredelenii zaryadov kapel' v kuchevykh oblakakh (On the Distribution of Droplet Charges in Cumulus Clouds).— Izvestiya AN SSSR, seriya geofizicheskaya, No.7. 1961.
48. Pudovkina, I.B. and Yu.S. Sedunov. O nachal'nom mekhanizme zaryazheneiya aerozol'nogo sloya i podynversionnykh sloisto-kuchevykh oblakov (On the Initial Mechanism of Charging of an Aerosol Layer and Subinversion Stratocumulus Clouds).— Izvestiya AN SSSR, seriya geofizicheskaya, No.12. 1963.
49. Programma izmereniya elementov atmosfernogo elektrichestva na okeanakh (Program of Measurement of Atmospheric Electricity Elements at the Oceans).— Informatsionnyi sbornik GUGMS, No.4. 1957.
50. Programma izmerenii napryazhennosti elektrostaticheskogo polya v svobodnoi atmosfere (Program of Measurements of the Electric Field in the Free Atmosphere).— Informatsionnyi sbornik GUGMS, No.4. 1957.
51. Reshetov, V.D. Problema atmosfernogo elektrichestva i aerozol' (The Problem of Atmospheric Electricity and Aerosols).— Trudy TsAO, No.30. 1959.
52. Reshetov, V.D. Issledovanie unipolyarnykh aerozolei (Investigation of Unipolar Aerosols).— Trudy TsAO, No.30. 1959.
53. Saluvere, T.A. Sutochnyi khod ploshchadi, osveshchennoi chasti sushi i okeana (Diurnal Variation of the Illuminated Land and Ocean Area). — Trudy GGO, No.157. 1964.
54. Selezneva, E.S. Rezul'taty nablyudenii za atmosfernymi yadrami kondensatsii v period MGG i MGS (Results of Observations of Atmospheric Condensation on Nuclei During the IGY and Year of International Geophysical Collaboration).— Materialy konferentsii po itogam MGG (1960) i meteorologicheskogo izucheniya Antarktidy (1959). Moskva, Gidrometeoizdat. 1961.
55. Selezneva, E.S. O yadrakh kondensatsii v atmosfere (On Condensation Nuclei in the Atmosphere).— Trudy NIU GUGMS, seriya I, No.7. 1945.
56. Selezneva, E.S. and M.I. Yudin. O zakonomernosti vertikal'nogo raspredeleniya yader kondensatsii v atmosfere (On the Regularity of the Height Distribution of Condensation Nuclei in the Atmosphere).— Trudy GGO, No.105. 1960.
57. Sergieva, A.P. Ob elektricheskikh zaryadakh oblachnykh chastits (On Electric Charges of Cloud Particles).— Izvestiya AN SSSR, seriya geofizicheskaya, No.3. 1958.
58. Stekol'nikov, I.S. Fizika molnii (Physics of Lightnings).— Moskva, Izvestiya AN SSSR. 1943.
59. Tverskoi, P.N. Atmosfernoe elektrichestvo (Atmospheric Electricity).— Leningrad, Gidrometeoizdat. 1949.
60. Tverskoi, P.N. Kurs meteorologii (A Course in Meteorology).— Leningrad, Gidrometeoizdat. 1962.
61. Fedorov, E.K. Elektricheskie zaryady chastits osadkov (Electric Charges of Precipitation Particles).— DAN SSSR, Vol.78. 1951.

62. Frenkel', Ya.I. *Teoriya yavlenii atmosfernogo elektrichestva* (Theory of Atmospheric Electricity Phenomena).— Leningrad-Moskva, Gostekhizdat. 1949.
63. Fuks, N.A. Mekhanika aerozolei (Mechanics of Aerosols).— Moskva, Izdatel'stvo AN SSSR. 1955.
64. Chubarina, E.V. Svyaz' elektricheskogo polya atmosfery s yadrami kondensatsii (Relationship between the Atmospheric Electric Field and Condensation Nuclei).— Trudy GGO, No.157. 1964.
65. Shmeter, S.M. O soderzhanii khlora v vode oblakov v svyazi s ikh mikrostrukturoi (On the Chlorine Content in the Water of Clouds as Related to Their Microstructure).— Trudy TsAO, No.9. 1955.
66. Allee, P.A. and B.B. Philipps. Measurements of Cloud Droplet Charge, Electric Field and Polar Conductivities in Supercooled Clouds.— J. Met., Vol.16, p.405. 1959.
67. Best, A.C. The Size Distribution of Raindrops.— Quart. J. Roy. Met. Soc., Vol.76, p.16. 1950.
68. Brooks, C.E.P. The Distribution of Thunderstorms over the Globe.— Geoph. Mem., No.24, p.145. 1925.
69. Browne, I.C., A.L. Palmer, and T.W. Wormell. The Physics of Rainclouds.— Quart. J. Roy. Met. Soc., Vol.80, p.291. 1954.
70. Bulletin WMO, No.21, p.1. 1953.
71. Chalmers, I.A. The Electricity of Nimbostratus Clouds.— Recent Advances in Atmospheric Electricity, Pergamon Press, London. 1958.
72. Chalmers, I.A. Vertical Electric Current during Continuous Rain and Snow. — J. Atmos. Terr. Phys., Vol.9, p.311. 1956.
73. Chalmers, I.A. and F. Pasquill. The Electric Charges on Single Raindrops and Snowflakes.— Proc. Phys. Soc., Vol.50, p.1. 1958.
74. Clark, J.F. The Fair Weather Atmospheric Electric Potential and Its Gradient. — Recent Advances in Atmospheric Electricity, Pergamon Press, London. 1959.
75. Clelland, I.A. and I. Nolan. The Electric Charge on Rain.— Proc. Roy. Irish Acad. A., Vol.28, p.81. 1912; A., Vol.30, p.61. 1912.
76. Clelland, I.A. and A. Gilmour. Further Observation of the Electric Charge on Rain.— Proc. Roy. Irish. Acad., A., Vol.35, p.13. 1920.
77. Dinger, I.E. and R. Gunn. Electrical Effects Associated with a Change of State of Water.— J. Terr. Magn. Atm. Electr., Vol.51, p.477. 1946.
78. Dreisbach, K. Die Vertikalverteilung der groben Kerne in der unteren Troposphäre und ihr Zusammenhang mit dem elektrischen Potentialgefälle.— Archiv für Meteorologie, Geophysik und Bioklimat., Bd.9, No.1. 1956.
79. Gish, O.H. and G.R. Wait. Thunderstorms and Earth's General Electrification.— J. Geophys. Res., Vol.55, p.473. 1950.
80. Gish, O.H. Universal Aspects of Atmospheric Electricity.— Compendium of Meteorology, T.E. Malone, editor, pp.108, 113, 115. American Meterological Society, Boston. 1951.

81. Goyer, G., I. Mc. Donald, F. Baer, and R. Braham (Jr.). Effects of Electric Fields on Water Droplets Coalescence.— J. Met., Vol. 17, p. 442. 1960.
82. Holzer, R.E. and D.S. Saxon. Distribution of Electrical Conduction Currents in the Vicinity of Thunderstorms.— Journ. Geoph. Res., Vol. 57, p. 207. 1952.
83. Israel, H. Atmosphärische Elektrizität, Bd. 1. 1957; Bd. 2. 1961, Leipzig.
84. Israel, H. and H.W. Kasemir. In welcher Höhe geht der weltweite luftelektrische Ausgleich vor sich?—Ann. der Geophysik, Bd. 5, S. 313. 1949.
85. Isted, G.A. Irregularities in the E-Region Caused by Atmospheric Electricity, London. 1955.
86. Israel, H. and R. Knopp. Zum Problem der Ladungsbildung beim Verdampfen.— Archiv für Meteorologie, Geophysik und Bioklimat., Bd. 13, H. 2. 1962.
87. Kraakevik, J.H. Electrical Conduction and Convection Currents in the Troposphere.— Recent Advances in Atmospheric Electricity, Pergamon Press, London. 1958.
88. Kraakevik, J.H. The Airborne Measurement of Atmospheric Conductivity.— Journ. Geoph. Res., Vol. 63, No. 1. 1958.
89. Krumm, H.C. Der weltzeitliche Tagesgang der Gewitterhäftigkeit.— Zeitschr. f. Geophys., Bd. 28, No. 2. 1962.
90. Lewis, W. Meteorological Aspects in Aircraft Icing.— Compendium of Meteorology. 1951.
91. Lieberman, A. Warm Fog and Cloud Dissipation.— Armour Res. Foundat., Chicago (Ill.). 1960.
92. London, J. A Study of the Atmospheric Heat Balance.— New York University Department of Meteorology and Oceanography. Final Report, Contract, No. Af 19 (122)-165. 1957.
93. Lukomski, H. Preliminary Studies on Electrification of the Atmosphere.— Acta Geophys., Polon., Vol. 8, p. 94. 1960.
94. Magono, C. et al. On the Positive Electrification of Snow Crystals in the Process of Their Melting.— Journ. Met. Soc. Japan, Ser. 11, Vol. 41, p. 270. 1963.
95. Mauchly, S.I. Studies in Atmospheric Electricity Based on Observations Made on Carnegie 1915-1921.— Researches of the Department of Terrestrial Magnetism, Vol. 5, p. 387. 1926.
96. Moore, C.B., B. Vonnegut, and A.T. Botka. Results of an Experiment to Determine Initial Precedence of Organized Electrification in Thunderstorms.— Recent Advances in Atmospheric Electricity. Pergamon Press, London. 1958.
97. Müleisen, R. The Influence of Water on the Atmospheric Electrical Field.— Recent Advances in Atmospheric Electricity. Pergamon Press, London. 1958.
98. Pierce, E. Some Topics in Atmospheric Electricity.—Recent Advances in Atmospheric Electricity. Pergamon Press, London. 1958.

99. Reiter, R. Observation of the Electricity of Nimbostratus Clouds.— Recent Advances in Atmospheric Electricity, Pergamon Press, London. 1958.
100. Sagalyn, R.C. and G.A. Fausher. Space and Time Variations of Charged Nuclei and Electrical Conductivity of the Atmosphere.— Quart. J. Roy. Met. Soc., Vol. 82, p. 428. 1956.
101. Sagalyn, R.C. and J.A. Fausher. Aircraft Investigation of the Large Ion Content and Conductivity of the Atmosphere and Their Relation to Meteorological Factors.— Journ. Atm. Terr. Phys., Vol. 5, p. 253. 1954.
102. Sartor, I. and M.A. Davis. A Comparison of Hydrodynamic and Electrostatic Forces on Cloud Droplets.— Proc. 8-th Weather Radar Conf., San Francisco, Calif. 1960.
103. Shaw, N. Manual of Meteorology, Vol. 2, 2nd edition, Cambridge. 1936.
104. Schotland, R.M. and E.J. Kaplin. The Collision Efficiency of Cloud Droplets.— New York Univ., Dept. Met. Oceanogr. Rep. AFCRC-TH-55-867. 1936.
105. Simpson, G.C. Atmospheric Electricity during Disturbed Weather.— Geophys. Mem., No. 8, p. 1, London. 1949.
106. Sivaramakrishnan, M.V. The Origin of Electricity Carried by Continuous, Quiet Type of Rain in the Tropics.— Ind. Journ Meteor. and Geoph., Vol. 13, p. 196. 1962.
107. Stergis, C., G. Rein, and T. Kangas. Electric Field Measurements above Thunderstorms.— J. Atmos. Terr. Phys., Vol. 11, p. 83. 1957.
108. Sverdrup, H.U. Observation of the Atmospheric-Electric Potential Gradient, 1922-1925.— Researches of the Department of Terrestrial Magnetism, Vol. 6. 1927.
109. Telford, I.W., N.S. Thorndike, and E.G. Bowen. The Coalescence between Small Water Droplets.— Quart. J. Roy. Met. Soc., Vol. 81, p. 241. 1955.
110. Turner, D. The Salinity of Rainfall as a Function of Drop Size.— Quart. J. Met. Soc., Vol. 81, No. 349. 1955.
111. Uchikava, K. Atmospheric Electric Phenomena.— Geophysical Magazine, Vol. 30, No. 4. 1961.
112. Vonnegut, B. and C.B. Moore. Preliminary Attempts to Influence Convective Electrification in Cumulus Clouds by the Introduction of Space Charge into the Lower Atmosphere.— Recent Advances in Atmospheric Electricity. Pergamon Press, London. 1958.
113. Vonnegut, B. and O. McCaig. Airbone Instrument for Measurement and Vectorial Presentation of Electric Potential Gradient.— Journ. Geoph. Res., Vol. 65. 1959, 1960.
114. Whipple, F.I.W. and F.I. Scrase. Point Discharge in the Electric Field of the Earth.— Geoph. Mem., Vol. 7, No. 68. 1936.
115. Workman, E.I. and S.E. Reynolds. Electrical Phenomena Occurring during the Freezing of Dilute Aqueous Solutions and Their Possible Relationship to Thunderstorm Electricity.— Phys. Rev., Vol. 78, p. 254. 1950.

116. Wormell, T.W. Lightning.— Quart. J. Roy. Met. Soc., Vol. 79, No. 342, p. 474. 1953.
117. Wormell, T.W. Atmospheric Electricity; Some Trends and Problems.— Quart. J. Roy. Met. Soc., Vol. 79, p. 3. 1953.

APPENDIX I

Electric field variation with altitude on clear days ($E \pm \sigma$, v/cm). Leningrad, 1958-1959

H, m	Group			
	I	II	III	IV
100	1.38±0.04	1.17±0.36	0.77±0.14	0.57±0.10
200	1.24±0.09	0.91±0.33	0.90±0.13	0.52±0.08
400	1.01±0.07	0.58±0.09	1.15±0.09	0.50±0.05
600	0.83±0.05	0.40±0.05	1.28±0.09	0.48±0.06
800	0.69±0.04	0.32±0.06	1.20±0.09	0.44±0.06
1000	0.59±0.04	0.25±0.06	1.00±0.10	0.41±0.06
1200	0.51±0.03	0.18±0.05	0.81±0.08	0.37±0.05
1400	0.45±0.04	0.14±0.05	0.66±0.06	0.35±0.04
1600	0.39±0.04	0.09±0.05	0.54±0.05	0.34±0.04
1800	0.31±0.03	0.06±0.04	0.47±0.06	0.33±0.04
2000	0.22±0.03	0.05±0.05	0.44±0.06	0.32±0.05
2200	0.16±0.03	0.03±0.03	0.44±0.06	0.30±0.04
2400	0.13±0.03	0.03±0.04	0.46±0.07	0.28±0.04
2600	0.11±0.03	0.02±0.03	0.45±0.09	0.27±0.04
2800	0.10±0.03	0.02±0.03	0.41±0.07	0.26±0.04
3000	0.09±0.03	0.01±0.02	0.38±0.06	0.25±0.04
3200	0.08±0.03	0.02±0.03	0.34±0.04	0.23±0.04
3400	0.07±0.03	0.03±0.02	0.31±0.04	0.22±0.03
3600	0.07±0.03	0.00±0.03	0.28±0.03	0.21±0.03
3800	0.07±0.03	0.02±0.03	0.26±0.02	0.20±0.03
4000	0.07±0.04	0.01±0.03	0.23±0.02	0.20±0.02
4200	0.07±0.03	0.00±0.02	0.21±0.01	0.20±0.02
4400	0.06±0.02	0.00±0.02	0.20±0.01	0.20±0.02
4600	0.06±0.02	0.00±0.02	0.20±0.01	0.20±0.02
4800	0.06±0.03	0.00±0.02	0.20±0.01	0.20±0.02
5000	0.06±0.02	0.00±0.02	0.20±0.01	0.20±0.02
No. of cases	72	23	79	20

APPENDIX II

Electric field variation with altitude on clear days ($E \pm \sigma$, v/cm). Kiev, 1958-1959

H, m	Group I	Group II	Group III
100	1.42±0.13	1.64±0.24	1.27±0.13
200	1.29±0.13	1.55±0.23	1.40±0.16
400	1.10±0.10	1.44±0.22	1.65±0.14
600	0.94±0.12	1.33±0.23	1.84±0.23
800	0.79±0.11	1.22±0.26	1.87±0.24
1000	0.65±0.06	1.05±0.25	1.79±0.21
1200	0.58±0.08	0.90±0.18	1.71±0.24
1400	0.56±0.07	0.79±0.18	1.58±0.27
1600	0.54±0.08	0.71±0.16	1.25±0.27
1800	0.50±0.08	0.65±0.17	0.98±0.22
2000	0.44±0.07	0.61±0.18	0.87±0.21
2200	0.40±0.06	0.57±0.14	0.93±0.19
2400	0.36±0.06	0.49±0.11	0.89±0.16
2600	0.33±0.07	0 37±0.14	0 81±0.17
2800	0.30±0.05	0.22±0.12	0.72±0.17
3000	0.27±0.04	0.09±0.10	0.62±0.17
3200	0.24±0.05	0.01±0.10	0.48±0.14
3400	0.21±0.04	—0.05±0.09	0.32±0.11
3600	0 19±0.03	—0 12±0.11	0.19±0.08
3800	0.17±0.02	—0.17±0.10	0.10±0.10
4000	0.16±0.03	—0.20±0.08	0.05±0.08
4200	0.15±0.03	—0.21±0.09	0.00±0.09
4400	0.14±0.03	—0.22±0.09	—0.07±0 08
4600	0.13±0.02	—0.22±0.07	—0.12±0.08
4800	0.12±0.02	—0.21±0.08	—0.14±0.07
5000	0.11±0 02	—0.22±0.07	—0.13±0.06
5200	0.11±0.02	—0.22±0.06	—0.14±0.06
5400	0.10±0.02	—0 22±0.07	—0.16±0.06
5600	0.08±0.02	—0.22±0.06	—0.16±0.07
5800	0.07±0.02	—0.23±0.04	—0.16±0.07
6000	0.07±0.01	—0.24±0.04	—0.16±0.08
No. of cases	20	23	43

APPENDIX III

Electric field variation with altitude on clear days ($E \pm \sigma$, v/cm). Tashkent, 1958-1959

H, m	Group			
	I	II	III	IV
100	1.23±0.09	0.81±0.56	0.64±0.10	0.37±0.05
200	1.13±0.06	0.66±0.41	0.75±0.09	0.38±0.06
400	0.95±0.05	0.48±0.48	0.88±0 06	0.39±0.05
600	0.78±0.04	0.41±0.39	0.96±0.08	0.41±0.04
800	0.66±0.05	0.38±0.41	0.98±0.08	0.43±0.04
1000	0.57±0.04	0.36±0 40	0.95±0.09	0.43±0.04
1200	0.48±0.04	0.32±0.06	0.90±0.09	0.40±0.04
1400	0.41±0.05	0.28±0 09	0.83±0.10	0.37±0.04
1600	0.38±0.04	0.24±0.04	0.76±0.09	0.36±0.04
1800	0.36±0.04	0.21±0.00	0.69±0.08	0.35±0.04
2000	0.35±0.03	0.16±0.00	0.61±0.08	0.32±0.04
2200	0.32±0.03	0.11±0.04	0.52±0.07	0.29±0.05
2400	0.29±0.04	0.08±0.04	0.44±0.06	0.26±0.04
2600	0.26±0.03	0.07±0.05	0.37±0.04	0.26±0.02
2800	0.24±0.02	0.06±0.06	0.30±0.03	0.25±0.03
3000	0.22±0.02	0.04±0.06	0.23±0.03	0.22±0.02
3200	0.19±0.02	0.02±0.04	0.18±0 03	0.20±0.02
3400	0.17±0.02	0.01±0.03	0.14±0.03	0.19±0.02
3600	0.17±0.02	—0.01±0.00	0.09±0.04	0.19±0.03
3800	0.15±0.02	—0.02±0.00	0.05±0.08	0.19±0.02
4000	0.13±0.02	—0.02±0.04	0.03±0.04	0.19±0.02
4200	0.11±0.03	—0.01±0.09	0.04±0.04	0.20±0.04
4400	0.11±0.02	—0.02±0.05	0.05±0.05	0.20±0.02
4600	0.11±0.02	—0.05±0.08	0.05±0.04	0.20±0.02
4800	0.10±0.02	—0.07±0.06	0.04±0.03	0.20±0.02
5000	0.10±0.02	—0.08±0.04	0.03±0.03	0.20±0.02
No. of cases	49	4	61	21

APPENDIX IV

Space charge density variation with altitude on clear days ($\rho \times 10^2$ e.s.u./m^3). 1958-1959

H, m	Group						
	I	II	III	IV	I	II	III
	Leningrad				Kiev		
100	0.37	0.69	—0.35	0.13	0.35	0.24	—0.35
200	0 31	0.44	—0.33	0.03	0 25	0.15	—0.33
400	0.24	0.24	—0.17	0.03	0.21	0.15	—0.25
600	0.19	0.11	0.11	0.05	0.20	0.15	—0.04
800	0.13	0.09	0.27	0.04	0.19	0.23	0.11
1000	0.11	0.09	0.25	0.05	0.09	0.20	0.11
1200	0.08	0.05	0.20	0.03	0.03	0.15	0.17
1400	0.08	0 07	0.16	0.01	0.03	0.11	0.44
1600	0.11	0.04	0.09	0.01	0.05	0.08	0.43
1800	0.12	0.01	0.04	0.01	0.08	0.05	0.08
2000	0.08	0.03	0.00	0.03	0.05	0.05	—0.08
2200	0.04	0.00	—0.03	0.03	0.05	0.11	0 05
2400	0.03	0.01	0.01	0.01	0.04	0.16	0.11
2600	0.01	0.00	0.05	0.01	0.04	0.20	0.12
2800	0.01	0.01	0.04	0.01	0.04	0.17	0.13
3000	0.01	—0.01	0.05	0.03	0.04	0.11	0.19
3200	0.01	—0.01	0.04	0.01	0.04	0.08	0.21
3400	0.00	0.04	0.04	0.01	0.03	0.09	0.17
3600	0.00	0.03	0.03	0.01	0.03	0.07	0.12
3800	0 00	—0.01	0.04	0.00	0.01	0.04	0.07
4000	0.00	—0 01	0.03	0.00	0.01	0.01	0.07
4200	0.01	0.00	0.01	0.00	0.01	0.01	0.09
4400	0.00	0.00	0.00	0.00	0.01	0.00	0.07
4600	0.00	0.00	0.00	0.00	0.01	—0.01	0.03
4800	0.00	0.00	0.00	0.00	0.01	0.01	—0 01
5000	0.00	0.00	0.00	0.00	0.00	—0.01	0.01

APPENDIX V

Space charge density variation with altitude on clear days ($\rho \times 10^2$ e.s.u./m^3). Tashkent, 1958-1959

H, m	Group			
	I	II	III	IV
100	0.27	0.40	—0.29	—0.03
200	0.24	0.24	—0.17	—0.01
400	0.23	0.09	—0.11	—0.03
600	0.16	0.04	—0.03	—0.03
800	0.12	0.03	0.04	0.00
1000	0.12	0.05	0.07	0.04
1200	0.09	0.05	0.09	0.04
1400	0.04	0.05	0.09	0.01
1600	0.03	0.04	0.09	0.01
1800	0.01	0.07	0.11	0.04
2000	0.04	0.07	0.12	0.04
2200	0.04	0.04	0.11	0.04
2400	0.04	0.01	0.09	0.00
2600	0.03	0.01	0.09	0.01
2800	0.03	0.03	0.09	0.04
3000	0.04	0.03	0.07	0.03
3200	0.03	0.01	0.05	0.01
3400	0.00	0.03	0.07	0.00
3600	0.03	0.01	0.05	0.00
3800	0.03	0.00	0.03	0.00
4000	0 03	—0.01	—0.01	—0.01
4200	0.00	0.01	—0.01	0.00
4400	0.00	0.04	0.00	0.00
4600	0.01	0.03	0.01	0.00
4800	0.00	0.01	0.01	0.00
5000	0.00	0.01	0.01	0.00

APPENDIX VI

Diurnal transformation of the electric field profile ($E \pm \sigma$, v/cm), local time. Leningrad, 1958-1959

Group I

H, m	2 hours	5 hours	14 hours	17 hours
100	1.56±0.22	1.42±0.22	1.83±0.62	1.65±0.17
200	1.33±0.19	1.19±0.09	1.60±0.40	1.38±0.10
400	1.06±0.20	0.94±0.09	1.32±0.19	1.05±0.06
600	0.82±0 07	0.83±0.09	1.06±0.15	0.84±0.07
800	0.64±0.06	0 74±0.10	0.76±0.16	0.70±0 06
1000	0.57±0.07	0.62±0.09	0.49±0.11	0.58±0.06
1200	0.50±0.06	0.52±0.07	0.34±0 13	0.50±0.04
1400	0.44±0.06	0.44±0.06	0.30±0.15	0.47±0.05
1600	0.41±0.08	0.35±0.04	0.30±0.16	0.46±0.06
1800	0.41±0.09	0.28±0.06	0.29±0.11	0.43±0.05
2000	0.39±0.06	0.25±0.02	0.26±0.11	0.41±0.04
2200	0.35±0.04	0.26±0.04	0.22±0.09	0.39±0.04
2400	0.32±0.04	0.27±0.04	0.19±0.13	0.35±0.04
2600	0.29±0.06	0.25±0.04	0.19±0.25	0.32±0.03
2800	0.26±0.05	0.23±0.04	0.20±0.20	0.30±0.03
3000	0.23±0.05	0.22±0.03	0.19±0.10	0.29±0.03
3200	0.23±0.05	0.20±0.02	0.17±0.17	0.27±0.02
3400	0.25±0.05	0.19±0.03	0.17±0.15	0.26±0.02
3600	0.26±0.04	0.19±0.02	0.17±0.08	0.23±0.03
3800	0.24±0.04	0.18±0.02	0.17±0.03	0.23±0.03
4000	0.22±0.03	0.18±0.02	0.18±0.05	0.26±0.07
4200	0.21±0.03	0.18±0.02	0.19±0.05	0.25±0.03
4400	0.20±0 02	0.18±0.02	0 18±0.04	0.22±0.02
4600	0.19±0.02	0.18±0.04	0.19±0.06	0.22±0.02
4800	0.18±0.02	0.18±0.02	0.20±0.06	0.22±0.03
5000	0.19±0.01	0.18±0.02	0.20±0.05	0.21±0.03
No. of cases	14	14	10	23
Q_{0-6000}	4.15	3.30	4.35	3.83

APPENDIX VII

Diurnal transformation of the electric field profile ($E \pm \sigma$, v/cm), local time. Leningrad, 1958-1959

Group III

H, m	2 hours	5 hours	14 hours	17hours
100	0.37±0.24	0.20±0.24	0.79±0.46	0.83±0.20
200	0.45±0.24	0.31±0.27	0.83±0.37	0.88±0.17
400	0.62±0.14	0.68±0 14	0.79±0.44	0.88±0.07
600	0.65±0.08	0.77±0.14	0.77±0.26	0.86±0.09
800	0.76±0.09	0.76±0.14	0.77±0.10	0.84±0.08
1000	0.67±0.09	0.68±0.20	0.70±0.22	0.75±0.12
1200	0.56±0.08	0.59±0.14	0.52±0.10	0.64±0.09
1400	0.48±0.08	0.48±0.14	0.37±0.06	0.54±0.10
1600	0.42±0.08	0.41±0.16	0.28±0.06	0.49±0.12
1800	0.39±0.10	0.41±0.10	0.24±0.00	0.47±0.10
2000	0.40±0.16	0.51±0.10	0.25±0.10	0.45±0.11
2200	0.44±0.15	0.59±0.12	0 31±0.14	0.47±0.14
2400	0.49±0.14	0.64±0.12	0.37±0.24	0.53±0.17
2600	0.53±0.14	0.70±0.18	0.38±0.20	0.49±0.14
2800	0.54±0.16	0.81±0.16	0.36±0.12	0.39±0.10
3000	0.51±0.12	0.87±0.21	0.30±0.12	0.34±0.10
3200	0.43±0.09	0.68±0.12	0.23±0.08	0.31±0.09
3400	0.36±0.06	0.42±0.10	0.18±0.07	0.30±0.08
3600	0.35±0.03	0.32±0.07	0.15±0.03	0.28±0.09
3800	0.35±0.03	0.27±0.04	0.13±0.02	0.25±0.06
4000	0.26±0.03	0.22±0.03	0.12±0.05	0.22±0.04
4200	0.19±0.03	0.19±0.02	0.11±0.00	0.18±0.03
4400	0.18±0.03	0.18±0.02	0.11±0.00	0.17±0.02
4600	0.17±0.04	0.17±0.02	0.11±0.00	0.18±0.02
4800	0.16±0.04	0.16±0.03	0.12±0.00	0.17±0.01
5000	0.14±0.03	0.15±0.02	0.09±0.04	0.15±0.01
No. of cases	20	29	6	29
Q_{0-6000}	3.00	5.65	2.80	2.53

APPENDIX VIII

Diurnal transformation of the electric field profile ($E \pm \sigma$, v/cm), local time. Kiev, 1958-1959

H, m	Group I		Group III	
	3 hours	15 hours	3 hours	15 hours
100	1.35±0.12	2.17±0.19	1.35±0.14	1.07±0.15
200	1.12±0.14	1.88±0.34	1.42±0.22	1.22±0.23
400	0.92±0.09	1.64±0.33	1.62±0.18	1.61±0.24
600	0.83±0.11	1.56±0.29	1.83±0.22	2.07±0.74
800	0.76±0.09	1.26±0.46	1.90±0.29	1.98±0.69
1000	0.72±0.09	0.86±0.22	1.88±0.28	1.65±0.55
1200	0.68±0.16	0.75±0.17	1.90±0.30	1.48±0.55
1400	0.38±0.11	0.74±0.22	1.93±0.35	1.39±0.68
1600	0.69±0.15	0.70±0.18	1.80±0.38	1.34±0.55
1800	0.65±0.13	0.63±0.19	1.50±0.22	1.23±0.53
2000	0.57±0.12	0.55±0.17	1.32±0.22	0.96±0.52
2200	0.51±0.10	0.49±0.16	1.20±0.20	0.73±0.40
2400	0.47±0.12	0.46±0.12	1.12±0.21	0.56±0.27
2600	0.42±0.13	0.48±0.15	1.06±0.22	0.42±0.27
2800	0.39±0.08	0.42±0.09	0.99±0.22	0.28±0.24
3000	0.38±0.09	0.32±0.06	0.87±0.22	0.11±0.31
3200	0.35±0.08	0.25±0.12	0.66±0.19	0.04±0.21
3400	0.32±0.07	0.17±0.10	0.44±0.17	0.03±0.19
3600	0.28±0.05	0.14±0.06	0.27±0.11	0.00±0.19
3800	0.26±0.04	0.14±0.03	0.15±0.13	0.05±0.18
4000	0.25±0.04	0.11±0.03	0.07±0.12	0.08±0.18
4200	0.24±0.05	0.06±0.00	0.00±0.12	0.08±0.14
4400	0.22±0.04	0.03±0.10	0.07±0.12	0.09±0.13
4600	0.20±0.04	0.05±0.03	0.12±0.08	0.07±0.11
4800	0.18±0.03	0.06±0.05	0.14±0.07	0.06±0.09
5000	0.17±0.04	0.05±0.00	0.14±0.06	0.04±0.11
5200	0.16±0.03	0.05±0.04	0.16±0.05	0.02±0.12
5400	0.15±0.04	0.05±0.00	0.18±0.06	0.03±0.15
5600	0.14±0.03	0.05±0.03	0.18±0.07	0.05±0.12
5800	0.11±0.03	0.05±0.00	0.18±0.08	0.09±0.15
6000	0.09±0.03	0.05±0.00	0.18±0.08	0.10±0.23
No. of cases	9	4	24	10
Q_{0-6000}	3.35	5.63	7.04	8.42

APPENDIX IX

Diurnal transformation of the electric field profile ($E \pm \sigma$, v/cm), local time. Tashkent, 1958-1959

Group I

H, m	6 hours	12 hours	18 hours	24 hours
100	1.08±0.19	1.76±0.42	1.35±0.12	1.50±0.31
200	0.90±0.09	1.73±0.33	1.23±0.08	1.27±0.23
400	0.72±0.06	1.33±0.30	0.97±0.08	0.99±0.15
600	0.65±0.08	0.69±0.31	0.75±0.07	0.83±0.12
800	0.65±0.08	0.37±0.00	0.64±0.07	0.79±0.13
1000	0.63±0.06	0.32±0.00	0.53±0.06	0.80±0.20
1200	0.55±0.06	0.34±0.00	0.44±0.06	0.72±0.00
1400	0.49±0.06	0.39±0.16	0.38±0.04	0.62±0.00
1600	0.46±0.07	0.37±0.16	0.34±0.04	0.59±0.07
1800	0.43±0.06	0.32±0.00	0.31±0.03	0.57±0.06
2000	0.40±0.06	0.28±0.00	0.27±0.03	0.54±0 06
2200	0.38±0.06	0.22±0.00	0.24±0.03	0.49±0.06
2400	0.36±0.05	0.16±0.00	0.21±0.02	0.42±0.05
2600	0.33±0.06	0.15±0.00	0.19±0.02	0.38±0.05
2800	0.29±0.03	0.13±0.00	0.18±0.02	0.37±0.07
3000	0.25±0 01	0.09±0.00	0.17±0.02	0.34±0.04
3200	0.23±0.01	0.08±0.00	0.15±0.02	0.29±0.04
3400	0.23±0.03	0.06±0.00	0.14±0.02	0.26±0.02
3600	0.23±0.04	0.05±0.00	0.14±0.04	0.24±0.02
3800	0.23±0.03	0.03±0.00	0.15±0.04	0.23±0.02
4000	0.25±0.03	0.00±0.00	0.16±0.02	0.21±0.02
4200	0.26±0.06	0.01±0.00	0.16±0.01	0.21±0.02
4400	0.24±0.03	0.07±0 00	0.15±0.01	0.20±0.00
4600	0.22±0.04	0.12±0.00	0.15±0.01	0.19±0.00
4800	0.20±0.03	0.15±0.00	0.14±0.01	0.19±0.02
5000	0.20±0.03	0.16±0.00	0.15±0.01	0.20±0.04
No. of cases	16	2	25	6
Q_{0-6000}	2.34	4.25	3.19	3.46

APPENDIX X

Diurnal transformation of the electric field profile ($E \pm \sigma$, v/cm), local time. Tashkent, 1958-1959

Group III

H, m	3 hours	9 hours	15 hours	21 hours
100	0.21±0.14	0.59±0.26	0.90±0.16	0.36±0.10
200	0.44±0.07	0.87±0.26	1.01±0.16	0.50±0.14
400	0.73±0.08	0.95±0.81	1.10±0.09	0.68±0.08
600	0.87±0.10	0.94±0.92	1.10±0.11	0.79±0.10
800	0.94±0.16	1.00±1.09	1.03±0.10	0.83±0.17
1000	0.95±0.16	0 96±0.95	0.96±0.12	0.85±0.13
1200	0.88±0.16	0.85±1.00	0.94±0.14	0.90±0.14
1400	0.83±0.16	0.83±0.92	0.85±0.14	0.98±0.33
1600	0.81±0.16	0.82±0.35	0.69±0.11	0.95±0.31
1800	0.77±0.17	0.64±0.44	0.57±0.08	0.86±0.23
2000	0.69±0.14	0.46±0 49	0.49±0.08	0.82±0.40
2200	0 61±0.14	0.39±0.54	0.40±0.06	0.75±0.27
2400	0.51±0.12	0.30±0.44	0.32±0.04	0.63±0.16
2600	0.41±0.07	0.14±0.26	0.26±0.04	0.56±0.14
2800	0.33±0.06	0.02±0.33	0.22±0.03	0.48±0.10
3000	0.28±0.05	0.17±0.00	0.19±0.03	0.38±0.07
3200	0.29±0.05	0 17±0.16	0.16±0.03	0.31±0.06
3400	0.18±0.05	0.16±0.00	0.13±0.04	0.26±0.04
3600	0.08±0.06	0.19±0.00	0.09±0.05	0.22±0.03
3800	0.01±0.20	0.20±0.00	0.06±0.05	0.21±0.03
4000	0 01±0.07	0.15±0.17	0.05±0.05	0.19±0.03
4200	0.06±0.06	0.14±0.17	0.04±0.06	0.18±0.02
4400	0.09±0.08	0.18±0.00	0.03±0.06	0.16±0.04
4600	0.07±0.05	0 19±0.00	0.02±0.05	0.13±0.03
4800	0.05±0.04	0.23±0.00	0.01±0 05	0.10±0.04
5000	0.04±0.04	0.31±0.00	0.02±0.05	0.09±0.04
No. of cases	23	2	28	7
Q_{0-6000}	4.65	4.57	3.40	4.02

APPENDIX XI

Diurnal transformation of profiles of Group III, excepting 15 cases having two maxima. Leningrad, 1958-1959

H, m	Hours					
	3	6	7	12	15	18
100	0.21	0.73	0.76	—2.00	1.61	0.69
200	0.41	1.42	0.91	1.17	1.71	0.78
400	0.67	1.92	1.51	0.84	1.44	0.85
600	0.79	2.02	2.35	1.28	1.05	0.92
800	0.79	1.98	3.04	1.30	0.82	0.92
1000	0.67	1.79	3.24	1.14	0.79	0.81
1200	0.50	1.54	2.55	0 58	0.48	0.62
1400	0.39	1.29	1.47	0.40	0.32	0.49
1600	0.33	1.07	0.99	0.11	0.32	0.45
1800	0.28	1.01	0.97	—0.02	0 34	0.42
2000	0.24	1.09	0.87	—0.01	0.21	0.41
2200	0.24	1.14	0.71	0.01	0.11	0.40
2400	0.26	1.06	0.59	0.04	0.12	0.37
2600	0.26	0.90	0.51	0.07	0.15	0 29
2800	0.25	0.81	0.48	0.07	0.17	0.23
3000	0.24	0.81	0.49	0.06	0.15	0.21
3200	0.23	0.71	0.54	0.06	0.10	0.19
3400	0.23	0.61	0.68	0.05	0.09	0.17
3600	0.22	0.57	0.78	0.03	0.08	0 16
3800	0.21	0.54	0.68	0.05	0.08	0.16
4000	0.21	0.47	0.50	0.07	0.08	0.17
4200	0.21	0.45	0.42	0.08	0.09	0.15
4400	0.21	0.43	0.40	0.08	0.10	0.15
4600	0.20	0.41	0.38	0.07	0.11	0.16
4800	0.18	0.41	0.34	0.04	0.12	0.15
5000	0.16	0.30	0.22	0.00	0.10	0.10
No. of cases	16	11	2	2	5	12

APPENDIX XII

Diurnal variations on clear days of the electric field E (v/cm) at various altitudes, of the atmospheric potential V_{6000} at an altitude of 6000 m (kv), and of the space charge Q_{0-600} of an air column 6000 m high with a base of 1 m^2 (e.s.u./m^2). Leningrad, 1958-1959

Altitude, m	Hours							No. of cases
	0	3	6	12	15	18	24	
E at ground level	2.1	2.8	3.0	2.7	2.6	2.6	2.1	186
100	0.8	0.9	1.0	1.3	1.6	1.8	0.8	
200	0.7	0.9	0.8	1.4	1.2	1.6	0.7	
300	0.7	0.7	0.6	1 2	1.1	1.6	0.7	
500	0.9	0.7	0.6	0 9	1.0	1.1	0.9	
700	0.7	0.7	0.4	0 7	0.8	1.1	0.7	
1000	0.6	0.6	0.2	0.6	0.7	1 6	0.6	
1200	0.5	0.5	0.1	0.4	0.5	0.8	0.5	
1500	0.4	0.5	0.1	0.3	0.4	0.6	0.4	
2000	0.3	0.4	0.0	0.3	0.4	0.5	0.3	
3000	0.3	0.3	0.1	0 2	0.2	0.2	0.3	
4000	0.1	0.2	0.0	0.2	0.2	0.3	0.1	
5000	0.1	0.2	0.1	0.1	0.2	0.2	0.1	
V_{6000}	204	222	80	184	226	278	204	
Q_{0-6000}	2.0	1.9	2.4	3.6	3.0	4.9	2.0	
No. of cases	52	71	3	27	70	9	52	

APPENDIX XIII

Diurnal variations on clear days of the electric field E (v/cm) at various altitudes, of the atmospheric potential V_{6000} at an altitude of 6000 m (kv), and of space charge Q_{0-6000} of an air column 6000 m high with a base of 1 m^2 (e.s.u./m^2). Kiev, 1958-1959

Altitude, m	Hours						
	0	2	6	12	15	18	24
100	1.6	1.1	1.2	1.6	0.5	1.8	1.6
200	1.2	0.9	1.2	1.1	1.4	1.5	1.2
400	1.3	1.0	1.1	1.6	1.6	1.4	1 3
600	1.3	0.9	0.8	1.7	1.7	2.1	1.3
800	1.4	0.9	0.8	1.7	1.6	2.1	1.4
1000	1.3	0.9	0.4	1.4	1.3	1.3	1.3
1200	1.3	0.8	0.4	1.2	1.5	1.0	1.3
1600	1.3	0.5	0.2	1.1	1.1	0.9	1.3
2000	0.8	0.5	0.2	0.9	0.9	0.7	0.8
3000	0.5	0.3	0.2	0.1	0.5	0.2	0.5
4000	0.5	0.2	0.2	0.1	0.0	0.1	0.5
5000	0.2	0.0	0.1	0.1	0.3	0.0	0.2
V_{6000}	286	200	168	301	252	273	286
Q_{0-6000}	4.8	4.5	3.3	5.3	5.0	6.8	4.8

APPENDIX XIV

Diurnal variations on clear days of the electric field E (v/cm) at various altitudes, of the atmospheric potential V_{6000} at an altitude of 6000 m (kv), and of the space charge Q_{0-6000} of an air column 6000 m high with a base of 1 m^2 (e.s.u./m^2). Tashkent, 1958-1959

Altitude, m	Hours						
	0	1	6	11	12	18	24
100	0.4	0.5	0.5	1.5	1.0	0.8	0 4
200	0.5	0.4	1.1	2.1	1.1	0.8	0.5
300	0.6	0.4	1.0	1.1	1.0	0.8	0.6
500	0.7	0.4	0.7	1.0	1.0	0.8	0.7
700	0.6	0.3	0.8	0.5	0.9	0.8	0.9
1000	0.7	0.3	0.5	0.3	0.8	0.8	0.7
1200	0.6	0.3	0.5	0.2	0.7	0.7	0.6
1500	0.5	0.3	0.5	0.2	0.6	0.7	0.5
2000	0.4	0.2	0.2	0.2	0.4	0.7	0.4
3000	0.2	0.2	0.1	0.1	0.2	0.3	0.2
4000	0.1	0.1	0.1	0.0	0.1	0.2	0.1
5000	0.1	0.1	0.1	0.1	0.1	0.1	0.1
V_{6000}	203	167	233	147	203	243	203
Q_{0-6000}	1.0	1.6	3.3	3.9	2.2	2.0	1.0
No. of cases	55	11	6	4	56	15	55

APPENDIX XV

Unitary field variation observed over oceans (o) and at various altitudes over continents (c), and the coefficient of correlation (k) between them (1958-1959)

	Hours						E, mean v/cm	Correlation coefficient k%	Altitude H, m
	0	3	6	12	15	18			
					Leningrad				
o	1.31	1.32	1.17	1.18	1.58	1.69	1.36		0
c	0.7	0.7	0.4	0.7	0.8	1.1	0.7	84	700
c	0.6	0.6	0.2	0.6	0.7	1.6	0.7	84	1000
c	0.5	0.5	0.1	0.4	0.5	0.8	0.5	79	1200
c	0 4	0.5	0.1	0.3	0.4	0.6	0.4	74	1500
c	0.3	0.4	0.0	0.3	0.4	0.5	0.3	76	2000
c	0.3	0.3	0.1	0.2	0.2	0.2	0.2	12	3000
					Kiev				
o	1.31	1.30	1.17	1.18	1.58	1.69	1.36		0
c	1.6	1.1	1.2	1.6	0.5	1.8	1.3	10	100
c	1.2	0.9	1.2	1.1	1.4	1.5	1.2	75	200
c	1.3	1.0	1.1	1.6	1.6	1.4	1.3	37	400
c	1.3	0.9	0.8	1.7	1.7	2.1	1.4	71	600
c	1.4	0.9	0.8	1.7	1.6	2.1	1.4	68	800
c	1.3	0.9	0.4	1.4	1.3	1.3	1.1	46	1000
					Tashkent				
o	1.31	1.28	1.17	1.19	1.18	1.69	1.36		0
c	0.5	0.3	0.5	0.2	0.6	0.7	0.5	59	1500
c	0.4	0.2	0.2	0.2	0.4	0.7	0.3	70	2000
c	0.2	0.2	0.1	0.1	0.2	0.3	0.2	86	3000
c	0.1	0.1	0.1	0.0	0.1	0.2	0.1	56	4000
c	0.1	0.1	—0.1	0.1	0.1	0.1	0.06	16	5000

APPENDIX XVI

Recurrence of various values of the atmospheric potential at an altitude of 6000 m (1958-1959)

Observation point		Range of variation of the potential, kv																			
		<(—201)	(—200)—(—161)	(—160)—(—121)	(—120)—(—81)	(—80)—(—41)	(—40)—(—1)	0—40	41—80	81—120	121—160	161—200	201—240	241—280	281—320	321—360	361—400	401—440	441—480	481—520	>520
Leningrad	No. of cases	84	7	9	10	10	20	25	48	78	74	107	82	71	49	24	20	12	9	4	99
	%	10	1	1	1	1	2.5	3	5.5	9.5	9	12.5	10	8.5	6	3	2.5	1.5	10	5	12
Kiev	No. of cases	53	4	6	3	8	10	33	10	30	40	33	29	30	16	12	12	7	9	4	46
	%	13.5	1	1.5	1	2	2.5	8.5	2.5	7.5	10	8.5	7	7.5	4	3	3	2	2.5	1	11.5
Tashkent	No. of cases	19	2	1	4	4	6	22	18	44	34	38	36	27	13	17	5	4	1	2	29
	%	6	0.5	0.5	1	1	2	7	5.5	13.5	10.5	11.5	11	8.5	4	5	1.5	1	0.5	0.5	9
		Clear days																			
Leningrad	No. of cases	2	—	3	1	2	3	8	15	33	34	32	32	36	19	7	10	4	2	2	13
	%	0.5	—	1	0.5	0.5	1	3	6	12.5	13	12.5	12.5	14	7.5	2.5	4	1.5	0.5	0.5	5
Kiev	No. of cases	5	—	—	1	1	2	3	3	5	6	15	11	5	5	3	3	4	2	1	18
	%	5.5	—	—	1	1	2	3	3	5.5	6.5	16	12	5.5	5.5	3	3	4	2	1	19.5
Tashkent	No. of cases	—	—	—	—	1	1	10	10	19	14	19	24	13	10	8	4	2	1	1	2
	%	—	—	—	—	1	1	7	7	13.5	10	13.5	17	9.5	7	6	3	1.5	1	1	1.5

APPENDIX XVII

Annual variation of the atmospheric potentional V (kv) at an altitude of 6000 m, and of the charge Q (e.s.u./m^2) of an atmospheric column with a base of 1 m^2 and a height 0-6000 m, 0-500 m, 500-3500 m, 3500-6000 m on clear days (1958-1961)

Electric characteristics	I	II	III	IV	V	VI	VII	VIII	IX	X	XI	XII
Leningrad												
V_{6000}	204	212	162	98	30	53	144	208	220	234	130	108
Q_{0-6000}	3.0	4.6	5 1	4.4	2.5	1.4	1.5	1.9	1.8	1.8	1.8	1.6
Q_{0-500}	1.3	1.8	2.3	2.3	1.5	0.8	0.4	0.3	0.4	0.3	0.3	0.7
$Q_{500-3500}$	0.6	1.4	1.8	1.9	1.4	1.4	1.8	1.2	0.8	0.8	0.5	0.1
$Q_{3500-6000}$	0.6	0.4	0.1	0.0	0.1	0.1	0.1	0.2	0.2	0.2	0.4	0.4
No. of cases	15	27	54	47	45	54	59	37	40	19	24	15
Kiev												
V_{6000}	213	192	255	300	265	227	273	361	369	416	565	432
Q_{0-6000}	4.7	4.0	3.8	3.9	3.8	3.6	3.7	3 6	3.4	4.2	5.5	5.6
Q_{0-500}	1.0	1.1	0.7	0.5	0.7	0.6	0.6	—0.2	—0.8	—0.4	—0.5	—0.1
$Q_{500-3500}$	5.4	6.1	3.8	2.9	3.2	2.9	3.1	3.3	1.9	1.4	1.8	2.6
$Q_{3500-6000}$	—0.5	0.1	0.4	—0.1	—0.3	0.1	0.6	1.3	1.1	0.9	1.4	0.0
No. of cases	6	15	17	19	9	13	25	7	17	24	3	8
Tashkent												
V_{6000}	188	167	159	181	265	306	275	171	131	144	171	181
Q_{0-6000}	3.0	2.6	2.2	2.2	2.0	1.5	1.9	2.0	1.8	2.0	2.9	3.3
Q_{0-500}	1 9	1.1	0.1	0.1	—0.2	—0.5	—0.2	0.4	0.4	0.4	1.1	2.0
$Q_{500-3500}$	1.3	1.6	1.9	1.8	1.9	2.0	1.8	1.5	1.4	1.4	1.4	1.3
$Q_{3500-6000}$	—0.3	—0.3	0.0	0.1	0.5	0.6	0.5	0.1	0.0	0.0	0.1	—0.1
No. of cases	21	11	19	20	19	46	24	13	40	23	12	25

APPENDIX XVIII

Annual variation of the atmospheric potential V at an altitude of 6000 m and of the charge Q of an atmospheric column with a base of 1 m^2 and a height of 0-6000 m, 0-500 m, 500-3500 m, 3500-6000 m on all days (1958-1961)

Electric characteristics	I	II	III	IV	V	VI	VII	VIII	IX	X	XI	XII
Leningrad												
V_{6000}	197	206	148	83	119	153	233	289	267	204	127	118
Q_{0-6000}	1.7	3.7	4.0	2.8	1.8	2.0	1.6	1.0	0.5	0.4	0.7	1.0
Q_{0-500}	0.4	0.8	1.2	1.1	1.0	0.8	0.4	—0.2	—0.5	—0.2	0.2	0.3
$Q_{500-3500}$	1.3	2.0	2.1	1.8	1.5	1.3	1.2	1.2	1.2	1.2	1.2	1 1
$Q_{3500-6000}$	—0.3	0.2	0.0	0.3	0.2	0.3	0.1	0.2	0.1	0.0	0.1	—0.4
No. of cases	79	116	134	124	121	139	140	106	130	152	105	136
Kiev												
V_{6000}	192	215	145	86	185	231	176	176	180	196	185	172
Q_{0-6000}	2.4	2.8	2.8	2.8	3.1	3.3	3.9	4.1	4.1	5.6	5.0	2.9
Q_{0-500}	0.2	0.5	0.1	—0.1	0.6	0.8	0.7	0 3	0.2	0.1	—0.3	—0.3
$Q_{500-3500}$	2.5	2.5	2.7	2.8	2.4	2.6	2.9	2.6	1.9	2.6	3.3	2.9
$Q_{3500-6000}$	—0.4	—0.1	—0.3	—0.7	—0.4	—0.1	0.4	1.2	0.7	—0.5	—1 0	—0.7
No. of cases	63	58	64	70	48	58	44	18	43	61	61	78
Tashkent												
V_{6000}	409	454	427	253	192	281	274	164	224	379	504	463
Q_{0-6000}	1.0	0.0	—1.2	0.1	1.7	2.0	2.4	2.0	1.7	1.1	—0.4	0.0
Q_{0-500}	1.2	1.0	0.6	0.3	0.0	—0.4	—0.2	0.4	0.5	0.5	0.9	1.2
$Q_{500-3500}$	1.0	0.5	0.1	1.2	2.2	2.0	1.8	1.4	1.5	1.5	0 9	0.7
$Q_{3500-6000}$	0.1	0.4	0.4	0.2	0 3	0.7	0.6	0.1	0.2	0.4	—0.1	—0.3
No. of cases	77	69	83	63	43	63	35	16	47	51	45	111

APPENDIX XIX

Electric characteristics of stratified clouds

Form of cloud	No. of cases	Altitude of the lower cloud boundary, m	Cloud thickness, m	Atmospheric potential V_{6000}, kv	Charge of the air column, Q_{0-6000} e.s.u./m^2	Electric fields in the clouds, v/cm				Space charge density in the cloud, e.s.u./m^3 × 10^2			Excess charge of the cloud, e.s.u./m^2	Excess charge density, e.s.u./m^3 × 10^2			Potential difference between the cloud boundaries, kv
						$\bar{E}$	$\lvert\bar{E}\rvert$	E_{max}	E_{min}	$\lvert\bar{\rho}\rvert$	ρ_{max}	ρ_{min}		ρ_{ex}	$\rho_{ex\,max}$	$\rho_{ex\,min}$	
St	116	350	500	170	2.5	0.9	1.6	5.5	—15.0	2.8	16.0	—17.5	2.8	1.1	37	—29	17
Sc	357	1000	500	170	1.5	0.3	1.8	14.0	—16.0	3.0	41.0	24.5	3.4	1.7	40	—41	24
As	218	3400	950	265	4.0	—0.2	3.2	64.5	—14.5	8.0	370.0	—290.0	1.0	2.6	127	114	87
Ns	155	900	2100	550	4.2	0.3	5.6	180.0	—120.0	11.5	252.0	—181.0	—3.8	—1.6	438	—348	—78
Cs	48	5500	1100	245	2.8	0.0	2.8	20.0	—9.0	4.0	17.3	—30.6	—0.3	1.9	20	41.2	—323

APPENDIX XX

Absolute values of the mean space charge densities ($\rho \times 10^2$ e.s.u./m^3) in stratified clouds

Cloud form	Observation point	ρ_1	ρ_2	ρ_3	ρ_4	ρ_{ex}	ρ_{mean}
St	Leningrad	2.5	3.3	2.9	4.6	1.2	3.0
	Kiev	2.4	3.0	6.2	2.9	1.1	3.0
Sc	Leningrad	2.2	3.9	2.2	3.1	1.2	3.0
	Kiev	2.0	2.9	2.4	5.8	3.2	2.3
	Tashkent	2.8	3.1	4.0	3.5	0.7	3.0
As	Leningrad	2.6	3.5	5.0	4.3	1.2	3.8
	Kiev	3.9	11.0	7.4	4.5	0.6	9.2
	Tashkent	6.7	7.6	9.8	13.9	6.0	10.7
Ns	Leningrad	2.5	5.6	10.3	15.7	0.9	10.1
	Kiev	3.2	5.5	6.0	7.9	0.5	12.8
	Tashkent	5.8	4.4	10.2	9.7	3.4	11.4
Cs	Leningrad	3.9	2.9	4.0	4.1	1.9	4.0

Remark. In the calculation of ρ_{ex} and ρ_{mean}, complex structures were taken into account.

APPENDIX XXI

Space charge density ($\rho \times 10^2$ e.s.u./m^3) in St clouds of different structures (1958-1959)

Singly-charged clouds		Doubly-charged clouds		Singly-charge clouds		Doubly-charge clouds	
$\rho+$	$\rho-$	ρ_{low}	ρ_{up}	$\rho+$	$\rho-$	ρ_{low}	ρ_{up}
Leningrad				Kiev			
2.4	—1.2	—1.6 2.4	2.2 0.5	1.7	—0.9	—2.7 2.9	2.5 —1.9

APPENDIX XXII

Space charge density ($\rho \times 10^2$ e.s.u./m^3) in Sc clouds of different structures (1958-1959)

Observation point	Singly-charged clouds		Doubly-charged clouds	
	$\rho+$	$\rho-$	ρlow	ρup
Leningrad	2.0	—1.9	—2.1 2.6	3.5 —4.1
Kiev	2.5	—1.0	—1.8 3.3	2.6 —3.0
Tashkent	0.8	—0.9	—1.1 5.3	1.3 —4.4

APPENDIX XXIII

Space charge density ($\rho \times 10^2$ e.s.u./m^3) in As clouds of different structures (1958-1959)

Observation point	Singly-charged clouds		Doubly-charged clouds	
	$\rho+$	$\rho-$	ρlow	ρup
Leningrad	2.9	—2.8	—1.9 1.5	2.3 —3.6
Kiev	1.9	—2.7	—3.9 4.4	12.2 —4.7
Tashkent	2.4	—2.3	—2.9 6.0	2.7 —2.7

APPENDIX XXIV

Space charge density ($\rho \times 10^2$ e.s.u./m^3) in Cs clouds of different structures (1958-1959)

Observation point	Singly-charged clouds		Doubly-charged clouds	
	$\rho+$	$\rho-$	ρlow	ρup
Leningrad	2.5	—5.1	—3.2 2.0	1.4 —2.6

APPENDIX XXV

Space charge density ($\rho \times 10^2$ e.s.u./m^3) in Ns clouds of different structures (1958-1959)

Observation point	Singly-charged		Doubly-charged	
	$\rho+$	$\rho-$	ρlow	ρup
Leningrad	2.1	—1.3	3.8 —2.8	6.8 2.7
Kiev	1.1	—1.8	—1.0 4.0	1.8 —1.2
Tashkent	5.3	—2.5	—6.1 2.9	3.8 —6.3

APPENDIX XXVI

Electric field distribution (%) in stratified clouds. Leningrad, 1958-1959

Cloud form	Field, v/cm																												
	<(—14)	(—14)—(—13)	(—13)—(—12)	(—12)—(—11)	(—11)—(—10)	(—10)—(—9)	(—9)—(—8)	(—8)—(—7)	(—7)—(—6)	(—6)—(—5)	(—5)—(—4)	(—4)—(—3)	(—3)—(—2)	(—2)—(—1)	(—1)—0	0—1	1—2	2—3	3—4	4—5	5—6	6—7	7—8	8—9	9—10	10—11	11—12	12—13	13—14
St							1	1	1	1	1	2	2	3	16	24	32	11	4	1									
Sc						0.5	0.5	2.5	1	1	2.5	3.5	2.5	6	13	24	25	10	4	1.5	1	0.5	0.5						
As	1		1	1	1	1	1	1	1	1	1.5	1	1.5	3.5	10	12.5	18.5	15.5	8	5	4	3	1	0.5	0.5	1	1	1	1
Cs					1	0.5		0.5	1		1	2	3	1.5	22	15	15	8	5	3	1	1	2	2	1				
Ns	3	0.5	0.5	1	1	1	1	2	3	4	6	7	5	10	10	10	9	6	3	2	1.5	1.5	1.5	1.5	1	1	1	1	1

APPENDIX XXVII

Electric characteristics of clouds as dependent on their thickness. Leningrad, 1958-1959

Cloud thickness, m	$\bar{E}$ v/cm	$\bar{E}_{max}$ v/cm	$\rho_{ex} \cdot 10^2$ e.s.u./m^3	$V_u - V_1$, kv	$\bar{Q} \cdot 10^{-3}$ e.s.u.	$\bar{Q}_{max} \cdot 10^{-3}$ e.s.u.	No. of cases	$\bar{E}$ v/cm	$\bar{E}_{max}$ v/cm	$\rho_{ex} \cdot 10^2$ e.s.u./m^3	$V_u - V_1$, kv	$\bar{Q} \cdot 10^{-3}$ e.s.u.	$\bar{Q}_{max} \cdot 10^{-3}$ e.s.u.	No. of cases
	St							Sc						
0—200	1	2	0	4	3	4	12	2	2	1	—	16	31	21
200—500	2	2.5	1	6	12	21	25	2	3	0	—	29	44	108
500—1000	2	4	2	0	35	61	12	2	4	1	—	35	73	50
1000	2	1	0	7	18	44	2	2	5	0	—	51	74	13
	As							Ns						
0—500	1	2	0.0	6	21	40	28	2	4	4	8	16	27	17
500—1000	2	3	0.0	13	27	52	20	2	5	—2	12	32	68	20
1000—2000	4	8	3	126	49	91	18	4	8	5	—23	49	85	24
2000—4000	3	12	0.0	268	69	126	12	10	20	—27	343	87	170	22
4000	8	52	4	265	404	260	6	7	31	4	265	201	275	19

APPENDIX XXVIII

Electric characteristics of clouds as dependent on their thickness. Kiev, 1958-1959

Cloud thickness, m	$\overline{\lvert E \rvert}$ v/cm	$\lvert E \rvert_{max}$ v/cm	$\rho_{ex} \cdot 10^2$ e.s.u./m^3	$V_u - V_l$, kv	$\overline{\lvert Q \rvert} \cdot 10^{-3}$ e.s.u	$\lvert Q \rvert_{max} \cdot 10^{-3}$ e.s.u.	No. of cases
			St				
0—200	1.0	1.4	1.3	8.2	23.0	25.9	10
200—500	1.4	2.3	0.6	42.9	22.3	37.7	23
500—1000	1.9	3.4	1.0	39.5	39.5	65.6	20
1000	2.3	4.6	0.9	68.9	44.7	86.5	5
			Sc				
0—200	1:4	1.6	1.0	—0.4	34.2	42.5	25
200—500	1.5	2.7	1.7	19.1	43.9	64.2	43
500—1000	1.4	2.9	1.1	5.9	53.0	80.4	19
1000	2.8	4.3	0.3	149.2	52.7	84.4	8
			As				
0—500	1.7	3.3	10.1	12.7	77.0	95.8	52
500—1000	2.6	2.8	0.6	41.7	86.4	121.0	8
1000—2000	3.0	6.4	0.7	—60.7	101.6	169.0	10
2000—4000	13.0	68.1	0.3	1501.5	208.7	370.1	5
			Ns				
0—500	0.0	0.5	0.2	—2.4	51.2	84.0	1
500—1000	2.0	3.8	—0.4	47.7	70.8	99.6	7
1000—2000	2.6	7.0	0.2	309.6	55.8	107.0	7
2000—4000	4.7	22.9	0.3	1230.8	147.7	334.2	10

APPENDIX XXIX

Electric characteristics of clouds as dependent on their thickness. Tashkent, 1958-1959

Cloud thickness, m	$\overline{\lvert E \rvert}$ v/cm	$\lvert E \rvert_{max}$ v/cm	$\rho ex \cdot 10^2$ e.s.u./m^3	$V_u - V_l$, kv	$\lvert \overline{Q} \rvert \cdot 10^{-3}$ e.s.u.	$\lvert \overline{Q} \rvert_{max} \cdot 10^{-3}$ e.s.u.	No. of cases
			Sc				
0—200	1.0	1.5	0.5	26.5	32.2	39.8	17
200—500	1.3	2.3	0.2	—1.9	63.4	99.2	18
500—1000	0.9	1.2	0.2	—15.1	93.8	147.8	6
1000	1.3	3.5	0.0	124.0	80.6	140.1	2
			As				
0—500	2.5	4.0	0.5	—2.9	106.5	177.8	19
500—1000	8.3	9.8	1.6	430.0	194.0	357.2	13
1000—2000	4.8	13.1	0.0	235.4	229.9	444.6	10
2000—4000	5.3	18.3	0.3	866.7	283.6	468.1	10
4000	6.1	29.0	—0.7	1861.0	430.6	620.0	1
			Ns				
0—500	3.1	5 4	3.0	—43.9	110.0	134.9	8
500—1000	6.1	9.7	—2.1	—7.8	155.6	290.9	5
1000—2000	3.0	6.6	—0.2	40	152.3	257.8	9
2000—4000	11.9	63 6	—1.3	2472.4	324.8	597.5	6
4000	12.8	30.0	0.4	—163.4	393.5	728.6	2

APPENDIX XXX

Magnitude and distribution of charges in stratified clouds. Leningrad, 1958-1959

Cloud form	Distribution of charges	Polarized clouds, e.s.u./m²					Unipolarly-charged clouds, e.s.u./m³	
		doubly-charged		triply-charged		quadruply-charged		
		$\pm$	$\mp$	$\frac{\mp}{-}$	$\frac{\pm}{+}$	$\frac{\mp}{+}$	positively	negatively
St	Lower polarized charge	—1.6	2.9					
	Upper polarized charge	1.6	—2.9				6.9	—10.6
	Excess charge	4.2	3.3					
	No. of cases	77	23				41	13
Sc	Lower polarized charge	—1.6	8.0					
	Upper polarized charge	1.6	—8.0				7.2	—6.4
	Excess charge	2.7	2.5					
	No. of cases	27	5				16	6
As	Lower polarized charge	—2.9	3.2					
	Upper polarized charge	2.9	—3.2					
	Excess charge	0.0	0.0				15.7	—6.1
	No. of cases	26	23				18	10
Ns	q_1 (below)	—10.1	2.9	—11.4	12.7	4.8		
	q_2 (above)	10.1	—2.9	13.0	—20.5	—22.4		
	q_3	—	—	—5.3	14.3	20.8		
	q_4	—	—	—	—	—7.4		
	Excess charge	0.5	3.7	—3.7	6.6	—4.2	3.4	—8.8
	No. of cases	27	23	15	22	13	13	10
Cs	q_1 (below)	—2.6	1.6	—5.3	3.5			
	q_2 (above)	2.7	—3.5	5.0	—3.7			
	q_3	—	—	—2.4	3.5			
	Excess charge	0.1	—1.9	—2.7	3.2			
	No. of cases	7	6	11	6			

APPENDIX XXXIa

Mean thickness of clouds of different types and different electric structures. Leningrad, 1958-1959

Cloud form	Distribution of charges in the clouds				Multiply-charged clouds
	±	∓	+	—	
St	450	450	200	200	700
Sc	400	430	260	210	700
As	800	900	640	700	1500
Ns	940	1600	630	700	2000

APPENDIX XXXIb

Mean altitude of the lower boundary of clouds of different electric structures

Cloud form	Distribution of charges in the clouds				Multiply-charged clouds
	±	—	+	—	
St	350	200	400	400	350
Sc	900	800	950	800	800
As	3000	3300	3100	3000	3000
Ns	800	850	800	800	800

APPENDIX XXXII

Electric characteristics of stratified clouds in different seasons. Leningrad, 1958-1959

Cloud form	$\lvert\bar{E}\rvert$ v/cm	$\lvert\bar{E}\rvert_{max}$ v/cm	$\rho_{ex} \cdot 10^2$ e.s.u./m^3	$V_u - V_l$ kv	$\lvert\bar{Q}\rvert \cdot 10^{-3}$ e.s.u.	$\lvert\bar{Q}\rvert_{max} \cdot 10^{-3}$ e.s.u.	No. of cases
			Summer				
St	1.7	4.5	4.0	—7.4	65.0	135.0	1
Sc	—1.1	2.6	5.1	11.3	49.1	84.3	17
As	3	8	3	—31	45	85	29
Ns	9	27	14	220	158	160	
			Winter				
St	1.5	2.2	2.1	4.8	10.6	21	20
Sc	0.6	2.3	3.4	1.7	16.3	23.3	43
As	1	3	0	—34	25	26	17
Ns	3	6	2	55	279	95	

APPENDIX XXXIII

Electric characteristics of stratified clouds in different seasons. Kiev, 1958-1959

Cloud form	$\lvert\bar{E}\rvert$ v/cm	$\lvert\bar{E}\rvert_{max}$ v/cm	$\rho_{ex} \cdot 10^2$ e.s.u./m^3	$V_u - V_l$, kv	$\lvert\bar{Q}\rvert \cdot 10^{-3}$ e.s.u.	$\lvert\bar{Q}\rvert_{max} \cdot 10^{-3}$ e.s.u.	No. of cases
			Summer				
St	—	—	—	—	—	—	—
Sc	1.6	4.4	2.1	20.9	47.5	71.8	16
As	2.8	4.9	—0.2	—253.5	—123.0	174.0	24
Ns	4.6	25.7	—1.4	1084.3	95.1	325.7	6
			Winter				
St	1.5	2.4	0.5	44.6	29.9	46.3	43
Sc	1.4	2.4	1.0	39.8	35.1	52.8	33
As	2.0	4.3	—0.6	9.7	58.3	102.5	17
Ns	1.9	3.5	0.8	—205.0	100.0	158.9	8

APPENDIX XXXIV

Electric characteristics of stratified clouds in different seasons. Tashkent, 1958-1959

Cloud form	$\lvert\bar{E}\rvert$ v/cm	$\lvert\bar{E}\rvert_{max}$ v/cm	$\rho_{ex} \cdot 10^2$ e.s.u./m^3	$V_u - V_l$, kv	$\lvert\bar{Q}\rvert \cdot 10^{-3}$ e.s.u.	$\lvert\bar{Q}\rvert_{max} \cdot 10^{-3}$ e.s.u.	No. of cases
			Summer				
St	—	—	—	—	—	—	—
Sc	—	—	—	—	—	—	—
As	25.0	71.0	3.0	2470.0	55.5	840.0	1
Ns	—	—	—	—	—	—	—
			Winter				
St	—	—	—	—	—	—	—
Sc	1.1	1.8	0.4	—0.9	61.8	125.0	26
As	4.2	10.2	0.4	348.4	171.1	319.3	26
Ns	4.2	13.3	—0.3	402.2	187.6	322.4	22

APPENDIX XXXV

Space charges (e.s.u./m^2) in St clouds of different electric structures, referred to reduced cloud thicknesses

No. of cloud layer	Distribution of charges			
	$\pm$	$\mp$	—	+
1	—1.06	1.68	—0.26	1.59
2	—0.74	2.33	—0.06	1.39
3	—0.26	2.06	—0.46	0.98
4	0.19	1.88	—1.12	0.79
5	0.39	1.32	—1.32	0.79
6	0.35	0.92	—1.32	0.66
7	0.58	—0.53	—1.06	0.72
8	0.88	—3.05	—0.53	0.65
9	0.70	—4.42	—0.17	0.43

APPENDIX XXXVI

Space charges (e.s.u./m^2) in Cs clouds of different electric structures, referred to reduced cloud thicknesses

No. of cloud layer	Distribution of charges					
	$\frac{+}{-}$	$\frac{-}{+}$	$-$	$\frac{-}{\pm}$	$\frac{+}{\mp}$	$\frac{\pm}{\pm}$
1	—0.73	0.23	—0.66	—1.78	2.07	—2.89
2	—0 75	—0.29	—1.46	—1.62	1.34	—1.68
3	—0.30	0.55	—1.52	—1.70	—0.70	0.77
4	0.36	0.46	—0.70	0.00	—2.31	2.63
5	0.35	—1.72	—0.19	2.65	—1.38	0.45
6	0.23	—2.03	—0.05	1.90	—0.52	—1.47
7	0.27	—0.60	—0.04	0.01	2.12	—2.88
8	0.24	—0.29	—0.07	—1.10	1.60	—2.32
9	0.18	—0.85	—0.07	—1.83	0.01	3.54

APPENDIX XXXVII

Space charges (e.s.u./m^2) in Sc clouds of different electric structures, referred to reduced cloud thicknesses

No. of cloud layer	Distribution of charges			
	$\pm$	$\mp$	$-$	$+$
1	—0.98	0.80	1.00	0.44
2	—0.87	1.06	—0.53	0.59
3	0.13	1.39	—0.86	0.73
4	0.73	1.19	—0.52	0.86
5	0.66	0.86	—0.72	0.92
6	0.80	0.93	—1.76	0.79
7	1.20	0.46	—2.72	0.59
8	1.40	—1.13	—2.32	0.65
9	1.51	—1.73	—0.97	0.79

APPENDIX XXXVIII

Space charges (e.s.u./m^2) in As clouds of different electric structures, referred to reduced cloud thicknesses

No. of cloud layer	Distribution of charges				Uncharged clouds
	$\pm$	$\mp$	$-$	$+$	
1	—0.79	1.32	—1.15	0.71	0.0
2	—0.86	1.05	—1.59	2.65	0.0
3	—0.79	0.92	—0.53	2.46	0.1
4	0.12	0.26	—0.07	1.13	0.0
5	0.46	—0.40	—0.86	1.32	0.0
6	0.00	0.13	—1.32	1.32	0.0
7	0.59	—0.13	—1.66	1.46	0.0
8	1.45	—1.46	—1.26	1.52	0.0
9	1.32	—1.85	—0.13	0.97	0.0

APPENDIX XXXIX

Space charges (e.s.u./m^2) in Ns clouds with different electric structures, referred to reduced cloud thicknesses

No. of cloud layer	Distribution of charges					
	$\frac{+}{-}$	$\frac{-}{+}$	$-$	$+$	$\frac{\pm}{+}$	$\frac{-}{\pm}$
1	—4.69	4.42	—2.57	0.35	6.91	—4.07
2	—3.05	1.57	—1.39	0.39	4.12	—2.85
3	1.06	—0.20	—0.53	0.32	—1.06	—0.33
4	2.33	—0.13	—0.99	0.32	—4.58	—1.97
5	1.19	—0.08	—1.19	0.46	—4.58	—0.96
6	0.79	0.13	—0.59	0.59	—3.05	0.54
7	0.66	—0.53	—0.39	0.59	—2.25	—0.21
8	0.99	—1.25	—0.39	0.32	—0.48	—1.79
9	1.33	—0.53	—0.43	0.08	0.79	—2.56

APPENDIX XL

Reduced variation of the electric field (v/cm) in St clouds. Leningrad, 1958-1959

No. of cloud layer	30/I 3 hr	10/II 6 hr	11/VIII 6hr	10/XI 15 hr	11/XI 6 hr	11/XI 6 hr	15/XII 3 hr	17/XII 3 hr	21/XII 7 hr	26/I 18 hr	4/II 18 hr
	a. Positively polarized clouds										
	1958									1959	
1	1.8	0.5	0.8	1 1	1.1	0.1	0.4	0.4	1.8	0.8	1.9
2	2 0	0.8	0.8	1.3	1 6	0.2	1.0	1.0	1.8	0 9	2.4
3	2.0	0.9	1.0	1.3	1.7	0.4	1.0	1.4	2.2	1.0	2.6
4	1.6	1.0	0.8	1.6	1 0	0.0	0.9	2.5	2.4	1.3	3.0
5	1.6	1 2	0.7	1.3	2.2	0.0	0.0	1.4	1.9	1.3	1.7
6	1.6	1.2	0.6	1.4	2.0	0.1	0.2	2.0	2.2	1.2	1.0
7	1.1	1.2	0.5	1.4	1.8	—0.4	—0.4	1.4	2.2	1.1	0.3
8	0.6	0.6	0.5	1.0	1.1	—0.8	—0.1	1.0	1.1	0.2	—0.4
9	0.0	0.0	0.5	0.7	0.6	—0.5	—0.6	0.9	0 7	—0.2	—1.6
10	—0.2	—0.7	0.5	0.0	0.6	—0.2	—0.2	0.4	0.4	—0.1	—2.0

No. of cloud layer	11/II 18 hr	14/II 18hr	15/II 3 hr	24/III 18hr	27/III 18hr	9/IV 18 hr	27/V 6 hr	5/XI 3 hr	10/XI 15 hr	15/XI 15 hr	20/XI 15hr
	1959										
1	0.9	1.2	1.2	1.5	0.6	3.1	—2.0	1.5	2.0	—5.0	1.5
2	1.3	1.7	1.4	1.8	0.7	3.6	—2.0	2.0	2.2	3.5	2.1
3	1.8	1.8	1.3	2.4	0.8	4.0	—0 5	2.0	2.8	—0.5	2.3
4	2.2	1.6	0.9	1.8	0.8	4.8	—0.5	1.9	3.6	1.5	2.3
5	2.0	1.2	0.2	1.9	0.5	5.2	—0.5	1.8	4.2	2.0	1.5
6	1.9	1.2	0.0	2.2	0.0	5.5	—0.5	2.5	3.2	2.4	1.6
7	1.9	1.0	—0.6	1.9	—0.4	5.5	—0.5	1.8	2.5	2.6	1.3
8	1.8	1.0	—1.4	1.0	—0.8	5.1	—0.5	2.1	2.5	2.1	1.1
9	0.9	0.0	—1.4	1.0	—0.4	2.6	—2.0	—0.8	1.4	1.8	1.0
10	0.6	0.5	—1.6	0.8	—0.6	2.0	—0.5	—2.1	0.2	1.4	0 8

No. of cloud layer	1/XII 6 hr	2/XII 18 hr	23/XII 18hr	24/XII 18hr	28/XII 18hr	30/XII 3 hr	Total	No. of cases	$\bar{E} \pm \sigma$, v/cm
1	1.4	1.9	1.2	1.5	0.5	2.4	24.2	28	0.9±0.29
2	4.1	2.4	1.9	1.3	1.5	2.8	37.1		1.4±0.28
3	1.0	3.5	1.9	1.6	2.2	2.8	44.7		1.6±0.20
4	1.0	4.0	2.0	1.8	1.6	2.4	48.2		1.8±0.22
5	0 0	3.7	2.7	1.8	1.3	1.8	43.0		1.6±0.25
6	0.1	2.6	2.2	1.6	1.2	1.5	41.1		1.5±0.24
7	0.9	2.2	2.4	0.8	0.8	1.2	34.4		1.3±0.25
8	0 5	2 1	2.6	—1.0	0.3	1.2	23.9		0.9±0.26
9	3.4	2.1	2.0	—1.4	0.1	1.3	9.1		0.3±0.23
10	0.2	2.2	2.0	—1.4	0.4	1.1	4.7		0.2±0.21

No. of cloud layer	27/V 6 hr	22/VI 3 hr	21/X 18 hr	15/XII 21hr	27/V 6 hr	20/XI 15 hr	31/XII 6 hr	Total	No. of cases	$\bar{E} \pm \sigma$, v/cm

b. Negatively polarized clouds

	1958				1959					
1	0.0	0.8	1.0	2.4	—1.2	1.4	0.3	4.7	7	0.7±0.43
2	—0.2	1.6	0 8	2.2	—2.0	1.4	0.0	3.8		0.5±0.53
3	—0.2	0.0	0.8	0.5	—9.6	1.2	0.0	—7.3		—1.0±1.44
4	—2.1	—0.5	0.6	3.5	—11.5	1.1	—0.2	—9.1		—1.3±1.82
5	—0.4	—3.5	0.6	1.0	—14.5	0.9	—0.2	—16.1		—2.3±2.11
6	0.0	—4.0	0.6	—0.5	—14.5	1.0	0.0	—17.4		—2.5±2.09
7	—3.6	—4.0	0.8	—1.0	—15.0	1.0	—0.2	—22.0		—3.1±2.11
8	—0.1	—5.5	0.7	—2.5	—15.0	0.8	0.1	—21.5		—3.1±2.16
9	—1.0	—5.0	0.7	—1.0	—7 0	1.0	0.2	—12.2		—1.7±1.16
10	—0.1	—1.8	0.7	—0.5	0.5	1.2	0.4	0.4		0.1±0.37

No. of cloud layer	22/IV 18 hr	17/V 6 hr	30/XII 18hr	10/I 15 hr	10/IV 18 hr	11/XII 6hr	Total	No. of cases	$\bar{E} \pm \sigma$, v/cm

c. Negatively charged clouds

	1958			1959					
1	—3.8	—1.8	0.2	—1.8	—	0.0	—7.2	6	—1.4±0.73
2	—2.9	—1.9	0.2	—1.9	—	0.2	—6.3		—1.2±0.62
3	—2.4	—2.0	0.3	—2.0	—2.0	0.4	—7.7		—1.3±0.52
4	—2.4	—1.9	0.4	—1.6	—2.0	0.4	—7.1		—1.2±0.51
5	—0.8	—1.9	0.4	—1.2	—0.5	0.5	—3.5		—0.6±0.37
6	0.8	—2.0	0.5	—0.9	—0.5	1.0	—1.1		—0.2±0.47
7	2.0	—0.8	0.6	—0.8	1.0	0.5	2.5		0.4±0.49
8	2.4	—0.6	0.6	—0.7	2.0	2.0	4.7		0.8±0.52
9	2.5	—0.8	0.7	—0.5	1.6	2.8	6.3		1.0±0.62
10	2.4	—0.8	0.8	—0.2	1.2	2.9	6.3		1.0±0.58

d. Positively charged clouds

No. of cloud layer	22/I 6 hr	12/III 18hr	11/XI 18 hr	16/XI 18 hr	20/XI 15 hr	16/XII 15hr	19/XII 15hr	19/XII 15hr	20/XII 7 hr	20/XII 15hr
1	3.0	1.6	3.0	1.1	1.6	2.6	1.8	2.1		3.2
2	2.5	1.8	3.0	1.1	1.7	2.5	1.4	1.4	1.6	1.0
3	2.4	1.6	2.7	1.1	1.5	2.6	1.3	1.4	1.6	0.6
4	2.0	1.8	2.6	1.1	0.8	2.4	1.2	1.4	1.5	0.7
5	1.8	1.6	2.0	1.0	0.9	2.5	0.8	1.2	1.2	0.7
6	1.0	1.8	1.2	1.0	0.4	2.3	0.7	1.2	0.8	0.6
7	0.6	1.3	1.0	0.9	0.2	1.2	0.7	1.0	0.0	0.6
8	0.3	0.9	0.8	0.9	−2.0	1.6	0.7	0.6	0.8	0.6
9	−1.6	1.0	0.7	0.8	−3.5	0.6	0.7	−0.2	0.8	0.5
10	−1.1	0.8	0.7	0.8	−8.0	0.9	0.7	0.2	0.9	0.5

No. of cloud layer	3/I 6 hr	27/I 6 hr	28/III 6 hr	30/XI 15hr	3/XII 6 hr	3/XII 18hr	28/XII 18hr	28/XII 18hr	Total	No. of cases	$\bar{E} \pm \sigma$, v/cm
					1959						
1	0.9	1.2	1.8	1.0	2.4	10.6	1.1	1.6	36.0	18	2.4±0.61
2	0.7	1.2	1.9	0.9	2.4	5.6	1.0	1.6	29.0		1.8±0.39
3	0.6	−3.0	1.7	0.8	2.4	2.5	1.0	1.2	20.0		1.2±0.23
4	0.4	−5.0	1.1	0.8	2.4	0.9	0.7	1.3	14.3		0.9±0.42
5	0.2	−6.5	0.7	0.8	2.4	0.6	0.6	1.0	10.1		0.6±0.50
6	0.0	−8.5	0.6	0.7	2.4	0.7	0.4	0.9	5.4		0.3±0.61
7	−0.3	−10.0	0.6	0.7	2.2	0.7	0.4	0.6	1.5		0.1±0.69
8	−0.6	−11.5	0.6	0.7	2.1	0.8	0.2	0.4	−3.3		−0.2±0.78
9	−0.9	−11.5	0.5	0.7	2.1	0.8	0.2	0.6	−7.1		−0.5±0.79
10	−1.1	−10.0	0.4	0.7	2.1	1.0	0.4	0.6	−9.2		−0.6±0.84

e. Multiply-charged clouds

No. of cloud layer	10/XI 15hr	11/XII 6hr	19/XII 7hr	3/I 6 hr	10/II 3 hr	10/II 3 hr	27/V 6 hr	15/XII 3 hr	15/XII 3 hr
	1958			1959					
1	0.7	1.5	1.1	0.3	1.0	2.0	0.0	3.3	1.3
2	0.6	1.8	0.3	0.1	1.2	2.5	−0.2	3.2	0.8
3	0.4	1.9	0.2	−0.7	2.0	2.5	−0.2	1.8	1.5
4	0.5	1.0	−0.2	−0.1	1.8	2.5	−2.1	2.8	1.5
5	0.3	1.2	−0.6	−0.2	1.0	2.5	−0.4	3.3	1.4
6	0.9	1.9	0.0	0.3	0.2	2.5	0.0	3.3	1.3
7	0.3	0.8	0.8	0.4	−1.4	1.0	−3.6	3.3	0.9
8	0.2	0.8	0.4	0.2	1.0	2.5	−0.1	3.1	0.4
9	0.2	0.6	0.2	−0.8	1.0	2.5	−1.0	2.2	0.4
10	0.0	0.5	−0.1	−0.8	1.0	1.0	−0.1	1.6	−0.4

APPENDIX XLI

Reduced variation of the electric field in Sc clouds. Leningrad, 1958-1959

a. Positively polarized clouds

No. of cloud layer	6/II 18hr	20/IV 15hr	26/IV 6hr	29/IV 18hr	16/V 18hr	11/V 18hr	24/V 18hr	12/VI 6hr	22/VI 15hr	4/VII 6hr	5/VII 3hr
1	0 6	0.2	—0.6	0.6	—0.3	0.2	0.6	1.4	0.0	1.9	0.2
2	0.5	0.5	—1.7	0.0	—0.6	1.1	1.6	1.5	0.3	2.8	0.2
3	1.3	2.0	—1.8	0.0	—0.9	1.2	1.9	1.8	2.5	2.4	0.8
4	1.2	2.0	2.3	2.0	—0.5	2.2	2.1	1.8	3.5	2.0	0.4
5	0.8	0.8	0.2	2.0	1.4	5.5	2.0	1.4	0.5	2.2	1.0
6	0.4	0.8	0.3	1.0	2.8	0.5	1.6	1.0	2.0	1.5	1.0
7	0.5	0.6	0.8	1.0	2.2	0 5	1.2	0.8	0.0	0.8	1.0
8	0.5	0.3	0.6	2.5	2.2	1.0	1.5	0.7	0.0	0.4	1.0
9	0.6	0.5	0.4	1.0	1.7	1.0	1.2	0.6	—3.0	0.1	1.0
10	0.6	—0.4	0.4	2.5	1.2	0.0	1.0	0.2	—2.5	0.2	0.4

No. of cloud layer	5/VII 3hr	8/VII 6hr	15/VII 15hr	6/VIII 18hr	21/VIII 18hr	25/VIII 3hr	9/IX 7hr	10/IX 6hr	18/IX 3hr	18/IX 9hr	18/IX 15hr
1	1.2	0.4	0.6	1.4	0.5	0.5	1.0	0.8	0.8	1.9	1.2
2	3.0	0.7	0.9	1.2	0.4	0.5	1.2	1.0	0.8	1.8	1.3
3	2.2	0.6	1.2	1.1	2.7	0.6	1.5	1.0	1.0	2.2	1.4
4	2 2	0.6	1.6	1.2	3.0	0.6	1.2	0.8	1.0	2.0	1.0
5	2.6	0.8	0.9	1.3	1.8	0.6	1.2	0.5	1.0	1 9	0.8
6	1.8	0.4	0.8	1.5	0.5	0.7	1.1	0.5	—1.0	1 4	0.6
7	1.3	2.0	0.8	1.5	1.2	0.5	1.1	0.6	0.0	1.1	0.5
8	0 5	2.0	0.4	1.4	1.8	0.4	0.4	0.5	—0.5	0.5	0.3
9	0.5	1.0	0.6	1.3	1.8	0.4	0.2	0.4	—0.4	0.5	0.3
10	0 0	1.0	0 4	0.9	1.6	0.3	0.3	0.3	0.4	0.4	0.4

No. of cloud layer	2/X 6hr	5/X 15hr	16/X 18hr	22/X 18hr	24/X 6hr	27/X 20hr	5/XI 15hr	6/XI 6hr	15/XI 3hr	24/XI 18hr
1	1.0	1.4	2.0	1.1	1.3	0.5	0.1	1.1	1.9	1.7
2	1.2	1.8	2.6	1.2	0.3	0.2	1.8	1.3	2.0	2.1
3	1.5	1.6	2.2	1.7	2.0	3.5	1.5	1 3	2.2	2.1
4	2.0	0.9	2.8	1.4	1.0	3.5	0.8	1.3	2.1	0.9
5	1.8	0.6	2.9	1.2	1.0	5.0	0.5	0.8	1.8	—0.9
6	1.6	0.8	2.9	1.8	5.0	4.5	0.6	0.8	0.8	0.0
7	0.9	0.7	2.3	2.6	3.5	7.5	1.1	0.7	1.2	0.0
8	0.8	0.6	1.9	2.8	2.5	6.0	1.0	0.6	1.1	0.2
9	0.3	—1.0	1.4	2.2	3.5	6.0	0.3	0.8	0.9	0.0
10	0.3	—0.5	1.0	0.9	2.0	0.5	0.4	0.2	0.5	0.2

No. of cloud layer	26/XI 6hr	7/XII 18hr	10/XII 18hr	12/XII 3hr	12/XII 7hr	12/XII 15hr	15/XII 7hr	15/XII 7hr	16/XII 3hr	19/XII 21hr
1	1.2	0.8	1.4	1.0	1.2	1.3	1.5	0.2	1.3	0.8
2	0 3	0.8	2.1	2.5	1.4	1.4	1.9	0.3	1.3	1.1
3	2.8	0.9	1.6	3.2	1.6	1.4	2.1	0.0	1.3	0.9
4	—0 5	1.2	1.4	3.4	1.8	1.4	2.2	0.4	1.2	0.9
5	—2.5	1.5	1.0	2.7	1.9	1.5	2.2	0.2	1.4	1.1
6	—4.0	1.2	0.6	2.3	2.2	1.2	2.2	0.2	1.7	0.5
7	—4.0	0.9	—0.2	2.0	2.0	1.2	1.4	0.1	1.6	0.5
8	—4.0	0.8	—1.4	1.6	2.2	1.2	0.5	0.0	1.3	0.2
9	—4.0	0.7	—1.2	1.5	1.9	0.6	0.1	0.0	1.2	0.5
10	—5.5	0.5	—1.4	1.6	1.6	0.4	0.1	0.0	0.9	0.6

No. of cloud layer	7/I 18hr	14/I 6hr	16/I 6hr	30/I 15hr	10/II 15hr	6/III 18hr	10/IV 18hr	18/IV 15hr	7/VII 18hr	16/VII 21hr	1/VIII 6hr	8/VIII 6hr	29/VIII 18hr
1959													
1	1.0	2.9	1.7	—3.4	1.2	1 5	0.8	0.6	1.5	1.8	1.0	0.9	1.3
2	1.4	2.9	2.0	—0.5	1.0	1.9	1.2	0.6	1.8	1.8	1.0	0.9	1.8
3	1.9	3.2	1.6	—1.6	1.2	2.4	2.0	5.4	1.4	2.0	0.8	1.0	2.2
4	1.2	3.3	1.6	0.3	1.4	3.5	2.2	6.5	0.2	1.6	1.0	1.3	1.6
5	0.4	3.3	1.6	—0.2	0.4	3.5	2.1	9.0	0.0	1.2	1.0	1 2	0.5
6	—0.7	3.0	1.6	1.0	1.9	3.5	2.0	9.5	2.5	1.3	1.1	1.2	1.0
7	—1.4	2.7	1.4	1.0	2.1	3.4	1.5	9.5	1.0	1 0	0.8	1.0	—0.5
8	—1.8	2.3	1.4	0.6	2.0	3.6	1.2	6.5	—0.5	0.7	2.5	0.8	—2.0
9	—6.5	2.0	1.4	—0.1	1.3	2.8	0.3	6.5	2.5	0.6	0.0	1.0	—3.5
10	—6.5	2.2	1.2	—0.4	1.6	1.2	0.2	6.5	0.4	0.4	—0.2	0.8	—2.0

No. of cloud layer	2/IX 6hr	11/IX 18hr	18/IX 18hr	1/X 18hr	2/X 6hr	2/X 18hr	3/X 6hr	5/X 18hr	7/X 6hr
1	1.9	0.5	—9.5	—3.5	1.8	1.9	1.5	2.8	1.8
2	1.2	1.8	—5.0	—2.0	1.8	1.7	2.7	3.4	2.8
3	1.8	2.0	—2.0	—5.0	2.6	2.3	3.2	3.0	2.2
4	1.8	1.9	—2.0	—0.5	—4.0	1.3	—2.0	1.7	2.4
5	0.3	2.0	—5.5	—0.5	—7.5	0.8	—6.0	3.0	2.4
6	6.5	3.5	—7.0	—2.5	—9.0	—1.6	—2.0	—0.5	2.5
7	6.5	2.0	—7.5	—5 5	—9.0	—2.0	—3.5	—2.0	3.6
8	5.0	2.0	—9.0	—7.5	—10.5	—5.0	—4.0	—2.5	2.5
9	6.0	—1.0	—10.5	—9.0	—11.0	—6.5	—7.0	—4.0	2.5
10	2.0	—2.0	—15.0	—10.0	—12.5	—6.5	—6.0	—8.0	2.6

No. of cloud layer	8/X 18hr	9/X 6hr	10/X 6hr	14/X 18hr	17/X 18hr	11/XI 6hr	11/XI 18hr	17/XI 18hr	18/XI 18hr	21/XI 6hr
1	2.4	2.6	3.8	1.3	2.8	1.2	0.8	1 4	3.4	1.5
2	2.4	5.2	4.2	1.3	3.2	2.0	1.5	1.0	3.8	1.5
3	2.8		4.0	1.8	3.4	4.0	2.2	0.9	4.6	1.4
4	2.7		3.7	2.3	3.3	2.1	2.4	0.9	4.6	1.4
5	2.4	—5.5	3.6	2.8	2.8	2.0	1.6	0.9	4.7	1.6
6	2.8	—2.5	2.8	0.8	2.6	1.4	—0.6	1.2	4.6	1.2
7	1.1	—2.5	1.6	0.5	2.4	0.8	—3.0	1.4	3.8	0.6
8	0.0	—4.5	1.4	—2.5	2.2	0.8	—3.5	1 7	3.2	0.7
9	—5.0	—6.0	1 6	—2.5	1.5	—0.5	—2.0	1.8	0.9	0.0
10	—4.0	—6.0	1.6	—5.0	1.2	—0.5	—2.0	1.2	0.9	—0.8

No. of cloud layer	2/XII 18hr	3/XII 6hr	16/XII 6hr	17/XII 6hr	18/XII 6hr	19/XII 6hr	19/XII 18hr	20/XII 3hr
1	1.0	0.4	1.9	1.5	0 8	6.0	1.4	1.1
2	0.9	0.5	2.2	1.4	1 6	6.0	2.2	1.4
3	1.2	0.8	2.5	1.4	1.8	6.8	2.4	1.8
4	1.6	1.2	2.6	1.8	1.0	3.9	2.4	2.0
5	0.5	1.0	2.4	2 1	—0.4	6.5	2.3	2.0
6	1.0	1.0	2.4	2.0	—2.0	5.7	2.3	1.9
7	0.7	0.7	2.5	2.0	—2.0	6.4	2.0	1.6
8	0.4	0.2	2.8	2.1	—2.0	5.4	1.6	1.2
9	0.4	0.1	2.4	1.5	3.5	4.4	1.2	1.0
10	0.0	0.1	1.2	0.9	—5.0	3.2	1.1	1.0

No. of cloud layer	23/XII 6hr	30/XII 15hr	31/XII 6hr	Total	No. of cases	$\bar{E} \pm \sigma$, v/cm
1	1.8	1.2	2.6	90.8	85	1.1±0.2
2	2.0	1.3	3.3	121.7		1.4±0.2
3	2.8	1.2	3.9	147.4		1.7±0.2
4	3.4	1.2	3.9	139.0		1.6±0.2
5	3.3	1.6	3.4	111.5		1.3±0.3
6	3.0	1.6	3.2	103.6		1.2±0.3
7	2.0	1.7	2.4	78.8		0.9±0.3
8	1 2	1.0	1.6	41.5		0.5±0.3
9	1.0	2.8	0.4	—3.8		0.0±0.4
10	—1.2	0.3	—0.2	—48.2		—0.5±0.4

No. of cloud layer	14/III 6hr	22/IV 6hr	22/IV 6hr	1/V 6hr	10/VII 15hr	21/VIII 6hr	17/IX 3hr	18/IX 15hr	31/X 18hr
b. Negatively polarized clouds									
1	0.8	0.0	—1.0	1.3	1.0	1.0	0.9	2.1	2.0
2	0.7	—2.0	—1.1	1.4	0.8	|	1.1	1.9	1.9
3	0.4	—3.5	—1.4	1.1	0.7	0.6	0.7	1.5	1.8
4	0.7	—2.5	—0.8	0.4	0.8	—0.5	0.3	1.6	1.7
5	0.5	—2.5	—1.7	—1.0	0.6	—0.5	—1.0	1.8	1 3
6	0.2	—1.0	—1.4	—1.5	0.6	—0.5	0.2	1.9	1.0
7	0 2	—2.0	—1.2	—1.6	0.9	—1.0	—2.6	2.1	1.0
8	0 4	—5.5	—1.4	—2.0	1.0	0.0	—2.0	2.2	1.1
9	0.4	—3.5	—2.1	—3.5	1.0	—0.2	—2.0	2.1	1.2
10	0.4	—0.5	—1.5	—1.0	0.7	—0.1	0.5	1.9	1.4

No. of cloud layer	23/XI 6hr	24/XI 6hr	1/XII 6hr	5/XII 6hr	5/XII 18hr	15/XII 7hr	17/XII 3hr	19/XII 7hr	19/XII 7hr
1	0.8	|	—4.0	0.8	0.0	—0.1	0.3	—0.2	1.1
2	0.4	—3.5	—5.5	1.0	—0.2	—0.2	0.5	—0.5	0.3
3	|	—5.5	—4.9	0.8	—0.5	—0.2	0.6	—1.1	0.2
4	—3.5	—5.5	—9.0	—0.3	—0.2	—0.2	0.2	—1.5	—0.2
5	—5.5	—7.0	—5.0	—2.2	0.0	—1.0	0.2	—1.4	—0.6
6	—5.5	—5.5	—4.5	—3.5	—0 5	—0.1	—0.2	—0.9	0.0
7	—5.5	—6.0	—4 5	—3.5	—0.6	0.1	—0.1	—0.2	0.8
8	—7.0	—6 0	—3.5	—3.0	—0.4	0.0	0.0	—0.2	0.4
9	—5.5	—5.5	—2.0	—2.0	0.0	—0.2	—0.2	—0.2	0.2
10	—5.5	—3.5	—3.5	—2.0	—0.1	—0.1	0.3	—0.4	—0.1

No. of cloud layer	21/I 6 hr	25/I 3 hr	3/II 6 hr	29/VIII 6hr	12/IX 6 hr	23/IX 6 hr	19/XI 6hr	19/XI 18hr	20/XII 15hr	Total	No. of cases	$\overline{E} \pm \sigma$, v/cm
1959												
1	0.3	—9.5	0.8	—0.8	—0.6	0.2	—2.0	4 8	1.6	1 3	26	0.0±0.5
2	—1.6	—8.0	0.5	—1.0	—0.6	0.6	—3.5	4.6	1.0	— 9.4		—0.3±0.5
3	—1.3	—8.0	0.4	—0.3	—1.2	0.9	—4.0	4.3	0.4	—16.2		—0.6±0.5
4	—3.5	—9.5	0.5	—0.2	—0.9	—0.5	—7.0	2.8	—0.2	—33.5		—1.3±0.6
5	—5.0	—11.0	0.5	—1.3	—4.4	—0.5	—1.0	+0.4	—1.0	—43.0		—1.7±0.6
6	—5.0	—9.5	0.5	—0.3	—13.0	—6.0	—1.0	—1.2	—1.6	—53.7		—2 0±0.7
7	—5.0	—8.0	0.4	—0.5	—16.0	—8.0	—1.5	—1.4	—1.8	—60.5		—2.3±0.8
8	—8.0	—8.0	0.6	1.0	—10.5	—12.5	—16.0	—0.6	—2 1	—74.0		—2.8±0.9
9	—6.0	—6.0	0.6	1.0	—14.5	—6.5	—7.5	—0.6	—2 2	—57.7		—2.2±0.7
10	—4.5	—6.0	0.4	1.0	—3.5	—5.0	—5.0	—0.6	—1.0	—32.8		—1.2±0.4

No. of cloud layer	16/V 18 hr	22/VI 15hr	16/IX 3 hr	18/IX 21hr	28/X 6hr	29/X 18 hr	30/X 3 hr
			c. Negatively charged clouds				
1	—0.8	0.7	0.8	0.8	0.3	—	0.9
2	—0.2	0.6	0.8	0.9	0.4	—	0.3
3	—0.4	0.6	0.9	0.8	0.4	—	0.6
4	0.0	0.7	1.6	1.0	0.4	2.9	0.6
5	0.0	1.0	0.8	1.4	0.4	2.3	1.0
6	—0.2	0.7	0.8	1.4	0.8	2.4	1.4
7	0.1	—	—	1.0	0.7	4.6	2.2
8	0.1	—	—	1.2	0.4	9.5	2.5
9	0.4	1.2	2.4	1.4	0.4	9.5	3.4
10	0.1	1.8	2.2	1.3	1.0	8.0	3.5

No. of cloud layer	25/I 3 hr	24/III 6hr	24/III 6 hr	27/V 18hr	18/VI 18hr	4/XII 18hr	15/XII 15hr	Total	No. of cases	$\bar{E}\pm\sigma$, v/cm
					1959					
1	—3.4	0.6	1.2	0.0	1.6	—0.7	1.0	3.8	14	0.3±0.4
2	—3.0	1.0	1.2	0.0	—0.1	—0.6	1.0	2.5		0.2±0.3
3	—2.7	1.0	1.2	0.1	0.6	—0.2	1.7	5.0		0.4±0.3
4	—2.4	2.4	1.4	0.0	1.2	0.0	1.8	11.6		0.9±0.4
5	—2.1	3.3	1.3	0.0	1.6	0.4	1.5	12.9		1.0±0.3
6	—1.8	3.2	1.0	0.0	1.6	0.9	1.4	13.8		1.1±0.3
7	—1.5	8.2	1.8	0.1	1.8	0.8	1.4	21.1		1.9±0.7
8	—1.5	13.5	1.9	0.2	1.0	0.9	1.8	31.5		2.9±1.2
9	—1.0	14.0	9.0	0.2	13.0	0.4	1.7	55.6		4.2±1.4
10	—1.3	12.5	10.5	0.8	10.5	0.7	1.9	53.4		4.1±1.3

No. of cloud layer	6/II 6 hr	28/VI 6 hr	15/VII 3 hr	21/VIII 6 hr	22/VIII 6 hr	9/IX 18 hr	16/IX 15 hr	16/IX 21 hr
				d. Positively charged clouds				
				1958				
1	1.3	0.7	2.6	1.3	1.2	1.2	—0.5	1.2
2	1.2	0.6	2.6	1.0	1.1	1.1	—0.5	1.2
3	1.2	0.2	2.2	1.2	0.7	1.1	—0.4	1.1
4	1.2	0.2	2.0	1.1	0.6	1.1	—0.5	1.1
5	—	0.2	1.5	1.0	0.4	1.1	—0.4	0.4
6	1.4	0.1	1.4	0.8	0.3	1.2	—0.4	1.0
7	0.9	0.2	1.6	0.4	0.3	0.9	—0.4	0.9
8	0.4	0.2	1.6	0.6	0.5	0.6	—0.4	0.8
9	0.4	0.1	0.5	0.7	0.4	0.9	—0.2	0.6
10	0.0	0.2	0.5	0.8	0.4	0.6	—0.1	0.7

No. of cloud layer	17/IX 15hr	19/IX 15hr	30/IX 18hr	2/X 6 hr	7/X 6 hr	16/X 18 hr	30/X 15 hr	31/X 6 hr
1	1.2	1.2	1.3	2.3	1.3	0.7	2.3	1 5
2	1.1	1.0	1.3	2.4	1.3	0.7	1.6	1.4
3	1.2	1.1	1.3	2.4	1.4	0.3	1.3	1.6
4	1.0	1.0	1.2	2.2	1.4	—0.4	1.4	1.4
5	0.5	0.8	1.1	2.4	1.4	—0.6	1.0	1.2
6	0.4	0.8	0.9	2.2	1.2	—0.4	0.5	1.1
7	0.2	0.6	0.9	2.2	1.1	—0.2	0.2	0.9
8	—0 2	0.6	0.7	2.2	1.0	—0.2	0.0	0.4
9	0.4	1.1	0.6	2.1	0.8	—0 6	—0.8	0.6
10	0.4	0.0	0.6	1.0	0.8	—0 6	—0.6	0.0

No. of cloud layer	15/XI 15hr	16/XI 6 hr	24/XI 6 hr	25/XI 3 hr	16/XII 7hr	20/XII 3hr	25/I 3 hr	5/II 15hr	16/II 6 hr
				1958				1959	
1	0.9	1.6	1.0	1.6	2 0	1.5	—0.3	0.4	2.3
2	1.0	1.4	1.0	1.5	2.2	1.6	—0.3	0.7	2.3
3	0.6	1.2	1.0	1.2	1.7	1.3	—0.3	0.5	2.4
4	0.1	1.3	0.9	1.0	1.5	1.1	—2.8	0.4	2.3
5	0.4	1.2	0.6	0.9	1.3	0.6	—3.1	0 3	2.0
6	0.2	0.5	0.3	0 7	1.6	0.5	—4.5	—0.2	1.4
7	—0.2	0.5	0.0	0.6	1.4	0.6	—8.3	—0.8	1.4
8	—0.2	—0.5	0.2	—0.2	1.5	0.2	—11.3	—0.9	1.2
9	—0.6	—0.5	0.2	—0.5	1.0	0.5	—11.0	—0.8	0.6
10	—0.4	—1.0	0.4	—0.5	0.8	0.6	—11.3	—0.6	1.2

No. of cloud layer	24/III 6hr	24/IV 21hr	9/V 6 hr	12/X 18hr	14/X 6 hr	19/X 3hr	20/X 21hr	23/X 15 hr	27/X 15hr	30/X 6 hr
					1959					
1	1.8	1.4	0.9	2.8	1.0	3.0	4.0	—6.5	0.0	1.8
2	1.8	0.8	1.2	2.2	1.0	3.8	3.8	—6.5	—0.8	2.0
3	1.6	0.4	1.2	2.2	—5 0	2 6	3.4	—6.5	—1.4	1.8
4	1.4	—0.4	0.3	1.8	—4 0	1 0	2.4	—6.5	—1.8	1.4
5	1.5	0.4	—1.3	1.8	—5.5	0.7	1.7	—6.5	—1.9	1.4
6	1.4	—0.8	—2.7	1.6	—5.5	0.6	1.3	—8.0	—1.8	0 8
7	1 2	0.0	—5.0	1.6	—7.0	0.5	1.4	—8.0	—1.7	—0.5
8	1.4	0.4	—5.0	1.6	—7.0	0.4	1.4	—6.5	—1.6	0.5
9	1.4	—0.6	—5.5	1.3	—5.5	0.4	1.4	—8.0	—1 3	—3.0
10	1.2	—0 5	—5.5	1.3	—9.5	0.4	1.3	—9.5	—1.6	—3.5

No. of cloud layer	3/XI 20 hr	12/XI 6 hr	28/XI 6 hr	3/XII 6 hr	20/XII 3 hr	22/XII 18 hr	Total	No. of cases	$\bar{E} \pm \sigma$, v/cm
1	2.4	1.0	2.7	2 8	0.8	3.0	54.7	41	1.3±0.2
2	2.4	1.0	2.6	2.7	0.8	2.8	52.1		1.2±0.2
3	2.4	—	2.3	2.6	0.3	3.0	38.4		0.9±0.3
4	2.2	—	2.4	2.2	0.4	3.3	27.9		0 7±0 3
5	2.0	—6.0	2.2	2.1	0.0	2.9	11.7		0.3±0.3
6	1.9	—6.0	2.2	1.6	—0.8	2.2	10.0		0.0±0.4
7	1.0	—6.5	1.6	—0.6	—1.0	0.9	—16.3		—0.4±0.4
8	0.8	—6.5	1.0	—0 8	—0.8	0.6	—21.4		—0.5±0.4
9	0.4	—8.0	—0.2	—0.4	—2.0	0.8	—32.3		—0.8±0.4
10	0.4	—11.0	—0.6	—0.5	—1.6	1.1	—44 2		—1.1±0.5

No. of cloud layer	14/IV 18 hr	16/X 6 hr	29/V 18 hr	30/V 3 hr	23/IX 18 hr	23/X 21 hr	26/X 15 hr	26/X 21 hr

e. Multi-charge clouds

	1958		1959					
1	1.6	0.7	—	—2.5	1.0	—2.0	3.2	1.9
2	1.8	0.6	—	5.0	0.0	—3.5	4.0	0.8
3	1.6	—	—	3.5	—4.0	—4.0	2.5	—2.0
4	0.8	—	—0.8	—2.0	—2.0	—1.0	0.4	—3.5
5	1.4	0.9	—0.6	—1.8	—1.0	—2.0	0.0	—0.5
6	1.4	—2.0	—6.5	—1.1	0.1	—1.0	—0.5	—1.1
7	1.4	—0.5	—3.5	5.0	—3.5	—0.5	—0.5	0.9
8	1.6	—0.5	—3.5	2.0	—0.5	—2.0	—2.0	—5 0
9	1.6	—0.5	—5.0	—2.5	2.5	—2.0	—3.5	—3.5
10	1.3	—2.5	—2.0	—1.0	—2.0	—3.5	—2.0	—2.0

8/XII 18 hr	14/IV 18 hr	30/IV 15 hr	8/I 6 hr	9/X 18 hr	8/X 6 hr

f. Uncharged clouds

1959	1958		1959		
1.0	0.1	0.3	1.0	3.0	2.2
—0.5	0.1	0.3	1.0	3.0	2.0
—2.0	0.1	0.3	1.0	2.9	2.0
—0.5	0 1	0.3	1.1	3.0	2.0
—0.5	0.0	0.3	1.1	3.0	2.2
1.0	—0.1	0.3	1.1	3.0	2.2
1.0	—0.1	0.3	1.1	3.0	2.2
—0.4	—0.1	0.3	1.1	3.0	2.0
—1.6	—0.1	0.3	1.1	3.0	2.2
—2.2	—0.2	—0.3	1.1	3.0	2.0

APPENDIX XLII

Reduced variation of the electric field in As clouds. Leningrad, 1958-1959

No. of cloud layer	25/I 15 hr	16/VI 9hr	17/VII 6hr	18/VII 6hr	19/VII 6hr	28/IX 18hr	29/IX 18hr
	a. Positively polarized clouds						
	1958						
1	—0.6	—1.5	—2.0	0.0	2.5	0.4	0.3
2	0.8	—1.4	0.5	2.9	2.5	0.3	0.3
3	0.1	—	—0.5	2.5	2.0	—2.5	0.5
4	0.0	—	—0.5	4.0	1.0	12 0	1.2
5	0.1	—0.5	—0.5	3.0	2 0	1.4	0.2
6	0.2	—0.5	—0.5	4.5	2.0	0.8	0.1
7	0.2	—0.5	—0.2	0.3	0.5	0.5	0.1
8	0.3	—2.0	0.4	0 2	0.0	0.2	0.1
9	0.7	—1.0	0.3	0.2	—2.5	0.0	0.2
10	0.9	—2.0	—0.5	0.7	—1.5	—0 3	0.3

No. of cloud layer	29/IX 18hr	30/IX 6hr	16/X 18hr	21/X 18hr	22/X 18hr	25/X 15hr	29/X 6hr	29/X 18hr
1	0.3	0.2	0.0	3.5	0.7	0.1	0.0	2.7
2	0.4	0.7	—0.1	2 5	—0.5	0.2	0.0	5.2
3	0.9	3.4	—0.6	1 5	—4.0	0.2	0.5	11.0
4	0.9	2.7	—3.5	1.5	—1 0	0.2	0.5	13.5
5	0.7	2 8	—3.5	4.0	—1.5	0.2	0.2	13 5
6	1.0	2.4	—3.5	3.5	—1.0	0.3	—	13.5
7	1.3	1.8	—2.5	3.5	—2.5	0 1	1.6	16.0
8	1.0	1.8	—2.5	4.0	—1.0	2.3	1.6	10.5
9	0.5	1.1	—2.5	4.0	—1.0	0.0	1.0	9.5
10	—1.0	1.1	—3.5	1.5	—2.0	—0.1	0.2	9.5

No. of cloud layer	3/XI 18hr	24/XI 18hr	4/XII 18hr	31/I 6 hr	10/IV 18hr	22/IV 3hr	1/VII 6hr
				1959			
1	0.3	0 5	0.6	—2.0	—0.5	—2.2	—7.5
2	0.4	0.0	0.7	—2.0	—0 2	—0.4	—2.5
3	0.5	2.0	0.8	0.6	0.0	—1.1	—7 5
4	0.5	0.5	0.8	0.1	0.0	—0.9	—8.0
5	0.6	1.0	0.7	0.0	0.0	—0.7	—0 5
6	0.4	0.5	0.7	—2.0	—0.3	—0 4	0.3
7	0.3	1.0	0.6	0.0	—0.2	—0.1	—2.5
8	0.2	1.0	0.6	4.5	—0 3	—1.0	—5.0
9	0.4	0 6	0.3	2.3	—0.8	—1.0	—6.5
10	0.2	0.5	0.1	0.6	—0.6	—1.0	—5.5

No. of cloud layer	30/VII 18hr	10/IX 15hr	19/IX 18hr	10/XI 3hr	Total	No. of cases	$\bar{E} \pm \sigma$, v/cm
			1959				
1	0.0	0.5	—0.6	0.2	—4.1	26	0.1±0.4
2	0.5	0.3	—0.7	0.2	12.6		0.5±0.3
3	3.5		—0.4	0.2	15.8		0.6±0.6
4	5.0	3.0	—0.4	0.3	33.4		1.3±0.8
5	3.0	0.0	0.2	0.2	26.6		1.0±0.6
6	0.0	3.0	0.0	0.4	18.6		0.7±0.6
7	3.0	—0.5	0.2	0.8	22.9		0.9±0.7
8	2.0	—1.0	—0.1	3.5	21.3		0.8±0.6
9	—4.0	—2.0	—0.8	—0.5	—1.6		—0.1±0.5
10	—3.5	—3.5	—1.9	—0.5	—11.8		—0.4±0.5

No. of cloud layer	1/II 6 hr	18/VII 6 hr	6/VIII 6 hr	23/X 6 hr	27/I 6 hr	8/IV 6 hr

b. Negatively polarized clouds

	1958				1959	
1	0.0	0.2	—0.2	—0.8	—0.7	—3.5
2	—1.0	0.0	—0.5		—0.5	—4.0
3		—0.1	—0.6		—0.5	—5.5
4		—0.4	—0.3		—0.1	—4.0
5		—0.5	—0.3	0.3	—0.1	—4.5
6		—0.3	—0.6	—1.0	—1.2	—3.0
7	—3.5	—0.3	—0.3	—0.9	0.4	—6.0
8	—5.0	1.0	—0.1	—0.8	0.1	—7.5
9	—5.0	1.0	0.0	—0.5	0.0	—2.5
10	—3.0	1.0	0.0	—0.3	1.0	—2.5

No. of cloud layer	10/IV 6 hr	10/IV 6 hr	17/IV 15hr	14/V 6 hr	26/V 18 hr	28/VIII 18hr	29/VIII 18hr
1		0.2	—12.5	0.1	—1.0	3.5	9.3
2	—7.0	—0.5	—0.5	0.0	—2.0	2.5	2.0
3	—7.0	—1.2	2.5	—0.5	—2.0	4.0	0.2
4	—8.5	—2.6	0.5	—0.9	—2.0	4.0	2.4
5	—6.5	—2.8	1.0	—1.0	—3.0	4.0	—0.5
6	—3.5	—2.4	1.0	—2.2	—2.0	4.0	—2.0
7	—2.2	—1.5	—0.5	—3.0	—3.5	4.0	—2.0
8	—2.2	—1.5	—1.6	—5.0	—5.0	5.0	—0.5
9	—1.4	—1.4	—0.1	—3.5	—5.0	3.5	—0.5
10	—1.4	—1.0	0.1	—3.5	—3.5	5.0	0.0

No. of cloud layer	17/IX 18hr	24/IX 6 hr	30/IX 15hr	15/X 18hr	16/X 6hr	16/X 18hr	21/X 7hr
1	0.2	—7.0	—2.0	0.0	1.0	—0.1	—0.5
2	0.2	—7.5	—2.0	—0.5	0.6	—0.3	—2.0
3	0 8	—9.0	—2.0	—2.0	1.1	—0.4	—4.0
4	—3.0	—7.5	—2.0	—3.5	—2.0	—0.4	—5.5
5	—3.0	—7.5	—3.5	—3.5	—5.5	—0.6	—4.0
6	—4 5	—5.5	—2.0	—3.0	—2.0	—0.6	—3.5
7	—5 5	—5.5	—5.5	—2.0	—2.0	—0.5	—2.0
8	—8.5	—5.5	—3.5	—3 5	—2.0	—0.2	—2.0
9	—2.5	—3.5	—2.0	—2.0	0.0	0.4	—2.0
10	—2 5	—3.5	—2.0	—0.5	0.0	0.2	—2.0

No. of cloud layer	6/XI 6hr	9/XI 18hr	24/XI 6hr	Total	No. of cases	$\overline{E} \pm \sigma$, v/cm
1	0.0	—2.0	—5.5	—21.0	23	—0.9±0.8
2	—1.2	—2.5	—7.0	—33.7		—1.5±0.6
3	—1.5	—4.0	—7.0	—40.6		—1.8±0.7
4	—3.0	—4.5	—5.0	—49.8		—2.2±0.6
5	—2.0	—7.5	—5.0	—57.5		—2.5±0.6
6	—2.0	—3.5	—3.0	—45.0		—1.9±0.4
7	—3 5	—6.0	—1.0	—51.8		—2.2±0.5
8	—2.0	—4.0	—1.2	—55.5		—2.4±0.6
9	—3.5	—3.0	—1.6	—35.1		—0.5±0 4
10	—2.9	1.0	—0.4	—20.7		—0.9±0.4

No. of cloud layer	18/IV 6hr	9/V 18hr	29/X 6hr	29/X 18hr	29/XI 6hr	5/I 3hr	26/VIII 18hr

c. Negatively charged clouds

	1958					1959	
1	—0.4	—7.5	0.1	2.8	—3.5	—11.0	0.4
2	—0 3	—11.0	0.1	2.8	—1.0	—10.5	0.3
3	3.5	—7.0	0.2	3 4	—1.3	—7.0	0.4
4	2 0	—4 0	0.3	3.6	—2.0	—10.5	0.6
5	2.0	—6.5	0.4	5.3	—2.0	—0.0	1.8
6	2.0	—5.0	1.2	8.0	—2.0	—7.5	1.0
7	1.0	—6.5		6.5	—0.5	—7.5	1.0
8	—0.1	—3.2	2.3	9.5	—1.0	—7.5	1.0
9	—0.4	—2.7	2.7	9.5	—0.2	—5.5	1.8
10	1.0	—4.0	2.6	8.0	0.0	—5.5	1.4

No. of cloud layer	22/IX 18hr	5/XI 3 hr	25/XII 15hr	Total	No. of cases	$\bar{E} \pm \sigma$, v/cm
			1959			
1	0.4	0 2	—2.0	—20.5	10	—2.0±1.3
2	—0.6	0.5	—0.5	—20.2		—2.0±1.5
3	0.4	0.5	—0.5	—7.4		—0.7±1.1
4	1.0	0.4	—0.5	—9.1		—0.9±1.2
5	0.2	0 0	—2.0	—9.6		—1.0±1.3
6	0.0	—0.6	—2.0	—4.9		—0.5±1.3
7	0.4	—1.2	—2.0	—8.8		—0.9±1.4
8	0.1	—2.2	—0.5	—1 6		—0.2±1.4
9	0.1	—1.0	—0.2	4.9		0.5±1.2
10	0.6	—1.0	—0.1	3.0		0.3±1.1

No. of cloud layer	27/II 18hr	28/II 3 hr	29/IV 18hr	10/V 15 hr	28/IX 6hr	1/X 6 hr	10/XI 15hr	20/XII 15hr
				d. Positively charged clouds				
				1958				
1	2.5	0.0	—0.4	—0.2	56.5	8.0	—0.1	0.7
2	2.2	0.0	—0.6	—0.4	64.5	9.0	—0.1	0 8
3	2.0	0.0	—0.6	—0.5	52.5	7.0	—0.1	0.8
4	1.9	—0.2	—0.6	—0.4	45.5	8.0	0.0	0.9
5	1.2	0.0	—0.5	—0.7	51.0	8.5	0.0	0.5
6	0.8	0.1	—0.4	—0.6	34.5	8.5	—0.1	0.4
7	0.9	—	—0.3	—0.6	37.5	6.0	—0.1	0.3
8	0.3	—	—0.3	—0.6	29.0	6.0	—0.1	0.2
9	—0.2	—0.5	—0.3	—0.4	19.0	5.0	—0.6	0.0
10	0.2	—1.7	—0.2	—0.8	23.0	5.0	—0.3	0.0

No. of cloud layer	9/I 6hr	26/I 18 hr	19/II 6 hr	19/IV 15hr	3/VII 18hr	27/VIII 18hr
			1959			
1	0.1	—	—0.1	—0.5	—3.6	0.8
2	0.0	—	—0.8	—0.6	—3.8	0.8
3	—0.1	—	—11.5	—0.6	—3.6	0 2
4	—0.3	—1.2	—11 5	—0.3	—3.6	0.2
5	—0.3	—1.2	—13.5	—0.8	—3.9	—0.8
6	—0.8	—1.6	—13.5	—2 0	—4.2	—0.4
7	—1.6	—1.6	—13.5	—2.0	—4.7	—0.3
8	—2.4	—1.4	—13.5	—2.0	—4.8	—0.6
9	—2.8	—2.2	—13.5	—2.0	—4.8	—0.5
10	—6.5	—2.4	—14.5	—3.5	—4.8	—0.3

No. of cloud layer	10/IX 15hr	17/IX 6hr	18/XII 12hr	24/XII 6hr	Total	No. of cases	$\bar{E} \pm \sigma$, v/cm
			1959				
1	5.8	—4.0	—	1.6	67.1	18	4.2±3.6
2	5.5	—4.0	3.6	1.6	77.7		4.6±3.8
3	4.6	—4.0	3.9	1.0	51.0		3.0±3.2
4	2.0	—5.5	—1.0	0.3	34.2		1.8±2.7
5	1.6	—2.0	0.3	—1.2	38.2		2.1±3.0
6	1.6	—2.5	0.3	—2.0	18.0		1.0±2.2
7	1.4	—4.0	0.2	—2.0	16.3		0.9±2.5
8	1.8	—4.5	0.0	—3.5	3.6		0.2±2.0
9	1.9	—4.5	0.1	—3.0	—9.3		—0.5±1.4
10	2.0	—6.0	0.2	—2.0	—12.6		—0.7±1.7

No. of cloud layer	25/VI 6hr	4/XII 18hr	24/IV 15hr	17/IX 6hr	24/IX 18hr
	e. Multiply-charged clouds				
	1958		1959		
1	0.5	—2.1	9.0	—4.0	1.2
2	2.0	—6.5	7.5	—4.0	—0.7
3	2.0	—3.0	9.5	—4.0	—2.0
4	4.5	—3.5	8.0	—5.5	—0.5
5	3.5	—2.3	9.0	—2.0	—1.5
6	2.0	—2.1	9.0	—2.5	—0.2
7	5.0	—3.1	9.5	—4.0	0.3
8	3.5	—4.5	9.5	—4.5	—2.1
9	2.0	—2.5	9.0	—4.5	—0.5
10	3.5	—2.3	11.0	—6.0	—0.2

No. of cloud layer	9/VII 18hr	8/I 6hr	13/I 6hr	19/III 6hr	24/III 6hr	16/X 18hr	25/XII 15hr	Сумма	Число случаев	$\bar{E}$, в/см
				f. Uncharged clouds						
	1958	1959								
1	0.0	0.4	—2.0	0.1	1.5	—2.0	—0.1	—2.1	7	—0.3
2	0.0	0.5	—1.8	0.1	1.5	—2.0	—0.1	—1.8		—0.3
3	0.1	0.5	—1.8	0.1	1.5	—2.0	—0.2	—1.9		—0.3
4	0.1	0.4	—1.6	0.1	1.4	—2.0	—0.2	—1.8		—0.3
5	0.1	0.4	—1.6	0.2	1.4	—2.0	—0.1	—1.6		—0.2
6	0.1	0.4	—1.8	0.2	1.8	—2.0	—0.2	—1.5		—0.2
7	0.0	0.4	—1.8	0.0	1.5	—2.0	—0.2	—2.1		—0.3
8	0.0	0.4	—1.8	0.0	1.6	—2.0	—0.1	—1.9		—0.3
9	0.0	0.4	—1.8	0.1	1.2	—2.0	—0.2	—2.3		—0.3
10	0.0	0.2	—1.6	0.0	1.7	—3.5	—0.2	—3.4		—0.5

APPENDIX XLIII

Reduced variation of the electric field in Cs clouds. Leningrad, 1958-1959

No. of cloud layer	28/II 15 hr	1/X 6 hr	21/X 18 hr	25/X 15 hr	29/XI 6 hr
	a. Positively polarized clouds				
	1958				
1	0.0	0.5	0.1	0.1	0.1
2	0.4	0.8	0.5	0.1	0.1
3	0.5	1.4	0.3	2.0	0.1
4	1.0	1.3	0.1	3.5	0.2
5	1.0	1.1	1.0	1.0	0.2
6	—	1.4	0.5	2.0	0.1
7	0.7	1.4	—0.3	0.5	0.1
8	0.5	0.9	0.1	0.5	0.0
9	0.3	0.2	0.0	0.5	—0.2
10	0 2	0.6	—0.2	—0.5	0.0

No. of cloud layer	17/II 6 hr	9/VI 6 hr	28/VIII 6 hr	Total	No. of cases	$\bar{E} \pm \sigma$, v/cm
	1959					
1	—0.1	0.4	0.2	1.4	8	0.2±0.1
2	—0.1	1.6	0.2	3.7		0.5±0.2
3	—0.2	1.5	0.1	5.8		0.7±0.3
4	—	1.1	0.1	7.3		1.0±0.4
5	—0.2	0.4	0.2	4.8		0.5±0.2
6	—0.2	0.4	0.3	4.5		0.6±0.3
7	0.4	0.3	0.6	3.7		0.5±0.2
8	0.5	0.2	0.0	2.7		0.3±0.1
9	0.6	0.3	0.0	1.8		0.2±0.1
10	0.4	0.3	0.2	1.1		0.1±0.1

No. of cloud layer	29/IX 6 hr	11/XI 18 hr	7/XII 18 hr	14/V 6 hr	31/V 6 hr	30/X 6 hr	Total	No. of cases	$\bar{E} \pm \sigma$, v/cm
	b. Negatively polarized clouds								
	1958			1959					
1	0.6	0.1	—0.1	—5.5	—0.6	0.2	—5.3	6	—0.9±0.9
2	0.0	—	0.0	—5.5	—1.2	0.2	—5.4		—1.3±1.1
3	0.1	—0.5	—0.2	—5.5	0.8	0.1	—4.5		—0.7±0.9
4	0.1	—0.1	—1.0	—5.5	0.6	0.1	—5.9		—1.0±0.9
5	0.1	—0.1	—0.7	—9.0	—	0.2	—9.4		—1.9±1.8
6	—0.5	—0.1	—0.5	—9.0	0.4	0.4	—9.2		—1.5±1.5
7	0.0	0.0	—0.2	—5.0	0.6	0.1	—4.4		—0.7±0.9
8	—0.3	0.0	—0.4	—3.0	+0.6	—0.6	—3.7		—0.6±0.5
9	—1.6	—	—0.2	—2.0	0.2	0.0	—3.7		—0.7±0.4
10	—1.2	—	0.4	—1.5	0.4	0.0	0.9		—0.2±0.4

No. of cloud layer	24/I 6 hr	11/XI 6 hr	Total	No. of cases	$\bar{E}$, v/cm
	c. Negatively charged clouds				
	1958				
1	—0.2	—3 5	—3.7	2	—1.8
2	—0 2	—3.5	—3.7		—1.8
3	0.2	—2.0	—2.2		—1.1
4	0.0	—0.6	—0.6		—0.4
5	—0.2	—0.2	—0.4		—0.2
6	0.0	—0.2	—0.2		—0.1
7	0.0	—0.2	—0.3		—0.2
8	0.0	—0.2	—0.2		—0.1
9	0.0	—0.2	—0.2		—0.1
10	0.1	—0.2	—0.1		—0.0

No. of cloud layer	3/IV 15 hr	6/VIII 6 hr	9/IX 18 hr	8/X 18 hr	8/XII 18 hr	29/VIII 6 hr	Total	No. of cases	$\bar{E} \pm \sigma$, v/cm
	d. Triply-charged clouds $(\pm)$								
	1958					1959			
1	—1.7	—1.4	—0.5	6.0	0.2	0.6	3.2	6	0.5±1.2
2	—0.6	1.5	0.1	8.5	0.4	0.4	7.4		1.2±1.5
3	—0.2	—0.5	0.2	11 0	0.2	0.5	11.3		1 9±1.8
4	—0.1	—2.0	—0.8	16.5	0.2	0.1	14.0		2.3±2.8
5	—0.2	—1.0	—0.3	20.0	0.1	1 4	20.1		3.3±3.4
6	—1.0	0.1	—0.2	6.5	0.0	—0.2	5.2		0.9±1.1
7	—1.4	—0.2	0.0	6.5	—0.4	0.3	4.8		0.8±1.2
8	—1.2	—0.4	0.2	3.5	0.2	0.8	3.2		0.5±0.6
9	—3.4	—0.8	0.6	9.0	0.4	1.0	6.8		1.1±1.7
10	—0.6	—0.3	1.1	9.5	0.5	1.0	11.2		1.9±1.6

No. of cloud layer	10/V 15 hr	21/VI 3 hr	1/X 6 hr	1/X 18 hr	7/IV 18 hr	17/IX 18 hr	Total	No. of cases	$\bar{E} \pm \sigma$, v/cm
	e. Triply-charged clouds $\begin{pmatrix} + \\ - \\ + \end{pmatrix}$								
	1958				1959				
1	—2.0	—6.0	1.4	10.0	1.4	—0.5	4.4	6	0.7±2.2
2	—2.4	—3.5	1.4	3.5	0.3	—0.5	—1.2		—0.2±1.0
3	—3.0	—5.0	1.2	3 5	0.2	—0.8	—4.0		—0.7±1.2
4	—3.5	—6.0	1.6	3.5	0.3	—1.0	—5.1		—0.8±1.4
5	—0.8	—3.5	5.0	6.5	1.0	—2.0	6.2		1.0±1.6
6	—1.4	—4.5	5.0	6.5	1.0	—1.0	5.6		0.9±1.7
7	—1 5	—0.4	6.5	3.0	—	—0.5	7.2		1.4±1.5
8	—2.2	—3.5	5.0	0.5	—0.6	0.4	—0.4		—0.1±1.2
9	—3.0	—3.5	5.0	0.5	—0.1	—2.9	—4.0		—0.7±1.3
10	—2.5	—1.2	3.5	0.6	—0.1	—2.6	—2.2		—0.4±0.9

No. of cloud layer	3/VI 6 hr	22/VI 15 hr	27/VI 6 hr	17/VII 6 hr	17/VII 18 hr	28/IX 6 hr	15/XII 7 hr
	f. Quadriply-charged clouds $\left(\begin{smallmatrix}+\\+\\-\end{smallmatrix}\right)$						
	1958						
1	5.0	0 4	0.1	0.1	1.2	1.1	—1.5
2	5.0	0.4	0.1	0.4	2.5	8.0	0.0
3	4.0	5.5	1.0	—0.2	1.0	11.0	0.0
4	5.0	3.5	1.0	0.4	1 8	11.0	0.5
5	2.0	—3.5	0.5	0.6	1 4	5.8	—1.0
6	3.5	3.1	0.5	0.6	1.2	1.0	—0.5
7	3.5	11.0	1.0	0.4	1.9	9.5	—0.5
8	2.0	4.2	2.0	0.4	1.8	7.0	—0 5
9	2.5	2.0	0.5	0.2	1.8	46.0	1.0
10	1.0	2.5	2.0	0.4	1.6	0.9	—0.5

No. of cloud layer	24/II 6 hr	19/IV 7 hr	Total	No. of cases	$\overline{E} \pm \sigma$, v/cm
	1959				
1	0.6	—3.5	3.5	9	0.4±0.8
2	1.2	—2.0	15.5		1.7±1.0
3	1.6	—3.5	20.4		2.3±1.4
4	0.9	—4.0	20.2		2.2±1.4
5	1.1	—2 5	4.5		0.5±0.9
6	0.8	—1.4	8.8		1.0±0.5
7	1.3	—1.4	26.8		3.0±1.5
8	0.6	—2.6	14.8		1.6±0.9
9	0.2	—3.5	50.6		5.6±3.1
10	0.1	—2.0	4.2		0.5±0.5

No. of cloud layer	29/IV 18 hr	9/IX 7 hr	9/IX 7 hr	22/X 18 hr	29/VII 18 hr	25/XII 15 hr	Total	No. of cases	$\overline{E}$, v/cm
	g. Uncharged clouds								
	1958				1959				
1	—0.9	0.2	0.2	0.2	—0.1	0.6	0.2	6	0.0
2	—1.0	—	0.2	0.1	0.0	0.6	—0.1		0.0
3	—0.8	—	0.2	0.1	0.1	—0.1	0.5		0.1
4	—0.8	0.2	0.2	0.1	0.1	0.2	0.3		0.0
5	—0.9	0.2	0.2	0.1	0.1	0.6	—0.1		0.0
6	—0.8	0.2	0.2	0.1	0.1	0.2	0.0		0.0
7	—0.8	0.2	0.2	0.1	0.1	0.7	0.5		0.1
8	—0.8	0.2	0.2	0.1	0.1	0.2	0.0		0.0
9	—0.8	0.2	0.2	0.1	0.1	0.1	0.1		0.0
10	—0.7	0.1	0.2	0.1	0.1	—0.4	—0.6		—0.1

APPENDIX XLIV

Electric potentials ($v \times 10^{-4}$) in rain-producing and in snow-producing nimbostratus clouds, calculated by Chalmers /71/ and measured by the authors

No. of layer	Ns snow clouds			Ns rain clouds		
	according to Chalmers		measured by the authors (1958-1964)	according to Chalmers		measured by the authors (1958-1964)
	Figure 40			Figure 40		
	curve			curve		
	3	4		4	6	
	Beneath the cloud					
1	—1	—2.5	0.8	—2	—1	0.8
2	0	—4.5	1 6	—3	—2	1.6
3	2	—6 5	2.4	—5	0	2.2
4	4	—8.0	3.4	—6	3	2.7
5	6	—9 0	5.0	—7	5	2.9
	In the cloud					
1	11	—11	7.3	—9	9	4.3
2	15	—12	10.2	—10	12	7.8
3	22	—8	13.7	—9	15	15.0
4	33 5	0	17.5	—8	18	26.3
5	41	16	22.0	—5	21	40.2
6	44	31	26.3	3	23	54.1
7	46	37	30.0	10	25	67.0
8	45	41	33.3	18	27	80.9
9	43	42	36.0	25	30	95.7
10	41	41	37.2	31	31	108.5
	Above the cloud					
1	37	37	36.6	33	32	121.0
2	35	35	35.8	34	33	130.5
3	35	35	36.6	35	34	137.5
4	35	35	37.3	36	34	144.5
5	35	35	38.9	36	34	150.0

APPENDIX XLV

Variation of the electric field ($E \pm \sigma$, v/cm) with altitude in cloudy days in the presence of clouds of only one of the following types. Leningrad, 1958-1959

H, m	St	Sc	As	Cs	Ns
100	1.1±0.2	0.8±0.1	0.3±0.0	0.6	—0.8±0.7
200	1.3±0.2	0.9±0.1			—0.7±0.6
300	1.3±0.2	0.9±0.1			—0 7±1.0
400	1.2±0.2	1.0±0.1			—0.9±1.2
500	1.0±0.2	1 0±0.1	0.5±0.0	0.6	—1.2±1.4
600	0.6±0.2	1.0±0.1			—1.2±1.3
700		0.9±0.1			—1.3±1.2
800	0.3±0.2	0.9±0.1			—1.6±1.6
900		0.8±0.1			—2.2±1.4
1000	0.1±0.2	0.6±0.1	0.9±0.0	0.5	—2.7±1.5
1100					—2.8±1.2
1200	0.2±0.1	0.5±0.2			—2.4±1.2
1300					—1.6±1.4
1400	0.2±0.1	0.4±0.2			0.0±1.3
1500			1.1±0.4	0.4	1.4±1.1
1600	0.2±0.1	0.2±0.2			1.6±2.3
1700					1.4±1.4
1800	0.1±0.0	0.0±0.2			0.5±2.0
1900					1.1±1.6
2000	0.1±0.1	—0.1±0.2	1.3±0.4	0.3	1.2±1.5
2100			1.7±0.8		0.6±1.3
2200	0.1±0.1	0.1+0.1	2.1±0.8		0.3±1.6
2300			2.4±1.1		0.7±1.4
2400	0.2±0.1	0.3±0.1	2.3±1.0		2.0±2.2
2500			2.2±0.5	0.2	2.7±1.9
2600	0.2±0.1	0.4±0.1	2.4±0.7		2.8±2.1
2700			2.5±0.7		2.3±1.0
2800	0.2±0.1	0.4±0.1	2.2±0.6		2.0±1.5
2900			1.7±0.7		2.2±2.0
3000	0.1±0.1	0.5±0.1	1.1±0.6	0.1	2.7±2.6
3100			0.9±0.5		2.9±2.9
3200	0.2±0.1	0.5±0.1	1.1±0.7		2.9±1.0

H, m	St	Sc	As	Cs	Ns
3300			1.4±0.6		2.9±2.0
3400	0.2±0.1	0.5±0.1	1.4±0.7		2.8±1.4
3500			1.1±0.6	0.2	2.5±1.4
3600	0.2±0.1	0.5±0.1	0.6±0.5		2.0±2.7
3700			0.3±0.5		1.6±2.2
3800	0.2±0.1	0.5±0.1	0.1±0.5		1.3±2.6
3900			0.0±0.5		1.1±2.2
4000	0.1±0.0	0.4±0.1	0.0±0.4	0.2	0.9±1.9
4100			0.0±0.5	0.1	0.6±1.5
4200	0.1±0.0	0.3±0.1	0.0±0.4	0.1	0.5±1.3
4300			0.1±0.4	0.1	0.7±1.2
4400	0.1±0 0	0.3±0.0	0.3±0.6	0.1	0.8±1.1
4500			0.6±0.6	0.1	0.8±1.4
4600	0.1±0.0	0.3±0.0	0.6±0.6	0.1	0.6±1.2
4700			0.0±0.5	0.1	0.3±0.8
4800	0.1±0.1	0.3±0.1	—0.6±0.6	0.1	0.4±0.7
4900			—0.6±0.6	0.0	0.8±1.0
5000	0.1±0.1	0.3±0.0	—0.2±0 6	—0.1	0.5±0.9
5100			0.1±0.5	—0.5	0.1±0.6
5200	0 1±0.0	0.2±0.1	0.3±0.5	1.4	1.0±0.4
5300			0.3±0.5	—2.1	0.4±0.9
5400	0.1±0.0	0 2±0.1	0.3±0.5	—2.3	0.6±0.6
5500			0.3±0.6	—2.1	0.8±1.2
5600	0.1±0 0	0.2±0.1.	0.3±0.5	—1.9	0 8±1.4
5700			0.3±0.4	—1.5	0.5±0.4
5800	0.1±0.0	0.2±0.1	0.3±0.4	—1.1	0.5±0.5
5900			0.3±0.5	—0.9	0.4±0.6
6000	0.0±0.0	0.2±0.1	0.4±0.6	—0.7	0.2±0.6
V_{6000}, kv	128±0.8	164±58	511±136	216	457
Q_{6000}, e.s.u./m^3	2.7±0.5	3.5±0.3	0.4±1.5	2.3	2.0
No. of cases	37	117	30	11	75

APPENDIX XLVI

Reduced variation of the electric field in Ns clouds (rain-producing, positively polarized). Leningrad, 1958-1963

No. of layer	27/II 18 hr	14/V 6 hr	2/VI 18 hr	5/VI 6 hr	11/VI 6 hr	20/VIII 15 hr	1/X 18 hr
				1958			
				Beneath the cloud			
1	0.71	0.32	0.10	0.67	1.41	0.23	—0.63
2	1.30	0.30	—0.60	2.65	0.93	0.03	—0.23
3	1.64	0.15	—0.39	1.35	0.66	0.38	0.38
4	1.91	0.12	—0.22	0.90	0.36	1.23	0.71
5	2.14	0.12	—0.22	2.15	0.60	1.23	0.97
				In the cloud			
1	0.35	—0.35	1.00	33.00	0.35	1.36	1.28
2	0.65	—1.50	2.50	51.00	0.05	1.57	2.30
3	0.55	1.00	8.50	100.50	—0.50	1.84	2.70
4	0.05	1.00	26.50	110.00	—0.50	2.13	3.30
5	0.25	1.00	25.00	160.00	0.50	2.15	3.65
6	0.25	9.00	0.50	150.00	2.00	2.20	2.40
7	—0.10	25.00	6.50	125.00	2.00	1.87	1.40
8	—0.10	1.45	9.00	140.00	0.50	1.58	1.30
9	—0.05	2.10	6.50	95.00	0.50	1.47	1.45
10	—0.04	0.05	2.00	85.00	—0.50	1.44	1.60
				Above the cloud			
1	—0.20	0.90	1.00	25.00	0.00	0.43	0.94
2	—0.35	—0.27	1.00	8.00	0.25	0.32	0.16
3	—0.35	0.25	1.00	1.65	—0.50	0.35	—0.01
4	—0.35	0.04	1.00	2.35	—0.50	0 38	0.35
5	—0.20	0.07	1.50	0.70	—0.10	0.36	0.00

No. of layer	3/VI 17 hr 45 min	28/VI 17 hr 51 min	7/VIII 5 hr 45 min	25/VIII 15 hr 04 min	26/VIII 5 hr 45 min	17/X 5 hr 54 min	21/X 7 hr 02 min
				1959			
				Beneath the cloud			
1	—1.42	0.75	0.80	0.04	0.87	1.15	—
2	—1.51	—1.70	0.34	0.88	3.05	1.60	—
3	—3.00	—3.05	—0.05	0.57	2.35	2.05	—
4	—3.50	—3.20	0.90	1.05	1.65	2.05	—
5	—0.85	—7.50	0.69	0.55	0.80	2.25	—

No. of layer	3/VI 17 hr 45 min	28/VI 17 hr 51 min	7/VIII 5 hr 45 min	25/VIII 15 hr 04 min	26/VIII 5 hr 45 min	17/X 5 hr 54 min	21/X 7 hr 02 min
				In the cloud			
1	0.84	—7.00	0.72	—0.70	5.00	2.50	2.35
2	1.45	—22.00	1.16	—1.15	3.50	2.50	4.10
3	1.91	—11.00	1.17	—2.65	—7.50	2.65	3.00
4	2.38	—11.00	1.34	—4.50	—11.00	2.30	2.40
5	1.45	—6.50	1.41	—20.50	—13.50	2.30	2.70
6	0.75	10.00	1.62	—1.25	—2.20	2.10	1.80
7	—0.25	35.00	0.93	2.50	14.00	1.55	—7.50
8	—0.35	3.00	0.90	8.50	10.00	1.40	—8.00
9	—0.65	3.00	0.87	4.50	125.00	1.30	—6.00
10	—0.60	4.50	0.79	—7.00	21.00	1.45	—1.50
				Above the cloud			
1	—0.55	8.00	0 68	—	13.50	1.75	1.00
2	—0.45	8.00	0.55	—	12.50	1.80	0.85
3	—0.25	4.00	0.36	—	7.90	1.60	0.55
4	—0.65	0.50	0.28	—	0.66	1.10	0 65
5	12.00	—0.20	0.20	—	1.41	0.75	0.55

No. of layer	21/X 15 hr 02 min	21/X 21 hr 18 min	25/XII 15 hr 00 min	16/VI 17 hr 45 min	15/VIII 20 hr 36 min	15/VIII 20 hr 36 min
				Beneath the cloud		
	1959			1960		
1	—	—	—	0.08	0.61	0.61
2	—	—	—	0.07	0.68	0.68
3	—	—	—	—	0.74	0.74
4	—	—	—	0.09	0.74	0.74
5	—	—	—	0.06	0.81	0.81
				In the cloud		
1	—0.47	—30.50	1.34	—0.03	1.42	6.75
2	—0.41	—29.50	1.84	0.02	0.74	10.00
3	—0.38	—17.50	1.78	0.04	0.68	10.00
4	—0.26	—13.50	1.45	0.07	0.54	7.00
5	—0.18	—10.00	—0.40	0.11	0.54	7.00
6	0.07	—2.50	—1.10	0.10	0.34	2.00
7	0.19	—9.50	—1.65	0.11	0.47	7.00
8	0.27	—16.50	—0.70	0.14	0.74	7.00
9	0.30	—10.50	0.95	—0.10	0.54	3.50
10	0.39	—7.50	—2.00	0.04	1.35	7.00

No. of layer	21/X 15 hr 02 min	21/X 21 hr 18 min	25/XII 15 hr 00 min	16/VI 17 hr 45 min	15/VIII 20 hr 36 min	15/VIII 20 hr 36 min
			Above the cloud			
1	10.00	0.25	—0.50	0.02	—	—
2	8.50	0.10	—0.50	0.03	—	—
3	5.50	0.29	—7.00	0.06	—	—
4	6.50	—0.18	—0.50	0.08	—	—
5	4.50	—0.15	—7.00	0.11	—	—

No. of layer	8/IX 5 hr 46 min	9/IX 17 hr 47 min	30/IX 15 hr 15 min	10/III 20 hr 31 min	10/III 20 hr 31 min	30/X 15 hr 19 min	30/X 15 hr 19 min
				Beneath the cloud			
	1960			1961			
1	—1.07	—1.96	—	—0 31	—	0.45	—
2	—0.14	—1.69	—	—1.89	—	0.60	—
3	—0.47	—1.62	—	—1.06	—	0.65	—
4	—0.20	—1.55	—	—2.01	—	0.80	—
5	0.07	—1.48	—	—2.10	—	1.75	—
				In the cloud			
1	0.74	—1.07	—0.20	—7.50	3.50	2.45	0.80
2	0.00	2.00	0.47	—7.50	0.50	3.15	0.75
3	—3.50	3.50	3.05	1.00	1.00	3.75	1.05
4	0.00	—3.50	4.70	3.50	1.50	3.45	1.25
5	3.50	—7 00	4.40	1 50	0.50	2.70	1.05
6	0.00	—7.00	3.70	3.50	0.50	2.05	0.75
7	3.50	—7.00	3.70	4.00	0.50	1.35	0.40
8	3.00	—3.50	3.70	3.50	—0.50	1.70	0.60
9	3.50	0.00	3.70	3.00	—0.50	1.25	0.25
10	10.00	—3.50	3.70	2.50	—0.70	0.00	0.20
				Above the cloud			
1	0.35	3.70	1.55	—	—0.19	—	0.10
2	0.70	0.70	0.94	—	—0.19	—	0.10
3	0.35	2.00	0.81	—	—0.10	—	0.30
4	0.35	20.00	0.68	—	—0.32	—	0.25
5	0.35	9.80	0.68	—	—0.05	—	0.20

No. of layer	1/XI 4 hr 37 min	15/II 3 hr 02 min	6/VIII 15 hr 09 min	12/X 15 hr 04 min
		Beneath the cloud		
	1961	1962		1963
1	0.21	7.00	1.35	—1.28
2	0 26	7.00	0.74	—1.28
3	0 27	10 00	—1.07	—1.55
4	0.39	8.10	—2.23	—1.62
5	1.42	0.70	—3.38	—1.22
		In the cloud		
1	1 50	—0.35	—1.22	—1.00
2	1.60	—0.70	—2.00	—0.35
3	—0.50	—1 00	—2.00	2.00
4	1.00	—0.70	4.70	1.35
5	1.00	—0.70	5.35	1.00
6	1.00	—0.70	0.00	0.00
7	0.95	—0.35	—53.50	0.00
8	1.25	0.35	—10.00	0.00
9	—2.00	1.35	—3.50	3.50
10	—2.00	1.70	3.50	3.50
		Above the cloud		
1	—2.00	1.00	0.34	7.00
2	—0.80	—	—	3.50
3	—0.20	—0.35	—0.14	10.00
4	—0.13	—0.34	—0.07	10.00
5	0.05	—0.27	—0.07	13.50

No. of layer	Total	No. of cases	Mean	Smoothed value
		Beneath the cloud		
1	10.69	24	0.44	0.5
2	13.27	24	0.55	0.5
3	9.67	24	0.40	0.4
4	7.21	24	0.30	0.3
5	0.37	24	0.02	0.1
		In the cloud		
1	16.86	31	0.54	0.6
2	26.74	31	0.86	1.4
3	105.14	31	3.39	3.0
4	136.95	31	4.42	4.7
5	201.28	31	6.50	5.8
6	181.88	31	5.87	5.8
7	158.07	31	5 10	5.3
8	160.73	31	5.20	5.8
9	240.23	31	7.76	6.2
10	126.37	31	4.08	5.3
		Above the cloud		
1	74.07	26	2.85	2.5
2	45.44	24	1.89	1.9
3	28.07	26	1.08	1.4
4	42.13	26	1.61	1.4
5	38.69	26	1.49	1.5

APPENDIX XLVII

Reduced variation of the electric field in Ns clouds (rain-producing negatively polarized). Leningrad, 1958-1962

No. of layer	27/II 18 hr	22/VI 18 hr	30/VI 3 hr	30/VI 3 hr	30/VI 15 hr	19/VII 6 hr	6/VIII 6 hr
			1958				
			Beneath the cloud				
1	0.71	—4.55	—0.89	—0.89	—	0.18	—9.55
2	1.30	—4.50	—0.55	—0.55	—	0.30	—12.65
3	1.64	—	—0 24	—0.24	—	0.16	—14.70
4	1.91	—5.45	0.07	0.07	—	0.13	—14.35
5	2.14	1.00	0.70	0.70	—	0.06	—10.70
			In the cloud				
1	3.15	—9.50	1.27	—0.50	2.11	0.10	—0.90
2	2.05	—9.00	1.84	—7.50	—1.50	0.25	—9.35
3	1.90	—19.00	0.90	—13.50	1.75	0.10	—25.00
4	1.90	—15.50	0.70	—8.50	0.35	—0.30	—8.50
5	1.50	1.50	—6.50	—4.50	—1.65	—0.50	—2.40
6	0.80	—4.50	—7.50	—1.00	—2.00	—1.00	—1.85
7	0.65	—4.50	—3.50	—7.50	—0.90	—0.50	—1.05
8	0.20	—3.50	—3.50	—2.00	—1.25	—0.50	—1.55
9	0.20	—3.50	—2.10	—3.50	—1.45	—0.50	5.00
10	0.10	—1.00	—1.60	—1.50	—1.95	—0 80	2.70
			Above the cloud				
1	—0.20	0.10	—0.50	—0.50	—0.95	—	—0.06
2	—0.35	—	0.05	—0.05	—0.12	—	—0.03
3	—0.35	0.29	0.27	0.27	0.11	—	—0.95
4	—0.35	0.52	0.10	0.10	0.20	—	—0.09
5	—0.20	0.52	0.10	0.10	—0.10	—	—0.07

No. of layer	20/VIII 15 hr	27/VIII 18 hr	28/VIII 6 hr	8/X 6 hr	6/V 6 hr	26/V 6 hr	26/V 18 hr
			Beneath the cloud				
		1958			1959		
1	0.23	0.45	—2.00	—1.03	0.23	—1.95	—6.95
2	0.03	0.25	—2.45	—1.60	0.66	3.85	6.80
3	0.38	0.40	—2.55	—2.32	0.49	—15.65	—8.30
4	1.23	0.40	—2.45	—0.43	0.26	—5.75	—13.00
5	1.23	0.35	—2.45	—0.84	—0.40	—2.75	—6.00

No. of layer	20/VIII 15 hr	27/VIII 18 hr	28/VIII 6 hr	8/X 6 hr	6/V 6 hr	26/V 6 hr	26/V 18 hr
				In the cloud			
1	0.25	0.60	—10.00	—4.45	—3.50	—3.50	—2.00
2	0.95	0.95	—30.00	—6.00	—7.00	—8.00	—6.50
3	—1.25	—2.00	—37.50	—2.75	—7.00	—9.50	—6.50
4	—0.05	—2.00	—44.00	4.00	—6.00	—7.50	—12.00
5	—0.05	—1.00	—33.50	—2.00	—5.50	—5.00	—12.50
6	—0.05	—0.50	5.50	—1.00	—6.50	—13.00	—14.00
7	0.02	—2.00	—0.50	—3.50	—4.00	—12.00	—9.50
8	0.02	—0.50	—4.50	—1.00	—5.50	—14.00	—1.50
9	0.04	—1.00	—12.50	0.50	—5.50	13.50	2.00
10	0.01	—3.50	—13.00	1.00	—7.50	—18.50	—0.50
				Above the cloud			
1	0.43	—0.05	—10.50	—	—	—4.50	—0.50
2	0.32	0.51	0.44	—	—0 65	—0.05	—1.00
3	0.35	0.51	0.21	—	0.07	—0.15	—0.50
4	0.38	0.62	0.21	—	0.13	—0.45	—0.20
5	0.36	1.01	1.17	—	—0.01	—0.53	—0.19

No. of layer	28/VIII 18 hr	28/VIII 18 hr	19/IX 18hr	22/IX 18 hr	30/IX 15hr	6/X 18 hr
				1959		
				Beneath the cloud		
1	—0.05	—0.05	0.80	2 20	0.47	2.85
2	0.10	0 10	1.85	1.95	0.70	1.95
3	0.25	0.25	1.14	1.45	1.00	1.10
4	0.40	0.40	1.05	1.55	1.30	0.98
5	0.55	0.55	3.25	0.65	1.45	0.60
				In the cloud		
1	0.40	—2.00	—2.00	1.90	1.00	0.01
2	0.30	—2.50	—2.50	1.70	1.00	—1.00
3	—0.60	—4.00	—4.00	—3.50	—2.00	—7.00
4	—0.55	—3.50	—3.50	—3.00	—8.50	—4.00
5	—0.20	—0.50	—2.00	—5.00	—3.50	—6.00
6	—0.10	—0.50	—2.00	—6.50	—0.25	—5.50
7	0.20	—0.15	—5.00	—3.50	—0.95	—2.00
8	0.20	—0.50	—	—6,50	—5.00	—2.50
9	0.35	—0.50	—0.50	—5.00	—10.00	—8.50
10	—0.30	—0.50	—1.35	—4.00	2.45	—10.50

No. of layer	28/VIII 18 hr	28/VIII 18 hr	19/IX 18 hr	22/IX 18 hr	30/IX 15 hr	6/X 18 hr
			Above the cloud			
1	—0.50	—0.50	1.90	—3.50	0.43	—2.00
2	—0.50	—0.50	0.41	—3.00	0.41	—6.50
3	—1.00	—1.00	0.63	—1.50	0.14	—0.50
4	0.50	0.50	0.35	0.00	0.06	—0.50
5	1.00	0.50	—0.20	—0.30	—	—

No. of layer	15/X 18 hr	15/X 18 hr	25/VIII 21 hr	9/XI 18 hr	7/VII 6 hr	9/IV 18 hr
			Beneath the cloud			
	1959		1960		1961	1962
1	0.15	0.15	3.24	—1.01	2.02	—3.05
2	—0.01	—0.01	2.70	—0.88	7.75	—3.40
3	0.33	0.33	1.76	—0.86	4.40	—3.40
4	0.44	0.44	0.07	—0.81	4.40	—3.70
5	0.01	0.01	—1.22	—0.61	1.70	—3.70
			In the cloud			
1	0.90	—3.50	—3.24	—0.81	6.75	—3.70
2	0.85	—3.50	—3.78	—0.54	10.10	—2.00
3	0.60	—5.50	—4.39	—0.88	4 70	—1.55
4	1.00	—5.50	—5.35	—1.28	—3.05	—1.22
5	1.00	—7.50	—3.40	—1.42	—3.40	—1.28
6	—0.50	—7.50	—4.05	—1.48	—0.70	—1.00
7	—1.00	—5.50	—4.05	—1.48	0.00	—0.70
8	—2.00	—3.50	—4.40	—1.55	0.00	0 70
9	—2.00	—3.50	—4.40	—1.55	3.50	1.35
10	—2.00	—5.00	—3.40	—1.48	3.50	1.35
			Above the cloud			
1	—3.50	—3.50	—	—1.15	—0.07	1.00
2	—3.50	—3.50	—3.70	—0.61	—0.07	—
3	—0.40	—0.40	—3.70	—0.40	0.07	0.70
4	—0.20	—0.20	—	—0.81	0.07	0.20
5	—0.25	—0.25	—	—0.61	0.07	0.47

No. of layer	8/VIII 9 hr	Total	No. of cases	Mean	Smoothed value
		Beneath the cloud			
	1962				
1	2.77	—15.52	26	—0.60	—0.60
2	3.38	—12.24	26	—0.50	—0.70
3	3.38	—29.75	26	—1.10	—0.90
4	2.77	—28.07	26	—1.10	—0.90
5	1.42	—12.30	26	—0.50	—0.70
		In the cloud			
1	3.05	—28.11	27	—1.00	—1.60
2	2 00	—78.68	27	—2.90	—3.10
3	—1.70	—149.17	27	—5.50	—4.80
4	—3.70	—139.55	27	—5.20	—5.00
5	—3.70	—109.00	27	—4.00	—4.00
6	—3.50	—80.18	27	—3.00	—3.00
7	0.00	—72.91	27	—2.70	—2.70
8	0.00	—64.43	27	—2.40	—2.20
9	—2.35	—41.91	27	—1.50	—1.90
10	7.00	—65.17	27	—2.40	—2.10
		Above the cloud			
1	0.00	—28.62	23	—1.20	—1.10
2	—	—21.75	22	—1.00	—0.90
3	0.00	—7.03	25	—0.30	—0.40
4	0.07	1.21	24	0.00	0.00
5	0.07	2.66	22	0.10	0.10

APPENDIX XLVIII

Reduced variation of the electric field in Ns clouds (mixed, positively polarized). Leningrad, 1958-1962

No. of layer	14/V 6 hr	2/VI 18 hr	3/VI 6 hr	5/VI 6 hr	28/VIII 15 hr	1/X 6 hr	7/X 18 hr
				1958			
				Beneath the cloud			
1	—0.2	0.8	2.2	0.9	2.7	0.2	1.0
2	—0.2	—0.6	2.2	2.9	1.4	—0.4	1.0
3	—0.2	—0.5	2.2	1.2	0.2	—1.2	0.9
4	—0.2	—0.4	2.2	0.9	0.5	—3.3	0.9
5	—0 2	0.0	2.2	1.2	1.0	—2 7	0.5
				In the cloud			
1	0.2	0.8	1.3	23.5	1.0	4.7	0 5
2	5.0	—1.7	—0.6	40.0	1.5	4.7	0.5
3	2.0	—5.5	—2.5	48.5	1.5	2.6	0.5
4	0.0	10.0	—6.0	57.0	0.5	0.6	0.5
5	—0.3	—7.5	—2.1	62.5	0.3	0.6	0.4
6	—0.1	4.6	—1.2	110.0	—0.4	0.4	0.4
7	—1.0	11.3	—2.7	136.0	—0.7	0.5	0.4
8	—1.7	8.0	6.0	133.0	—0.7	5.5	0.3
9	—1.4	8.0	—2.0	133.0	—0.4	2.0	0.3
10	0.0	5.0	0.2	100.0	—0.4	3.2	0.5
				Above the cloud			
1	0 i	0.0	—1.5	17.9	—1.5	—	—
2	0.0	0.0	—0.2	5.4	—1.4	—	—
3	—0.1	0.0	0.0	3.5	—0.4	—	—
4	0.3	0.0	0.0	0.8	—0.5	—	—
5	0.0	0.0	4.3	0 6	—0.6	—	—

No. of layer	8/X 18 hr	15/X 3 hr	3/VI 18 hr	22/VI 18 hr	26/VIII 6 hr	27/VIII 6 hr	28/VIII 6 hr
				Beneath the cloud			
	1958				1959		
1	—1.0	—0.6	—0.7	—4.8	0.8	0.5	—2 3
2	—1.2	0.7	—0 4	—3.7	1.9	2.4	—2.3
3	—2.5	1.0	—0.9	—4.6	3.0	3.4	—2.3
4	—0.1	1.4	—0.1	—5.2	2.6	—15.5	—2 3
5	—0.5	1.8	—0.3	0.9	2 2	—15.5	—2.3

No. of layer	8/X 18 hr	15/X 3 hr	3/VI 18 hr	22/VI 18 hr	26/VIII 6 hr	27/VIII 6 hr	28/VIII 6 hr
				In the cloud			
1	—3.1	0.9	0.0	—12.0	5.4	—6.2	—2 8
2	—4.5	1.0	0.8	—12.0	6.7	—2.0	—23.3
3	—4.5	1.2	1.6	—12.0	—1.6	2.0	—37.0
4	—3.1	1.4	1.8	—12.0	—9.3	3.0	—43.5
5	0 0	1 8	2.0	—12.0	7.5	20.0	—12.6
6	4.0	14.3	2.6	—9.0	12.7	24.5	5.7
7	0.5	18.6	1.1	—16.0	63.2	45.5	—2.7
8	4.5	—6.1	—0.1	—4.1	152.5	45.0	—9.0
9	13.0	—3.9	—0.7	—4.3	45.5	0.1	—11.7
10	5.7	—4.9	—0.9	—1.1	12.0	—1.8	—12.0
				Above the cloud			
1	—	—	—	—0.2	14.6	—	—6.5
2	—	—	—	—0.6	9.2	—	—3.5
3	—	—	—	0.3	4.4	—	0.3
4	—	—	—	0.4	0.4	—	0.1
5	—	—	—	0.4	0.6	—	0.2

No. of layer	6/X 6 hr	21/X 7 hr	21/X 15 hr	25/XII 15 hr	14/IV 6 hr	25/IV 6 hr	25/IV 15 hr
				Beneath the cloud			
		1959				1960	
1	—	—0.5	—	—	0.7	3.4	7.8
2	—	—0.3	—	—	0.7	3.7	16.6
3	—	0.3	—	—	1.2	3.2	13.5
4	—	0.2	—	—	1.7	2.7	3.8
5	—	1.2	—	—	1.7	3.0	1.2
				In the cloud			
1	0.4	1.5	5 3	0.9	—2.4	3.7	3.7
2	0.2	2.6	6.4	0.9	—4 5	4.2	3.7
3	0.2	4.2	1.4	0.9	3.0	4.7	3.7
4	—2.5	3 8	5.1	0.9	3.5	5.0	3.7
5	0.0	3.2	3.3	0.9	7.0	5.4	3.7
6	1.5	3.4	—4.2	1.6	12.8	9.3	6.4
7	—1.8	1.4	—4.8	1 5	16.2	11.1	2.4
8	0.5	—5.7	3.4	—0.8	12.8	4.8	0 8
9	0.1	—5.7	5.0	—1.8	3.5	4.8	0.9
10	—2.7	—1.2	—5.2	—1.6	—1.1	4.4	0.5

No. of layer	6/X 6 hr	21/X 7 hr	21/X 15 hr	25/XII 15 hr	14/IV 6 hr	25/IV 6 hr	25/IV 15 hr
			Above the cloud				
1	—0.5	1.4	—	—2.3	—5.2	1.4	0.3
2	1.0	1 8	—	—3.1	—7.0	3.2	—0.2
3	0.4	1.1	—	—1.9	—7.0	4.5	—0.4
4	0.1	0.9	—	0.2	4.4	3.0	—0.3
5	0.1	0.8	—	0.0	2.3	2.6	—0.1

No. of layer	27/IV 6 hr	25/VI 15 hr	15/VIII 21 hr	30/VIII 6 hr	8/IX 6 hr	9/IX 18 hr	30/IX 15 hr
			1960				
			Beneath the cloud				
1	—1.0	0.4	0.8	—3.3	—1.4	—2.0	—
2	—0 5	—0.8	0.3	—1.9	—0.2	—1.8	—
3	0.0	—0.8	0 2	—0.3	—0.3	—1.8	—
4	—1.7	0.1	0.2	0.2	—0.5	—1.6	—
5	—2.3	0.3	0.3	—1.4	—0.1	—1.6	—
			In the cloud				
1	—	0.0	0.4	—1.2	0.0	—1.5	0.4
2	—	0.0	0.4	1.4	0.4	—1.4	0.0
3	—	0.4	0.5	0.7	1.5	—1.0	4.0
4	—	1.0	0.7	—1.9	0.3	—2.2	4.0
5	—	1.5	0.7	3.3	0.3	1.7	3.8
6	—3.5	2.4	7.3	35 0	—5.3	4.0	3.7
7	—3.9	—0.1	5.0	14.0	—3.5	—4.6	3.7
8	—3.9	0.7	2.5	18.0	10.4	—3.5	3.7
9	5.6	0.1	4.5	87.8	1.5	3.5	3.7
10	3.1	0.7	5.5	20.0	5.6	—1.0	3.7
			Above the cloud				
1	—3.7	0.0	—	23.5	0.4	—5.2	3.4
2	—3.9	0.1	—	23.5	0.2	—3.3	0.9
3	—3.7	0.0	—	22.0	0.0	0.6	0.9
4	—2.8	—0.1	—	20.9	0.0	1 5	0.9
5	—3.3	0.1	—	20.9	0.0	2.2	0.8

No. of layer	10/III 21 hr	7/IV 15 hr	7/VII 6 hr	1/XI 5 hr	6/XII 6 hr	27/IV 6 hr
			Beneath the cloud			
			1961			1962
1	—0.3	—	2.0	0.2	—1.0	0.5
2	—1.9	—	7.1	0.2	—1.0	—0.9
3	—1.9	—	5.2	0.3	—0.9	—1.0
4	—2.6	—	4.1	0.3	—0.9	—0.9
5	—2.5	—	4 7	0.4	—0.9	—1.1
			In the cloud			
1	—1.6	—30.2	3 3	1.1	0.5	—1.1
2	—9.5	—19.0	1.7	1.8	3.0	—1.1
3	—17.5	—3.5	7.6	1.0	2.3	—1.1
4	—13.2	0.5	9.4	2.5	1.2	—0.4
5	—9.1	1.0	—1.7	4.0	0 3	0.2
6	1.2	1.3	—2.1	1.0	—0.5	—1.5
7	4.6	7.2	0.4	0.9	—1.3	—1.4
8	5.1	—7.4	1.8	—0.5	—5.7	—0.7
9	2.5	—0.1	5.8	—1.5	—0.6	0.0
10	1.8	5.0	0.0	—2.0	—11.1	1.4
			Above the cloud			
1	—0.2	0.5	0.1	—0 8	—1.0	1.0
2	—0 1	1 8	0.1	—0.6	—1.7	0.5
3	0.1	3.7	—0.1	—0.2	—2.0	1.6
4	—0.3	3.2	0.0	—0.1	—2.0	0.9
5	—0.3	1.5	0.1	0.0	—2.0	1.2

No. of layer	23/VI 6 hr	30/VI 6 hr	Total	No. of cases	Mean	Smoothed value
			Beneath the cloud			
	1962					
1	—0.8	0.7	5.7	31	0.2	0.4
2	—0.9	0.7	22.8	31	0.7	0.5
3	—0.9	0.7	16.4	31	0.5	0.3
4	—0.9	0.7	—13.7	31	—0.4	—0.1
5	—1.0	0.7	—9 1	31	—0.3	—0.3
			In the cloud			
1	—1.1	0.5	—3.2	35	—0.1	—0.1
2	—1.3	1 3	7.3	35	0.2	0.2
3	—1.0	5.4	14.2	35	0.6	0.4
4	0.2	2.7	25.2	35	0.7	1.1
5	0.2	1.4	91.8	35	2 6	3.1
6	0.0	0.0	242 3	36	6.7	6 1
7	0.2	—1 1	300.1	36	8.3	8.4
8	0.3	0.6	366.3	36	10.2	9.2
9	0.3	0 0	290.4	36	8.1	7.5
10	—0.1	0.0	131.2	36	3.6	4.1
			Above the cloud			
1	—0.5	0.0	35.5	28	1.3	1.7
2	—0.3	0.0	21.8	28	0 8	1.0
3	—0.3	0.0	27.3	28	1.0	1.0
4	—0.1	—0 1	31.7	28	1.1	1.1
5	—0.1	0.0	32.3	28	1.2	1.2

APPENDIX XLIX

Reduced variation of the electric field in Ns clouds (snow-producing, negatively polarized). Leningrad, 1958-1962

No. of layer	4/II 6 hr	4/II 6 hr	28/II 15 hr	15/XII 15 hr	5/I 3 hr	9/I 6 hr	9/I 18 hr
			Beneath the cloud				
		1958				1959	
1	—0.95	—0.95	4.55	0.50	—	—1.50	0.50
2	—2.10	—2.10	6.00	0.50	—	—1.50	1.55
3	—1.80	—1.80	5.80	0.50	—	—1.50	1.10
4	—1.30	—1.30	6.25	0.50	—	—0.75	1.00
5	—0.85	—0.85	5.70	0.50	—	—0.60	0.35
			In the cloud				
1	—0.65	—5.50	2.50	0.50	—11.00	—0.10	—1.30
2	—1.80	—6.50	2.00	—1.00	—11.00	—0.10	—3.50
3	—3.00	—5.00	2.50	—1.50	—12.00	—0.30	—4.50
4	—3.00	—8.50	1.00	—2.50	—12.00	—0.95	—3.50
5	—2.00	—6.50	1.00	—3.00	—12.00	—1.10	—5.00
6	—2.00	—7.00	0.25	—1.00	—12.50	—1.35	—6.50
7	—0.75	—5.00	0.20	—1.00	—11.00	—0.90	—6.50
8	—0.95	—3.50	0.50	—0.50	—12.50	—0.70	—8.00
9	—3.50	—5.00	1.50	—0.50	—14.00	—0.85	—6.50
10	—3.00	—3.50	0.20	—0.25	—11.00	—0.80	—6.50
			Above the cloud				
1	—0.15	—0.15	0.10	—0.05	—12.00	—0.20	—10.00
2	—0.50	—0.50	—0.15	—0.21	—12.00	0.15	—13.50
3	—1.85	—1.85	—0.04	—0.13	—12.00	0.25	—13.50
4	—1.05	—1.05	0.20	—0.08	—11.00	0.40	—15.50
5	—1.40	—1.40	0.35	—0.03	—11.00	0.35	—13.50

No. of layer	26/I 18 hr	26/I 18 hr	31/I 18 hr	2/II 18 hr	2/II 18 hr	15/II 15 hr	17/II 6 hr
			1959				
			Beneath the cloud				
1	0.48	0.48	—0.15	—	—	0.55	—0.70
2	0.37	0.37	0.15	0.60	0.60	0.35	0.40
3	0 57	0.57	0.70	0.90	0.90	0.45	0.85
4	0.03	0.03	0.95	1.90	1.90	0.55	0.85
5	0.13	0.13	1.25	2.65	2.65	—1.00	0.70

No. of layer	26/I 18 hr	26/I 18 hr	31/I 18 hr	2/II 18 hr	2/II 18 hr	15/II 15 hr	17/II 6 hr
				In the cloud			
1	1.20	—0.01	0.95	2.50	—1.20	—0 50	1.00
2	1.40	0.46	—2.00	1.80	—3.50	—0.50	1.00
3	—0.15	—1.45	—6.00	1.15	—3.00	—1.00	—0.50
4	—0.65	—0.20	—6.00	0.60	—4.50	—2.00	—0.50
5	—0.50	—0.05	—2.50	0.30	—6.00	—1.00	—0.50
6	—0.50	—0.10	—2 00	—0.30	—5.00	—1.00	—0.50
7	—0.50	—0.35	—2.50	—0.75	—4.50	0.50	0.50
8	1.00	—0.80	—2.00	—1.80	—6.50	—0.50	1.00
9	0.55	—1.10	—1.00	—2.30	—4.50	0.50	1.00
10	—0.40	—0.90	1.00	—1 55	—5.00	0.50	1.00
				Above the cloud			
1	—0.35	—0 35	1.10	—1.60	—1.60	0.50	—
2	—0.35	—0.35	0.30	—0.13	—0.13	—0.50	—
3	—0.17	—0.17	1.00	—0.10	—0.10	—	—
4	—0.24	—0.24	—0.40	—0.12	—0.12	—	—
5	—0.20	—0.20	—	—0.09	—0.09	0.50	—

No. of layer	19/II 6 hr	28/III 18 hr	28/III 18 hr	8/IV	19/IV 7 hr	6/XI 6 hr
			1959			
			Beneath the cloud			
1	2.60	0.44	0.44	—	—6.50	0.75
2	1.85	0.53	0 53	—	—7 50	0.78
3	1.55	0.86	0.86	—	—4.50	0.98
4	1.44	0.66	0 66	—	—7.50	1.27
5	—1.25	0.55	0.55	—	—7.50	1.87
			In the cloud			
1	1.55	—0.10	1.00	—	—6.50	2.23
2	—17.00	—0.30	1.00	—6.50	—17.50	2.41
3	—8.50	—0.40	1.00	—13.00	—16.00	1.75
4	—4.50	—0.25	1.00	—12.00	—22.00	1.49
5	—2.50	—0.30	1.00	—10.00	—18.00	0.95
6	—2.50	—0.20	1.00	—7.00	—12.00	1.10
7	—2.50	—0.50	0.50	—3.50	—12.00	1.15
8	—4.00	—0.50	0.50	—2.50	—16.50	0.35
9	—2.50	—0.50	0.50	0.50	—13.00	1.15
10	—0.50	—0.65	0.50	2.50	—5.00	1.15

No. of layer	19/II 6 hr	28/III 18 hr	28/III 18 hr	8/IV	19/IV 7 hr	6/XI 6 hr
			Above the cloud			
1	—0.30	—	—	—	—	0.75
2	0.05	0.13	0.65	—	—	0.48
3	0.05	0.03	0.15	—	—	0.49
4	0 05	0.01	0.00	—	—	0.38
5	0.10	0.01	0.05	—	—	0.58

No. of layer	18/XI 6 hr	17/XII 18 hr	9/II 6 hr	10/II 6 hr	7/XII 6 hr	7/XII 6 hr	8/XII 6 hr
				Beneath the cloud			
	1959		1960				
1	—3.50	1.00	—1.35	0.61	0.07	0.07	—0.61
2	—0.50	0.55	—0.70	0.61	0.14	0.14	—0.68
3	—0.50	0.40	3.50	7.00	0.27	0.27	—0 34
4	—2.00	0.20	3,50	—10.00	0.27	0.27	0.14
5	—2.00	0.32	3,50	—7.00	0.27	0.27	0.27
				In the cloud			
1	—3.50	2.00	3.50	—7.00	0.20	—0.54	—0.47
2	—3.50	1.50	3.50	—7.00	0.20	—0.54	—1.15
3	—3.50	0.80	0.00	—10.00	0.14	—0.54	—1.35
4	—2.00	—0.05	0.00	—7.00	0.00	—0.47	—1.35
5	—3.50	—0.65	0.00	—7.00	—0.40	—0.54	—1.35
6	—2.00	—3.50	0.00	—7.00	—0.40	—0.61	—1.48
7	—5.50	—6.50	—3.50	—7.00	—0.47	—0.68	—1.55
8	—3.50	—7.00	—7.00	—7.00	—0.94	—0.74	—1.69
9	—2.00	—8.00	—7.00	—7.00	0.08	—0.74	—0.61
10	—2.35	—6.00	—10.00	—7.00	—0.40	—0.88	—0.81
				Above the cloud			
1	—	—0.70	—17.00	—	—0.27	—0.27	—
2	—	0.25	—7.00	—	0.40	0.40	—
3	—	0.23	0.00	—	0.27	0.27	—
4	—	0.13	0.20	—	0.14	0.14	—
5	—	0.13	0.40	—	—0.07	—0.07	—

No. of layer	20/II 21 hr	30/IV 7 hr	Total	No. of cases	Mean	Smoothed value
			Beneath the cloud			
	1962					
1	—0.70	—	—3.97	24	—0.02	—0.01
2	—2.00	—	—1.05	26	0.00	0.16
3	—1.35	—	16.24	26	0.62	0 30
4	—0.35	—	—0,83	26	—0.03	0.14
5	—0.35	—	—2.76	26	—0.10	—0.27
			In the cloud			
1	—0 35	—3.98	—23.57	28	—0.84	—1.11
2	—0.35	—8.80	—77.27	29	—2.67	—2.43
3	—1.00	—16.55	—102.90	29	—3.54	—3.37
4	—1.70	—15.85	—107.42	29	—3.72	—3.60
5	—2 00	—16 55	—99.69	29	—3.44	—3.45
6	—1.70	—16.55	—92.34	29	—3.20	—3.28
7	—2.00	—17.20	—94.80	29	—3.28	—3.40
8	—2.00	—17.50	—105.27	29	—3.63	—3.44
9	—0.35	—17.55	—91.92	29	—3.20	—3.18
10	—1.00	—17.20	—77.84	29	—2.68	—2.84
			Above the cloud			
1	—	—15.20	—57.74	20	—2.80	—2.55
2	—	—10.45	—42.44	22	—1.93	—2.06
3	—	—6.10	—33.28	21	—1.59	—1.64
4	—	—2.00	—30.06	21	—1.45	—1.42
5	—	—0.35	—25.53	21	—1.21	—1.29

APPENDIX L

Reduced variation of the electric field in Ns clouds (snow-producing, positively polarized). Leningrad, 1958-1961

No. of layer	14/I 18 hr	15/I 3 hr	21/II 6 hr	7/III 6 hr	15/III 6 hr	26/IX 18 hr	15/X 3 hr
				1958			
				Beneath the cloud			
1	0.25	8.00	1.00	2.00	0.37	1.80	—0.45
2	0.25	2.55	1.00	3.50	0.35	1.40	0.62
3	2.50	1.55	—0.50	2.00	0.34	1.15	0.95
4	3.30	0.80	—3.50	2.50	0.57	1.12	1.40
5	4.00	0.96	—2.00	6.90	0.76	0.86	3.65
				In the cloud			
1	2 50	2.60	—0.50	0.75	0.60	1 70	17.50
2	2.50	3.00	—1.00	1.00	0.78	3.25	19.50
3	1.50	2.50	0.50	1.05	0.91	4.65	18.50
4	1.00	2.90	1.50	1.25	1.26	—0.80	15.00
5	4.50	5.00	4.00	1.10	1.22	—4.45	1.00
6	6.00	6.50	4.50	1.25	1.45	2.50	—2.00
7	6.00	10.00	—2.00	0.80	1.23	—2.00	—2.50
8	6.00	15.50	0.50	0.40	1.09	—3.50	—4.00
9	4.00	19.50	—0.10	0.30	0 75	0.50	—1.00
10	2.50	14.00	1.00	0.30	0.20	0.50	—2.50
				Above the cloud			
1	2.50	3.50	—	0.55	0.19	3.50	—4.00
2	6.00	0.41	—	0.45	0.22	1.00	—5.00
3	12.50	0.24	—	0.13	0.16	0.20	0 00
4	4.00	0.19	—	0.04	0.10	1.55	0.50
5	0.50	0.15	—	0.20	0.05	1.35	0.50

No. of layer	14/XI 18 hr	14/XI 18 hr	14/XI 18hr	28/XI 6 hr	10/XII 6 hr	26/XII 6 hr	28/XII 18 hr	31/XII 6 hr
				Beneath the cloud				
1	—	—	—	2.00	0.80	—	1.35	—
2	—	—	—	2.50	1.15	—	0.55	2.10
3	—	—	—	2.50	0.95	1.00	0.70	1.35
4	—	—	—	3.50	0.65	1.00	0.40	1.05
5	—	—	—	4.50	0.55	1.15	0.65	0.80

No. of layer	14/XI 18 hr	14/XI 18 hr	14/XI 18 hr	28/XI 6 hr	10/XII 6 hr	26/XII 6 hr	28/XII 18 hr	31/XII 6 hr
				In the cloud				
1	1.55	1.65	—0.35	4.50	0.10	5.75	0.20	1.75
2	2.00	1.25	—0.70	3.00	1.00	—	—0.85	2.30
3	2.95	0.70	0.50	2.00	0.10	14.50	—0.75	0.60
4	2.15	0.25	2.00	3.50	0.20	—	0.50	1.23
5	2.30	0 25	2.50	3.50	0.30	50.00	0.80	0.60
6	2.30	0.25	2.50	2.00	0.20	19.50	0.10	0.15
7	2.60	0.25	2.00	2.00	0.10	1.00	0.05	0.45
8	2.60	0.10	0.50	5.00	0.10	1.00	0.40	—0.15
9	2.45	0.20	1.00	0.85	0.10	2.30	—0.70	—0.05
10	2.25	—0.05	0.50	0.22	0.10	1.70	—0.45	—0.55
				Above the cloud				
1	—0.10	—0.10	—0.10	0.37	0 03	0.10	0.30	—0.95
2	—0.20	—0.20	—0.20	0.11	0.00	0.10	0.50	—0.12
3	—0.50	0.50	0.50	0.39	0.06	0.05	0.33	1.45
4	—0.50	0.50	0.50	0.16	0.08	0.35	0.17	2.00
5	—0 15	—0.15	—0.15	0.59	0.06	—0.10	0.14	1.65

No. of layer	2/I 18 hr	5/I 3 hr	9/I 6 hr	10/I 3 hr	10/I 3 hr	20/II 15 hr	20/II 15 hr	24/II 18 hr
				1959				
				Beneath the cloud				
1	—	—	—1.50	0.00	0.00	1.19	1.19	0.50
2	—	—	—1.50	0 00	0.00	1.31	1.31	3.50
3	—	—	—1.50	—0.45	—0.45	1.26	1.26	3.50
4	—	—	—0.75	0.00	0.00	1.53	1.53	3.50
5	—	—	—0.60	—0.20	—0.20	2.03	2 03	3.50
				In the cloud				
1	0.88	—0.82	—0 05	—0.25	—0.15	2.47	—0.14	2.00
2	1.64	—0.92	0.60	0.25	—0.15	2.85	0.05	2.00
3	1.90	—1.14	1.50	1.20	—1.10	2.75	—0.65	5.00
4	1.80	—1.37	1.70	0.42	—2.10	2.70	—0.85	2.00
5	1.65	—1.31	1.50	—0.02	—2.55	2.85	1.00	1.00
6	0.60	—0 82	1.20	1.47	2.00	2.75	1.00	0.45
7	0.60	2.50	0.75	—0.55	0.50	2.70	0.50	2.00
8	0.85	4.00	0.10	—0.40	0.50	2 85	0.50	4.00
9	0.30	2.50	—0.50	—0.95	1.00	2.85	1.00	1.10
10	—0.25	1.00	—1.35	—1 80	0.50	1.55	0.50	1.00

No. of layer	2/I 18 hr	5/I 3 hr	9/I 6 hr	10/I 3 hr	10/I 3 hr	20/II 15 hr	20/II 15 hr	24/II 18 hr
				Above the cloud				
1	—0.40	—12.00	—0.20	1.00	1.00	0.25	0.25	1.00
2	—0.19	—12.00	0.15	0.32	0.32	0.02	—0.06	5.00
3	—0.05	—12.00	0.25	0.56	0.56	—0.11	—0.11	2.50
4	0.00	—11.00	0.40	0 67	0 67	—0.13	—0.13	0.85
5	0.37	—11.00	0.35	0.54	0.54	—0.10	—0.10	0.90

No. of layer	25/II 3 hr	25/II 3 hr	19/IV 3 hr	3/VI 18 hr	24/XII 6 hr	25/XII 3 hr	25/XII 3 hr
				Beneath the cloud			
1	—	—	—	—1.42	0.60	1.30	1.30
2	—	—	—3.35	—1.51	0.55	1.25	1.25
3	—	—	—3.50	—3.00	0.55	0.97	0.97
4	—	—	—4.50	—3.50	0.70	1.31	1.31
5	—	—	—4.50	—0.85	0.80	1.32	1.32
				In the cloud			
1	2 30	1.00	—0.20	0.84	1 10	1.72	0.00
2	2.50	2.00	—3.50	1.45	0.85	1.83	0.45
3	2.50	2.00	—10.50	1.91	0.55	1 66	0.60
4	2.05	3.00	—16 00	2.37	1.60	1.55	0.90
5	1.50	1.00	—14.50	1.45	1.70	1.40	0.90
6	1.10	1.00	0.50	0.75	0.95	1.28	1.55
7	0.80	2.00	20.00	—0.25	1.35	1.05	1.85
8	0.35	1.00	5.00	—0.35	1.35	0.65	1.80
9	0.50	0.50	15.00	—0.65	0 30	0.35	1.35
10	0 50	0.50	3.50	—0.60	—0 20	0.35	0.25
				Above the cloud			
1	—0.02	—0.02	—3.00	—0.55	—0.20	—0.21	—0.21
2	—0.06	—0.06	—2.50	—0.45	0.10	0.25	0.25
3	—0.07	—0.07	—2.00	—0.25	0.17	0.12	0.12
4	—0.10	—0.10	—2 00	—0.65	0.34	0.17	0.17
5	—0.11	—0.11	—2.50	12.00	1.65	0.14	0.14

No. of layer	28/XII 3 hr	7/I 6 hr	15/III 15 hr	15/III 21 hr	1/III 6 hr
			Beneath the cloud		
	1959		1960		1961
1	1.30	—1.90	—1.35	—0.70	—1.00
2	1.25	—0.40	—1.35	0.00	—1.35
3	0.97	1.95	—1.35	0.00	—1.35
4	1.31	2.15	—1.35	0.00	—2.00
5	1.32	1.00	—1 70	3.50	—2.00
			In the cloud		
1	0.45	—2.50	—1.70	3.50	—2.00
2	0.30	—2.85	2.00	3.50	—2.00
3	0.25	2.20	7.00	3.50	—1.70
4	0.10	8.50	3.50	7.00	0.00
5	0.10	9.50	7.00	3.50	0.70
6	—0.05	9.50	3.50	0.00	0.35
7	—0.20	8.00	1.35	0.00	0.00
8	—0.35	6.00	0.35	0.14	0.35
9	—1.10	6.50	0.94	0.27	0.70
10	—1.20	4.00	0.40	0.40	0.70
			Above the cloud		
1	—0.21	—2.80	—	—	—0.35
2	0.25	0.15	—	—	—0.70
3	0.12	0.09	—	—	—0.35
4	0.17	0.11	—	—	0.00
5	0.14	0.14	—	—	0.07

No. of layer	20/XI 21 hr	9/XII 15 hr	Total	No. of cases	Mean	Smoothed value
			Beneath the cloud			
	1961					
1	—1.35	—5.36	9.56	27	0.35	0.38
2	—1.00	—3.40	12.53	29	0.43	0.40
3	— 0 70	—1.35	12.27	30	0.40	0.41
4	—1.00	—1.00	12.03	30	0.40	0.51
5	—1.00	—3.40	25.15	30	0.84	0.81
			In the cloud			
1	0.35	—5.75	43.44	37	1.17	1.14
2	3.50	—2.70	50.68	36	1.40	1 48
3	3.50	—1.35	71.79	37	1.94	1 70
4	3.50	—1.00	53.32	36	1.50	1.90
5	3.50	0.00	95.19	37	2.60	2.22
6	3.50	0.70	80.48	37	2.20	2.20
7	0.00	0.70	65.63	37	1.80	1.84
8	0.00	3.50	57.53	37	1.56	1.66
9	0.00	3.50	64.16	37	1.73	1.37
10	—0.35	3.50	17.36	37	0.47	1.60
			Above the cloud			
1	—	0.70	—10.18	33	—0.31	—0.08
2	—	0.00	—4.96	33	—0.15	—0.10
3	—	—0.70	5.89	33	0.18	0.10
4	—	—0.70	6.31	33	0.19	0.19
5	—	—1.00	6.70	33	0.20	0.20

APPENDIX LI

Reduced variation of the electric field in Ns clouds (mixed, negatively polarized). Leningrad, 1958-1962

No. of layer	19/VII 5 hr 45 min	6/VIII 5 hr 45 min	26/V 5 hr 45 min	29/VI 17 hr 51 min	30/VI 3 hr 00 min	27/VIII 17 hr 47 min	19/IX 17 hr 46 min
				Beneath the cloud			
	1958				1959		
1	0.2	—6.7	—2.6	1.2	—0.6	0.3	0 9
2	0.3	—12.0	—4.3	—1.2	—0.6	0 3	0.7
3	0.2	—14.3	—3.7	—2.9	—0.4	0.3	1.0
4	0.2	—14.0	—0.1	—3.5	—0.2	0.3	1.1
5	0.2	—13.8	—1.4	—10.3	—1.2	0.3	0.8
				In the cloud			
1	0.1	—3.6	—6.5	—8.6	—1.9	0.5	1.5
2	0.1	—10.0	—6.5	—8.6	—3.0	0.3	1.5
3	0.2	—2.0	—9.5	—8.3	—9.5	0.2	1.5
4	0.1	—3.0	—11.0	—10.8	—17.6	—4.5	1.5
5	—0.2	—1.6	—11.0	—30.0	—7.2	—2.8	1.5
6	—1.0	—1.5	—11.1	—67.9	—3.7	—2.0	1.0
7	—0.5	—1.4	—6.9	—80.0	—4.6	—2.0	—4.0
8	—1.0	—3.6	—15.5	—78.4	—5.6	—1.8	—4.2
9	—0.5	11.0	—12.8	—12.1	—2.6	—4.0	—3.5
10	—0.6	6.0	—16.3	7.8	—7.0	—3.1	—1.1
				Above the cloud			
1	—	—0.3	—3.8	8.0	—0.6	0.3	—0.2
2	—	—0.5	—0.3	8.0	0.1	0.4	0.4
3	—	—0.2	—0 5	8.0	0.3	0.3	0.6
4	—	—0.1	—0.1	8.0	0.9	0.3	0.4
5	—	—0.1	0.1	8.0	0.9	0.8	0.0

No. of layer	22/IX 17 hr 43 min	30/IX 15 hr 00 min	6/X 17 hr 47 min	16/X 5 hr 45 min	31/X 5 hr 57 min	29/VI 17 hr 55 min	8/VIII 9 hr 02 min
				Beneath the cloud			
		1959			1961	1962	
1	2.4	0.9	1.3	—0.1	—2.4	3.8	2.8
2	0.1	0.9	1.7	—0.1	—4.3	2.5	2.8
3	2.1	0.9	1.2	—0.1	—3.3	4.6	2.8
4	1.7	0.9	1.0	—0.1	—4.9	10.1	2.8
5	1.6	0.9	0.5	—0.1	1.1	8.6	2.8
				In the cloud			
1	1.4	1.4	0.2	0 1	4.6	5.0	3.3
2	3.0	1.3	—6.7	—0.8	4.6	2.7	—7.7
3	2.4	0.0	—8.5	—0.5	4.6	0.7	—4.3
4	—3.8	—4.9	—6.0	—3.0	4.6	0.1	—1.6

No. of layer	22/IX 17 hr 43 min	30/IX 15 hr 00 min	6/X 17 hr 47 min	16/X 5 hr 45 min	31/X 5 hr 57 min	29/VI 17 hr 55 min	8/VIII 9 hr 02 min
5	—5.3	—1.6	—10.5	—2.5	4.6	—0.3	—0.4
6	—3.5	—0 2	—15.0	—2.4	0 7	—11.9	—1.0
7	—2.0	—0 8	—15.0	—3.4	0.4	—17.7	—0 6
8	—3 5	—4.1	—17.2	—2.0	—2.2	—7.7	—1.7
9	—3.5	—7.9	—19.5	—2.0	—2.4	—5.1	8.7
10	—2.0	2 8	—19.5	—3.5	—1.9	—0.4	3.5
			Above the cloud				
1	—5.6	21.5	—2.6	1.0	—3.2	—0.2	1.7
2	—5.6	22.0	—1.1	1.5	—0.1	—0.2	0.0
3	—3.4	22.5	—0.7	1.4	0.1	—0.2	0.1
4	—1.4	0.6	0.4	2.0	0.1	—0.1	—0.1
5	—1.4	—0.4	—0.4	1.4	0.9	0.0	0.1

No. of layer	6/VIII 15 hr 09 min	Total	No. of cases	Mean	Smoothed value
		Beneath the cloud			
	1962				
1	1.1	2.5	15	0.2	—0.1
2	1.1	—12.1	15	—0.8	—0.5
3	0.3	—11.3	15	—0.8	—0.7
4	—0.3	—5.0	15	—0.3	—0.5
5	—0.3	—10.3	15	—0.7	—0.5
		In the cloud			
1	—1.9	—4.4	15	—0.3	—0.8
2	—1.1	—30.9	15	—2.1	—1.7
3	—2.5	—35.5	15	—2.4	—2.8
4	—5.8	—65.7	15	—4.4	—3.9
5	2.1	—65.2	15	—4.3	—5 6
6	—20.2	—139.7	15	—9.3	—9.0
7	—57.3	—195.8	15	—13.0	—11.4
8	—9.3	—157.8	15	—10.5	—9.6
9	—9.3	—65.5	15	—4.4	—5.3
10	7.3	--28.0	15	—1.9	—1.7
		Above the cloud			
1	0.4	16.4	15	1.2	0.5
2	—0.9	23.7	15	1.7	1.6
3	—0.3	28.0	15	2.0	1.6
4	—0.2	10.7	15	0.8	1.0
5	—0.1	8.9	15	0.6	0.7

APPENDIX LII

Reduced variation of the electric field in Ns clouds (snow-producing, negatively polarized with additional charges). Leningrad, 1958-1962

No. of layer	4/II 18 hr	25/II 3 hr	26/I 6 hr	13/II 6 hr	19/IV 3 hr	19/IV 6 hr
			Beneath the cloud			
	1958			1959		
1	—3.50	—	—	—7.50	—	—
2	—3 50	—	—	—7.50	—3.35	—
3	—3.50	—	—	—8 00	—3.50	—
4	—3.50	—	—	—8.00	—4.50	—
5	—2.00	—	—	—6.50	—4.50	—
			In the cloud			
1	—3.00	—5.00	—5.00	—8.00	—4.50	—21.50
2	—2.00	—5.00	—5.50	—8.00	—2.00	—23.00
3	—2.00	—5.00	—5.50	—8.00	—2.00	—17 00
4	—1.80	—4.50	—5.00	—6 50	—2.00	—9.00
5	—1.70	—4 50	—3 50	—4.50	—1.50	—15.50
6	—1.60	—4.50	—4.00	—5.00	—2 65	—10.00
7	—0.90	—4.50	—4 00	—3.50	—1.50	—7 50
8	—0 10	—4.50	—2.00	—1 50	—2.00	—7.00
9	0.04	—5.00	—3.00	—3.50	—2.00	—21.50
10	—0.50	—6.50	—3.50	—8.00	—2.00	—23.00
			Above the cloud			
1	—2.60	0.30	—3.50	—6 50	—3.00	—
2	—0.40	0 10	—3.50	—6.00	—2.50	—
3	—0.50	0 50	—2.50	—5.00	—2.00	—
4	—0.20	0.15	—4.00	—3.50	—2.00	—
5	—0.90	0.04	—4.00	—2.10	—2.50	—

No. of layer	22/IV 3 hr	6/I 6 hr	29/III 18 hr	20/XI 15 hr	9/XII 9 hr	25/XII 6 hr
			Beneath the cloud			
	1959		1960		1961	
1	—0.07	—	—3.50	0.00	—	—1.00
2	0.17	—	0.00	0.00	—	—1.30
3	0.64	—4.00	—3.50	0.00	—	—1.00
4	0 10	—2.50	—7 00	0.07	—	—0.70
5	0 50	—4.00	—7.00	—	—	—0.35
			In the cloud			
1	—8.50	—7.00	—7.00	—0 35	—0 70	—1.30
2	—13.50	—7.00	—3.50	—0.07	0 00	—2 70
3	—12.00	—7.00	—4.40	—0.07	0.00	—2.35
4	—11.50	—5.50	—3 40	—0.35	0.00	—2.35

No. of layer	22/IV 3 hr	6/I 6 hr	29/III 18 hr	20/XI 15 hr	9/XII 9 hr	25/XII 6 hr
5	—4.50	—2.50	—3.40	—0.35	0.00	—1.70
6	—4.50	—2.00	—2.70	—0.35	0.00	—1.30
7	—14 00	—3.50	—3.05	—0.35	—0.35	—1.70
8	—12.50	—3.50	—3.70	—0.07	—0.35	—2.35
9	—12.00	—0.50	—3.40	—0.14	—0.35	—7.00
10	—7.00	—1.00	—2.35	—0.14	0.00	—3.50
			Above the cloud			
1	—0.75	—	—	0.00	0.35	—1.70
2	—0.04	—	—	0.00	0.35	0.70
3	0 03	—	—	0.00	0.14	—
4	0.09	—	—	0.00	0.14	—0.70
5	—0.90	—	—	0.00	0.14	—0.70

No. of layer	15/III 6 hr	Total	No. of cases	Mean	Smoothed value
		Beneath the cloud			
	1962				
1	—1.00	—14.57	7	—2.08	—2.08
2	—1.35	—16.73	8	—2.09	—2.20
3	—1.00	—23.86	9	—2.65	—2.60
4	—1.00	—27.03	9	—3.00	—3.19
5	—1.00	—24.85	8	—4.10	—4.22
		In the cloud			
1	—2.00	—73.85	13	—5.68	—5.28
2	—2.00	—73 77	13	—5.65	—5.54
3	—2.00	—67.32	13	—5 20	—5.05
4	—2.00	—53.90	13	—4.15	—4.25
5	—2.00	—45.65	13	—3.50	—3.56
6	—1.70	—40.30	13	—3.10	—3.32
7	—1.70	—46.55	13	—3.60	—3.37
8	—1.70	—41.27	13	—3.18	—3.63
9	—1.00	—59.35	13	—4.56	—4.19
10	—0.30	—47.79	13	—4 45	—4.49
		Above the cloud			
1	0.07	—17.33	10	—1.73	—2.26
2	0.07	—11.22	10	—1.12	—1.25
3	0.07	—9.31	9	—1.03	—1.04
4	0.07	—9.95	10	—1.00	—1.02
5	0.34	—10.58	10	—1.06	—1.04

EXPLANATORY LIST OF ABBREVIATED NAMES OF USSR INSTITUTIONS, ORGANIZATIONS, JOURNALS, ETC., APPEARING IN THIS TEXT

Abbreviation	Full name (transliterated)	Translation
GGO	Glavnaya Geofizicheskaya Observatoriya	Main Geophysical Observatory
LGMI	Leningradskii Gidrometeorologicheskii Institut	Leningrad Hydrometeorological Institute
MGG	Mezhdunarodnyi Geofizicheskii God	International Geophysical Year
NII GUGMS	Nauchno-Issledovatel'skii Institut Glavnogo Upravleniya Gidrometeorologicheskoi Sluzhby	Scientific Research Institute of the Main Administration of the Hydrometeorological Service
TsAO	Tsentral'naya Aerologicheskaya Observatoriya	Central Aerological Observatory
UFN	Uspekhi Fizicheskikh Nauk	Progress of Physical Sciences
ZhTF	Zhurnal Tekhnicheskoi Fiziki	Journal of Technical Physics

[1841] Printed in Jerusalem, Israel NASA TT F-425
TT 67-51374